

NONLINEAR-REGRESSION FLOW MODEL OF THE GULF COAST AQUIFER SYSTEMS IN THE SOUTH-CENTRAL UNITED STATES

By Logan K. Kuiper

U.S. GEOLOGICAL SURVEY

Water-Resources Investigations Report 93-4020



A Contribution of the
Regional Aquifer-System Analysis
Program

Austin, Texas
1994

U.S. DEPARTMENT OF THE INTERIOR
BRUCE BABBITT, *Secretary*

U.S. GEOLOGICAL SURVEY
Gordon P. Eaton, *Director*

Any use of trade, product, or firm names in this publication is for descriptive purposes only and does not imply endorsement by the U.S. Government

1994

For sale by the U.S. Geological Survey, Earth Science Information Center, Open-File Reports
Section, Box 25286, Mail Stop 517, Denver Federal Center, Denver, CO 80225

For additional information write to:

Project Chief
U.S. Geological Survey
8011 Cameron Road, Building B
Austin, Texas 78754-3898

CONTENTS

	Page
Abstract.....	1
Introduction.....	2
Description of study area.....	3
Geologic setting.....	7
Ground-water flow.....	12
Data available for hydraulic head and hydraulic conductivity...	12
Nonlinear-regression flow model.....	17
Modeling methodology and construction.....	18
Regression model.....	40
Prediction and confidence intervals.....	45
Depth dependence of hydraulic conductivity.....	48
Hydraulic conductivity zones.....	51
Subsidence.....	54
Preparation of observations of head and hydraulic conductivity, Y_i	54
Grid element volume-averaged heads.....	55
Averaging algorithm.....	56
Logarithms of hydraulic conductivity of sand.....	58
Residual weighting.....	61
Application of regression flow models and results.....	62
Descriptions of models used.....	63
Choosing the best regression model.....	75
Analysis of residuals.....	76
Comparison of models.....	78
Model error.....	94
Model truncation.....	98
Summary and conclusions.....	100
Summary.....	100
Conclusions.....	101
References.....	102
Attachments.....	105
Introduction.....	106
The Levenberg-Marquardt method.....	106
MAIN.....	107
Explanation of MAIN listing.....	108
Flow chart of MAIN.....	110
Definition of program variables.....	111
Listing.....	113
MODEL.....	122
Essential features of MODEL.....	123
Definition of program variables.....	124
Listing.....	130
SOLEQU listing....	158
PCG listing.....	159
SIP listing.....	166

ILLUSTRATIONS

	Page
Figures 1-7. Maps showing:	
1. Location of Gulf Coast Regional Aquifer-System Analysis study area and generalized outcrop of aquifer systems....	4
2. Generalized average land-surface altitude and bathymetry.....	5
3. Generalized structural features and location of geohydrologic section.....	6
4. Altitude of the base of the gulf coast aquifer systems and area of occurrence of geopressure.....	8
5. Ground-water pumpage from the gulf coast aquifer systems, 1980.....	13
6. Water-table altitude on shore and equivalent freshwater head at the sea floor offshore.	14
7. Estimate of depth to water containing 35,000 milligrams per liter dissolved solids....	15
8. Cumulative frequency distribution of concentration of dissolved solids in 18,000 sand beds in the gulf coast aquifer systems.....	16
9. Maximum areal extent of modeled area and outcrop of hydrogeologic units represented by model layers...	20
10-24. Maps showing:	
10. Areal extent of model layer 2 and simulated 1982 equivalent freshwater head from model 4.....	21
11. Areal extent of model layer 3 and simulated 1982 equivalent freshwater head from model 4.....	22
12. Areal extent of model layer 4 and simulated 1982 equivalent freshwater head from model 4.....	23
13. Areal extent of model layer 5 and simulated 1982 equivalent freshwater head from model 4.....	24
14. Areal extent of model layer 6 and simulated 1982 equivalent freshwater head from model 4.....	25
15. Areal extent of model layer 7 and simulated 1982 equivalent freshwater head from model 4.....	26
16. Areal extent of model layer 8 and simulated 1982 equivalent freshwater head from model 4.....	27
17. Areal extent of model layer 9 and simulated 1982 equivalent freshwater head from model 4.....	28
18. Areal extent of model layer 10 and simulated 1982 equivalent freshwater head from model 4.....	29

ILLUSTRATIONS--Continued

Page

Figures 10-24. Maps showing--Continued:

19. Areal extent of model layer 11 and simulated 1982 equivalent freshwater head from model 4.....	30
20. Areal extent of model layer 13. Represents confining unit between model layers 4 and 5.....	31
21. Areal extent of model layer 14. Represents confining unit between model layers 5 and 6.....	32
22. Areal extent of model layer 15. Represents confining unit between model layers 6 and 7.....	33
23. Areal extent of model layer 16. Represents confining unit between model layers 7 and 8.....	34
24. Areal extent of model layer 17. Represents confining unit between model layers 8 and 9.....	35
25. Idealized diagram from central Texas to the edge of the Continental Shelf showing vertical relation of aquifers and confining units.....	36
26. Map showing areal extent of the significantly overpressured parts of the geopressed zone.....	38
27-31. Graphs showing:	
27. Total pumping rate by layer for the years 1960, 1970, 1975, and 1980.....	41
28. Two potential regression models, $f_1(x,B)$, and $f_2(x,B)$ for describing the relation between cartesian coordinate (x) and the volume average of head ($Y(x)$).....	43
29. Decrease of hydraulic conductivity of sand with depth.....	49
30. Decrease of hydraulic conductivity of clay with depth.....	50
31. Effective hydraulic conductivity, equations (10) and (11), for $K_s/K_c = 10^4$	52
32. Map showing the 10 regions used to define hydraulic conductivity zones.....	53
33. Map showing the location of the 1,675 grid-element volume-averaged heads for 1982.....	59
34. Graph showing change in multiplier $[D^2(p,n,\alpha)]$ for prediction interval size with number of regression parameters.....	64
35. Diagram showing generalized pattern of ground-water flow.....	82
36-46. Maps showing:	
36. Recharge (discharge) into the top of the aquifer system for 1982, model 4.....	83
37. Simulated drawdown of equivalent freshwater head from 1937-82, model 4, model layer 2	84

ILLUSTRATIONS--Continued

	Page
36-46. Maps showing--Continued:	
38. Simulated drawdown of equivalent freshwater head from 1937-82, model 4, model layer 3.....	85
39. Simulated drawdown of equivalent freshwater head from 1937-82, model 4, model layer 4.....	86
40. Simulated drawdown of equivalent freshwater head from 1937-82, model 4, model layer 5.....	87
41. Simulated drawdown of equivalent freshwater head from 1937-82, model 4, model layer 6.....	88
42. Simulated drawdown of equivalent freshwater head from 1937-82, model 4, model layer 7.....	89
43. Simulated drawdown of equivalent freshwater head from 1937-82, model 4, model layer 8.....	90
44. Simulated drawdown of equivalent freshwater head from 1937-82, model 4, model layer 9.....	91
45. Simulated drawdown of equivalent freshwater head from 1937-82, model 4, model layer 10.....	92
46. Simulated drawdown of equivalent freshwater head from 1937-82, model 4, model layer 11.....	93

TABLES

		Page
Table	1. Relation of geologic units, previously defined geohydrologic units, and layers used in regional flow model.....	10
	2. Mean hydraulic conductivity by model layer and region.....	60
	3. Regression parameters for models 1 through 12.....	66
	4. Results from flow models 1 through 12.....	70
	5. 1982 ground-water flow rates for models 3 through 11..	80
	6. The effect of model alterations on: (1) layer-averaged predicted head, h_{layer} ; (2) hydraulic conductivity of parameters of clay and sand, P_c and P_s ; (3) $\omega_k^{1/2}e_k$; (4) the 15 flows of table 5; and (5) deep head for models 3 through 11, and model 4.....	96

**CONVERSION FACTORS, VERTICAL DATUM,
AND ABBREVIATED WATER QUALITY UNITS**

Multiply	By	To obtain
<u>Length</u>		
foot (ft)	0.3048	meter
inch (in.)	25.40	millimeter
mile (mi)	1.609	kilometer
<u>Area</u>		
square mile (mi ²)	2.590	square kilometer
<u>Flow</u>		
billion gallons per day (Ggal/d)	43.81	cubic meter per second
cubic foot per day (ft ³ /d)	0.02832	cubic meter per day
inch per year (in/yr)	25.4	millimeter per year
<u>Pressure</u>		
pound per square inch (lb/in ²)	6.895	kilopascal

Sea level: In this report, "sea level" refers to the National Geodetic Vertical Datum of 1929--a geodetic datum derived from a general adjustment of the first-order level nets of the United States and Canada, formerly called Sea Level Datum of 1929.

Chemical concentrations and seawater density are given in metric units. Chemical concentration is given in milligrams per liter (mg/L) and seawater density is given in grams per cubic centimeter (gm/cm³).

SYMBOLS AND DIMENSIONS

[Number in parentheses refers to the page or illustration where the symbol first appears or where additional clarification may be obtained. Symbols are also defined in the text.]

<i>Symbol</i>	<i>Dimensions</i>	<i>Description</i>
A	L^2	Cross sectional area (42).
B	-----	Parameter vector (40).
\hat{B}	-----	Value for parameter vector B at which S(B) is a minimum (46).
B_i to B_p	-----	Regression parameters.
C_s	1	Specific storage factor (54).
Chi^2	1	Probability distribution function (76).
D	-----	Function (63).
E	-----	Random vector (40).
F	1	F probability distribution function (46).
G	1	Function (63).
K	LT^{-1}	Hydraulic conductivity tensor (18).
K_c	LT^{-1}	Hydraulic conductivity of clay (51).
K_s	LT^{-1}	Hydraulic conductivity of sand (51).
M	1	Number of grid-elements with a specified head (39).
Mu	$ML^{-1}T^{-1}$	Mean weighted residual (76).
N	1	Number of grid-elements dependent upon regression parameters (19).
P	$ML^{-1}T^{-2}$	Pressure (18).
P_c	LT^{-1}	Hydraulic conductivity parameter of clay (96).
P_s	LT^{-1}	Hydraulic conductivity parameter of sand (76).
Q	L^3T^{-1}	Rate of discharge (18).
R	L	Radius (57).
S_s	T^{-1}	Specific storage (18).
S(B)	-----	Weighted mean square error (46).
T	-----	Transpose of a matrix (46).
V_c	L^3	Clay fraction of the grid element (51).
X	-----	Matrix (46).
\hat{X}	-----	Matrix X evaluated at $B=\hat{B}$ (46)
Y	-----	Random vector (40).
Y_i	-----	Set of observations (40).
Z_i	-----	Random variable (76).
a	-----	Width to vertical thickness ratio (51).
b	L	Grid element thickness (37).
b_1 to b_9	-----	Regression parameters (65).

SYMBOLS AND DIMENSIONS--Continued

<i>Symbol</i>	<i>Dimensions</i>	<i>Description</i>
dd	-----	Function, depth (48, 95).
e	-----	Base of Naperian logarithms, 2.71828 (46).
f(B)	-----	Expectation of Y (40).
g	LT ⁻²	Acceleration due to gravity (18).
h	ML ⁻¹ T ⁻²	Pressure head (18).
h _w	L	Water table altitude (37)
Δh _s	ML ⁻¹ T ⁻²	Head triggering value for subsidence (54).
k	L ²	Intrinsic permeability tensor (18).
n	1	Number of observations (40).
p	1	Number of parameters (46).
ns	1	Number of point observations of head used to formulate pressure head (56).
\bar{q}		Specific discharge (18).
r	L	Radius (56).
s	1	Aquifer layer (61).
t	T	Time.
u	1	Number expressing departure from ideal situation (63).
v ²	-----	Variance (76).
x	L	Cartesian coordinate in x-direction
y	L	Cartesian coordinate in y-direction
z	L	Cartesian coordinate in z-direction
α	1	F probability distribution function argument (46).
∂	-----	Partial derivative (18).
μ	ML ⁻¹ T ⁻¹	Dynamic viscosity (18).
ω	1	Matrix (40).
ρ	ML ⁻³	Density of fluid (18).
Δ	-----	Change in a quantity.
ε	-----	ε ² ω ⁻¹ is variance (40, 42).

NONLINEAR-REGRESSION FLOW MODEL OF THE GULF COAST AQUIFER SYSTEMS IN THE SOUTH-CENTRAL UNITED STATES

By

Logan K. Kuiper

ABSTRACT

Multiple-regression methodology was used to calibrate a time-dependent, variable-density ground-water flow model with subsidence of the deep, regional gulf coast aquifer systems in the south-central United States. The methodology was also used to help answer questions concerning model reliability. More than 40 different regression models having 2 to 31 regression parameters are used and detailed results are reported for 12 of the models. More than 3,000 values for grid-element volume-averaged head and volume-averaged hydraulic conductivity are used as observations in the regression models. Calculated prediction interval half widths, though perhaps inaccurate due to a lack of normality of the residuals, are smallest for those models having only four regression parameters. Because of this, and also because the root-mean weighted residual decreases very little with an increase in the number of regression parameters, the models having a small number of parameters are probably the most reliable.

The various models used show considerable overlap between the prediction intervals for shallow head and hydraulic conductivity of sand (K_s). Approximate 95-percent prediction interval half widths for volume-averaged freshwater head exceed 108 feet; for volume-averaged $\log_{10}(K_s)$, they exceed 0.89. All the models produce unreliable predictions of head and ground-water flow in the deeper parts of the aquifer system, including the amount of flow coming from the geopressed zone beneath the aquifer system. Truncating the domain of solution of one of the models to exclude that part of the system having a ground-water density greater than 1.005 grams per cubic centimeter does not appreciably change simulated heads or flow. Also, excluding that part of the system below a depth 3,000 feet below land surface, and setting the density to that of freshwater in the remaining shallow part of the domain of solution, does not appreciably change the results for head and ground-water flow from the model, except for locations close to the truncation surface.

The regression methodology allowed the testing of a wide range of models for the simulation of the aquifer system. It also provided estimates of the accuracy of results and a mechanism to determine sources of model error.

INTRODUCTION

A common approach used to determine the accuracy of a ground-water simulation model is to compare model-computed values and values of the hydraulic parameters used in the model with field observations of physical quantities. Such comparisons form the basis for model calibration, which is that process whereby these parameters are varied to obtain the best possible fit with the observed quantities (Konikow, 1978). Clearly, for such calibration to be possible, it is necessary to establish some criterion to decide whether a particular selection of regression parameters (regression model) gives a better or worse fit than some other selection of regression parameters. Furthermore, for calibrated models to be most useful it is necessary to be able to gage their reliability. Recent advances in regression modeling described by Vecchia and Cooley (1987), Cooley and others (1986), Cooley (1977, 1979, 1982), Neuman (1980), and Yeh and Yoon (1981) treat model calibration as a statistical procedure. These regression procedures provide the necessary fitting criterion and the estimates of model reliability.

The purpose of this report is to illustrate the application of a multiple regression methodology to help answer questions concerning model reliability, to use the method to calibrate a ground-water flow model for a thick regional aquifer system in the Gulf Coastal Plain of the south-central United States, and to develop an improved understanding of flow in the gulf coast aquifer systems.

First, the hydrologic and geologic setting of the gulf coast aquifer systems is described in detail to provide the background needed to understand the modeling effort. A short description of the flow model and the regression procedure for calibration follows. The next section gives formulae to determine the confidence of the model output and the regression parameters used in the model, and a procedure for selecting the model expected to give the best results. Following are sections on: model construction, preparation of observations, application of the model, model error, and analysis of residuals.

This report is one of several presenting the results of the Gulf Coast Regional Aquifer-System Analysis (RASA) study, one of many RASA studies which have been conducted by the United States Geological Survey since 1978, at which time the RASA program was initiated following a congressional mandate (Sun, 1986, p. 2). Professional Paper 1416 consists of several chapters dealing with various aspects of the ground-water flow system in the Gulf Coastal Plain of the south-central United States. Chapter B (Hosman and Weiss, 1991) and C (Weiss, 1992) present physical characteristics of geohydrologic units such as thickness, altitude of the top, and percentage of sand; Chapter D (Ackerman, 1993), E (Ryder and Ardis, in press), H (Martin and Whiteman, in press) and I (Arthur and Taylor, in press) present results of ground-water flow simulations for parts of the gulf coast aquifer systems using a grid element spacing of 5 mi. Chapter F (Williamson, in press) presents results of ground-water

flow simulations for the entire gulf coast aquifer systems using grid element spacing of 10 mi. The focus of this report is on regression methodology whereas chapter F of Professional Paper 1416 focuses on the predevelopment (prior to ground-water withdrawal) ground-water flow system and changes due to withdrawal of ground water. Simulations described in chapter F employ hydraulic conductivity estimates from regression analyses described in this report.

DESCRIPTION OF STUDY AREA

The Gulf Coast Regional Aquifer-System Analysis study area is approximately 290,000 mi² and consists of part of the states of Arkansas, Florida, Illinois, Texas, Louisiana, Mississippi, Tennessee, Kentucky, Alabama, and Missouri, as well as part of the Gulf of Mexico (fig. 1). The Mississippi River provides the main drainage from the land area. Other important streams are the Rio Grande, Colorado, Arkansas, and Sabine Rivers.

Three aquifer systems have been identified in the study area (Grubb, 1984): The Mississippi embayment aquifer system; its lateral equivalent, the Texas coastal uplands aquifer system; and the coastal lowlands aquifer system (fig. 1). For purposes of this report all three aquifer systems are treated as a unit and are usually referred to as the gulf coast aquifer systems, or simply aquifer system. Comparison among the aquifer systems and detailed discussions of each aquifer system have been presented by Grubb (1987), Williamson and others (1990), Ackerman (1989), Arthur and Taylor (1990), Brahana and Mesko (1988), Martin and Whiteman (1989), and Ryder (1988). The remainder of this section and the Geologic setting section were taken from Williamson and others (1990) with only slight modification.

The land-surface altitude in the study area varies from sea level to more than 800 ft (fig. 2). The dominant feature of the topography is the flat, low-lying Mississippi Alluvial Plain (Fenneman, 1938). The Plain generally lies south and west of the Mississippi embayment structural trough (fig. 3). The topography of the Mississippi embayment is asymmetrical in that the valley lies to the west side of the embayment and the topographically higher hills are mostly to the east side. The Mississippi River, an important feature of the hydrologic system, generally traverses the east side of the valley. The general slope of the land surface is toward the Gulf of Mexico and is incised by large stream valleys that are generally perpendicular to the coastline.

Much of the study area is humid and mean annual precipitation ranges from 20 in. near Mexico to more than 60 in. along the gulf coast of Louisiana, Mississippi, and Alabama. The average mean annual precipitation over the area is 48 in.

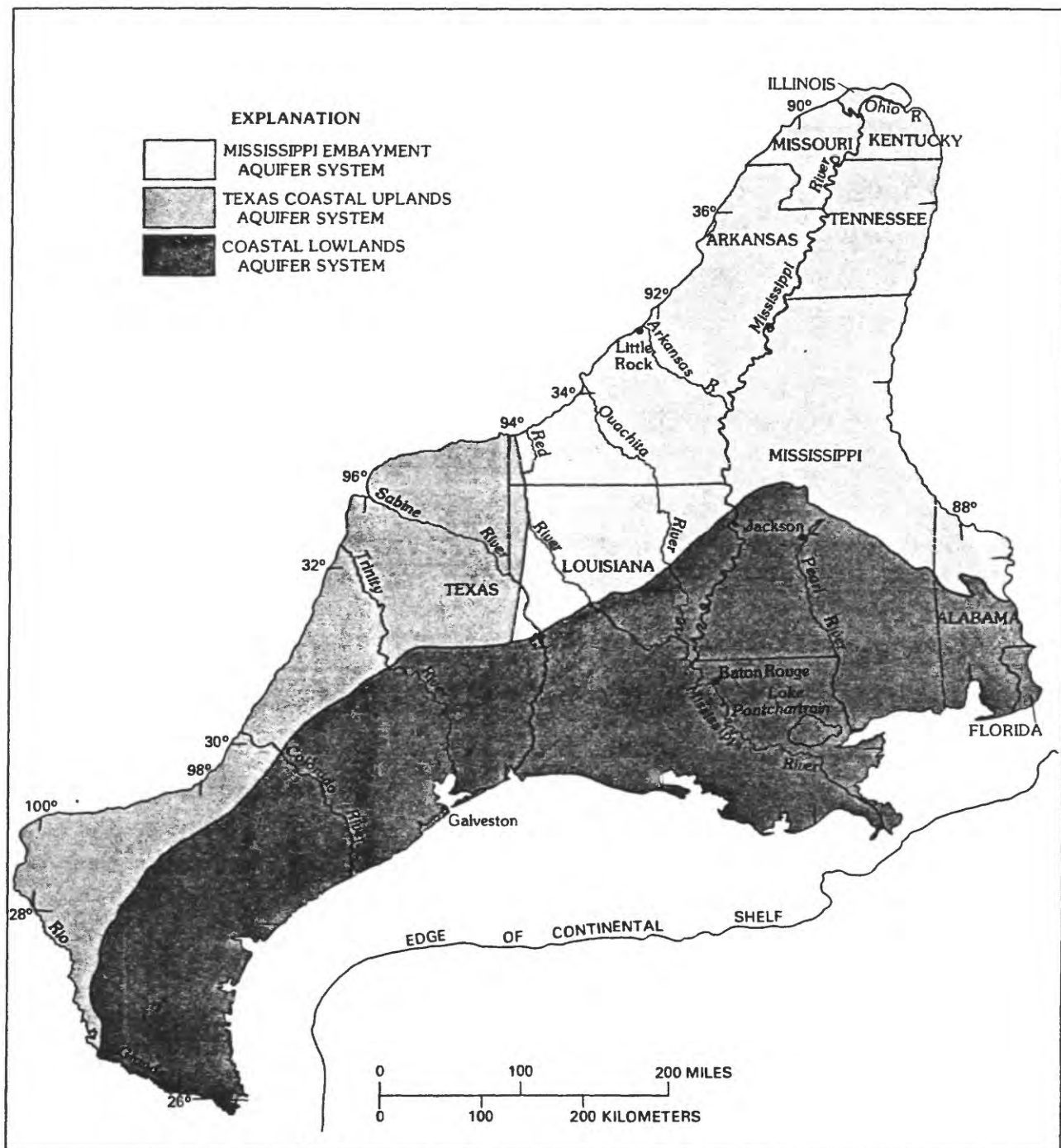
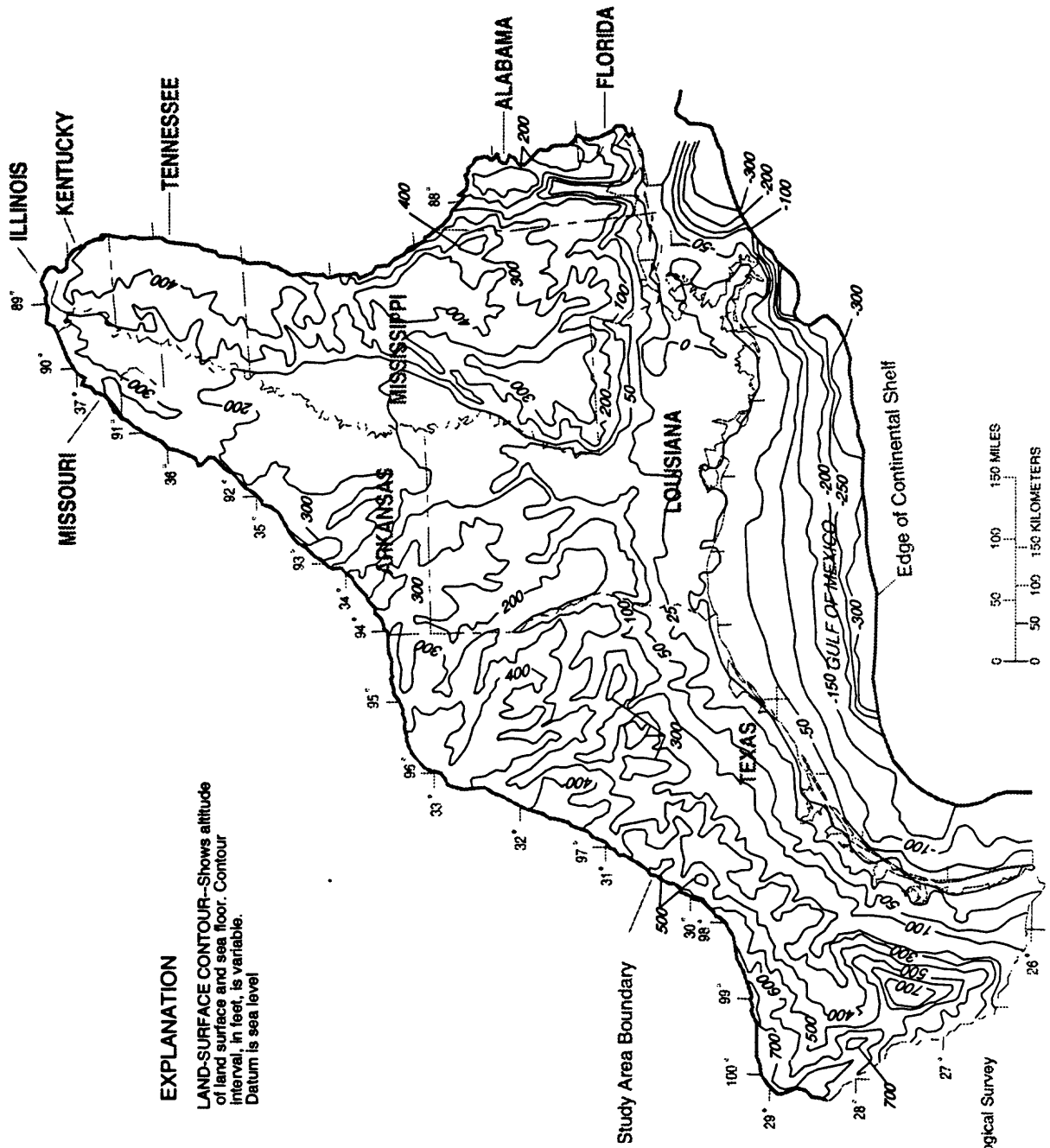


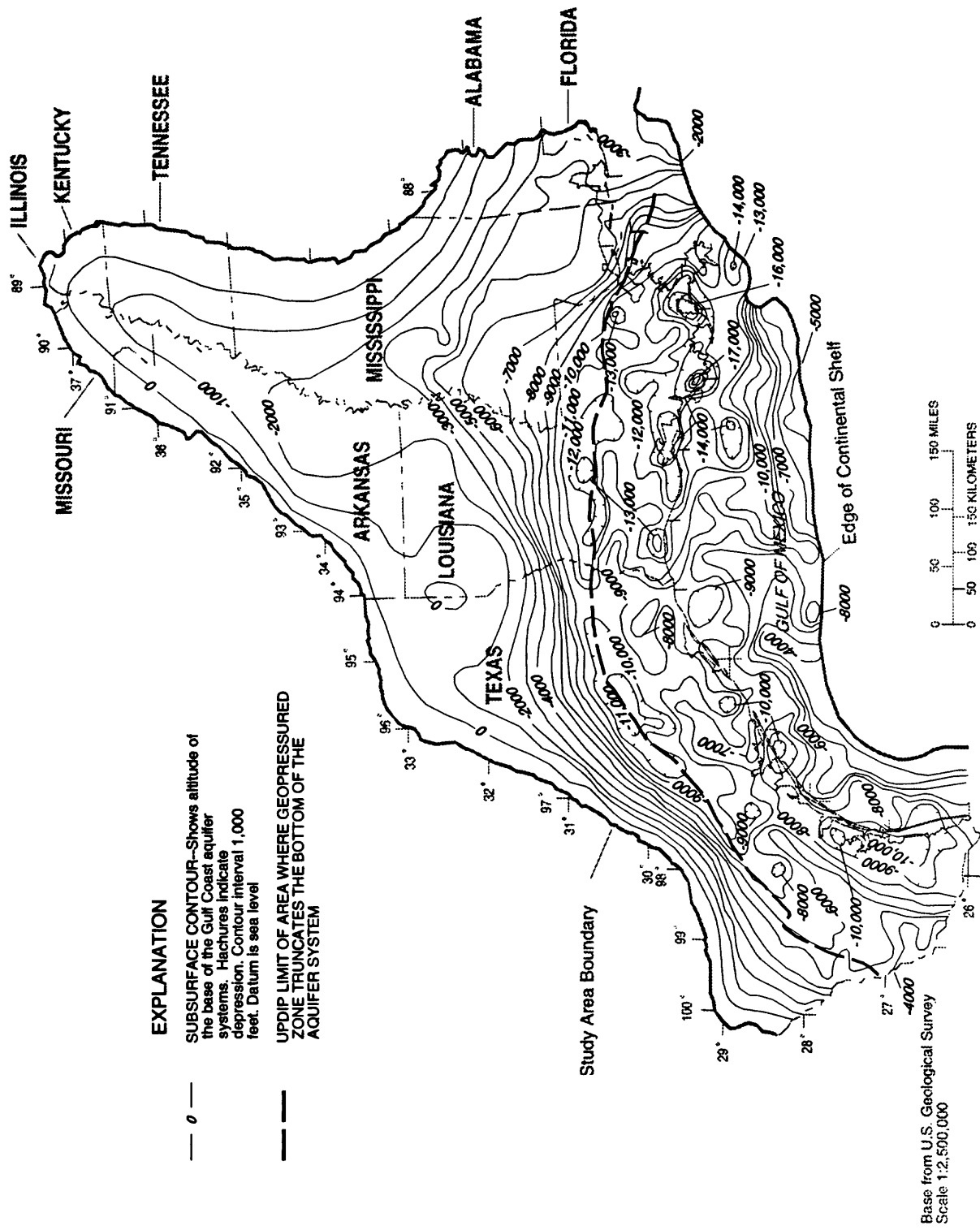
Figure 1.--Location of Gulf Coast Regional Aquifer-System Analysis study area and generalized outcrop of aquifer systems (from Hosman and Weiss, 1991).



EXPLANATION

---2X---
LAND-SURFACE CONTOUR—Shows altitude of land surface and sea floor. Contour interval, in feet, is variable. Datum is sea level

Figure 2. Generalized average land-surface altitude and bathymetry (from Williamson and others, 1990).

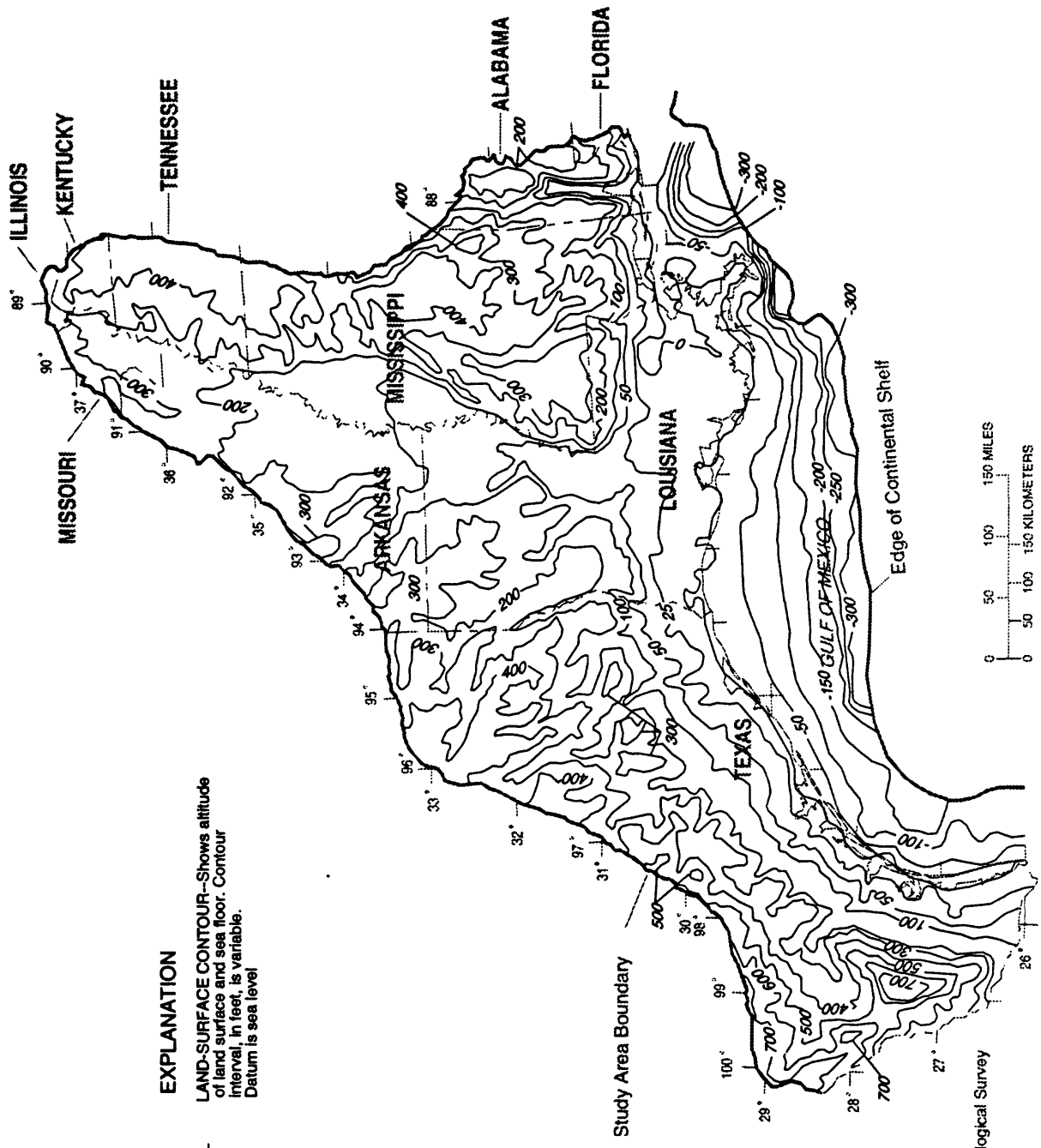


EXPLANATION

— 0 —
 SUBSURFACE CONTOUR—Shows altitude of the base of the Gulf Coast aquifer systems. Hatchures indicate depression. Contour interval 1,000 feet. Datum is sea level

 UPDIP LIMIT OF AREA WHERE GEOPRESSURED ZONE TRUNCATES THE BOTTOM OF THE AQUIFER SYSTEM

Figure 4. Altitude of the base of the aquifer systems and area of occurrence of geopressure. (From Williamson and others, 1990.)



EXPLANATION

--- 200' ---

LAND-SURFACE CONTOUR—Shows altitude of land surface and sea floor. Contour interval, in feet, is variable. Datum is sea level

Base from U.S. Geological Survey
Scale 1:2,500,000

Figure 2. Generalized average land-surface altitude and bathymetry (from Williamson and others, 1990).

In part of the study area, actual evapotranspiration is limited by the amount of rainfall, which is less than potential evapotranspiration. In south Texas, potential evapotranspiration exceeds rainfall most of the year, especially in the summer and fall; most of the rainfall returns to the atmosphere in a short time. In the eastern part of the area, rainfall substantially exceeds potential evapotranspiration, providing abundant surface-water runoff. The mean annual unit runoff varies from less than 1 in/yr in the southwestern part of the area to more than 20 in/yr in the northern and eastern parts and averages about 15 in/yr (Gebert and others, 1987).

Nearly 10 Ggal/d of ground water was pumped from the gulf coast aquifer systems in 1980 (Mesko and others, 1990). This amount corresponds to approximately 0.9 in/yr spread over the approximately 230,000 mi² land portion of the study area. Major areas of irrigation are the Mississippi Alluvial Plain, southwestern Louisiana, and south Texas. More than 60 percent of the municipal and industrial pumpage for public supply and industry is withdrawn from the coastal lowlands aquifer system (fig. 1).

Geologic Setting

The sediments of the gulf coast aquifer systems were deposited during Cenozoic time. Changes in sea level and accompanying transgressions and regressions of the sea caused cyclical sedimentation alternating from predominately continental to predominantly marine environments of deposition. Deposition occurred in fluvial, deltaic, or shallow-marine environments, and the interbedded sequences are composed of sand, silt, and clay, with some gravel, lignite, and limestone. Beds of sediment crop out at the surface in roughly parallel bands that are younger progressively gulfward in a typical offlap sequence. The shifting of facies, both laterally and vertically, resulted in a complex interbedding of sediment types. In general, the more clastic continental deposits have higher permeabilities characteristic of aquifers.

The Gulf Coast geosyncline and the Mississippi embayment, which are the major structural features of the study area (fig. 3), largely control the pattern and thickness of sedimentation (fig. 4). These structural features were present prior to Cenozoic deposition, and were accentuated as the basins subsided and accommodated the increased sediment buildup. Except where affected by local uplifts, the general pattern of sedimentation is one of increasing thickness in a gulfward, downdip direction. Uplift features that affected the deposition patterns are the Sabine uplift, San Marcos arch, Monroe uplift, Pascola arch, Jackson dome, LaSalle arch, and Wiggins uplift. Downwarp features associated with greater sediment buildup are the Desha basin, East Texas basin, Houston embayment, Rio Grande embayment, and Terrebonne embayment.

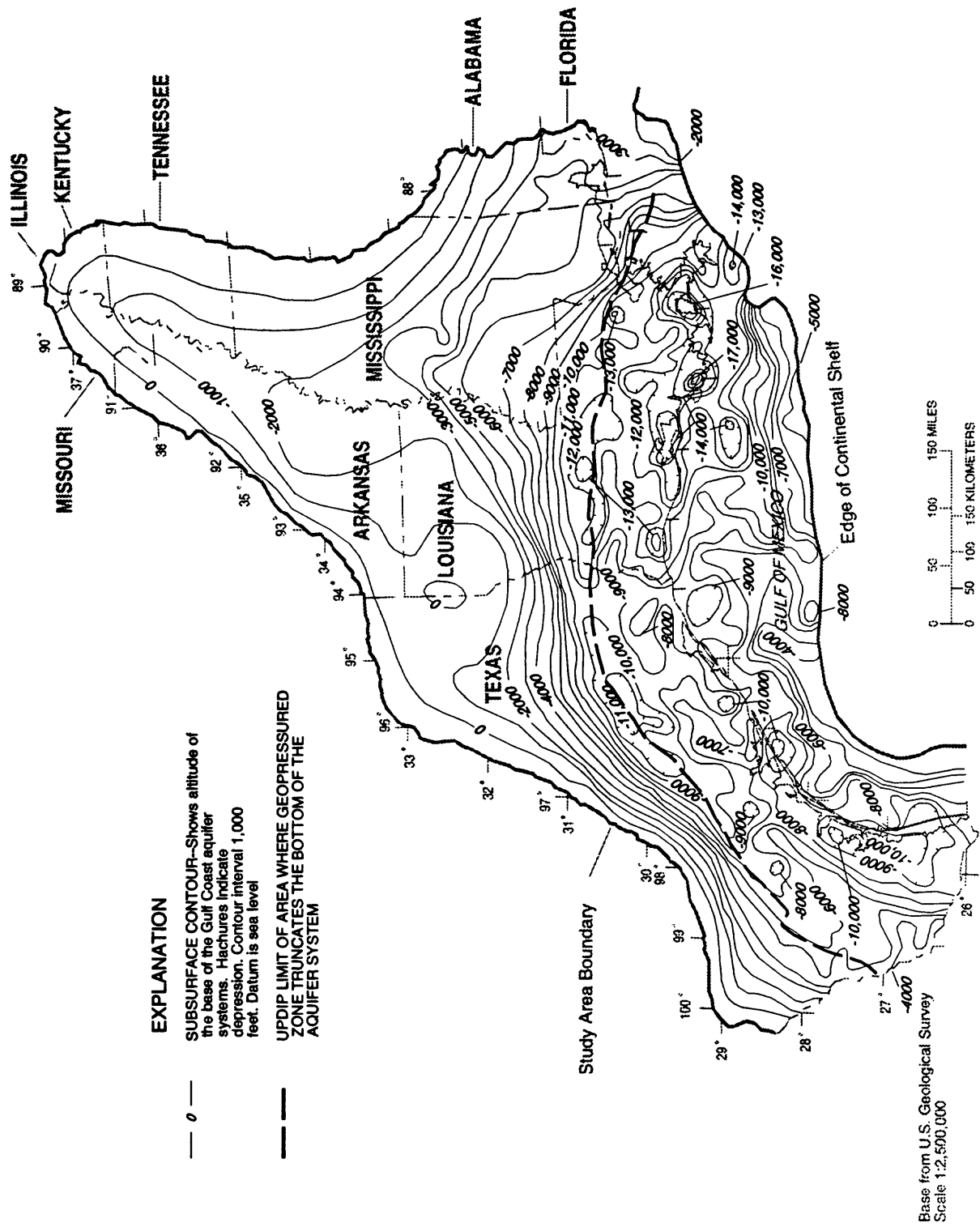


Figure 4. Altitude of the base of the aquifer systems and area of occurrence of geopressure. (From Williamson and others, 1990.)

Faults are common throughout the area, although their effect on regional ground-water movement is not known. In general, fault throws are not great enough to offset the full thickness of hydrologic units described in this report, although individual beds could be offset. Much of the faulting has led to zones of grabens and horsts. Particularly pronounced zones near the perimeter of the Mississippi embayment and the gulf coast geosyncline are the New Madrid fault zone, the Luling-Mexia-Talco fault zone, and the Pickens-Gilbertown fault zone (fig. 3). The Reelfoot rift zone is within the Mississippi embayment and may provide a pathway for upward discharge of ground-water from underlying Paleozoic rocks. Numerous growth faults, which occur contemporaneously with deposition, exist farther gulfward.

Geopressed zones (fig. 4) have fluid pressures significantly greater than normal hydrostatic pressure, and are enclosed by zones of very low permeability. The most probable cause for the development of these abnormally high fluid pressures is restriction of the escape of fluid during sediment compaction, causing pressure buildup and undercompaction of sediments (Fertl, 1976, p. 16).

Salt domes occur throughout the gulf coast aquifer systems, particularly in belts near and roughly parallel to the present-day coastline. The source of the salt domes is the deeply buried Louann Salt of Jurassic age, which has risen as diapirs that penetrate varying amounts of Cenozoic strata. The structural effects of the domes are relatively localized. However, the domes may have a significant effect on water quality due to dissolution of salt by ground water.

The gulf coast aquifer systems were subdivided into 15 hydrogeologic units that correspond to layers in a digital model used for simulation of regional ground-water flow. Five of these are considered to be confining units within which there is almost no horizontal flow. Weiss and Williamson (1985) describe the principles and methodology used for subdividing the aquifer systems into the 15 hydrogeologic units that is based on a combination of lithologic and hydraulic information. Hosman and Weiss (1991) provide a detailed description of the units of the Mississippi embayment and Texas coastal uplands aquifer systems. Weiss (1992) gives a detailed description of the units of the coastal lowlands aquifer system. Table 1, from Williamson and others (1990), gives the relationship and numbering convention for the 15 model layers used in this study to the geology and the previously mapped units in other reports in this series. The 15 model layers are numbered 2 through 11 for permeable layers or aquifers and 13 through 17 for confining units as shown in table 1. In this study, the model layers are referred to by number. The model construction described in the following section gives a detailed description of the geometry of the 15 model layers.

TABLE 1.—Relation of geologic units, previously defined geohydrologic units, and layers used in regional flow model (from Williamson and others, 1990, table 2)

[Note: correlations shown here are generalized. Exact relations vary widely from place to place.]

Mississippi embayment and Texas coastal uplands aquifer systems

Geologic Unit			Geohydrologic units defined by previous studies	Gulf Coast Regional Aquifer-System Analysis		
System	Series	Group		Model layer number	Geohydrologic units	
Quaternary	Pleistocene and Holocene		Mississippi River Valley alluvial aquifer (Boswell and others, 1968)	11	Mississippi River Valley alluvial aquifer *	
Tertiary	Eocene and Oligocene	Jackson and Vicksburg		15	Vicksburg-Jackson confining unit ^{1/}	
		Claiborne		Cockfield aquifer system (Payne, 1970)	6	Upper Claiborne aquifer
				Cockfield Formation (Hosman and others, 1968)		
				Cook Mountain Formation	14	Middle Claiborne confining unit
				Sparta hydraulic system (Payne, 1968)	5	Middle Claiborne aquifer
				Sparta Sand (Hosman and others, 1968)		
		Memphis aquifer (Hosman and others, 1968) (layers 4 and 5)				
		Cane River Formation	13	Lower Claiborne confining unit		
	Paleocene	Wilcox		Carrizo and Meridian Sand aquifer (Payne, 1975)	4	Lower Claiborne upper Wilcox aquifer
				Carrizo Sand and Meridian-upper Wilcox aquifer (Hosman and others, 1968)		
				Wilcox Group (Hosman and others, 1968)	3	Middle Wilcox aquifer
			Lower Wilcox aquifer (Hosman and others, 1968)	2	Lower Wilcox aquifer *	
Midway				12	Midway confining unit ^{1/}	

^{1/} The Midway confining unit was referred to as the coastal uplands confining unit and the Vicksburg-Jackson confining unit was referred to as the coastal lowlands confining unit by Grubb, (1984, p. 11).

* Not present in the Texas coastal uplands aquifer system.

TABLE 1.—Relation of geologic units, previously defined geohydrologic units, and layers used in regional flow model (from Williamson and others, 1990, table 2)—Continued

Coastal lowlands aquifer system

Geologic Unit			Geohydrologic units defined by previous studies	Gulf Coast Regional Aquifer-System Analysis	
System	Series	Group		Model layer number	Geohydrologic units
Quaternary	Pleistocene and Holocene		Upper Chicot aquifer (Jorgensen, 1975)	11	Permeable zone A (Holocene-upper Pleistocene deposits)
			Chicot aquifer (Meyer and Carr, 1979)	10	Permeable zone B (Lower Pleistocene-upper Pliocene deposits)
Tertiary	Pliocene		Evangeline aquifer (Whitfield, 1975) (Meyer & Carr, 1979)	9	Permeable zone C (Lower Pliocene-upper Miocene deposits)
			'2,000-foot' sand of the Baton Rouge area (Torak and Whiteman, 1982) Jasper aquifer (Whitfield, 1975)	17	Zone D confining unit
	8	Permeable zone D (Middle Miocene deposits)			
	16	Zone E confining unit			
	7	Permeable zone E (Lower Miocene-upper Oligocene deposits)			
	Eocene and Oligocene Jackson and Vicksburg			15	Vicksburg-Jackson confining unit ^{1/}

^{1/} The Midway confining unit was referred to as the coastal uplands confining unit and the Vicksburg-Jackson confining unit was referred to as the coastal lowlands confining unit by Grubb, (1984, p. 11).

Ground-Water Flow

The essential feature of the regional flow system is flow of ground water from upland recharge areas to discharge areas at lower altitudes on land or the sea floor. Differences from this simplified description are caused by the effect of a large volume of dense water that tends to flow beneath fresher water. Except for a small amount of water that may move upward from the geopressed zone into the aquifer system, little flow probably occurs through the aquifer system bottom. There is no lateral flow from beyond the landward boundary of the study area because the sediments that make up the aquifer systems pinch out. The potential for lateral flow exists along the Mexican border and along the north-south boundary of the study area in southern Alabama and western Florida. An arbitrary extension of the aquifer system thicknesses was made into Mexico because no data were available. The flows along the north-south boundary of the study area in southern Alabama and western Florida were ignored because of the minimal permeability of the sediments and the relatively short distance compared to the perimeter of the study area. Recharge from the uplands in south Texas may be limited by the availability of water, considering the fact that potential evapotranspiration exceeds precipitation at some locations. Flows are of course altered by pumping. The areal distribution of pumping from the 10 aquifers, model layers 2-11, for the year 1980 is shown in figure 5. The similarity between the water-table altitude and land-surface altitude is shown by comparing figure 6 with figure 2.

The presence of dense water in the system has a considerable effect upon ground-water flow. A large volume of water having a concentration of dissolved solids greater than seawater is contained within the aquifer systems (fig. 7). Sea water has a concentration of dissolved solids of about 35,000 mg/L and a density of 1.025 gm/cm³. The estimated depth to water with a concentration of dissolved solids the same as seawater is shown in figure 7. Estimates of dissolved-solids concentrations in ground water were made for about 18,000 sand beds in the study area (Weiss, 1987). About 66 percent of the beds have water with a dissolved-solids concentration greater than 10,000 mg/L (fig. 8). Although not a precise measure of the quantity of water dense enough to effect ground-water flow, the above indicate that much of the volume of water in the gulf coast aquifer systems has a density substantially greater than 1.0 gm/cm³.

Data Available for Hydraulic Head and Hydraulic Conductivity

More than 600,000 individual measurements of hydraulic head were available. When considered as observations of hydraulic head in a particular well at a particular instant in time, these hydraulic-head measurements are, in general, accurate; except for those cases where errors in recording were made, they usually have less than 0.5 ft of error. For each well, the hydraulic-head measurements were averaged over 2-year intervals to give a representative value of hydraulic head for the well for

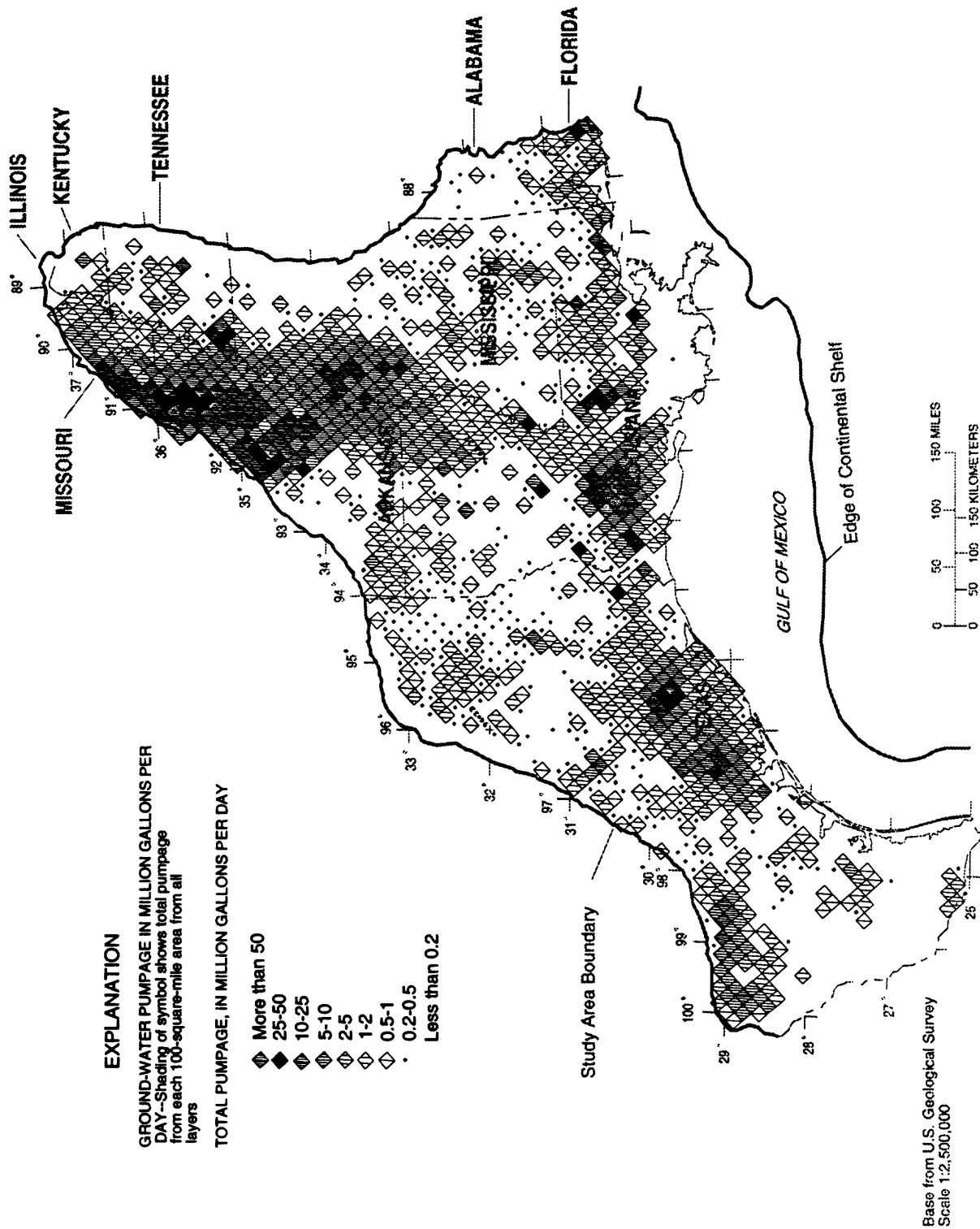


Figure 5. Ground-water pumpage from the gulf coast aquifer systems, 1980. (Modified from Williamson and others, 1990.)



Figure 6. Water-table altitude on shore and equivalent freshwater head at the sea floor offshore. (Modified from Williamson and others, 1990.)

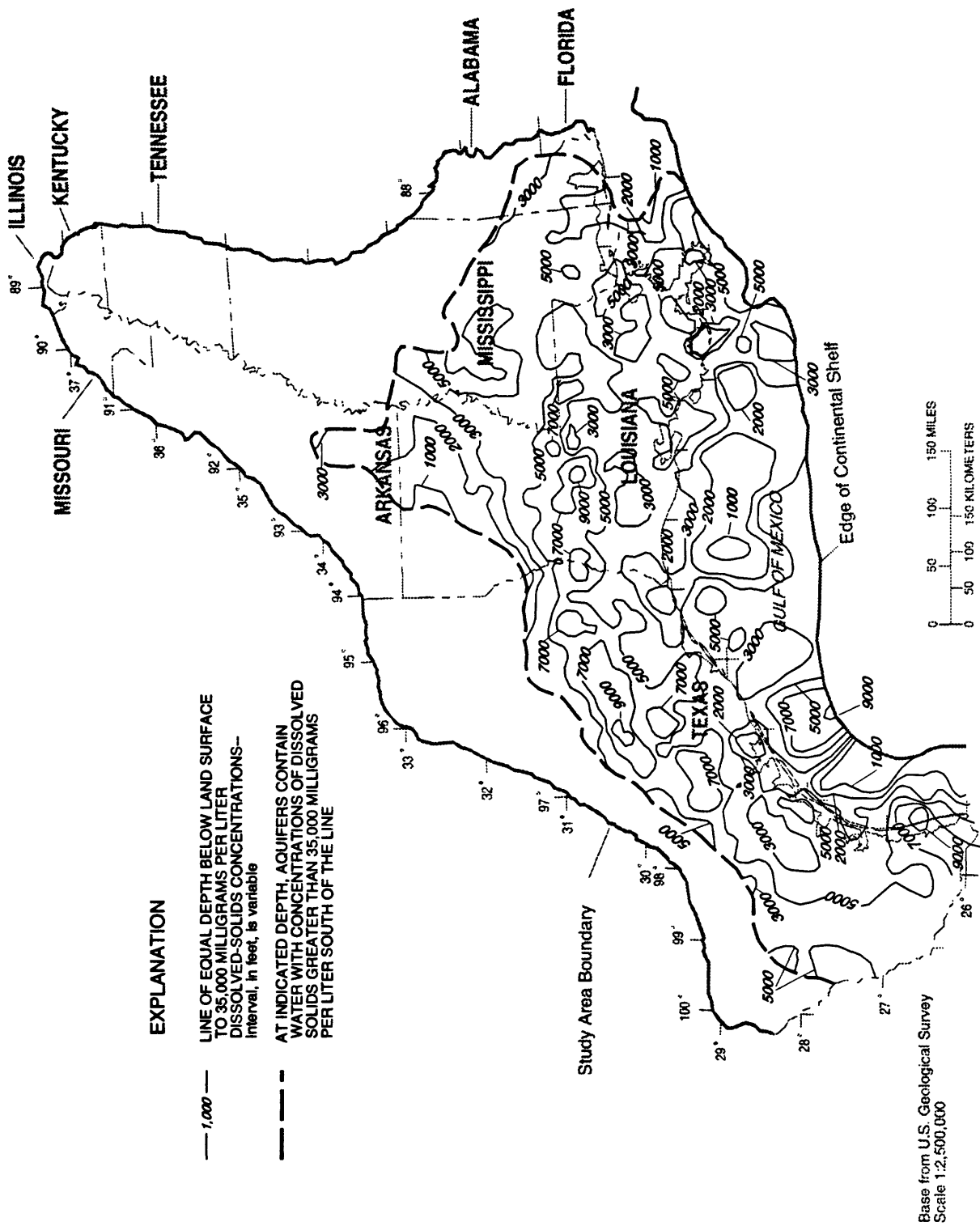


Figure 7. Estimate of depth to water containing 35,000 mg/L dissolved solids.

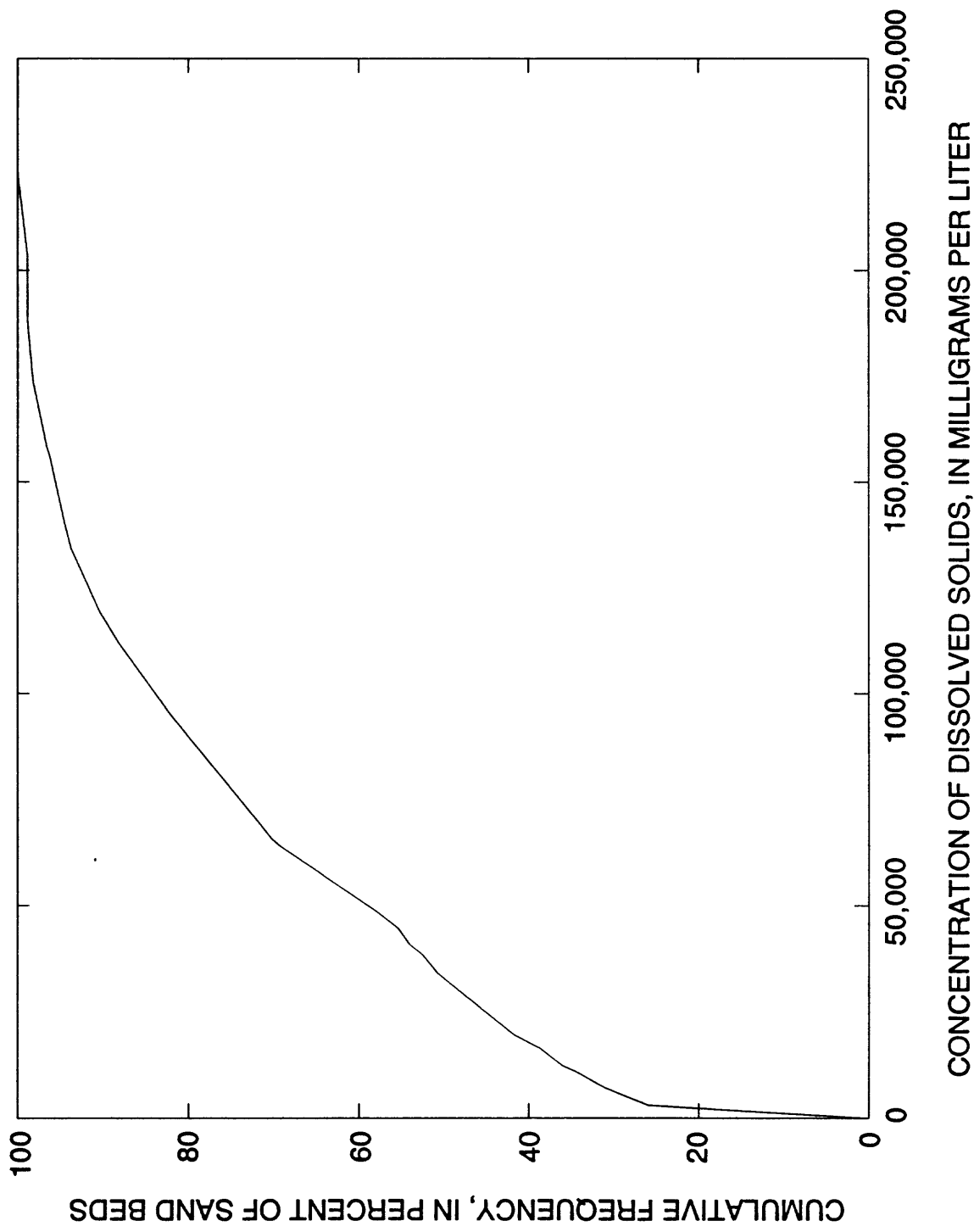


Figure 8. Cumulative frequency distribution of concentration of dissolved solids in 18,000 sand beds in the gulf coast aquifer systems

a given year centered within the 2-year interval. In this manner, the more than 600,000 measurements were reduced to approximately 50,000 time-averaged observations of hydraulic head at individual wells. In addition, there were approximately 15,000 measurements of formation pressure from drill-stem tests. These measurements were used to approximate point-pressure head values. Because of the indirect procedure used, these point pressure head values from drill-stem test can have errors much larger than 0.5 ft. As is generally the case, the numerical-flow model used in this study produces an approximation to grid-element volume-averaged head values that are not equal to values for head at a single point in the aquifer system.

More than 6,700 determinations of hydraulic conductivity were available (Prudic, 1991) from both specific capacity and pumping tests. As with the observations of hydraulic head, most of these determinations of hydraulic conductivity were made using water wells less than 1,000 ft deep.

Because the water-well based data on hydraulic head and hydraulic conductivity were from relatively shallow depths, (and the point pressure-head values from the drill-stem test were quite inaccurate, even though in some cases occurring at considerable depth) the aquifer systems may be characterized as having a paucity of data for all but relatively shallow depths.

NONLINEAR-REGRESSION FLOW MODEL

Ground-water flow in the aquifer systems is assumed to be governed by the general equations for variable-density flow (De Weist, 1969).

The domain of solution of the aquifer systems has as its top that surface consisting of either the water table or land surface or sea bottom, whichever is lowest. This surface is relatively static and is taken as a fixed head surface of the domain of solution. The movement of water outside the domain of solution, such as the flow of water moving downward to the water table, is not simulated. The bottom of the domain of solution is a no-flow boundary when above a geologic unit which is assumed to have no flow. When above the geopressured zone, flow may come from the geopressured zone which is given a specific head.

Along the perimeter, the aquifer system domain of solution thins out and has zero thickness at most locations, except along certain parts of the perimeter offshore in the Gulf of Mexico. Here, nonzero thicknesses are present below the sea floor, but are assumed to allow no flow due to the presence of extremely low permeability clacareous clays.

Specific storage is taken to be constant throughout the entire aquifer system domain of solution. Water density is assumed to be nearly constant in time but to vary with location in the domain of solution.

Hydraulic conductivity varies within the domain of solution. Effective hydraulic conductivity at any location is determined (Desbarats, 1982) from the hydraulic conductivities of the clay and sand at that location and the relative amounts of each of these components as determined from data. The hydraulic conductivities of the clay and sand components are allowed to vary, but use is made of existing data for these conductivities and the manner in which they decrease with depth.

Although the top of the domain of solution has a fixed head, a maximum allowable recharge from that surface is imposed. This maximum value ranges from 2 in/yr to 12 in/yr, decreasing towards the south.

Modeling Methodology and Construction

Ground-water flow in the aquifer systems is assumed to be governed by the following three-dimensional variable-density time-dependent flow equations (Kuiper, 1983). The general vector form of Darcy's equation (De Wiest, 1969; Bear, 1979; Kuiper, 1983), is

$$\bar{q} = -K[\nabla h + (\rho/\rho_0)\nabla z] \quad (L/T), \quad (1)$$

Here, \bar{q} is the specific discharge of the fluid, and h is pressure head equal to P/ρ_0g , where $\rho_0 = 1 \text{ gm/cm}^3$, g is the acceleration of gravity, and P is pressure. Equivalent freshwater head, equal to $(h+z)$, will be referred to simply as head in the following text. The quantity z is vertical distance measured upward above a datum, $\rho = \rho(x,y,z)$ is the density of the fluid and is assumed to vary with time so slowly that its time dependence is ignored (Kuiper, 1983). Equivalent freshwater head is approximately equal to hydraulic head $(P/\rho g + z)$ when fluid density is approximately equal to ρ_0 . The hydraulic conductivity tensor $K = K(x,y,z)$ is given by

$$K = k\rho_0g/\mu, \quad (2)$$

where k is the intrinsic permeability tensor of the porous medium, and μ is the dynamic viscosity of the fluid. The mass balance equation (De Wiest, 1969) is

$$\nabla \cdot (\rho \bar{q}) = -\rho S_s \partial h / \partial t - Q \quad (M/L^3 T), \quad (3)$$

where $S_s(x,y,z)$ is specific storage, t is time, and $Q(x,y,z,t)$ is the rate of discharge of fluid per unit volume due to pumping. When equation (1) is substituted for \bar{q} of equation (3), the governing flow equation for $h(x,y,z,t)$ is obtained.

Equation (3), when discretized, forms a matrix equation to be solved for the grid-element volume-averaged heads corresponding to each of the grid elements in the domain of solution. This matrix equation is used to formulate the regression equation for the regression technique (Cooley, 1982). The hydraulic parameters of the aquifer systems, such as specific storage and hydraulic conductivity, and also other unknowns such as specified head or flow on the domain of solution boundary, are specified in some chosen manner by the regression parameters of the regression technique.

The discretization of the domain of solution is defined vertically by the 15 model layers. Grid elements with a constant 10-mi spacing define horizontal discretization. The spacing is constant because of the use of finite-differences which require that grid element rows and columns follow straight lines, and because the regions of the aquifer system that would benefit from small grid element size are numerous and are spread over the aquifer system in an irregular manner. The 10-mi spacing is the smallest allowable, given computer-time constraints.

The total number of grid elements in the domain of solution of the aquifer system is $N = 29,345$. The grid elements are divided into 10 model layers mentioned earlier and numbered 2 through 11 from bottom to top. Layer 1 is for the geopressured zone. A very thin layer, model layer 12, is located on the top of all of the other layers. This 12th model layer represents the top several feet of the aquifer system. Maximum areal extent and outcrop areas of the hydrogeologic units represented by the model layers are shown in figure 9. The grid element row and column numbers are also shown. Five layers representing confining units mentioned previously and numbered 13 through 17 are interbedded between model layers 4 through 9. The layers representing confining units provide resistance to vertical flow between the adjacent aquifers above and below but do not have any horizontal flow themselves, nor do they store water. The layers that represent confining units do not have grid elements (Kuiper, 1985) and the associated approximating equations do not directly involve head in the confining units. The areal extent of model layers 2 through 11 are shown in figures 10 through 19, and the areal extent of model layers 13 through 17 which represent confining units are shown in figures 20 through 24. The vertical relation of aquifers and confining units across the central part of the study area is shown in figure 25.

Boundary conditions are either specified-flow or specified-head. Specified-flow boundaries are always no-flow boundaries. There are two separate specified-head boundaries, the top of the domain of solution and the geopressured zone part of the bottom of the domain of solution. Each of these two surfaces has two regression parameters associated with it. The specified-boundary head on such a surface is equal to the sum of the product of an initial head distribution, to be described later, with a regression parameter associated with the surface, and an additional second parameter for the surface.

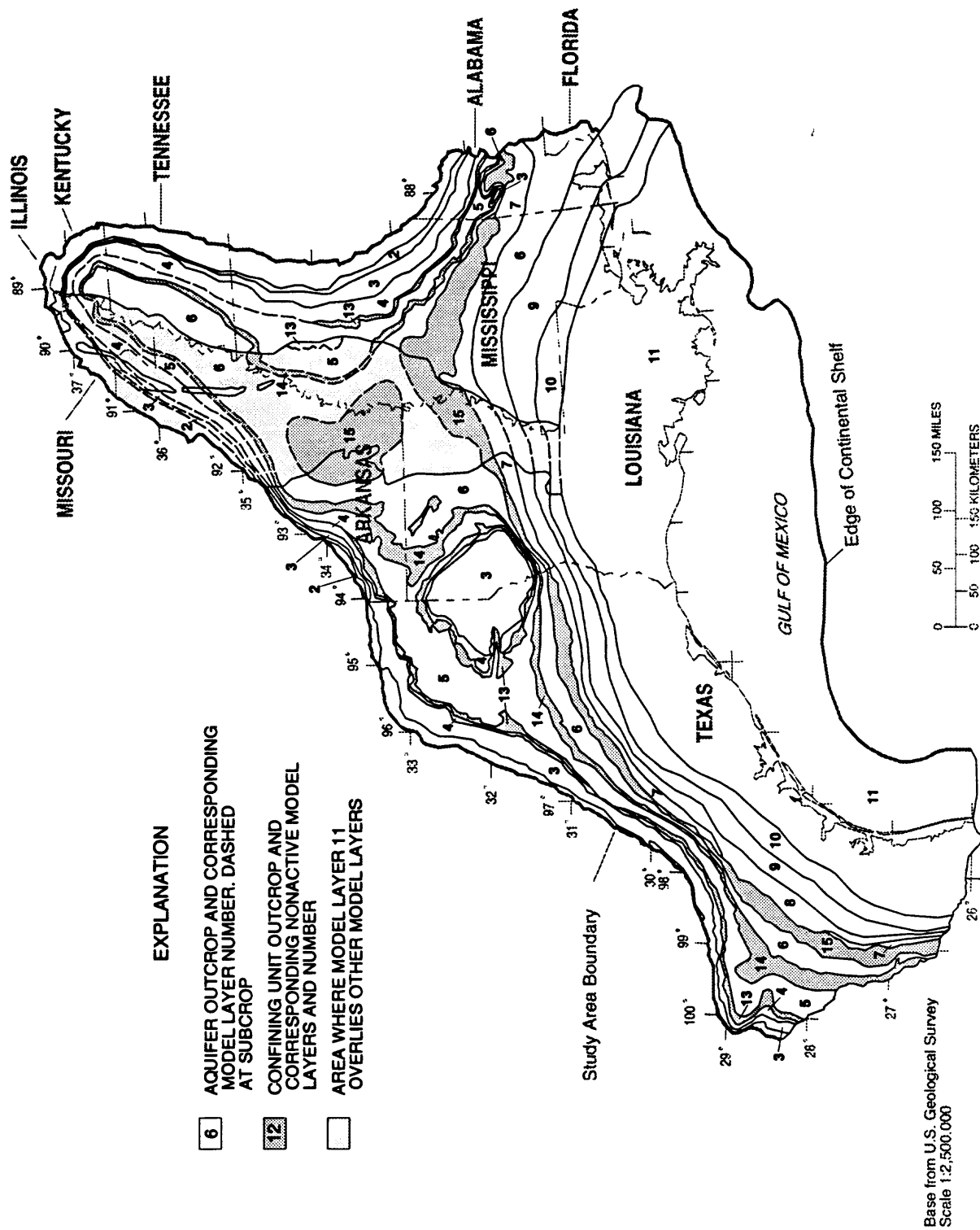


Figure 9. Maximum areal extent of modeled area and outcrop areas of hydrogeologic units represented by model layers (modified from Williamson and others, 1990).

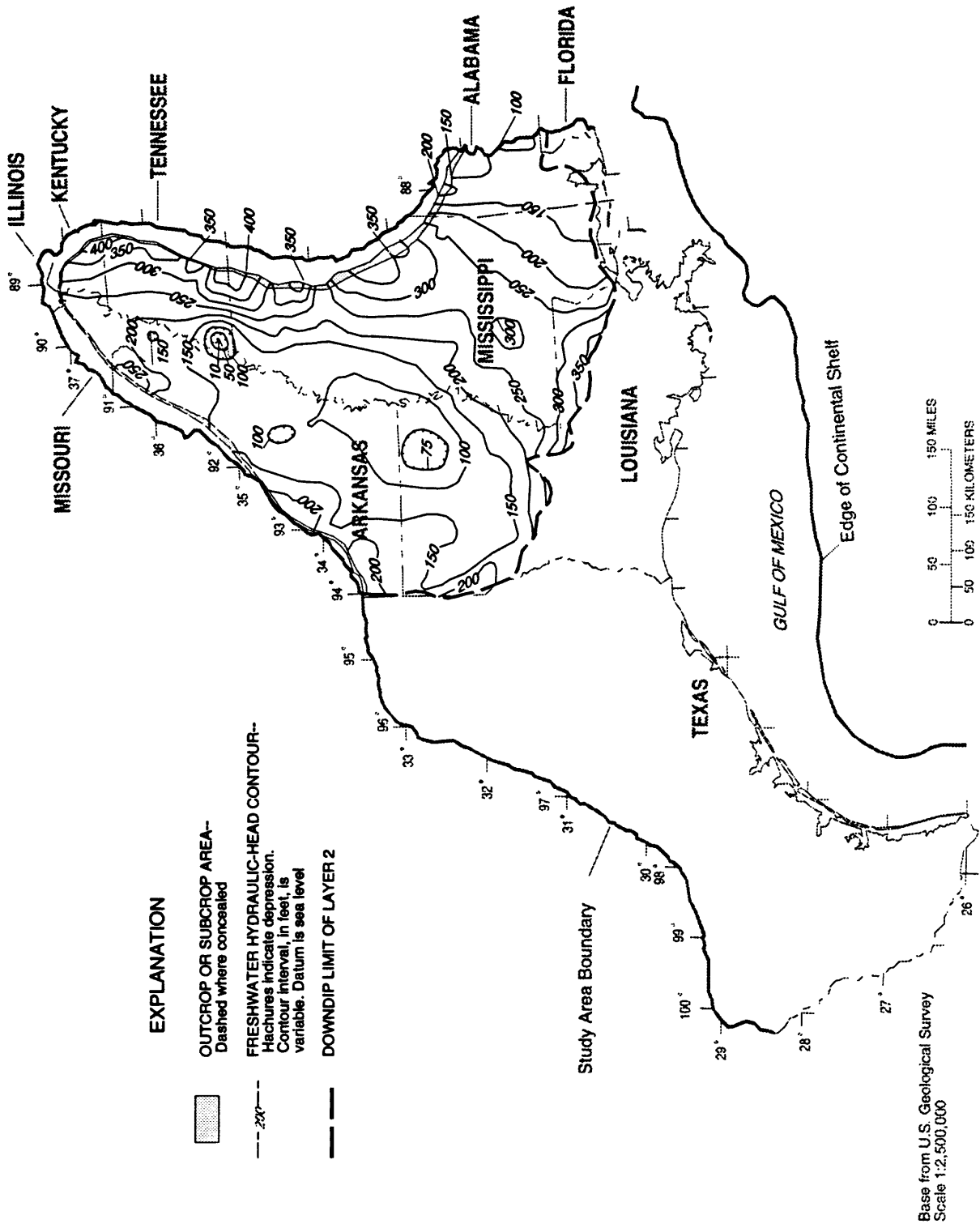


Figure 10. Areal extent of model layer 2 and simulated 1982 equivalent freshwater head from model 4.

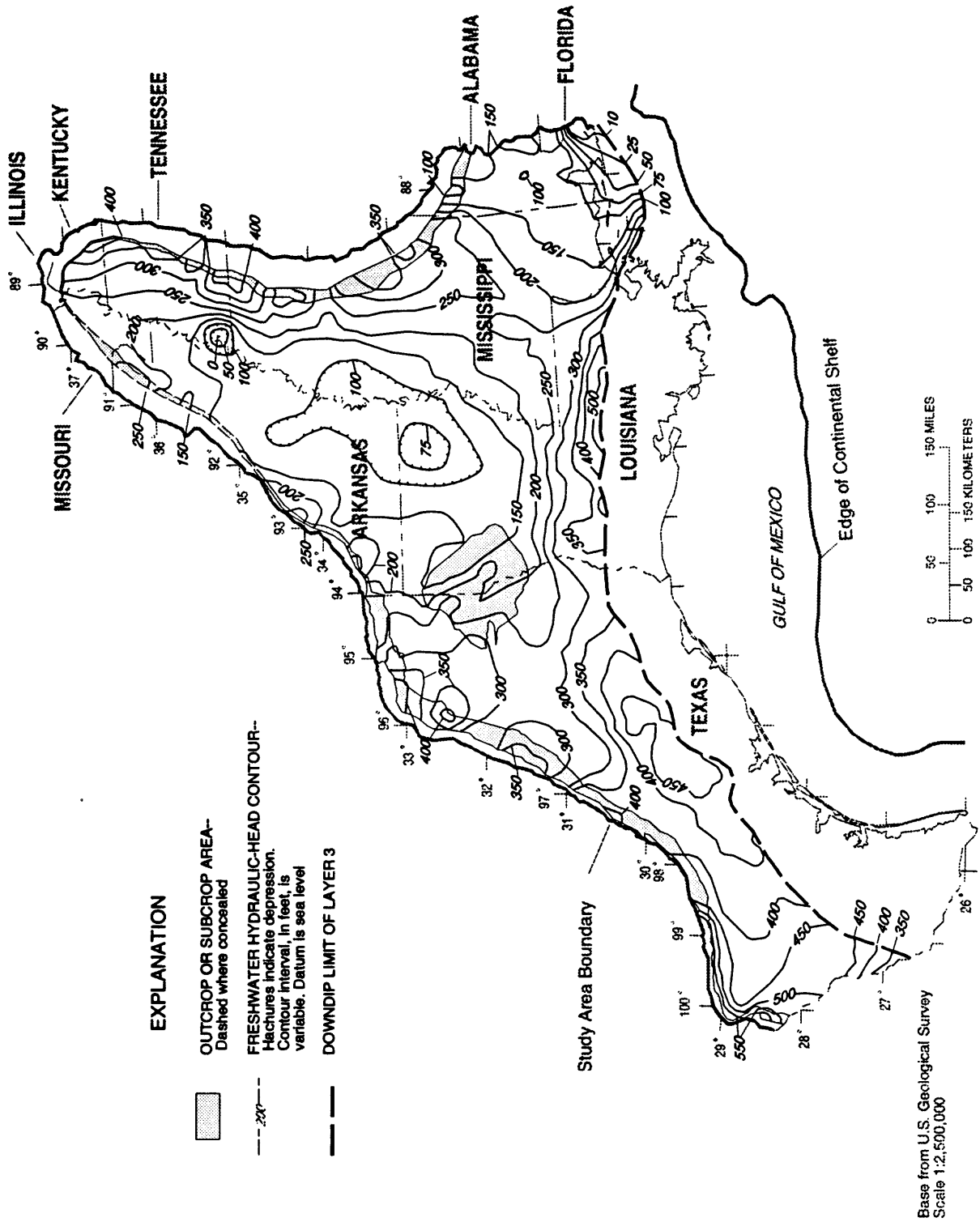


Figure 11. Areal extent of model layer 3 and simulated 1982 equivalent freshwater head from model 4.

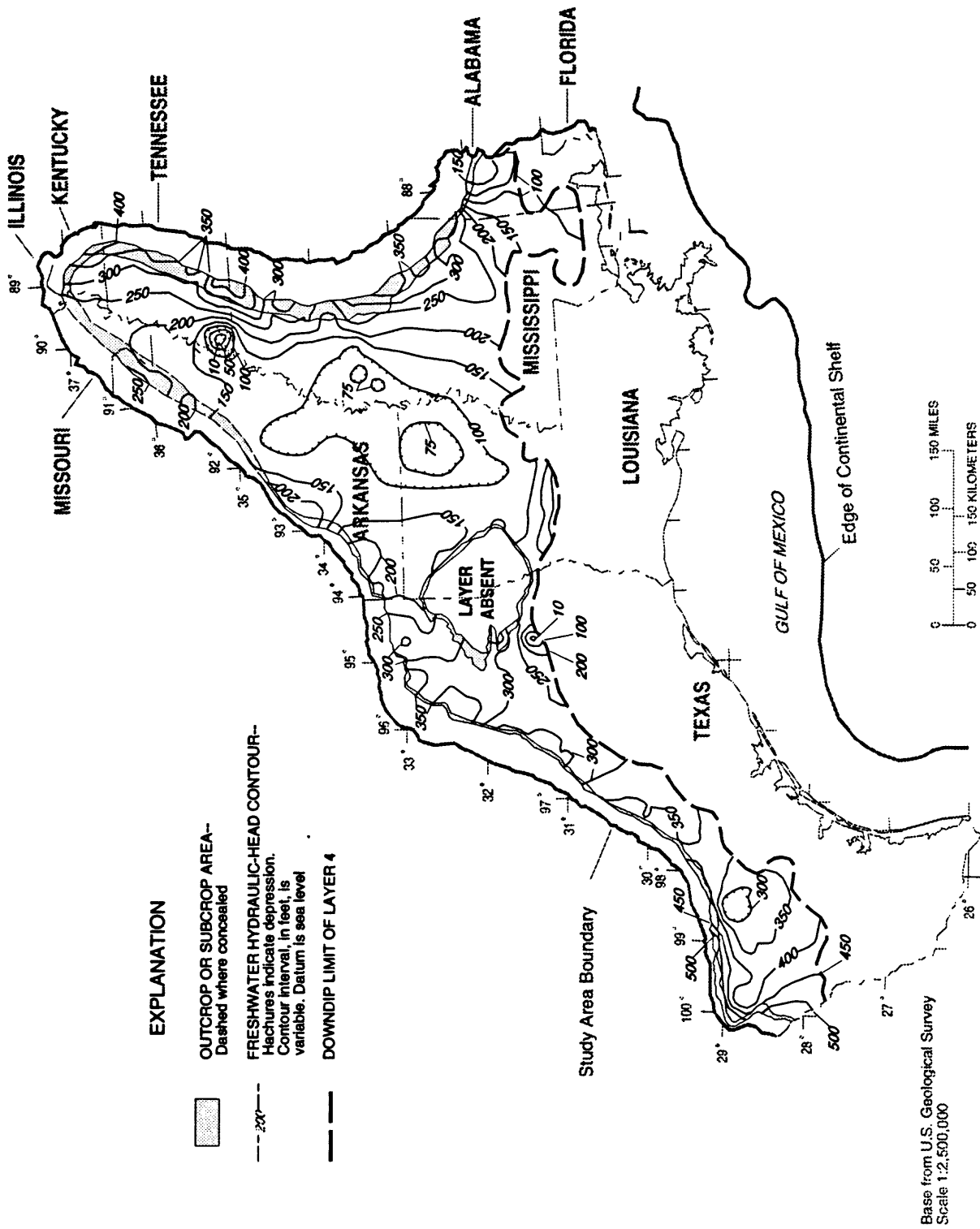


Figure 12. Areal extent of model layer 4 and simulated 1982 equivalent freshwater head from model 4.

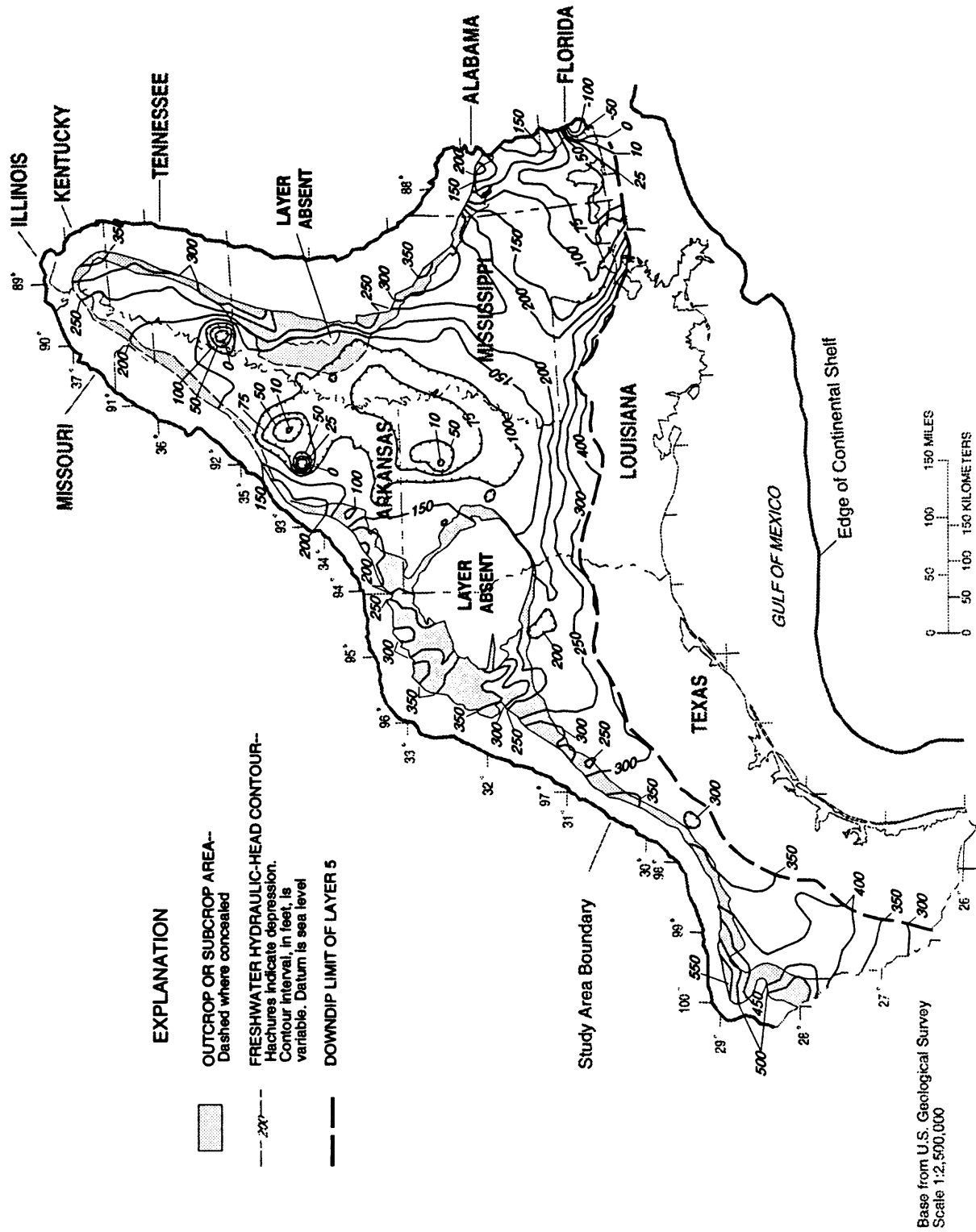


Figure 13. Areal extent of model layer 5 and simulated 1982 equivalent freshwater head from model 4.

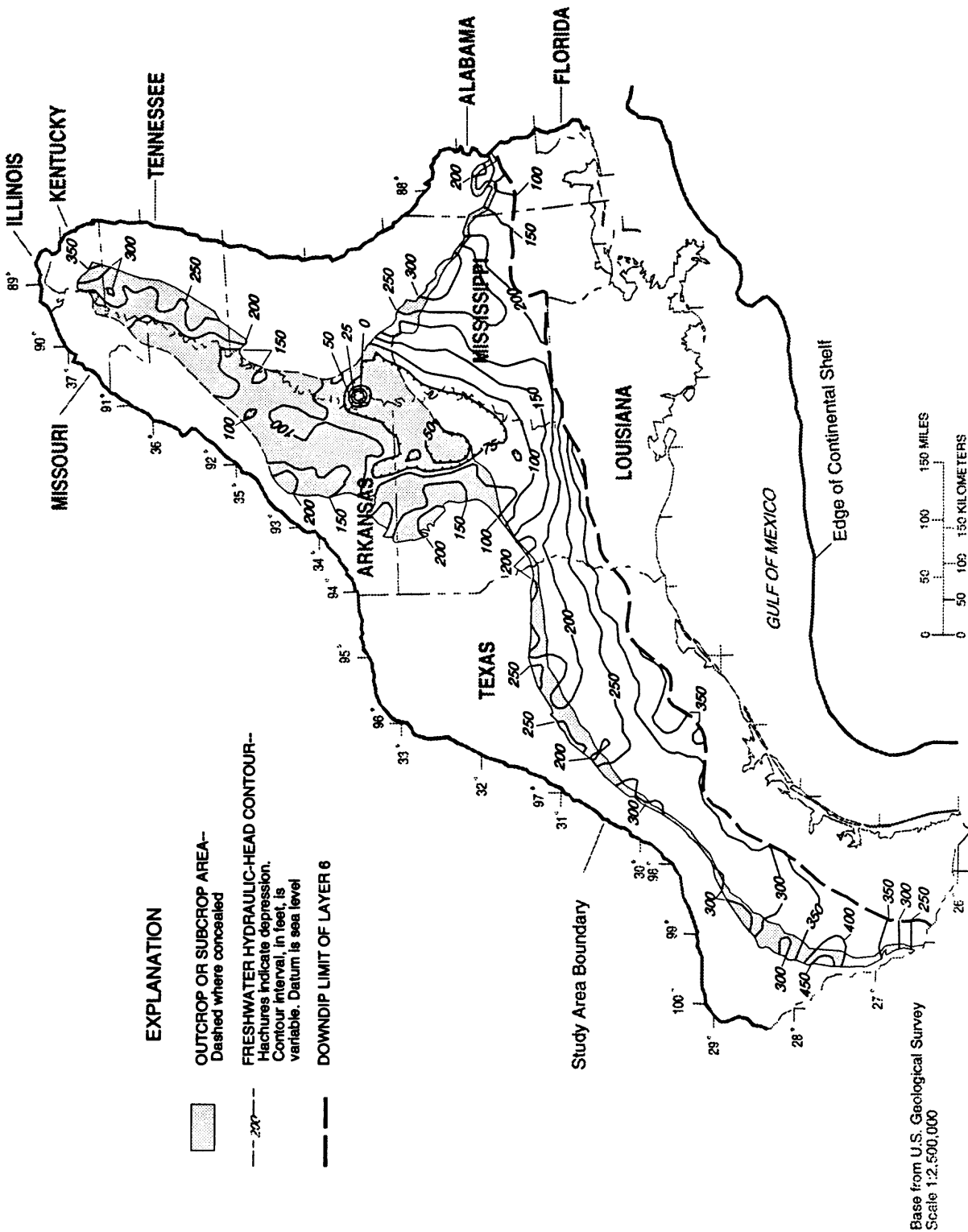


Figure 14. Areal extent of model layer 6 and simulated 1982 equivalent freshwater head from model 4.

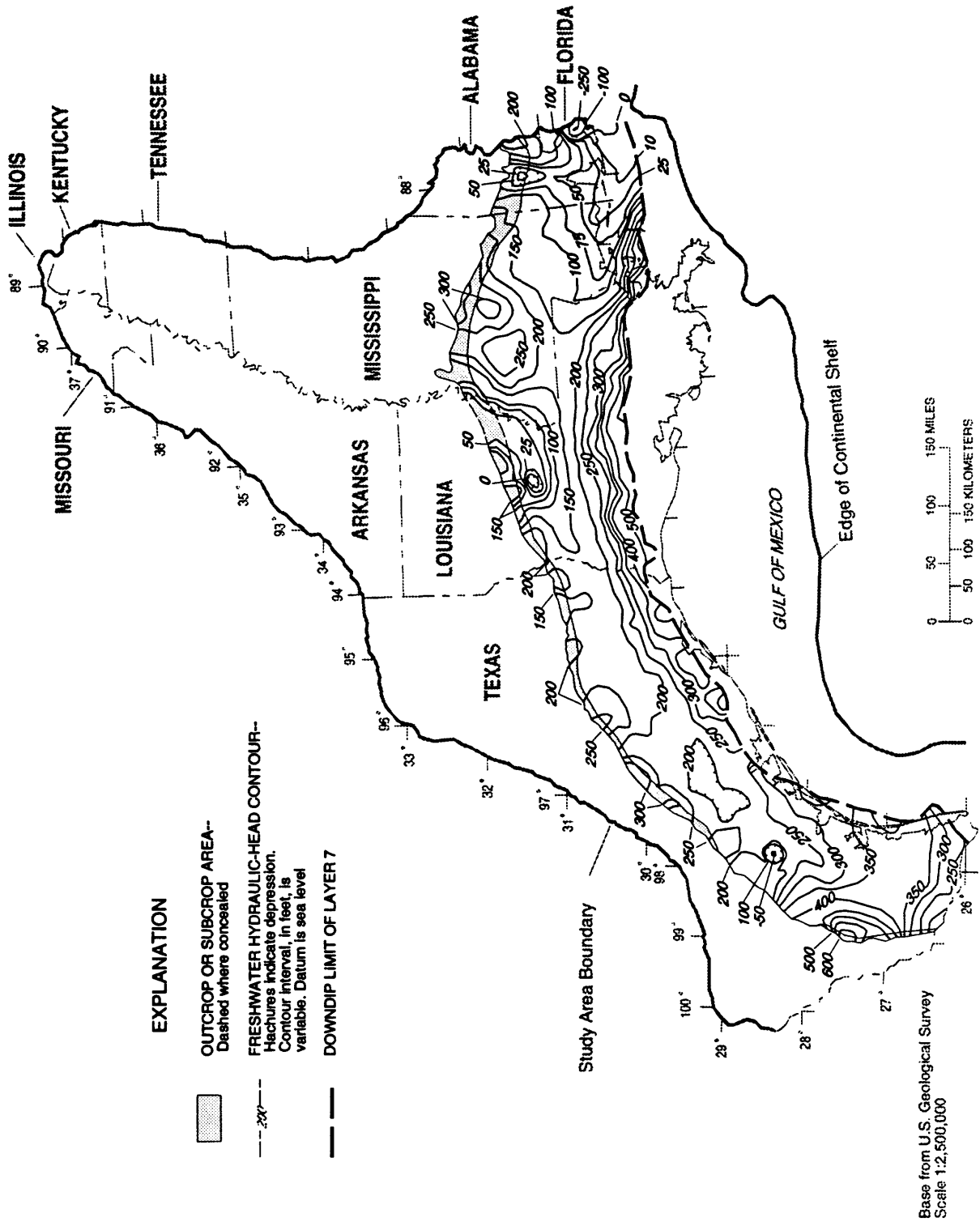


Figure 15. Areal extent of model layer 7 and simulated 1982 equivalent freshwater head from model 4.

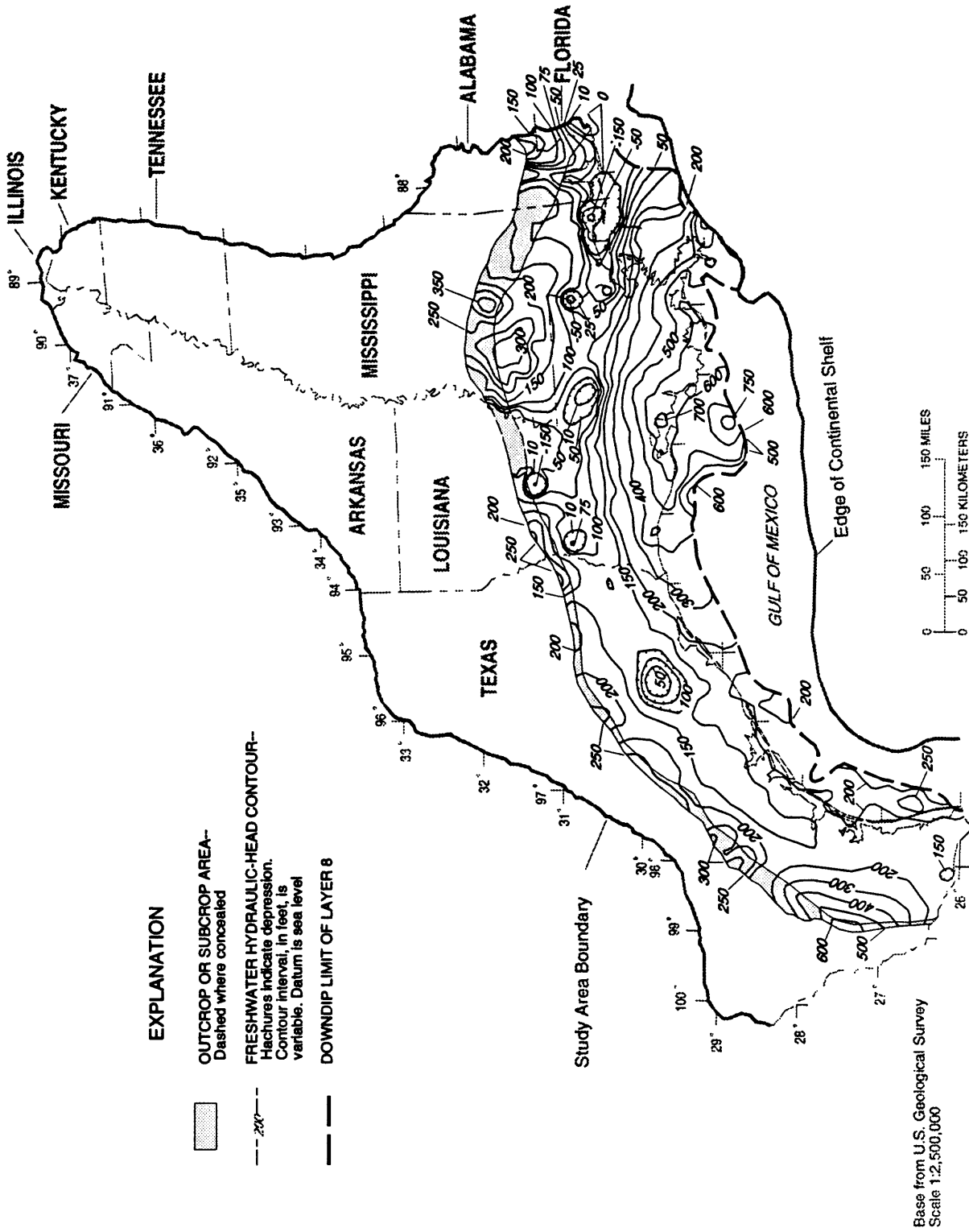


Figure 16. Areal extent of model layer 8 and simulated 1982 equivalent freshwater head from model 4.

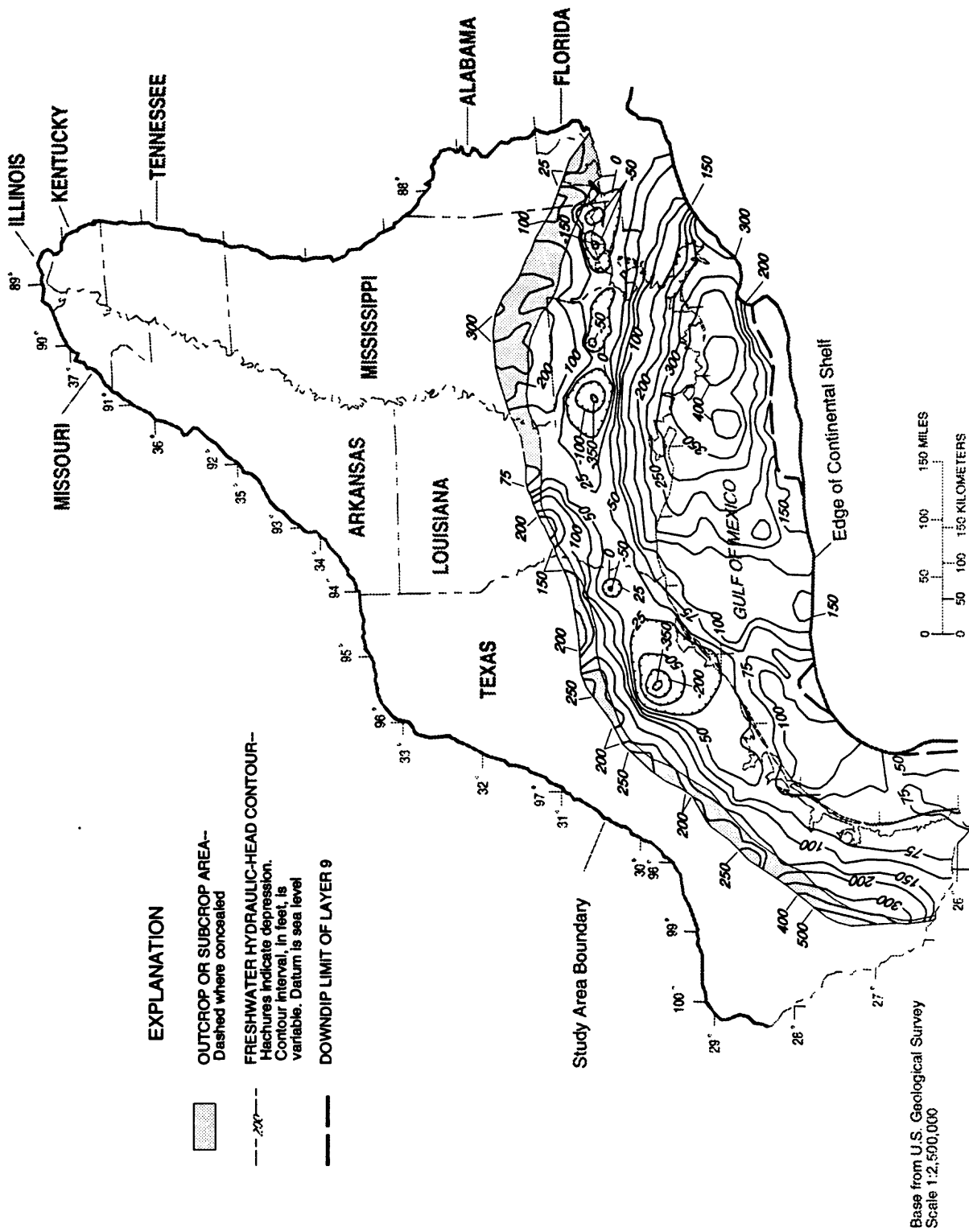


Figure 17. Areal extent of model layer 9 and simulated 1982 equivalent freshwater head from model 4.

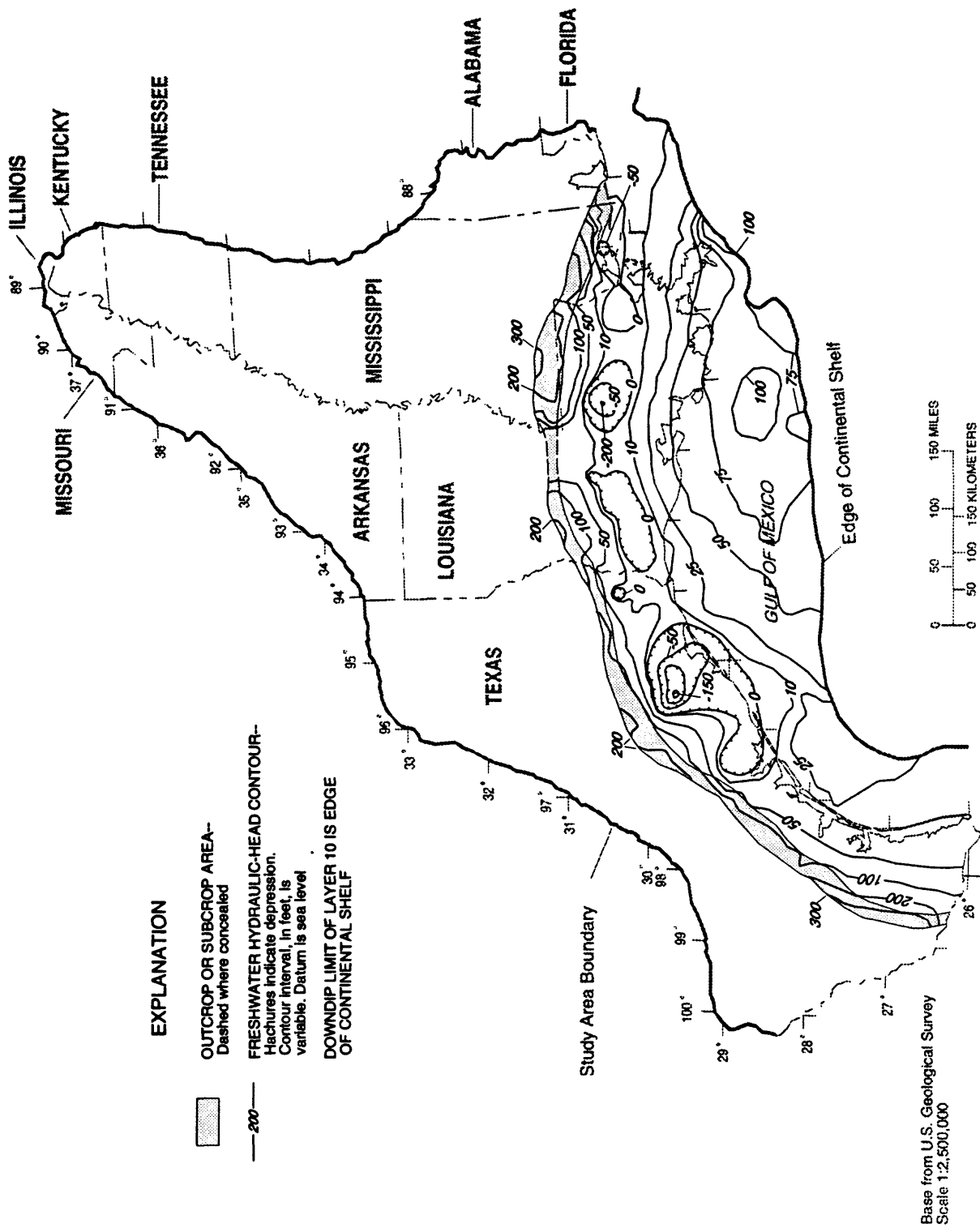


Figure 18. Areal extent of model layer 10 and simulated 1982 equivalent freshwater head from model 4.

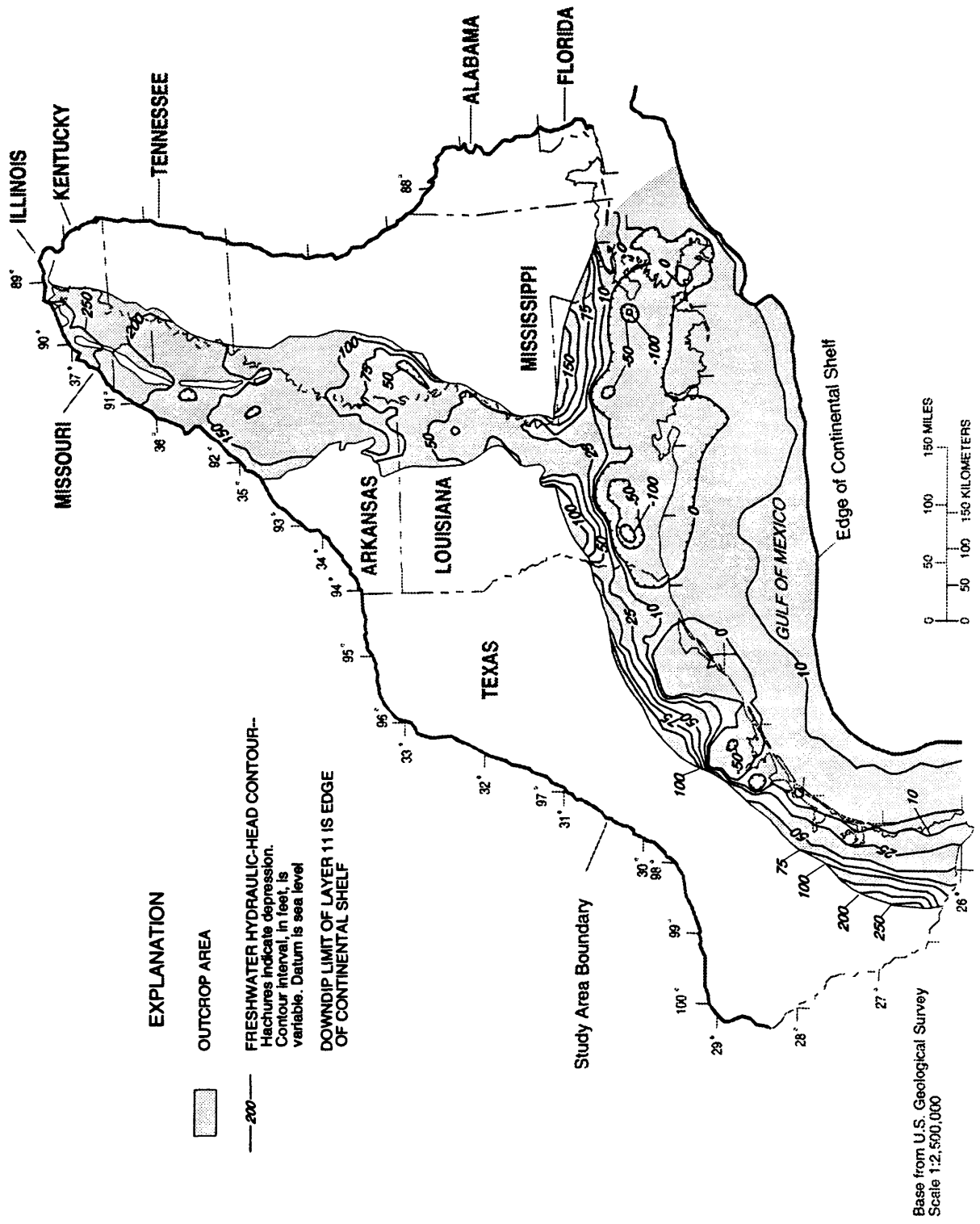


Figure 19. Areal extent of model layer 11 and simulated 1982 equivalent freshwater head from model 4.

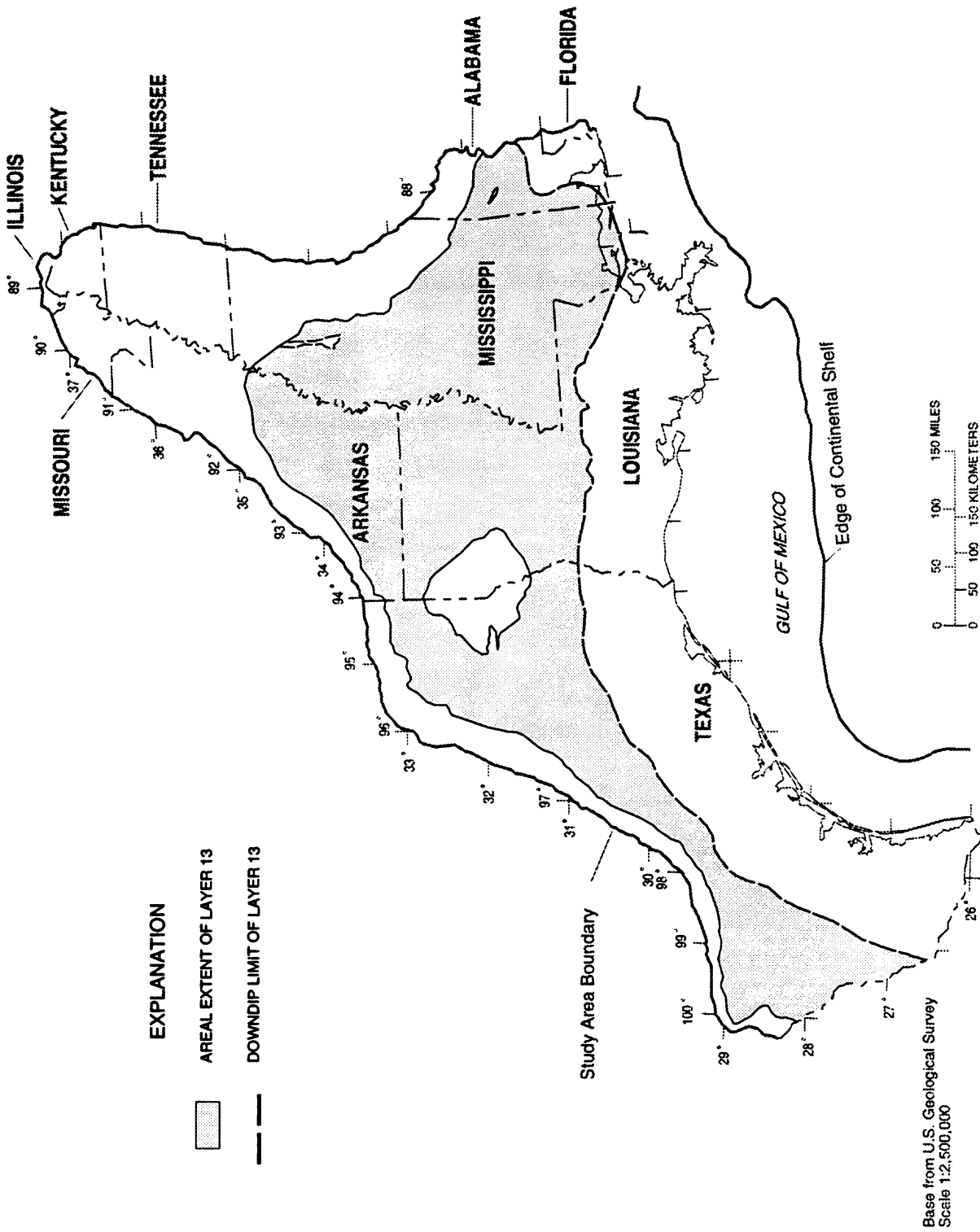


Figure 20. Areal extent of model layer 13. Represents confining unit between model layers 4 and 5.

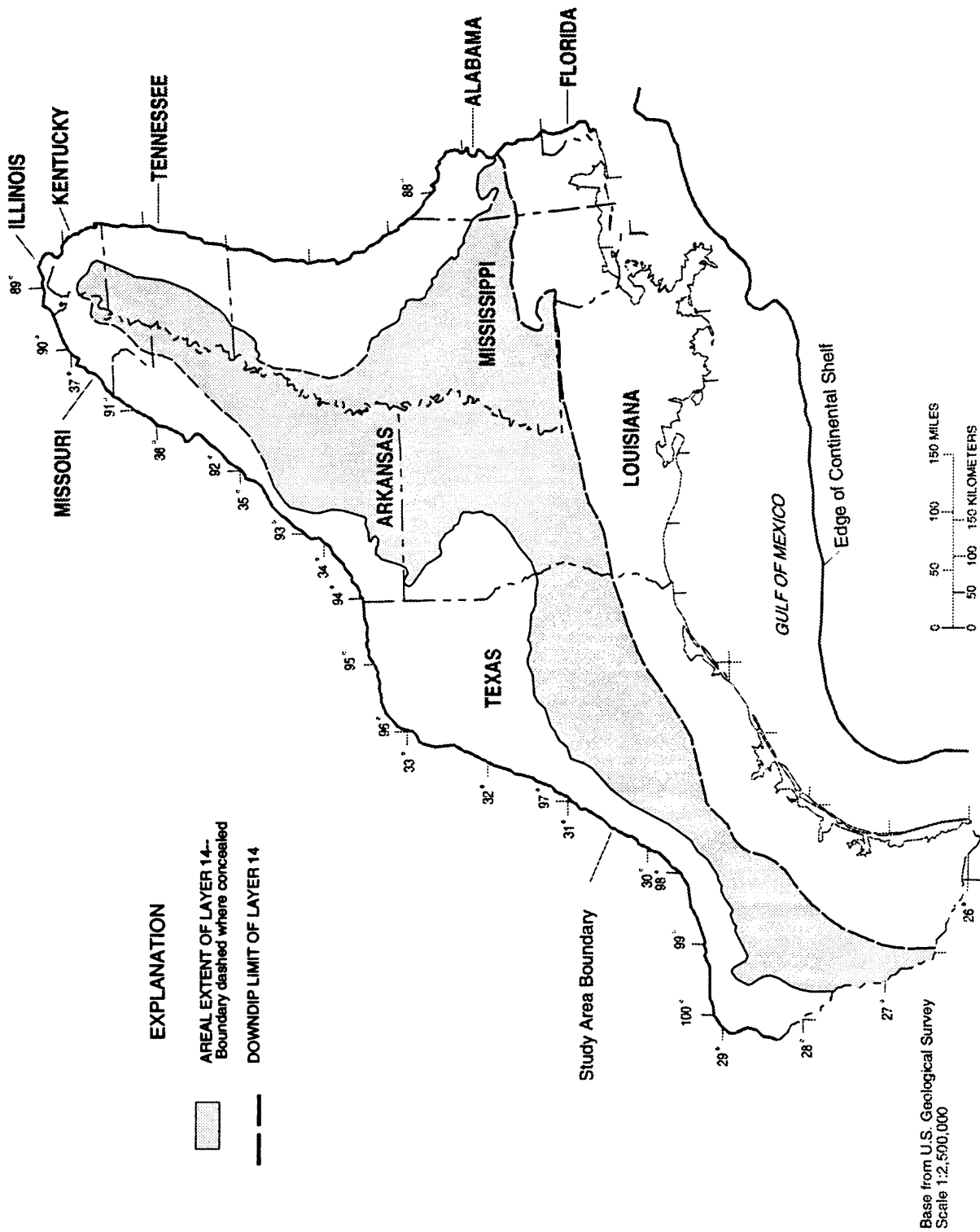


Figure 21. Areal extent of model layer 14. Represents confining unit between model layers 5 and 6.

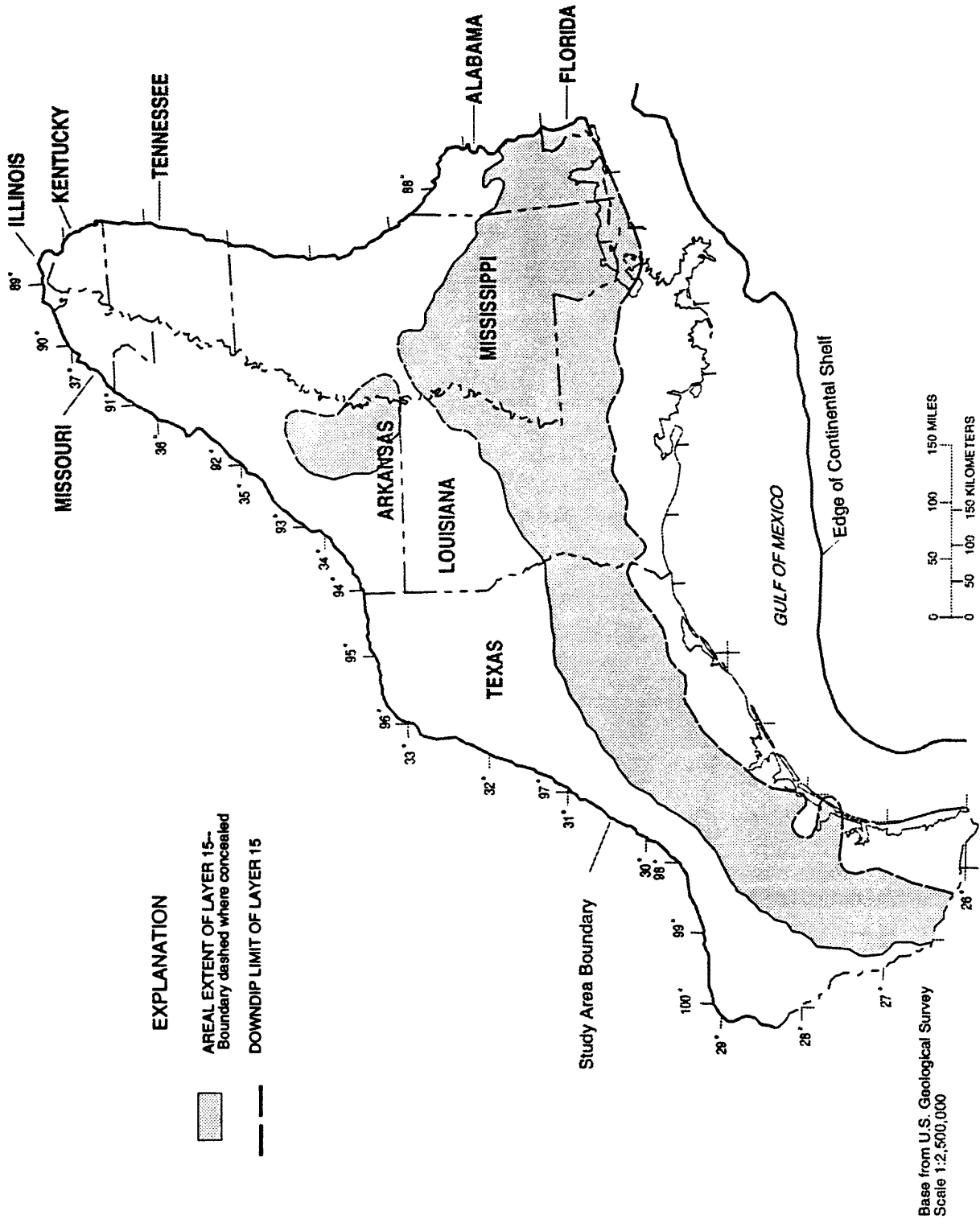


Figure 22. Areal extent of model layer 15. Represents confining unit between model layers 6 and 7

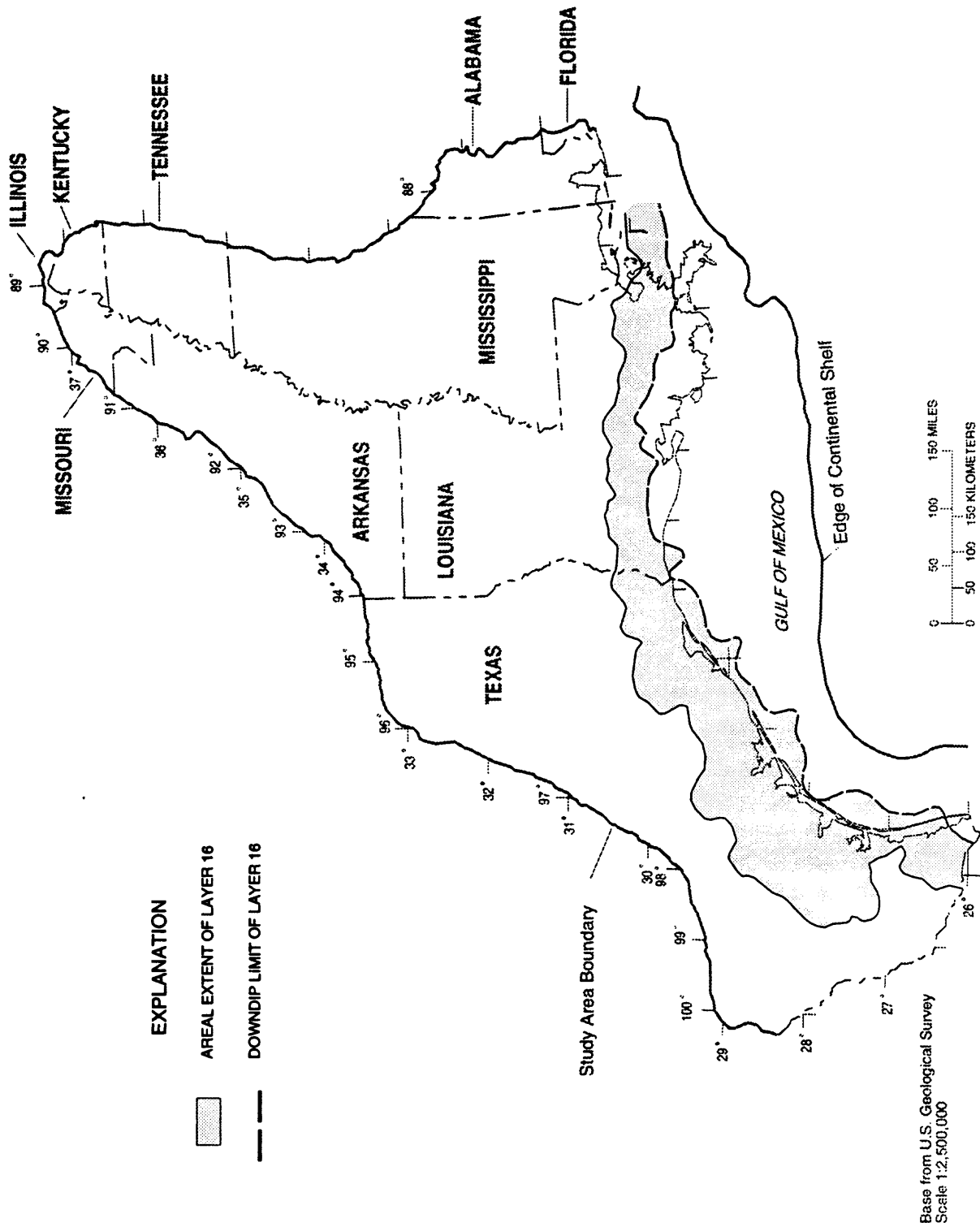


Figure 23. Areal extent of model layer 16. Represents confining unit between model layers 7 and 8.

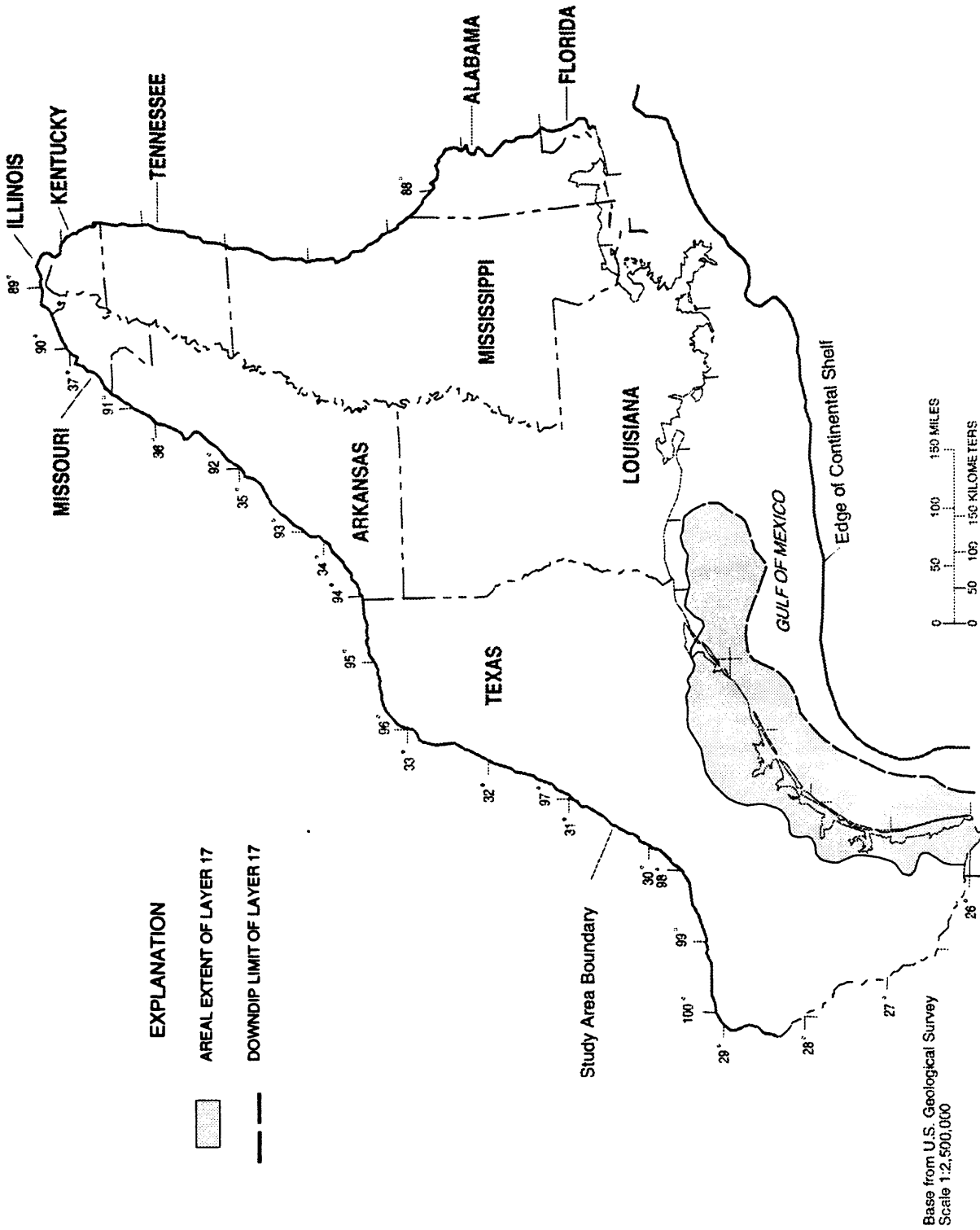


Figure 24. Areal extent of model layer 17. Represents confining unit between model layers 8 and 9.

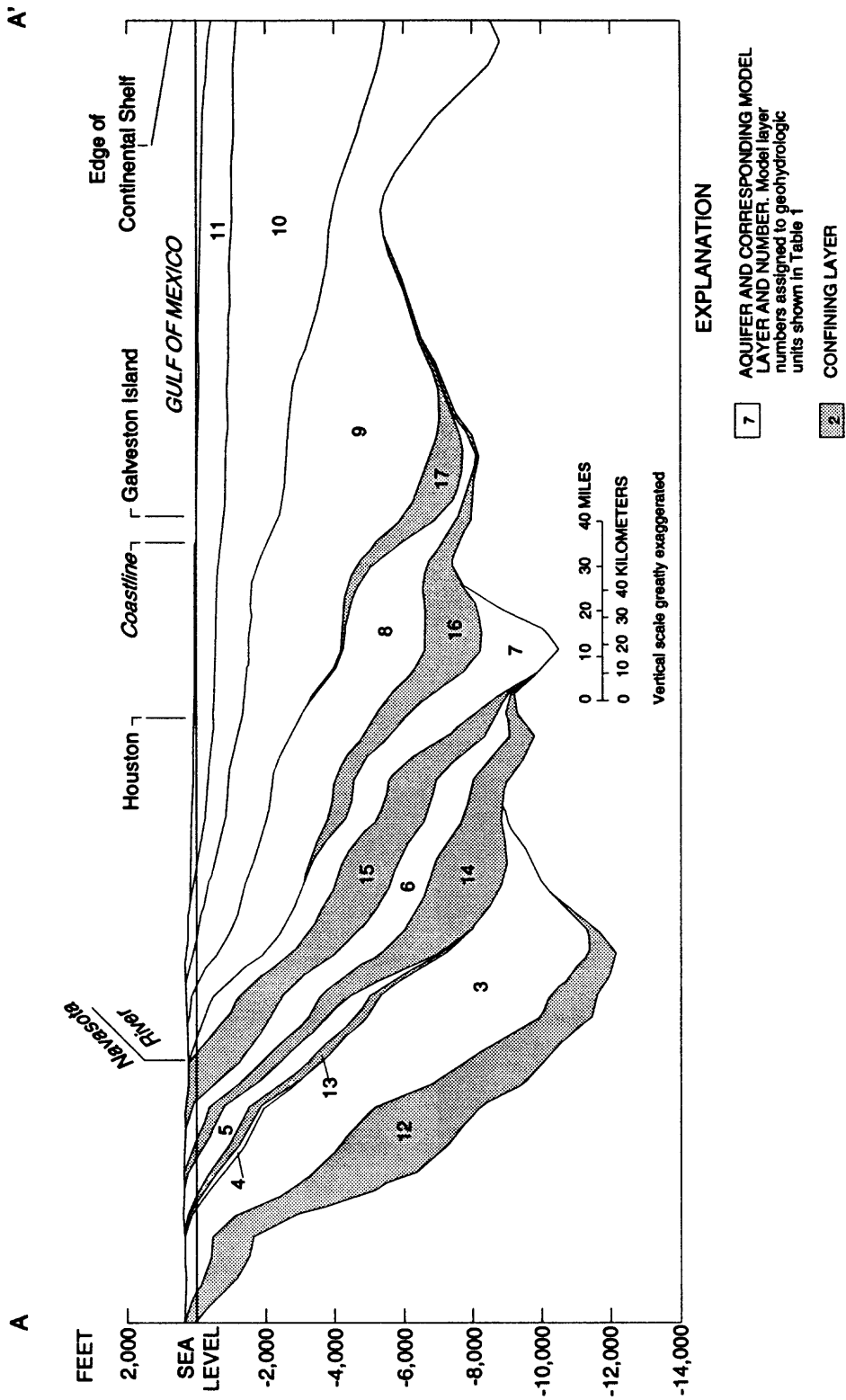


Figure 25. Idealized diagram from central Texas to the edge of the Continental Shelf showing vertical relation of aquifers and confining units (modified from Williamson and others, 1990).

The bottom surface of the aquifer system domain of solution is either in the geopressured zone or on the top of a geologic unit which is assumed to have no flow. The significantly overpressured parts of the geopressured zone beneath the aquifer system in the model are shown in figure 26. The updip extent of the significantly overpressured area is approximately equal to the line where model layer 7 is partially truncated by the geopressured zone as shown by Weiss (1993). Because the geopressured zone presumably extends further offshore than the aquifer system, the offshore limit of the region shown in figure 25 is the edge of the Continental Shelf. A layer of geopressured zone grid elements lies beneath all of the other layers mentioned above and has the areal extent shown in figure 26. The specified geopressured zone head in the geopressured zone layer is equal to the product of 1,000 ft with a regression parameter, plus an additional second regression parameter. For the grid elements in the geopressured zone, the quantity (K_z/b) , where K_z is grid element effective vertical hydraulic conductivity and b is grid-element thickness, is equal to the second regression parameter. Note that vertical flow between two grid elements, denoted 1 and 2, is

$$(h_1 - h_2)(\text{area}) \left[\frac{b_1}{(K_1)_z} + \frac{b_2}{(K_2)_z} \right]^{-1},$$

whence the choice of (K_z/b) as a regression parameter for the geopressured zone. The two basic properties of a source of fluid adjacent to the domain of solution are the pressure of the source and its ability to actually deliver fluid if permitted by lowering the pressure and increasing the conductivity in the domain of solution adjacent to the fluid source. Because of the way the two parameters determine flow, they relate directly to these two basic properties.

The top of the aquifer system domain of solution is that surface consisting of either the water table, land surface, or sea floor, whichever is lowest. The top model layer, layer 12, has the areal extent shown in figure 10 and overlies the aquifer system. This model layer has a specified head equal to the product of (1) an approximation to the water-table altitude h_w (Williams and Williamson, 1989) when on land, or equivalent freshwater head at the sea floor offshore, with (2) a regression parameter; plus a second regression parameter. The water-table altitude is coincident with the altitude of streams and lakes except when a layer of unsaturated material exists between a lake or stream bottom and the underlying water table. The two parameters function so as to allow for the possibility that the water-table altitude h_w may have an error proportional to h_w (likely assumption) and also a constant error.

The specific storage $S_s = S_s(x,y,z)$ is taken to be constant for the entire aquifer system domain of solution. This single value of S_s is taken to be one regression parameter.

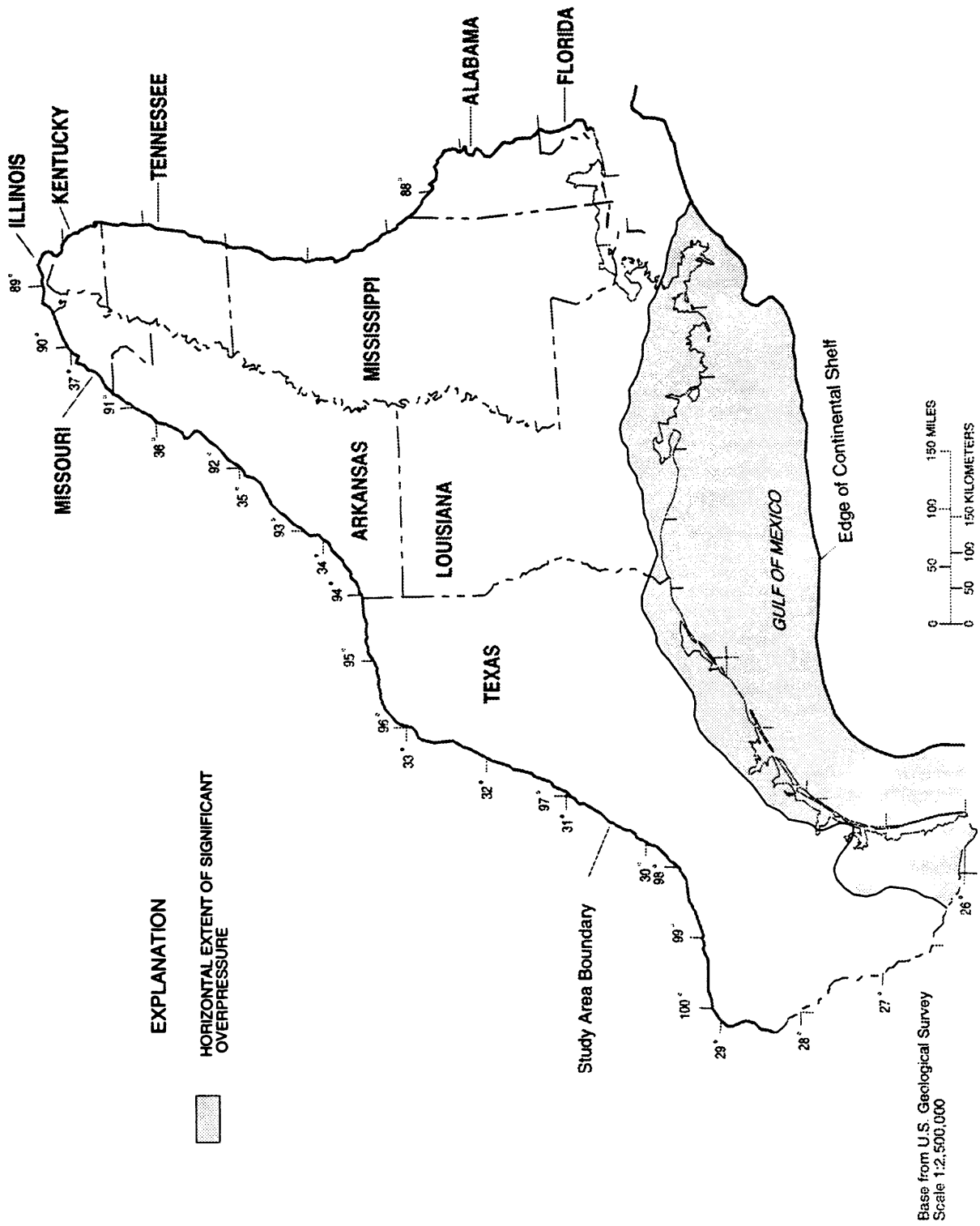


Figure 26. Areal extent of the significantly overpressured parts of the geopressed zone

The density $\rho(x,y,z)$ is given a separate fixed and measured value for each of the $N = 29,453$ grid elements. Density is assumed to be nearly constant in time. This approximation is valid when grid-element volume-averaged density values change very little during the time span being simulated (Kuiper, 1983; Weiss, 1982; Bennett, 1980). No regression parameters are assigned to $\rho(x,y,z)$. Because pumping is known sufficiently well, no regression parameters are assigned to pumping rate $Q(x,y,z,t)$.

The values for K_x , K_y , and K_z , the principal direction values of the hydraulic conductivity tensor K , are prescribed by subdividing the aquifer system domain of solution into a number of hydraulic conductivity zones, each of which contains many grid elements. For each zone or group of zones, two regression parameters are assigned, one for the hydraulic conductivity of the clay of the medium and one for the sand. Here, as elsewhere, the word clay is intended to mean fine-grained sediment including silt. The hydraulic conductivity of each of the components in each of the grid elements is given by the product of the appropriate regression parameter with a function of the depth of the center of the grid element below ground surface. Both of these functions, one for the clay component and one for the sand component, are described further on and give the rate of decrease of hydraulic conductivity with depth. The clay and sand component conductivity values for each grid element are then combined (Desbarats, 1987) with data on the relative amounts of clay and sand in each grid element to finally arrive at effective hydraulic conductivity values K_z , and $K_x = K_y$ for each of the grid elements. If one wishes to consider the horizontally anisotropic case where $K_x \neq K_y$, a single additional regression parameter is assigned to K_x/K_y , assumed to be constant throughout the domain of solution. A detailed description of the procedure for prescribing K_x , K_y , and K_z , is given in a later section on hydraulic conductivity.

Effective vertical hydraulic conductivity K_z for model layer 12 was adjusted to restrict the amount of recharge that flows into underlying model layers. On the basis of an approximation to precipitation less evaporation considerations the maximum allowable recharge rate was specified to vary linearly from 2 in/yr at row number 80 to 12 in/yr at row number 56, in figure 10. The remaining areas in row numbers greater than 80 and less than 56 were allowed a maximum of 2 and 12 in/yr, respectively. Individual layer 12 grid element values for K_z were reduced from an otherwise constant value of K_z for the layer. Only those few grid elements with a high water-table altitude in southern Texas, and several others near areas of heavy pumping, required adjustment.

The solution of equation (3) above is accomplished by obtaining the finite-difference approximating equations (Kuiper, 1983; Kuiper, 1985) using the implicit approximation for the time derivative. The set of $N-M$ simultaneous equations generated, where $N = 29,453$ is the total number of grid elements and M is the number with a specified head, is solved at each time step and gives values for the N heads at each of the time steps and at each of the grid elements not located on a specified-head boundary. All of the N heads are regarded as dependent variables depending upon the

regression parameters. A measured value of head is assumed to equal computed head, as a function of the regression parameters, plus an error term called the residual. The vector equation expressing these relationships becomes the regression equation for the regression technique (Vecchia and Cooley, 1987).

Quantities other than the heads are also dependent upon the regression parameters. Possibilities include the parameters themselves, values of the hydraulic conductivity in the various zones mentioned, storage depletion as measured by subsidence, ground-water flow rates, and so forth. Thus, the regression equation may include these quantities, also, if they have observed values.

Values for grid-element volume-averaged head were matched for the years 1972 and 1982, and were produced by the numerical flow model by using four time intervals of length 30, 5, 5, and 5 years, respectively. Starting with a steady-state predevelopment zero pumping solution for the year 1937, heads were determined for the years 1967, 1972, 1977, and 1982. For each of these four time intervals, appropriate time-averaged pumping values were used as determined from pumping data. For the three 5-year time intervals 1967-72, 1972-77, and 1977-82, the pumping rates for the years 1970, 1975, and 1980 were used. The pumping rates for these years are close to the average pumping rates during the three time intervals. For the 30-year time interval from 1937 to 1967, an approximation to the average pumping rate during the interval was obtained using the 1970 location of pumped wells, but decreased in accordance with total pumping by layer for the years 1960 and earlier. The total pumping rate by layer for the years 1960, 1970, 1975, and 1980 is shown in figure 27.

Regression Model

The nonlinear regression model (Draper and Smith, 1981; Vecchia and Cooley, 1987) supposes that a set of observations (Y_i , $i = 1, 2, \dots, n$) of the physical system are related to a $p \times 1$ vector of unknown regression parameters B through the stochastic model

$$Y = f(B) + E , \tag{4}$$

where Y and E are $n \times 1$ random vectors, and the $n \times 1$ vector $f(B)$ is the expectation of Y . The integer p is the number of regression parameters. The observations Y_i are thought of as a realization of the components of the $n \times 1$ random vector Y . The $n \times 1$ random error vector E is assumed to have the probability distribution

$$E \sim N(0; \epsilon^2 \omega^{-1}) , \tag{5}$$

where ω is a known $n \times n$ symmetric positive definite matrix and ϵ is a scalar constant. In the text below we shall frequently refer to $f(B)$ as being the numerical flow model. As explained above, it contains quantities

other than those coming from the numerical flow model as dependent variables.

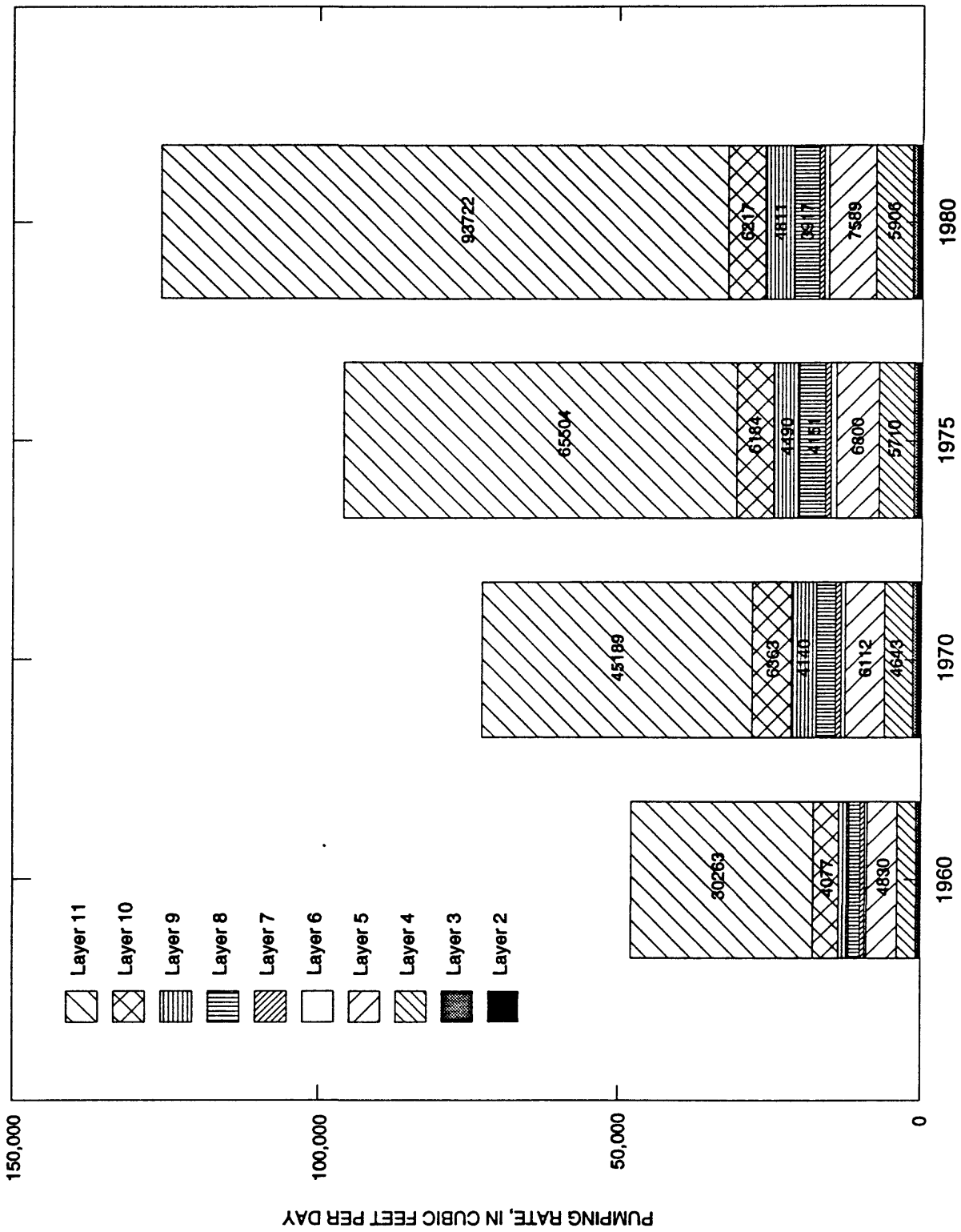


Figure 27. Total pumping rate by layer for the years 1960, 1970, 1975, and 1980.

In the case where n becomes large without limit and a continuum of points exists, such as the continuum of points corresponding to a cartesian coordinate (x,y,z) , the vectors Y and E become random fields $Y(x,y,z)$ and $E(x,y,z)$, and the vector $f(B)$ becomes a function $f(x,y,z,B)$. As an example, figure 28 shows a single realization of random field $Y(x)$ as a function of cartesian coordinate x , where realization $Y(x)$ is the volume average of head over a volume extending from the bottom of an aquifer to its top and having a given cross sectional area A . A second example is the volume average of hydraulic conductivity rather than head. The value of realization $Y(x)$ shown is the exact value of the volume average, even though only an approximation to this value could be obtained by measurement. Two different approximations to $f(x,B)$ are shown in figure 28. The first $f(x,B)$, denoted $f_1(x,B)$, is coarse compared to $f_2(x,B)$ and does not follow $Y(x)$ as closely as $f_2(x,B)$. Because $f_1(x,B)$ and $f_2(x,B)$ only approximate $f(x,B)$, the expectations of $E_1(x) = Y(x) - f_1(x,B)$ and $E_2(x) = Y(x) - f_2(x,B)$, though perhaps small, are not zero. Because $f_1(x,B)$ follows $Y(x)$ more closely than does $f_2(x,B)$, $E_1(x)$ has a larger apparent variance than does $E_2(x)$. Apparent variance, approximately equal to residual mean square (Draper and Smith, 1981, p. 34) is, in the case of individual observations Y_i , $i = 1, \dots, n$, defined to be:

$$\frac{1}{n} \left[\sum_{i=1}^n (Y_i - f_i(B))^2 \right],$$

where $n \gg 1$.

This demonstrates that the apparent variance of $E_1 = Y - f_1(B)$ is dependent upon the chosen degree to which an approximate $f_1(x,B)$ is capable of fitting realization Y , the observations. For a given realization Y , many different sets approximate $f(B)$ and corresponding E can be chosen, each with a different apparent variance. As the chosen $f(x,B)$ departs further from the true $f(x,B)$ the agreement will decrease and apparent variance will increase. Apparent variance values are inflated relative to the true value for variance $\epsilon^2\omega^{-1}$ that would obtain if the true $f(x,B)$ were being used. Criteria for this lack of agreement can sometimes be used (Draper and Smith, 1981, p. 35) to determine if a chosen approximate $f(x,B)$ is reasonably close to the hypothesized true $f(x,B)$.

If measurement error is also present, then E also includes this error component, the size of which depends on the accuracy of the measurements used.

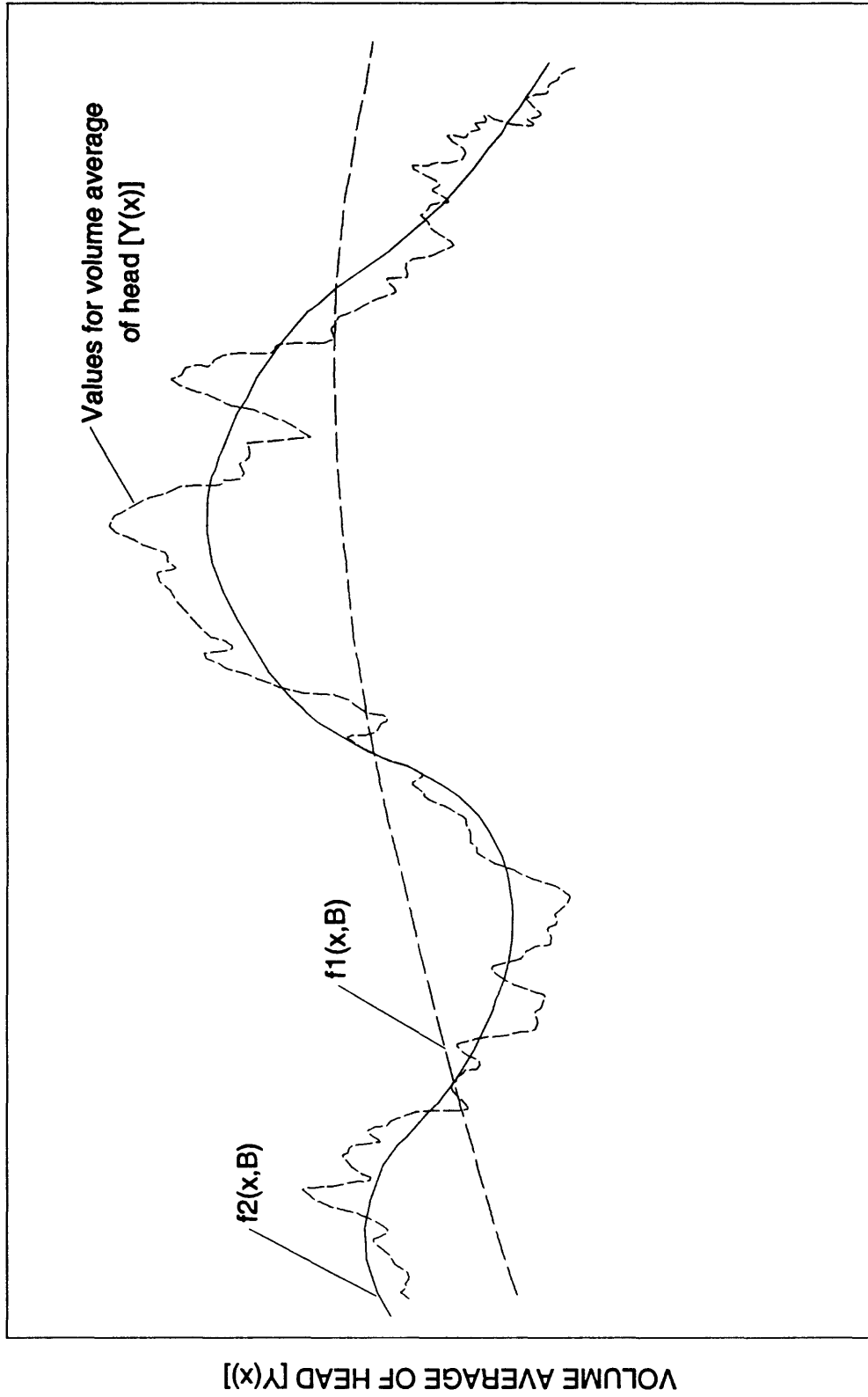


Figure 28. Two potential regression models, $f_1(x,B)$ and $f_2(x,B)$, for describing the relation between cartesian coordinate (x) and volume average of head [Y(x)]

In this study apparent variance is used to approximate true variance $\epsilon^2\omega^{-1}$, the possibility of this procedure was indicated by Draper and Smith (1981, p. 34). A single approximation ω_j is made for those ω_{ii} corresponding to observations of a given type occurring in a zone j of the domain of solution. Accordingly $\epsilon^2\omega_j$, is approximated by

$$\frac{1}{n_j} \left[\sum_{i=1}^{n_j} (Y_i - f_i(B)) \right]^2 ,$$

where n_j (for $n_j \gg 1$) is the number of observations occurring in zone j . The zones j were chosen so that those regions of the domain of solution with like variance were located in the same zone. Different types of observations had different zonations of domain of solution.

In practice, the number of observations is finite, so that in the example in figure 28, $f(B)$ would approximately fit a series of points on the curve $Y(x)$. In this study, when considering observations of head, area A mentioned above is 100 mi², the horizontal area of the grid elements of the multilayered numerical flow model used to simulate the system. Where observations of head are available, average values over the 10 mi by 10 mi by layer thickness grid elements have been assigned to the centers of the elements. These grid element head observations are determined, as will be discussed in more detail, from observations of hydraulic head obtained from wells located in or near the grid element. The observed value of head for a given element, as well as the corresponding value for head produced by the numerical flow model, $f(B)$, are considered to be volume averages of head over the grid element. Because of this, substantial measurement error occur in these grid-element volume-averaged heads. The flow model $f(B)$ of this study, is likewise coarse, so that even in the absence of measurement error, $f(B)$ differs substantially from the observations for any choice of B .

Regression modeling requires determining the variance of E . The apparent variance of E , which is an approximation to the true variance of E , depends upon both the degree to which $f(B)$ fits the observations without measurement error and the measurement error of the observations. In some cases, $f(B)$ may be structured with sufficient detail to fit the observations Y_i exactly. For example, in one method for treating hydraulic conductivity observations in this study (the method in model 9 below) the entire aquifer system domain of solution was divided into seven zones. Six of these zones had an observed value for zone volume-averaged hydraulic conductivity as estimated from individual point values of hydraulic conductivity from individual pump tests of wells within the zone. Flow model $f(B)$ was structured to allow seven different values for hydraulic conductivity in the seven zones, and was thus capable of fitting the six observed values for hydraulic conductivity exactly. Accordingly, the variance of E for these six observations was determined using the formula for the variance of an average of quantities, these quantities being the individual aquifer-test values for hydraulic conductivity.

Prediction and Confidence Intervals

The numerical flow model, $f(B)$, of equation (4) should be selected in such a manner that the model is capable of simulating the aquifer system as closely as possible. Many choices are available, not only with regard to the number and type of regression parameters in $f(B)$, but in what manner they are incorporated into the flow model $f(B)$. Some of these choices are mentioned above. As stated previously for example, the specific storage $S_s(x,y,z)$ in $f(B)$ has a single value throughout the domain of solution and is assigned only one regression parameter, but fluid density $\rho(x,y,z)$ and pumping $Q(x,y,z,t)$ are assigned no regression parameters. Hydraulic conductivity and specified boundary heads are assigned several regression parameters.

With regard to simulation, the confidence that one has in the head and flow values produced by the flow model is of primary importance, simply because head and flow measurements are of primary interest. Predictions of hydraulic conductivity and specific storage are really of interest only because of the way they affect head and flow. As such, they are of secondary importance. However, when the flow model $f(B)$ is used to predict head and flow values in the future, or when the regression equation is extrapolated beyond the vicinity of the observations, then the confidence of the regression parameters might seem to be important because of the fact that head and flow depend upon the parameters and no observations of head and flow are available for comparison. Unfortunately, even if the regression parameters of $f(B)$ are known well, some heads and flow rates may still have considerable error if $f(B)$ has not been constructed in a suitable manner. For example, suppose $f(B)$ has a single hydraulic conductivity value for the entire domain of solution, even though the hydraulic conductivity is variable. This single value may be thought of as the average hydraulic conductivity in the domain of solution. Even if it is shown that this so-called average hydraulic conductivity is known quite well, the heads and flow may still be known only very poorly because using a constant hydraulic conductivity is an inadequate approximation to the variable hydraulic conductivity distribution present. Very likely, the best information available on the confidence of heads and flow outside of the vicinity of the observations is the confidence of heads and flow within the vicinity of the observations. In conclusion, the confidence that one has in head and flow values in the vicinity of the observations is of primary interest in evaluating the ability of the flow model to simulate the aquifer system, past, present, and future. As will be shown later, it is sometimes possible to evaluate this confidence.

Equation (75) of Vecchia and Cooley (1987) gives an approximate prediction interval for Y_k :

$$Y_k^e = f_k(\hat{B}) \pm d_{1-\alpha} [\hat{X}_k (\hat{X}^T \omega \hat{X})^{-1} \hat{X}_k^T + \omega_k^{-1}]^{1/2}, \quad (6)$$

where k may correspond to a location at which there is no observation. Here

$$d_{1-\alpha}^2 = S(\hat{B}) [(p+1)/(n-p)] F_{\alpha}(p+1, n-p),$$

where as mentioned previously, the number of observations n is the length of the vector Y , and the number of regression parameters p is the length of the vector B . The upper α percentile of the F distribution with $p+1$ and $n-p$ degrees of freedom is denoted by $F_{\alpha}(p+1, n-p)$. The value of the vector of regression parameters B at which the sum of squared weighted residuals $S(B) = [Y-f(B)]^T \omega [Y-f(B)]$ is a minimum, is denoted by \hat{B} . The T superscript denotes the transpose of a matrix. The sensitivity matrix X is given by $X_{ij} = [\partial f_i(B) / \partial B_j]$, and matrix X evaluated at $B = \hat{B}$ is denoted \hat{X} . The j th component of the $1 \times p$ vector X_k is X_{kj} . $\epsilon^2 \omega_k^{-1}$ is the variance of $F_k = Y_k - F_k(B)$. If k is not an observation number, then ω does not have to be diagonal and ω_k is not an element of ω . In this case there is no correlation between Y_k and Y_i , one of the n observations of vector Y of equation 4. The interval given by equation 6 is a $(1-\alpha)100$ -percent prediction interval for Y_k , the k th member of the $n \times 1$ random vector Y . Thus, if the model is nearly linear, the probability is $1-\alpha$ that $Y_k \leq Y_k^e(+)$ where $Y_k^e(-)$ and $Y_k^e(+)$ are the two values of Y_k given in equation 6. If the model is nonlinear, the probability $1-\alpha$ is approximate. As noted above k need not be contained within the observed set of quantities Y_i . Thus, for example, equation 6 may be used for values of the head at locations where no observation occurs, provided that one is able to find a value for ω_k . If k corresponds to some distant future observation, then ω_k cannot easily be determined. Replacing $d_{1-\alpha}$ with $(S(\hat{B})/(n-p))^{1/2}$ in equation (6) causes the term to the right of the \pm sign, when squared, to give the variance of Y_k .

Equation (45) of Vecchia and Cooley (1987) gives an approximate confidence interval for the regression parameter B_i :

$$B_i^e = \hat{B}_i \pm d_{1-\alpha} [i^T (\hat{X}^T \omega \hat{X})^{-1} i]^{1/2}, \quad (7)$$

Here $d_{1-\alpha} = S(\hat{B}) [p/(n-p)] F_{\alpha}(p, n-p)$ where $S(\hat{B})$ and $F_{\alpha}(p, n-p)$ have been defined above. The $p \times 1$ vector i is a vector whose only nonzero component is the i th, which has the value unity. The two B_i^e extreme values given in equation (7) determine a $(1-\alpha)100$ -percent confidence interval for B_i , the i th member of the $p \times 1$ vector B . Replacing $d_{1-\alpha}$ with $(S(\hat{B})/(n-p))^{1/2}$ in equation (7) causes the term to the right of the \pm sign, when squared, to give the variance of B_i .

Equations (6) and (7) may be useful in choosing between the many possible choices for $f(B)$. The smaller the intervals in equations (6) and (7) are, the better the choice for $f(B)$ is considered to be. Especially important is the choice for the number of regression parameters p , because of the distinct way that the two intervals increase with p . A comparison of over 40 different choices for $f(B)$ with p varying from 2 to over 31 is presented in the application and results section.

Equations (6) and (7) require evaluations of $S(B)$, X , and $f(B)$ at $B = \hat{B}$. $S(B)$ may be approximated by

$$S(B) = \sum_{i=1}^n (Y_i - f_i(B))^2 \omega_i, \quad (8)$$

Approximate equation (8) has used $\omega_i = \omega_{ii}$ and $\omega_{ij} = 0$ for $i \neq j$, in the exact expression for $S(B)$ given previously. The minimization $S(B)$ in equation (8) in the p members of B was carried out by the Levenberg-Marquardt algorithm (Gill and others, 1981) for the minimization of the sums of squares. This algorithm is iterative and finds successively smaller values of $S(B)$ at a series of successive choices of B selected by the algorithm. During this iterative process it is interesting to evaluate to the left side of inequality (7) of Vecchia and Cooley (1987):

$$\frac{[Y-f(B)]^T \omega^{1/2} P \omega^{1/2} [Y-f(B)]}{[Y-f(B)]^T \omega^{1/2} (I-P) \omega^{1/2} [Y-f(B)]} \leq (p/n-p) F_{\alpha}(p, n-p), \quad (9)$$

where $P = \omega^{1/2} X (X^T \omega X)^{-1} X^T \omega^{1/2}$.

Inequality (9) expresses a $(1-\alpha)100$ -percent exact confidence region for B . As $S(B)$ decreases with the successive choices for B , the left-hand side of equation (9) also commonly decreases. The contours of $S(B)$ and the contours of the left-hand side of (9) as a function of B , coincide quite closely (Donaldson and Schnabel, 1987; Sundararaj, 1978; Wallace and Grant, 1977). Equation (9) with the equality sign may be used to solve for $\alpha = \alpha_m$, with $B = B_m$, where m is the Levenberg-Marquardt iteration number. With this definition of α_m , the successive values for B , B_m $m = 1, 2, 3, \dots$ lie somewhere on the boundary of the $(1-\alpha_m)$ 100-percent confidence region for B . For successively larger values of m , the left-hand side of equation (9), evaluated at $B = B_m$, decreases to zero as does $F_{\alpha_m}(p, n-p)$, and at the same time α_m increases to unity from $\alpha_0 > 0$.

Depth Dependence of Hydraulic Conductivity

The hydraulic conductivity of the porous medium in the domain of solution of the aquifer system, which is composed of interbedded fine-grained and coarse-grained sediments, usually decreases with depth below land surface.

The hydraulic conductivity of the coarse-grained sediments or sands, usually decreases with depth due to decreasing porosity, but increases with depth due to higher temperature and the resulting decrease in fluid viscosity. The net outcome of these factors, however, is usually decreasing hydraulic conductivity with depth. The function $10^{-0.8dd}$, where dd is measured in kilometers, was used to express the rate of the decrease of the hydraulic conductivity of sand with depth dd (Loucks and others, 1986; Lake and Carroll, 1986). Loucks and others (1986) presented data (fig. 29) on the hydraulic conductivity of sand from Tertiary deposits of the Texas Gulf Coastal Plain. The curve (constant) $10^{-0.8dd}$, which is an approximation, is also shown. The exponent of this curve was assigned a regression parameter, but because of the shallow depth of most head observations, the parameter had such a large confidence interval that it was decided that the model would be more accurate if the curve $10^{-0.8dd}$ was assumed.

The hydraulic conductivity of the fine-grained sediments, or clays, in the domain of solution of the aquifer system tends to decrease with depth because of compaction. Figure 30, taken from Neglia (1979), shows the decrease with depth of the hydraulic conductivity of various clay samples. The curve shown in figure 30, (constant) $10^{(-1.167dd+.0833dd^2)}$ where dd is measured in kilometers, was formulated to approximate the measured values shown and was used in this study to give the rate of decrease of hydraulic conductivity of clay with depth. As with the decrease of hydraulic conductivity of sand with depth, a regression parameter included in the exponent had a very large confidence interval and was removed.

The hydraulic conductivity of clay or sand of the fine-grained or coarse-grained sediments in a grid element is found by taking the product of the regression parameter associated with the hydraulic conductivity zone (described below) containing the grid element with the appropriate depth function, where the depth chosen was the depth below land surface of the center of the grid element. The clay and sand components have separate regression parameters, and use the clay and sand depth functions described above respectively. The effective hydraulic conductivity tensor K of the grid element will depend upon the shape, size, and distribution of the sand bodies in the grid element and also on the hydraulic conductivity of these sand bodies and the clay matrix surrounding them. Desbarats (1987) presented a statistically-based procedure for calculating grid element

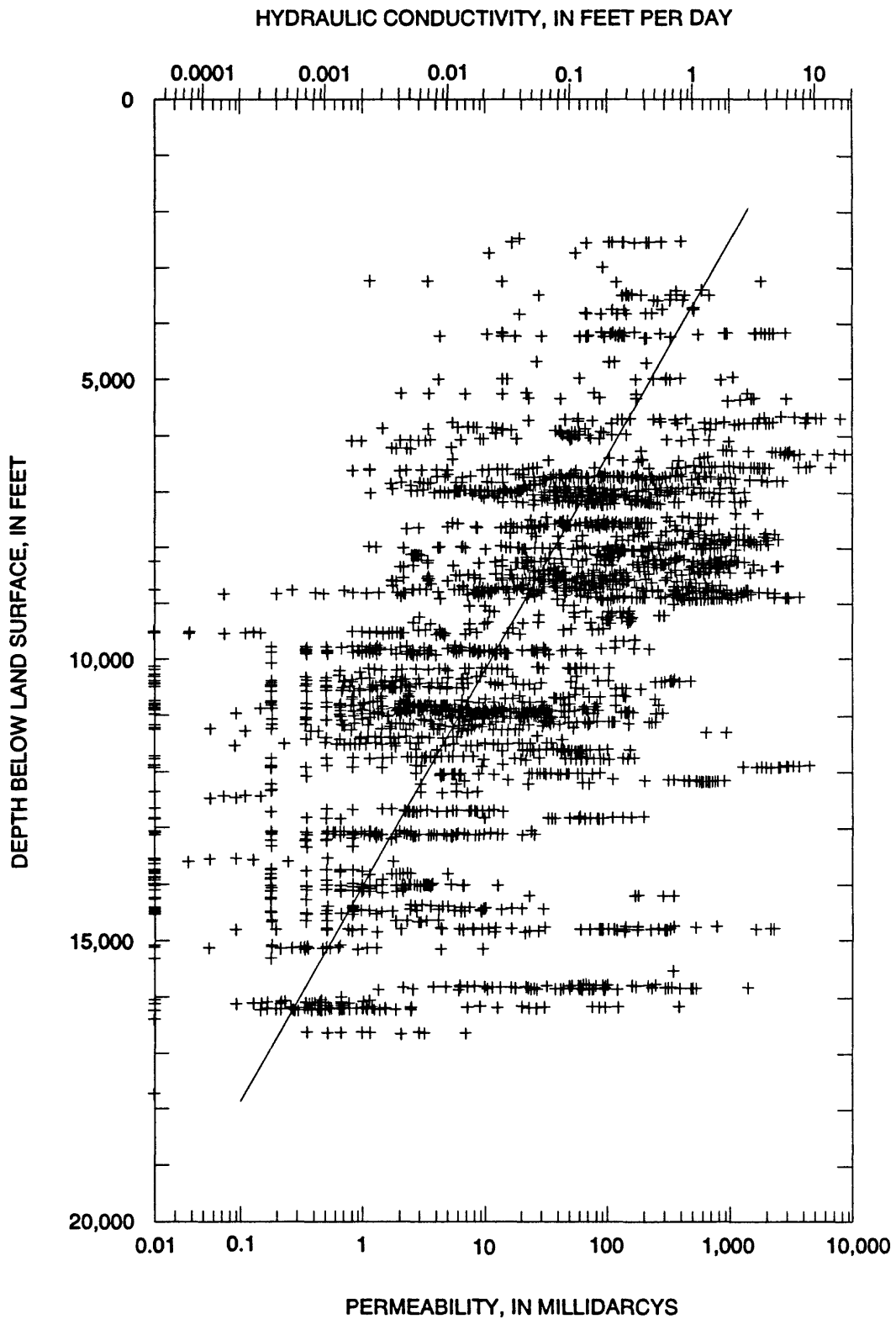


Figure 29. Decrease of hydraulic conductivity of sand with depth. (Modified from Loucks and others, 1986.)

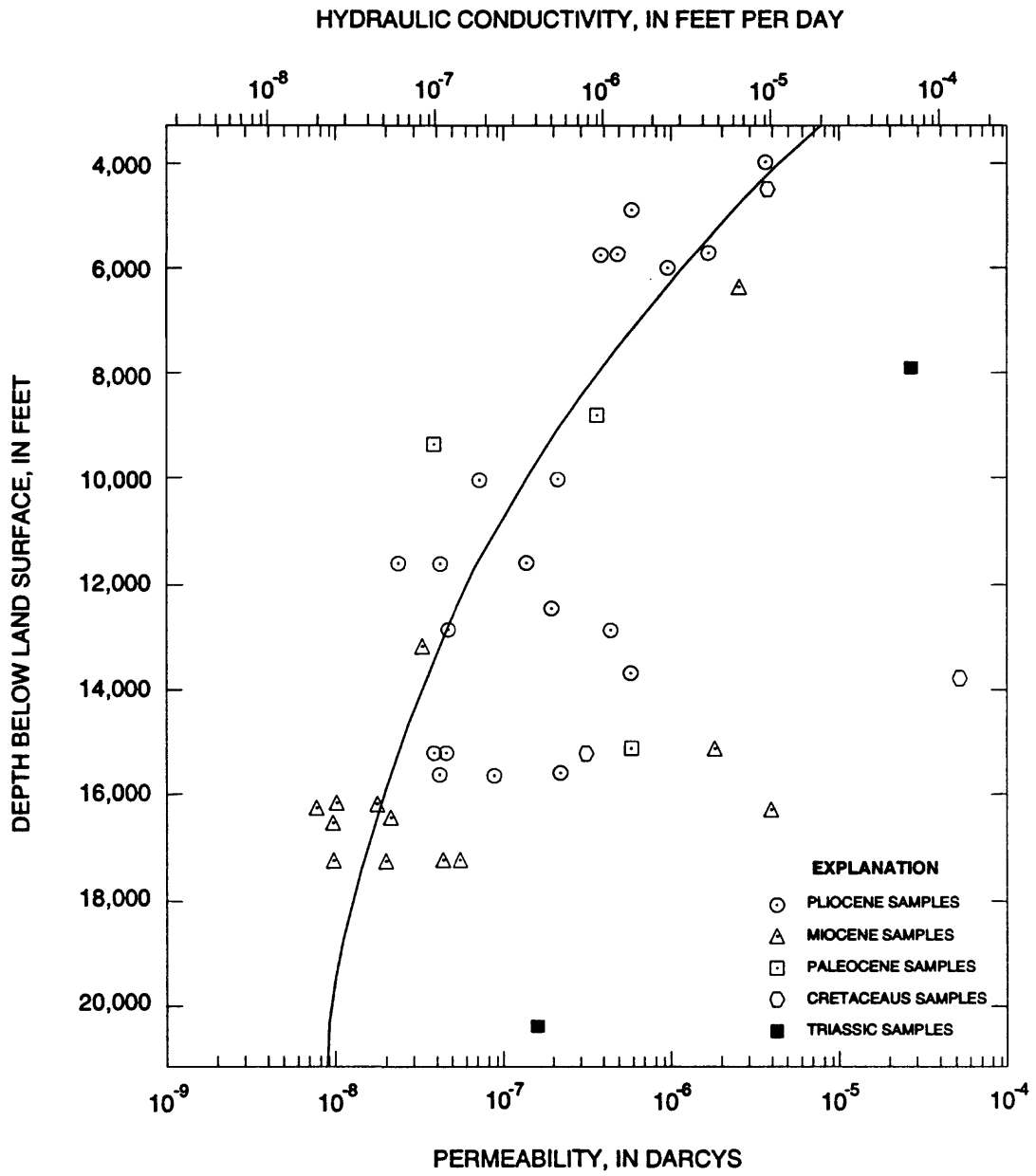


Figure 30. Decrease of hydraulic conductivity of clay with depth. (Modified from Neglia, 1979.)

effective hydraulic conductivity values. Figure 31 shows effective horizontal (K_h), and vertical (K_z) hydraulic conductivity values, as functions of V_c , the clay fraction of the grid element, for the case where $\log_{10}(K_c/K_s) = -4$, where K_c and K_s denote the hydraulic conductivity of the clay and sand components respectively. Then K_h and K_z can be calculated from:

$$\frac{K_z}{K_s} = [K_c/K_s]^{a^{-1}} (V_c)^{a^{-1}}, \quad (10)$$

$$\frac{K_h}{K_s} = [K_c/K_s]^{a} (V_c)^{a}. \quad (11)$$

Here, a , related to the width to vertical thickness ratio of the sand bodies, is set equal to 4.0 or to the product of 4.0 and a regression parameter. Horizontal anisotropy is introduced by setting $K_x = K_h$ and by setting K_y equal to the product of K_h with a regression parameter. If anisotropy is not desired, then $K_x = K_y = K_h$ and no additional regression parameter is used.

Hydraulic Conductivity Zones

The hydraulic conductivity zones previously discussed in the Modeling Methodology section are cross referenced by layer and region. The layers are the model layers 2 through 11, top-layer 12, and model layers 13 through 17. The regions are shown in figure 32. Note that the regions specify horizontal position and the layers specify vertical position. The hydraulic conductivity zones are thus specified in three dimensions by cross referencing. A hydraulic conductivity zone does not exist for each of the model layers 2 through 17 and each of the 10 regions because the domain of solution does not extend to all combinations of layers and regions. The function of the hydraulic conductivity zones and the assignment of regression parameters to them allows the model to approximate the heterogeneity of either the clay or sand component in the domain of solution. A particular volume within the domain of solution may consist of several or many adjacent hydraulic conductivity zones. Assigning the same regression parameter, clay or sand whichever the case maybe, to all of the hydraulic conductivity zones within the particular volume causes the hydraulic conductivity of the clay or sand in the volume to be constant except as altered by the depth function for clay as explained previously.

The actual number of regression parameters that may be assigned to the hydraulic conductivity zones is variable. Two regression parameters could, for example, be assigned to all of the zones, the first regression parameter for the clay component in all of the zones and the second for the sand component in all of the zones. Or, for example, 11 regression parameters could be used: 10 for the clay components of the 10 regions and the 11th regression parameter for the sand component of all of the zones,

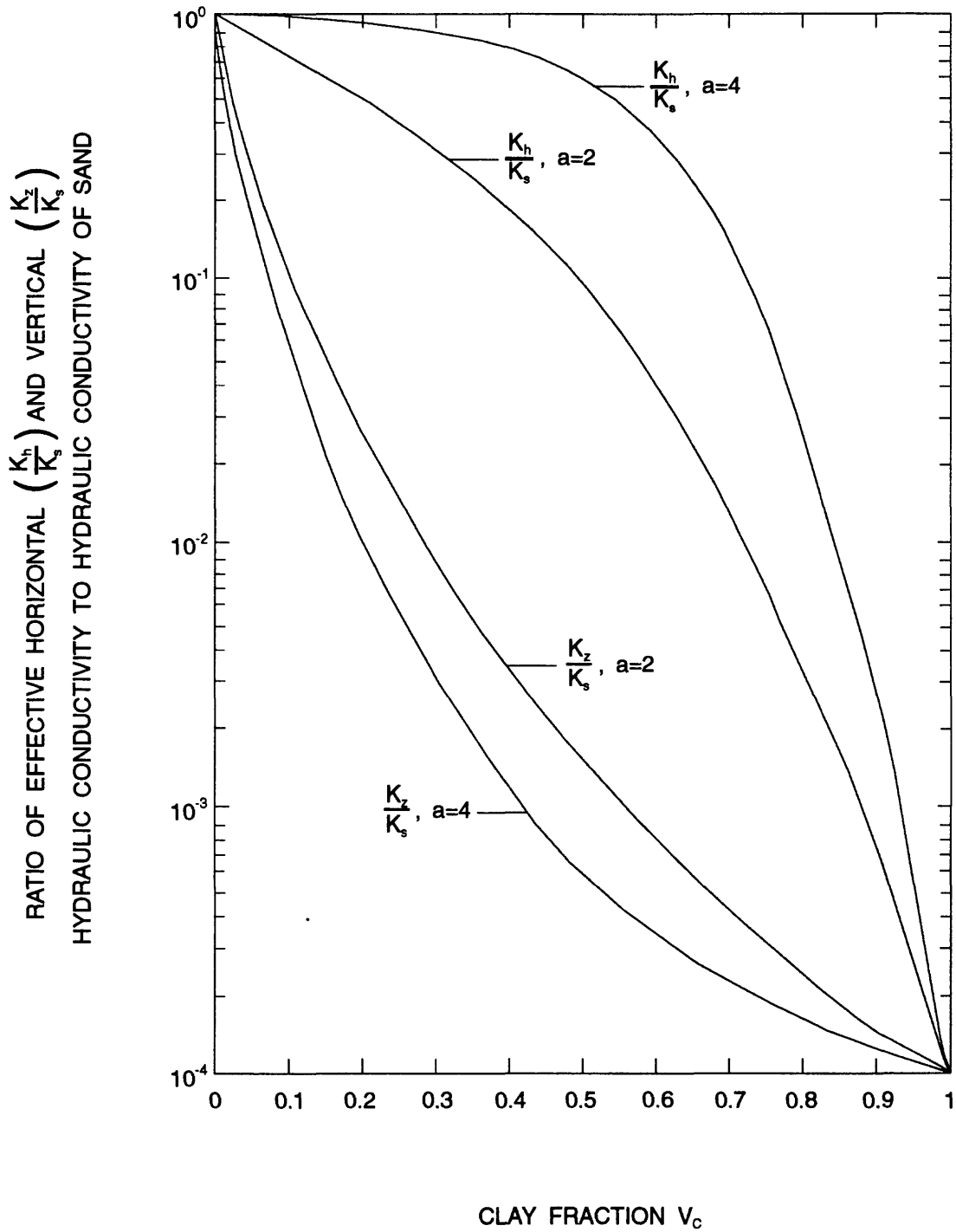


Figure 31. Effective hydraulic conductivity, equations (10) and (11), for $K_s/K_c=10^4$

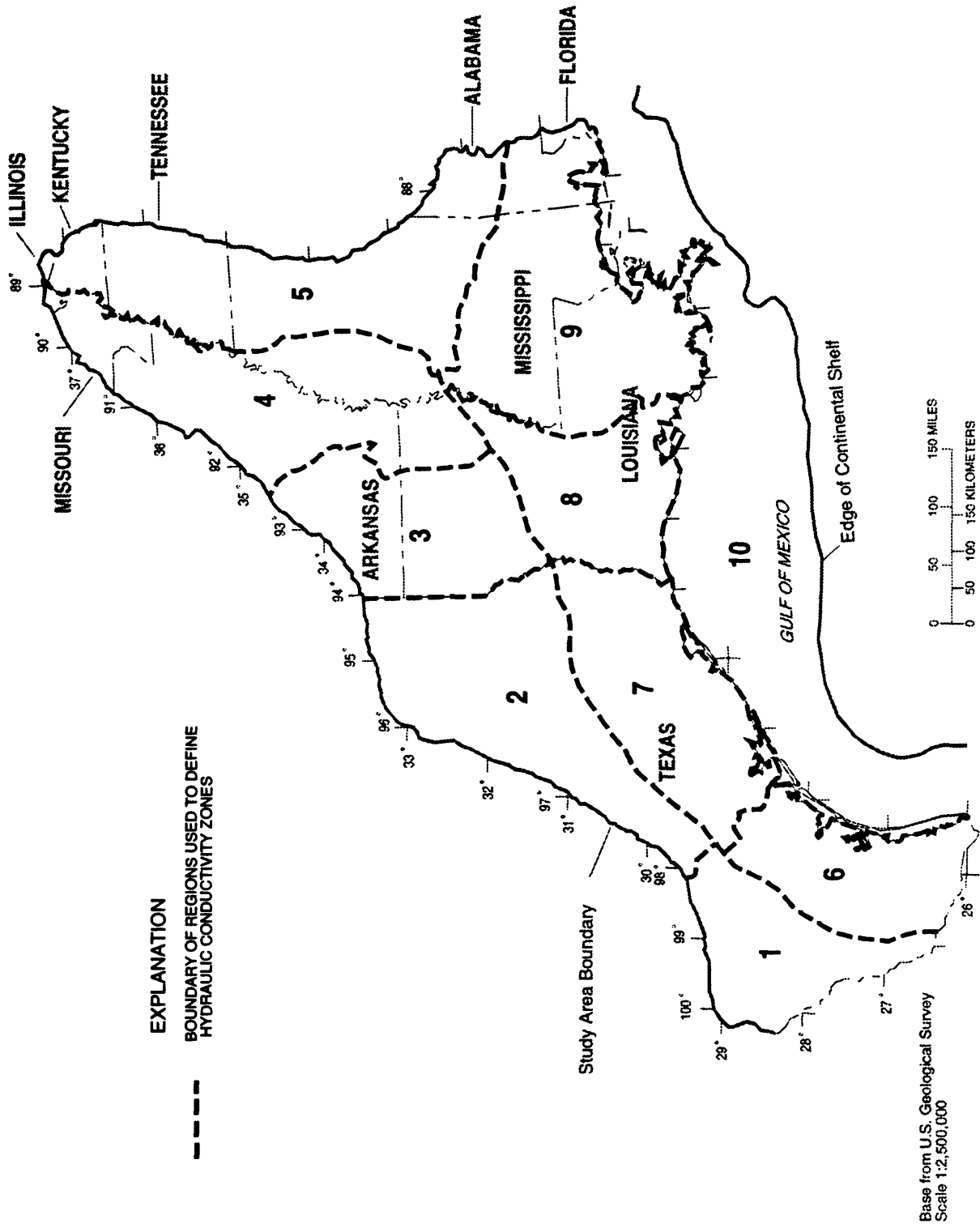


Figure 32. Extent of the 10 regions used to define hydraulic conductivity in the study area. The model layers having hydraulic conductivity data are given in table 2, by region.

and so forth. The application and results section below lists several of the many combinations used. Because the top-layer heads are specified, only the vertical effective hydraulic conductivity in this layer has any effect on the heads. For convenience, the top layer is assigned $V_c = 1$ and this layer has no regression parameters for hydraulic conductivity of sand. Also, the model layers 13 through 17 are mostly clay and, thus, have $V_c = 1$ and have no regression parameters for hydraulic conductivity of sand because little sand is present.

Subsidence

Certain areas of the aquifer system are affected by land subsidence due to ground-water withdrawals. In the numerical flow model, subsidence caused by inelastic compaction of clays was modeled using the procedure of Leake and Prudic (1988). Specific storage is increased from values characteristic of elastic compaction of clays to values characteristic of clays during inelastic compaction and land subsidence. The procedure increases the specific storage by some factor C_s when the grid-element volume-averaged head h declines through values of $h < h_1$, where h_1 is the lowest grid-element volume-averaged head achieved in the recent past. This factor C_s is unity, however, if h has not decreased by more than some triggering value Δh_s in the recent past. Recent past was taken to be all time since 1937, at which time a steady-state numerical flow model with zero pumping defined predevelopment conditions. The value C_s was either set to 40, or to the product of 40 with a regression parameter. In the grid elements of model layers 2 through 6, the subsidence mechanism was not thought to be operative as a result of the absence of materials capable of further compaction, so that C_s was fixed at unity. The triggering value Δh_s was either set equal to 80 ft, or the to product of 80 ft with a regression parameter. The grid area-averaged subsidence for a particular 10-mi by 10-mi grid area located at ground surface is approximately equal to the total volume of the fluid removed from storage in all grid elements lying below the grid area at ground surface, divided by 100 mi². This approximation would be nearly exact if water were incompressible. The slight compressibility of water will cause the subsidence to be slightly less than as calculated above, when the volume of the fluid removed is measured at the same temperature and measure of the water at the point of removal.

Preparation of Observations of Head and Hydraulic Conductivity, Y_i

In this study the observations Y_i included observations of head and hydraulic conductivity. The only other possible observations are flow and anthropogenic subsidence. As mentioned previously, recharge into the top of the aquifer system was restricted by adjusting the hydraulic conductivity of layer 12. This mechanism does not, however, involve any observations of flow Y_i . Remaining flow rates, including discharge upward from the aquifer system into layer 12 and also discharge from the geopressed zone, are known poorly so that they would have a very small influence on $S(B)$ because their weights ω_i in equation (8) would be small.

Land subsidence due to ground-water withdrawals can be observed and measured accurately, and measured values are available in locations where substantial subsidence occurs. However, subsidence was not included in the observations Y_i , because of the relatively small areas of those locations where measured values are available.

The point observations of both hydraulic head and hydraulic conductivity were volume-averaged for the grid elements and hydraulic conductivity zones respectively. These volume averages are the observations, Y_i , to which model-simulated values are compared.

Grid Element Volume-Averaged Heads

Approximately 50,000 point observations or measurements of hydraulic head were available. As mentioned previously, these approximately 50,000 values were obtained from time-averaging more than 600,000 individual measurements of hydraulic head in water wells. Accompanying each of these approximately 50,000 point observations was the year, well location, and usually the land-surface altitude. Any of these four items could, however, be in serious error so that the data needed considerable verification. Verification was done partially by persons other than the author and included correlations, such as land-surface altitude versus location, and other procedures. Upon receipt by the author these data were passed through a computer program that looked for anomalies in space and time. If an observation was not in correspondence with five or more adjacent observations in space and time, the observation was deleted. An observation was considered not in correspondence with a single adjacent observation if its hydraulic head was not within 70 ft of the adjacent observation and furthermore, not within 35 ft/mi of distance between the observation and the adjacent observation. Adjacent here means within in the same or an adjoining 10-mi grid element and within 10 years of time. Those point observations of hydraulic head passing verification, about 92 percent, were considered valid and were put into an averaging algorithm described below to form 3,107 grid-element volume-averaged heads.

In addition to the approximately 50,000 point observations of hydraulic head, there were approximately 15,000 measurements of formation pressure from drill-stem tests which were used to approximate point-head values (Lobmeyer, 1985). The resulting point-head values were culled of points in a geopressed condition by eliminating those with pressures outside of the interval of 0.38 to 0.55 (lb/in²)/ft. The culled point-head data were then used to form grid element averaged heads for those grid elements with 10 or more point heads from drill-stem tests, using a simple unweighted averaging of the culled point heads. The resulting 586 grid-element volume-averaged heads based on drill-stem tests were identified so that they could be distinguished from the grid-element volume-averaged heads based upon point observations of hydraulic head from water wells, because they were located deeper in the aquifer system and were less accurate.

Averaging Algorithm

As mentioned previously, equations (1) and (3) are discretized in order to arrive at finite-difference approximating equations. These approximating equations have N heads associated with the N grid elements in the domain of solution. These grid element heads should be thought of as grid-element volume-averages of head. This volumetric average perhaps should be weighted somewhat in favor of the central portion of the grid element volume. Such an average is not directly observable but must be approximated from point observations of head within the volume of the grid element, or perhaps adjacent grid elements. An averaging algorithm was used to form this average from point observations. Included in the algorithm is a criterion for deciding if there is a sufficient density of point observations of head to justify the determination of a grid-element volume-averaged head. If there is a paucity of point observations, then no grid-element volume-averaged head is calculated, and the grid element does not have an entry for the set of observations $(Y_i, i = 1, 2, \dots, n)$ associated with equation (4). The averaged head calculated by the algorithm is linear in the point observation of head (Gamut, 1986):

$$\hat{h}(t) = \sum_{i=1}^{ns} a_i \hat{h}_i \quad , \quad (12)$$

Here, $\hat{h}(t)$ is the grid-element volume-averaged head, t is time, and the \hat{h}_i are point observations of head measured within the time interval $(t-\Delta t, t+\Delta t)$. The integer ns is the number of \hat{h}_i used to formulate \hat{h} and the a_i are a set of weights which tend to be larger when the head \hat{h}_i is located closer to the center of the grid element. No consideration is given to the vertical dimension, so that only horizontal distances are considered and the depths of point observations of head within a grid element are disregarded. The justification for this is that vertical dimensions are very small compared to horizontal dimensions and because \hat{h} was formulated from data \hat{h}_i within the same layer as that of the grid element for which \hat{h} is being sought.

The weights a_i are determined by following these steps:

- 1) Divide the polar coordinate 0 space surrounding the center of the grid element at which an averaged head is desired into eight octants of 45° each.
- 2) For each octant, determine the $N3$ \hat{h}_i that are at the smallest distances $r_i, i = 1, 2, \dots, N3$, from the center of the grid element, where $r_1 < r_2 < \dots < r_{N3}$.

N3 is chosen as desired. Eliminate those \bar{h}_i that are at distances $r > R$, where R is a radius of choice. Note that there may be less than N3 points in the octant with $r < R$. Set all $r_i < R_0$ to R_0 , a second radius of choice where $R_0 < R$. Let $g_j = r_1$, where j denotes the octant number, $j = 1, 2, \dots, 8$. Form the average

$$H_j = \left(\sum_{i=1}^{N3} \bar{h}_i / r_i^2 \right) / \left(\sum_{i=1}^{N3} 1 / r_i^2 \right) \text{ for each of the octants.}$$

This calculation actually may involve up to N3 values \bar{h}_i . If there are no \bar{h}_i in the octant with $r < R$, then no H_j is found.

- 3) Determine $\hat{h} = \left(\sum_{j=1}^{\ell} H_j / g_j^2 \right) / \left(\sum_{j=1}^{\ell} 1 / g_j^2 \right)$, where the summations are over the ℓ octants for which a H_j has been found.

- 4) The value of \hat{h} found in the previous step is kept for use if

$$\ell \left[\sum_{j=1}^{\ell} 1 / r_j^2 \right] > C(N3, R, R_0) , \quad (13)$$

where $C(N3, R, R_0)$ is a coefficient of choice.

The use of radius R is to prevent the use of data at very large distances from the grid element center. The use of R_0 , in the step where those r_i within an octant are set to R_0 if less than R_0 , is to prevent a single point close to the center of the grid element from totally overwhelming the value of H , for that octant.

The use of $1/r^2$ weighting as opposed to some other power of r requires some justification. In the case of a uniform distribution of data points in two dimensions, a weighting of $1/r$ gives equal weight to points at any radius. This is true because the area between r and $r + \Delta r$ is $2\pi r \Delta r$ which when multiplied by the weighting factor $1/r$ gives $2\pi \Delta r$. Thus data at very large values of radius r ($r < \text{radius} < r + \Delta r$) are counted as heavily as those at small r . This is definitely not desired since we seek an average head \hat{h} that is representative of those heads somewhat centrally located within the single grid element for which \hat{h} is being found, not a uniformly weighted-average head over the entire region. Thus whatever the power n should be in the weighting factor $1/r^n$, it is clear that it should definitely be greater than 1. A value of $n = 2$ was used. This value for n would place twice as much emphasis on points that are twice as close. Several different values for n , all greater than 1.5 were used. For those values of n used, little effect was found on the ability of the model to fit the data as measured by values of mean weighted residual and root mean square weighted residual.

Estimators of the type described above are intended for noisy data with correlation dependent on the separation distance between values of h_i (Gamut, 1986). Such estimators are stable because they interpolate between the values of h_i , so that h must lie between the smallest and largest values of h_i $i = 1, \dots, s$. Note that h is octally weighted regardless of the number of h_i that may occur in a given octant, provided only that this number is at least 1. N_3 was chosen to be 3, $C(N_3, R, R_0)$ was $36(10 \text{ mi})^{-2}$, R_0 was 2 mi, and R was 15 mi which is 1.5 times the horizontal dimension of a grid element which was 10 mi. The number of grid-element volume-averaged heads calculated was 3,107: 1,432 for the year 1972, and the remainder of 1,675 for the year 1982, both with $\Delta t = 1$ year. The location of the 1,675 grid-element volume-averaged heads for 1982 is shown in figure 33.

Logarithms of Hydraulic Conductivity of Sand

Grid-element volume-averaged heads, the preparation of which is explained above, form part of the set of n observations Y_i , $i = 1, 2, \dots, n$. The remaining members of Y_i are volume averages of the hydraulic conductivity of sand. The volumes used here are much larger than a single grid element volume and consist of the hydraulic conductivity zones mentioned previously. A total of 33 zones based on the logarithm of the hydraulic conductivity of sand for the sand component of model layers 2 through 11 were constructed by using the layer and region combinations for which hydraulic conductivity data are given in table 2. The point estimates of the logarithm of hydraulic conductivity of sand were derived from aquifer or specific-capacity tests. The geometric mean of these test data were calculated by Prudic (1991) for each layer by region. Preliminary values for these tests, which generally are about 30 percent less than those given by Prudic (1991), were used in this study and are given in table 2. The logarithm of the hydraulic conductivity of sand for a zone is calculated as the simple average of the point observations of the logarithmic values of hydraulic conductivity of sand within the zone, whether determined by aquifer or specific-capacity tests. For one of the models, model 9 below, the 33 zones based on the logarithm of the hydraulic conductivity of sand were combined into six groups, each with a corresponding zone-averaged logarithmic hydraulic conductivity of sand.

It was mentioned previously that the hydraulic conductivity of sand for a grid element j in the numerical model $f(B)$ is given by $k_j = P_j 10^{-0.8d_j}$, where P_j is the hydraulic conductivity parameter for the grid element and d_j is the depth in kilometers of the center of the grid element below ground surface. Thus, when $\log_{10}(k_j) = \log_{10}(P_j) - 0.8d_j$ is averaged over a hydraulic conductivity zone containing m grid elements j but only a single value P for

P_j , $\frac{1}{m} \sum_{i=1}^m \log_{10}(k_j) = \log_{10}(P) - 0.8d$ is obtained where $d = \frac{1}{m} \sum_{j=1}^m d_j$. When viewed as an observation, $\frac{1}{m} \sum_{j=1}^m \log_{10}(k_j)$ is one of the observations of the logarithms

of hydraulic conductivity of sand, Y_i , but when predicted by the model it is the corresponding $f_i(\hat{B})$. The single hydraulic conductivity parameter associated with the hydraulic conductivity zone containing the grid elements $j = 1, 2, \dots, m$ is P .

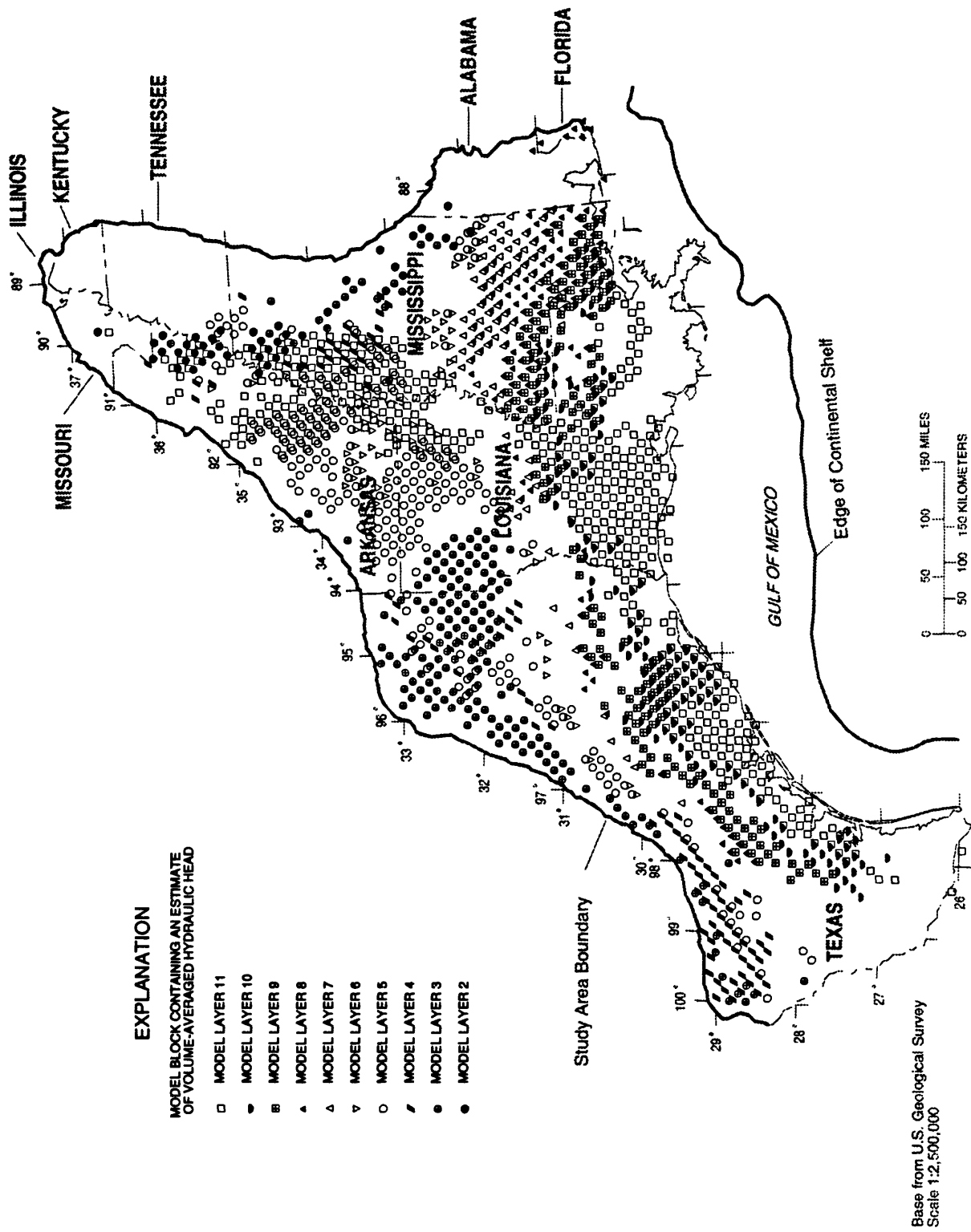


Figure 33. Location of the 1,675 grid-element volume-averaged heads for 1982.

TABLE 2.--Mean hydraulic conductivity by model layer and region

[Layer numbers are given in table 1 and region numbers are shown in figure 31. Mean base 10 logarithm of sand hydraulic conductivity is measured in units of feet per day (ft/d); mean \log_{10} hydraulic conductivity of sand is 1.481; average geometric mean hydraulic conductivity of sand is 30.3 ft/d]

Layer	Region	Mean \log_{10} sand hydraulic conductivity	Geometric mean sand hydraulic conductivity (ft/d)
2	5	1.761	57.68
3	2	0.844	6.98
3	3	1.117	13.09
3	5	1.386	24.32
4	1	1.493	31.12
4	2	1.345	22.13
4	5	1.689	48.87
5	2	1.048	11.17
5	3	1.507	32.14
5	4	1.628	42.46
5	5	1.906	80.54
5	9	1.073	11.83
6	2	0.881	7.60
6	3	1.352	22.49
6	4	1.685	48.42
6	5	1.605	40.27
7	8	1.543	34.91
7	9	1.565	36.73
8	7	1.473	29.72
8	8	1.524	33.42
8	9	1.704	50.58
9	6	0.698	4.99
9	7	1.162	14.52
9	8	1.663	46.03
9	9	1.750	56.23
10	6	0.938	8.67
10	7	1.259	18.16
10	8	1.688	48.75
10	9	1.726	53.21
11	4	2.292	195.88
11	7	1.573	37.41
11	8	2.074	118.58
11	9	1.926	84.33

The total number of observations Y_i , $i=1,2,\dots,n$ was either $n = 3,107 + 33 = 3,140$ or $n = (3,107+586) + 33 = 3,726$. Here, the number of observations of the logarithms of hydraulic conductivity of sand is 33. The number of grid-element volume-averaged heads from water-wells is 3,107; and the number of grid-element volume-averaged heads from drill-stem tests is 586. For model 9, there are 6 rather than 33 observations of the logarithms of hydraulic conductivity of sand.

Residual Weighting

In equation (5) ω is a known $n \times n$ symmetric, positive-definite matrix. The matrix ω is assumed to be diagonal. The minimization of $S(B)$ in equation (8) tends to cause $Y_i - f_i(B)$ to be small when ω_i is large, or equivalently, when the variance $\epsilon^2\omega_i^{-1}$ is small. Thus when the variance of an observable Y_i is small; that is, its value is known well, \hat{B} is found such that the model value $f_i(\hat{B})$ is close to the actual value Y_i . The variance of E_i , the i th member of the $n \times 1$ random vector E , is $\epsilon^2\omega_i^{-1}$ where ϵ is a common variance factor of choice. As explained in the modeling methodology section above, the true variance of E , $\epsilon^2\omega^{-1}$, may be approximated by apparent variance. The ω_i for the 3,107 values of grid-element volume-averaged head were separated into 10 groups, corresponding to the 10 model layers 2 through 11. Thus, $\omega_i = \omega_s$, $i = 1,2,\dots,3,107$, where s is the model layer containing the grid element i corresponding to observation Y_i .

For $s = 1,2,\dots,10$, the value of $\epsilon^2\omega_s^{-1}$ was set equal to $\frac{1}{n_s} \sum_{i=1}^{n_s} (Y_i - f_i(\hat{B}))^2$

where n_s is the number of observations in layer s . These ω_s depend upon the number of regression parameters p making up the $p \times 1$ vector of parameters B , and also upon the construction of $f(B)$. The ω_i corresponding to the 586 grid-element volume-averaged heads from drill-stem tests were

given a separate single value for $\epsilon^2\omega^{-1}$ equal to $\frac{1}{586} \sum_{i=1}^{586} (Y_i - f_i(\hat{B}))^2$. This

value was much larger than the values for $\epsilon^2\omega_s^{-1}$ above.

The $\epsilon^2\omega_i^{-1}$ for the 33 observations of the logarithms of hydraulic conductivities of sand, Y_i , were given a single value. This single value of the $\epsilon^2\omega_i^{-1}$ was calculated as the average of 10 variances. Each of these 10 variances was determined as the variance of those Y_i corresponding to model layer s , about their own mean. The value for $\epsilon^2\omega^{-1}$ obtained in this manner is approximately equal to the value for $\epsilon^2\omega^{-1}$ obtained by determining the variance of all of the 33 observations of the logarithms of the hydraulic conductivities of sand about their own single mean. In model 9, residual weighting for the six observations of the logarithms of the hydraulic conductivities of sand was done using six different values $\epsilon^2\omega_i^{-1}$ for variance. These variances were smaller than the single value of $\epsilon^2\omega^{-1}$ used for the 33 observations of the logarithms of the hydraulic conductivities of sand, as explained previously in the regression model section.

The above described estimation of the variances $\epsilon^2 \omega_i^{-1}$ for grid element volume-averaged head, made use of the values $Y_i - f_i(\hat{B})$. But to find \hat{B} in $f(\hat{B})$ one needs to minimize $S(B) = \sum_{i=1}^n (Y_i - f_i(B))^2 \omega_i$ which itself depends upon the very weights ω_i which are being sought. This apparent predicament is solved by doing several minimizations of $S(B)$, putting the ω_i from a given iteration into $S(B)$ for the next iteration. For the values ω_i , this process converges sufficiently in only two iterations.

Weighted mean square error $S(B) = \sum_{i=1}^n [Y_i - f_i(B)]^2 \omega_i$ may be written $\sum_{i=1}^n [Y'_i - f'_i(B)]^2 \omega'_i$, where $Y'_i = Y_i (\omega_i / \omega'_i)^{1/2}$, $f'_i = f_i (\omega_i / \omega'_i)^{1/2}$, and $\omega'_i = O(1)$. Thus, it is possible to normalize Y_i and f_i such that, for each of the three classes of observations: grid-element volume-averaged heads, from (1) water-well data and from (2) drill-stem tests, and (3) volume-averaged logarithms of hydraulic conductivity of sand; the weights ω_i are order unity. Normalizing heads from water wells, in conjunction with a selection for ϵ^2 , allowed the weights ω_i $i=1,2,\dots,3107$ for the grid element volume-averaged heads to satisfy $.4 < \omega_i < 1.7$ and $(1/3, 107) \sum_{i=1}^{3107} \omega_i = 1$.

In addition, the single weight for the grid-element volume-averaged heads from drill-stem tests and also the single weight for the 33 observations of the logarithms of the hydraulic conductivities of sand are allowed to both be unity.

APPLICATION OF REGRESSION FLOW MODELS AND RESULTS

The principal value of the regression methodology is that it allows one to measure the accuracy of the predictions produced by a model.

The principal use of the regression flow models in this study is to give an indication of the accuracy of the predicted values for grid-element volume-averaged head, and the logarithm of hydraulic conductivity of sand values in the models. Also desired is an indication of the accuracy of the values obtained for the regression parameters. These indications of accuracy are obtained from the prediction interval half widths and confidence interval half widths, available in equations (6) and (7) respectively.

Equation (6) above gives an approximate prediction interval for the k th member of the random vector Y of equation (4). The term in equation (6) containing the sensitivity matrix X was, except for the six observations of

the logarithms of the hydraulic conductivities of sand of model 9, always less than 4 percent of ω_k^{-1} . Dropping this term causes equation (6) to become:

$$\omega_k e_k^2 = d_{1-\alpha}^2 = S(\hat{B})D^2(p, n, \alpha) , \quad (14)$$

where

$$D^2(p, n, \alpha) = [(p+1)/(n-p)]F_\alpha(p+1, n-p) .$$

The probability is approximately (1-A)100 percent that $f_k(\hat{B}) - e_k < Y_k < f_k(\hat{B}) + e_k$, if $f_k(B)$ is a linear model. This result is exact when $f(B)$ is a linear model, and the $\omega_k^{1/2} e_k$ have a normal distribution. For fixed n, equation (14) shows that $S(\hat{B})$ will have to decrease faster with p than $D^2(p, n, \alpha)$ increases with p in order that the prediction interval half width e_k decrease with increasing p. Figure 34 shows plots of $D^2(p, n, \alpha)$ as a function of p.

Having considered the dependence of $\omega_k e_k^2$ upon p with fixed n, let us now consider its dependence upon n with fixed p. If $S(\hat{B})/(n-p)$ is written as $(1+u)\epsilon^2$, then equation (14) becomes

$$\omega_k e_k^2 = (1+u)\epsilon^2 G(p, n, \alpha) , \quad (15)$$

where

$$G = (p+1)F_\alpha(p+1, n-p) .$$

When $n \rightarrow \infty$ and $n \gg p$, it can be shown that $1+u = S(\hat{B})/[(n-p)\epsilon^2] \rightarrow 1$ (R.L. Cooley, U.S. Geological Survey, oral commun., 1989), so that when n is large, $1+u$ changes very little with n. Furthermore, for $n > 1,000$ and $p \ll n$ as in this study, G changes very little for any increase in n. Thus, $\omega_k e_k^2$ displays no strong dependence upon n.

Description of Models Used

All models have the basic features as given in the section on "Modeling Methodology and Construction." Each model has the same domain of solution. The differences between the models are: the degree and manner by which the domain of solution is partitioned into hydraulic conductivity zones; and the degree to which unknowns related to boundary conditions, the manner of the dependence of effective hydraulic conductivity on clay and hydraulic conductivity of sand, and subsidence, are parameterized. When an unknown is parameterized, an optimal value for the parameter is found by the model. If an unknown value is not parameterized, a fixed default value is used. Thus, models with a larger number of parameters are more flexible but not conceptually more complex.

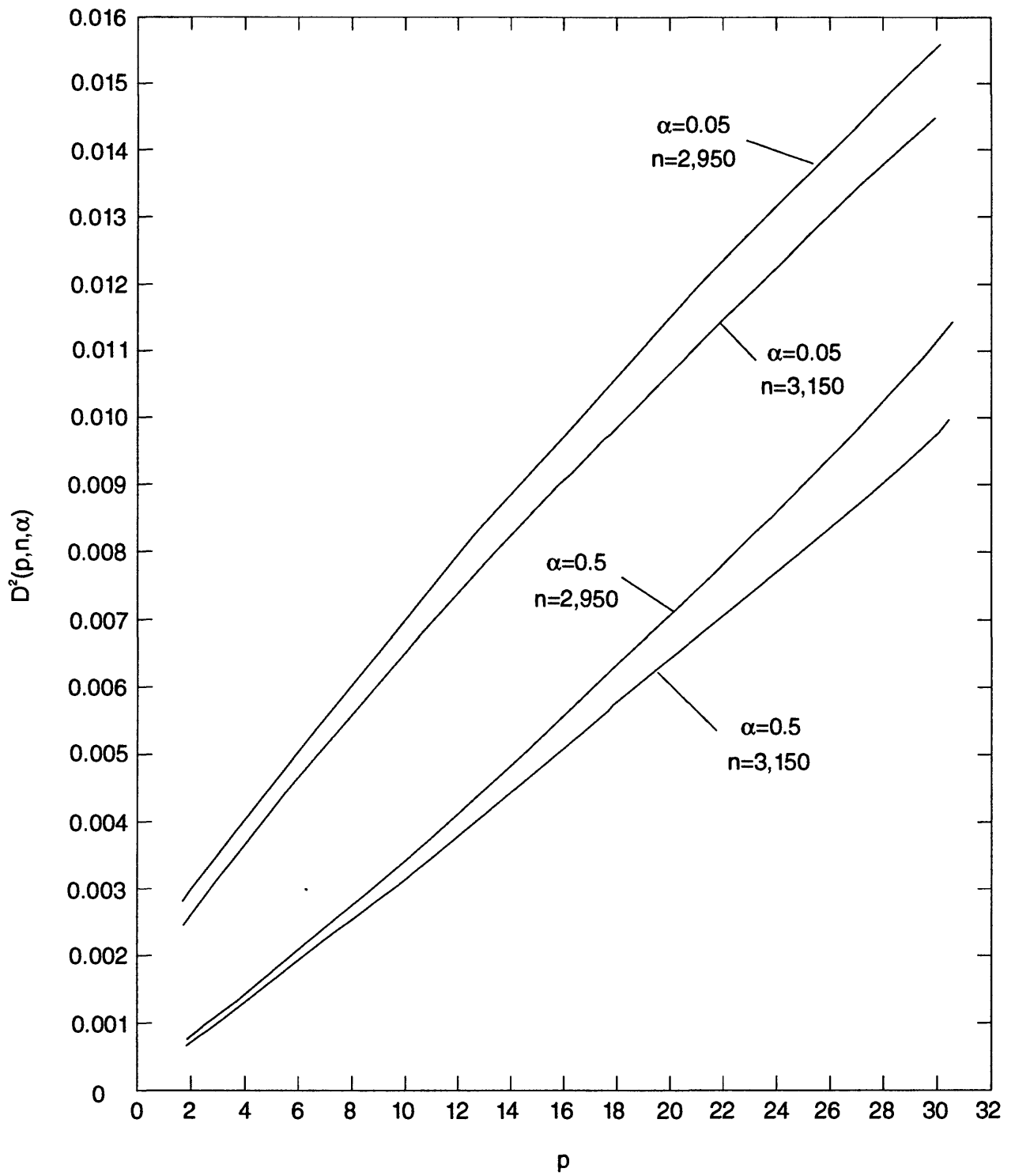


Figure 34. Change in multiplier $[D^2(p, n, \alpha)]$ for prediction interval size with number of regression parameters.

Many different numerical flow models $f(B)$, with different numbers of regression parameters p were used. Several of these are shown in table 3. The regression parameters b_i used in this table are defined as follows. The specified boundary head in the top-layer grid elements is equal to $h_w b_1 + b_2$. Here, h_w is water-table altitude or equivalent freshwater head at the sea floor, as discussed previously. The specified boundary head in the geopressured zone, shown in figure 26, is $(1,000 \text{ ft})b_3$. The value of (K_z/b) in the geopressured zone grid elements is equal to b_4 . Regression parameter b_5 is equal to .25a. Quantity a was discussed previously for use with equations (10) and (11) to calculate effective hydraulic conductivity. Regression parameter b_6 is K_y/K_x for horizontal anisotropy. Regression parameter b_7 is the parameter which when multiplied by 80 ft gives the subsidence triggering value Vh_s discussed previously. Regression parameter b_8 is the parameter that when multiplied by 40 gives the subsidence specific storage multiplication factor C_s . Regression parameter b_9 is specific storage.

In table 3, when B_j occurs in the row starting with b_i , it indicates that b_i is equal to B_j , the j th element of the $p \times 1$ regression parameter vector B . Note that more than one of the b_i may be equal to a single one of the B_j . When no entry occurs in the row b_i , it indicates that the regression parameter b_i is not used and that the default value applies. The default values for the regression parameters are $b_1 = 1$, $b_2 = 0$, $b_3 = 1$, $b_5 = 1$, $b_6 = 1$, $b_7 = 1$, and $b_8 = 1$. When b_4 is not used, (K_z/b) for the geopressured zone grid elements is set equal to either a very large number or zero. When b_4 is very large, the geopressured zone provides no resistance to vertical flow, and all resistance is provided by the model layers lying above the geopressured zone. When b_4 is zero, no flow is allowed from the geopressured zone. In table 3, entry 0 for b_4 denotes that (K_z/b) is zero, "very large" denotes that (K_z/b) is very large. Default values of regression parameters b_i were selected to prevent biasing results in favor of few regression parameter models. Such a bias occurs when results from models with many regression parameters are used to arrive at default values of the parameters in a model with few parameters. For example, if a given model $f(B)$ with many regression parameters determines that b_7 (the regression estimate for \hat{b}_7 corresponding to $B = \hat{B}$) should be 1.3, then in another model $f(B)$ with few parameters in which b_7 is not used, the default value of b_7 may not be set to 1.3, and so forth. The single value b_9 of the specific storage for the aquifer domain of solution, is always used and hence has no default value.

The entries in table 3 below row b_9 give the assignment of regression parameters to the hydraulic conductivity zones. For example, model 3 has $B_1 = b_1 = b_3$ and $B_2 = b_9$. Regression parameter B_3 is assigned to the hydraulic conductivity of clay of all those hydraulic conductivity zones contained in model layers 2 through 11, top-layer 12, and also model layers 13 through 17 which represent confining units. Regression parameter B_4 is

TABLE 3.—Regression parameters for models 1 through 12

[When B_j occurs in the row starting with b_j , it indicates that b_j is equal to B_j , the j^{th} element of the $p \times 1$ regression parameter vector B . Note that more than one of the b_j may be equal to a single one of the B_j . Shading indicates that combination of models and parameters was not used or was not applicable; do, ditto; VL, is very large]

Sediment	Model											
	1	2	3	4	5	6	7	8	9	10	11	12
Number of parameters	2	3	4	4	6	7	8	9	11	18	26	31
b_1 for head in top layer	B1	B1	B1	B1	B1	B1	B1	B1	B1	B1	B1	B1
b_2 for head in top layer (feet)												
b_3 for geopressed head			B1		B2	B1	B1	B2		B1	B1	B1
b_4 for geopressed head (day^{-1})	0	0	VL	0	B3	VL	VL	B3	0	B2	B2	B2
b_5 for .25a in equations 10 and 11								B4		B3	B3	B3
b_6 horizontal anisotropy												
b_7 for subsidence triggering head											B4	B4
b_8 for subsidence specific storage												
b_9 specific storage (feet^{-1})	B1	B2	B2	B2	B4	B2	B2	B7	B2	B5	B5	B5
Layer 2	B2	B3	B3	B3	B5	B3	B3 and B5	B8	B3	B6		B6
Layer 3	do	do	do	do	do	do	do	do	do	do		B7
Layer 4	do	do	do	do	do	do	do	do	do	do		B8
Layer 5	do	do	do	do	do	do	do	do	do	do		B9
Layer 6	do	do	do	do	do	do	do	do	do	do		B10
Layer 7	do	do	do	do	do	B4	do	do	do	do		B11

Clay hydraulic conductivity

TABLE 3.—Regression parameters for models 1 through 12—Continued

Sediment	Model											
	1	2	3	4	5	6	7	8	9	10	11	12
Layer 8	B2	B3	B3	B3	B5	B4	B3 and B5	B8	B3	B6		B12
Layer 9	do	do	do	do	do	do	do	do	do	do		B13
Layer 10	do	do	do	do	do	do	do	do	do	do		B14
Layer 11	do	do	do	do	do	do	do	do	do	do		B15
Layer 12	do	do	do	do	do	do	do	do	do	B7	B6	B16
Layers 13-17	do	do	do	do	do	B5	B4 and B6	do	B4	B8		B17-B21
Region 1							B3 and B4					
Region 2							do					
Region 3							do					
Region 4							do					
Region 5							do					
Region 6							B5 and B6					
Region 7							do					
Region 8							do					
Region 9							do					
Region 10							do					

Clay hydraulic conductivity

TABLE 3.—Regression parameters for models 1 through 12—Continued

Sediment	Model											
	1	2	3	4	5	6	7	8	9	10	11	12
Layer 2	B2	B3	B4	B4	B6	B6	B6	B9	B5-B11	B9	B9	B22
Layer 3	do	do	do	do	do	do	do	do	do	B10	B10	B23
Layer 4	do	do	do	do	do	do	do	do	do	B11	B11	B24
Layer 5	do	do	do	do	do	do	do	do	do	B12	B12	B25
Layer 6	do	do	do	do	do	do	do	do	do	B13	B13	B26
Layer 7	do	do	do	do	do	B7	do	do	do	B14	B14	B27
Layer 8	do	do	do	do	do	do	do	do	do	B15	B15	B28
Layer 9	do	do	do	do	do	do	do	do	do	B16	B16	B29
Layer 10	do	do	do	do	do	do	do	do	do	B17	B17	B30
Layer 11	do	do	do	do	do	do	do	do	do	B18	B18	B31
Region 1	do											
Region 2	do											
Region 3	do											
Region 4	do											
Region 5	do											
Region 6	B8	do	do	B17	do							
Region 7	do	do	do	do	do	do	do	do	do	do	B18	do
Region 8	do	do	do	do	do	do	do	do	do	do	B19	do
Region 9	do	do	do	do	do	do	do	do	do	do	B20	do
Region 10	do	do	do	do	do	do	do	do	do	do	B21	do
Region 6	do	do	do	do	do	do	do	do	do	do	B22	do
Region 7	do	do	do	do	do	do	do	do	do	do	B23	do
Region 8	do	do	do	do	do	do	do	do	do	do	B24	do
Region 9	do	do	do	do	do	do	do	do	do	do	B25	do
Region 10	do	do	do	do	do	do	do	do	do	do	B26	do

Sand hydraulic conductivity

assigned to the hydraulic conductivity of sand of model layers 2 through 11. Top-layer 12, and confining units represented by model layers 13 through 17 have no sand and thus need no regression parameter assignment.

Table 3 is self explanatory except for the following. The regions mentioned are those of figure 31, and allow for a horizontal discretization as opposed to vertical discretization using the layers. For hydraulic conductivity of clay, model 7 uses B_3 and B_5 for layers 2 through 11, B_3 in regions 1 through 5 and B_5 in regions 6 through 10. B_4 and B_6 are used for layer 12, B_4 for regions 1 through 5, and B_6 for regions 6 through 10. For hydraulic conductivity of sand, model 9 uses a discretization of the domain of solution into seven zones, selected on the basis of hydrogeologic considerations. Each of these zones correspond to various combinations of the layers and regions. B_5 through B_{11} are used for these seven zones. Model 12 uses B_{17} through B_{21} for layers 13 through 17.

The following is a short description of the models of table 3 in physical terms. The specific storage, the horizontal hydraulic conductivity of sand, and the vertical hydraulic conductivity of clay were allowed to vary within bounds and the values were determined as a result of the regression model and are tabulated in table 4. Other factors such as the head in the geopressed zone, the altitude of the water table, and head decline necessary for the onset of land subsidence were allowed to vary in some models but were fixed in other models.

The value of specific storage for layers 2 through 11 ranged from 4.5×10^{-7} to 8.0×10^{-7} , except that model 12 had a specific storage of 3.0×10^{-8} . The horizontal hydraulic conductivity of sand was uniform at about 30 ft/d for all layers in models 1, 2, 3, 4, 5, and 6. Both models 10 and 12 have different values of horizontal hydraulic conductivity of sand for each layer. The values range from about 8 ft/d for layer 3 in model 10 to 650 ft/d for layer 2 in model 12. Models 10 and 12 are similar in that layers that have large values of horizontal hydraulic conductivity of sand in one model also have large values in the other model. Two values of horizontal hydraulic conductivity of sand were used in model 6; the values are about 73 ft/d for layers 2 through 6 and 25 ft/d for layers 7 through 11. The horizontal hydraulic conductivity of sand varied by geographic region in models 7 and 11. The variability was greater in model 11 with 10 conductivity values ranging from 5 ft/d to 134 ft/d, than in model 7 with 2 values of about 24 ft/d and 68 ft/d. Six values of horizontal hydraulic conductivity of sand were used in model 9; the values range from about 6 ft/d to about 380 ft/d. These values were for combinations of layer and geographic region which, in general, correspond to area and layer combinations of Prudic (1991, p. 28), and the values used correspond closely to the geometric means presented by Prudic (1991).

The vertical hydraulic conductivity of clay was uniform for both the clay fraction within aquifers and for the confining units in models 1 through 5, and model 8; the values range from about 3.6×10^{-4} ft/d to about 30 ft/d. In models 6, 7, 9, 10, and 12 the hydraulic conductivity of

TABLE 4.—Results from flow models 1 through 12

[The 95 percent prediction intervals for the observations are obtained from $w_k^{1/2} \sigma_k$, the 95 percent confidence intervals for the parameters with entry $a(b)$ are from $a(b)^{-1}$ to $a(b)$. Shading indicates that combination of models and parameters was not used or was not applicable; do, ditto]

	Model											
	1	2	3	4	5	6	7	8	9	10	11	12
Number of parameters	2	3	4	4	6	7	8	9	11	18	26	31
$w_k^{1/2} \sigma_k$ of equation 14	175	166	141	141	157	162	168	178	167	214	219	243
(1+u) of equation 15	3.17	2.42	1.50	1.49	1.48	1.45	1.43	1.48	1.14	1.29	1.02	1.11
Mean weight residual	33.2	9.23	2.64	2.54	2.53	2.20	1.48	2.34	3.74	2.22	1.70	2.64
Root-mean-square weighted residual	60.5	53.0	41.6	41.5	41.4	40.96	40.72	41.4	36.3	38.6	34.4	35.9
Chi ²	678	413	316	324	326	204	242	321	260	261	164	188
Parameters:												
b_1 for head in top layer	.834 (1.04)		.898 (1.04)	.899 (1.04)	0.900 (1.04)	0.913 (1.05)	.901 (1.05)	0.900 (1.05)	.932 (1.05)	0.913 (1.07)	.920 (1.07)	.911 (1.06)
b_2 for head in top layer (feet)			.898 (1.04)									
b_3 for geopressured head					0.054 (>10 ³)	0.913 (1.05)	.901 (1.05)	0.25 (>10 ³)		.913 (1.07)	.920 (1.07)	.911 (1.06)
b_4 for geopressured head (day ⁻¹)					1.25x10 ⁻⁸ (>10 ³)			0.94x10 ⁻⁸ (>10 ³)		.16x10 ⁻⁴ (>10 ³)	1.5x10 ⁻⁵ (>10 ³)	.71x10 ⁻⁵ (>10 ³)
b_5 for 25s in equations 10 and 11								1.01 (1.14)		.97 (1.19)	1.09 (1.22)	.88 (1.20)
b_6 horizontal anisotropy												
b_7 for subsidence triggering head											1.28 (1.92)	2.75 (99.2)
b_8 for subsidence specific storage												
b_9 specific storage (feet ⁻¹)	.66x10 ⁻⁶ (>10 ³)	.66x10 ⁻⁶ (>10 ³)	.45x10 ⁻⁶ (1.73)	.45x10 ⁻⁶ (1.73)	.47x10 ⁻⁶ (1.93)	.46x10 ⁻⁶ (2.03)	.54x10 ⁻⁶ (2.04)	.54x10 ⁻⁶ (12.1)	.51x10 ⁻⁶ (1.83)	.68x10 ⁻⁶ (3.94)	.86x10 ⁻⁶ (4.70)	.30x10 ⁻⁷ (6.61)

TABLE 4.—Results for flow models 1 through 12—Continued

		Model											
		1	2	3	4	5	6	7	8	9	10	11	12
		Clay hydraulic conductivity parameters (feet per day)											
Layer 2	29.9 (1.63)	29.9 (1.66)	$.365 \times 10^{-3}$ (1.23)	$.362 \times 10^{-3}$ (1.23)	$.361 \times 10^{-3}$ (1.26)	$.12 \times 10^{-3}$ (2.27)	$.47 \times 10^{-3}$ (2.70) $.55 \times 10^{-3}$ (1.33)	$.374 \times 10^{-3}$ (1.53)	22×10^{-3} (1.32)	$.26 \times 10^{-3}$ (2.03)			$.78 \times 10^{-4}$ ($>10^3$)
Layer 3	do	do	do	do	do	do	do	do	do	do	do		$.26 \times 10^{-2}$ (22.3)
Layer 4	do	do	do	do	do	do	do	do	do	do	do		$.94 \times 10^{-3}$ ($>10^3$)
Layer 5	do	do	do	do	do	do	do	do	do	do	do		$.44 \times 10^{-4}$ (51.9)
Layer 6	do	do	do	do	do	do	do	do	do	do	do		22×10^{-1} ($>10^3$)
Layers 7	do	do	do	do	do	$.39 \times 10^{-3}$ (1.33)	do	do	do	do	do		$.53 \times 10^{-4}$ (4.90)
Layer 8	do	do	do	do	do	$.39 \times 10^{-3}$ (1.33)	do	do	do	do	do		$.83 \times 10^{-2}$ (26.7)
Layer 9	do	do	do	do	do	do	do	do	do	do	do		$.29 \times 10^{-2}$ (5.86)
Layer 10	do	do	do	do	do	do	do	do	do	do	do		2.98 ($>10^3$)
Layer 11	do	do	do	do	do	do	do	do	do	do	do		$.11 \times 10^{-3}$ (2.70)
Layer 12	do	do	do	do	do	do	do	do	do	do	$.98 \times 10^{-3}$ (670)	$.11 \times 10^{-2}$ ($>10^3$)	$.31 \times 10^{-2}$ ($>10^3$)
Layers 13-17	do	do	do	do	do	22×10^{-4} (2.72)	$.29 \times 10^{-4}$ (3.36) $.21 \times 10^{-5}$ ($>10^3$)	do	$.11 \times 10^{-3}$ (1.67)	$.67 \times 10^{-4}$ (2.19)			$.48 \times 10^{-6}$ (>9) $.16 \times 10^{-3}$
Region 1													$.24 \times 10^{-3}$ (2.76)
Region 2													$.10 \times 10^{-3}$ (3.23)
Region 3													$.33 \times 10^{-4}$ (2.28)
Region 4													$.66 \times 10^{-3}$ (4.34)
Region 5													$.35 \times 10^{-3}$ (5.41)
Region 6													$.21 \times 10^{-3}$ (4.75)
Region 7													$.30 \times 10^{-3}$ (1.88)
Region 8													$.31 \times 10^{-3}$ (3.53)
Region 9													$.68 \times 10^{-3}$ (2.43)
Region 10													$.27 \times 10^{-3}$ ($>10^3$)

TABLE 4.—Results for flow models 1 through 12—Continued

Model		1	2	3	4	5	6	7	8	9	10	11	12
		Sand hydraulic conductivity parameters (feet per day)											
Layer 2		29.9 (1.63)	29.9 (1.66)	29.9 (1.20)	30.3 (1.19)	30.3 (1.23)	72.7 (1.22)		29.0 (1.31)		266.0 (2.50)		650 (2.88)
Layer 3		do	do	do	do	do	do		do		7.6 (4.27)		8.70 (6.36)
Layer 4		do	do	do	do	do	do		do		75.0 (1.83)		57.6 (2.49)
Layer 5		do	do	do	do	do	do		do		35.8 (1.87)		47.0 (2.32)
Layer 6		do	do	do	do	do	do		do		58.7 (2.83)		58.3(4.38)
Layer 7		do	do	do	do	do	25.0 (1.35)		do		34.3 (4.72)		53.8 (5.10)
Layer 8		do	do	do	do	do	do		do		55.5 (2.95)		125 (3.07)
Layer 9		do	do	do	do	do	do		do		27.2 (2.54)		19.1 (3.77)
Layer 10		do	do	do	do	do	do		do		9.7 (2.18)		11.8 (2.48)
Layer 11		do	do	do	do	do	do		do		49.1 (1.92)		84.9 (2.11)
Region 1								68.2 (1.24)		group 1 383.0 (2.03)		17 (2.37)	
Region 2								do		group 2 115.0 (1.44)		12 (3.07)	
Region 3								do		group 3 94.3 (1.33)		10 (2.65)	
Region 4								do		group 4 30.0 (1.39)		134 (3.49)	
Region 5								do		group 5 14.9 (1.51)		67 (2.60)	
Region 6								24.2 (1.37)		group 6 6.53 (1.95)		19 (5.27)	
Region 7								do		group 7 16.4 (2.55)		18 (1.93)	
Region 8								do				72 (2.67)	
Region 9								do				72 (1.92)	
Region 10								do				5 (>10 ³)	

clay within the aquifers had a different value than that for the confining units. In model 11 the vertical hydraulic conductivity of clay was uniform throughout each of the 10 geographic areas for clay both within aquifers and confining units. In model 12 a separate value of vertical hydraulic conductivity of clay was used for each aquifer and each confining unit; the values range from 4.8×10^{-7} ft/d to about 3 ft/d.

The estimated water-table altitude was reduced by a factor ranging from 0.834 to 0.932, except that for model 1 the water-table was fixed at the values estimated by Williams and Williamson (1989). The flow of water to and from the water table was controlled by a hydraulic conductivity factor for the top layer 12 and the value was the same as that for the vertical hydraulic conductivity of clay within aquifers for models 1 through 9.

The top of the geopressured zone was assumed to be a no-flow boundary in models 1, 2, 4, and 9. A head of 1,000 ft at the top of the geopressured zone was reduced by a factor in models 3, 5, 6, 7, 8, 10, 11, 12; the reduction factors ranged from 0.054 to 0.92. A parameter analogous to the "vertical conductance" of MacDonald and Harbaugh (1988) for controlling flow from the geopressured zone was determined for models 5, 8, 10, and 11; the values range from 9.4×10^{-9} d⁻¹ to 1.6×10^{-5} d⁻¹. The resistance to vertical flow for models 3, 6, 7, and 12 was due to clay in the sediments above the geopressured zone and no "vertical conductance" value was used for the geopressured zone.

The onset of land subsidence began after a head decline of 80 ft from predevelopment in models 1 through 7 and model 9. The head decline necessary for the onset of land subsidence ranged between 102 ft and 220 ft for models 8, 10, 11, and 12.

The coefficient used to adjust hydraulic conductivity and obtain "effective" hydraulic conductivity according to equations 10 and 11 was allowed to vary in models 8, 10, 11, and 12; the values ranged from 0.22 to 0.27.

The results from the flow models f(B) defined in table 3 for $n = 3,107 + 33 = 3,140$, except for model 9 which has $n = 3,107 + 6 = 3,113$, are given in table 4. As mentioned previously, 3,107 is the number of grid-element volume-averaged heads from water wells, and 33 or 6 is the number of observations of the logarithms of the hydraulic conductivities of sand. Models using $n = 3,107 + 33 + 586 = 3,726$ and including the drill-stem data were also used and have similar results. These models were considered to be somewhat less reliable because of possible bias in the preparation of the drill-stem test data, and are thus not shown. Sources of bias are the proximity of wells to active oil fields and the indirect procedure for arriving at formation pressure from drill-stem tests. The second row of table 4 gives $\omega_k^{1/2}e_k$ of equation (14) for the 95-percent prediction interval for random variable Y_k . The number shown for $\omega_k^{1/2}e_k$ is

in feet for Y_k corresponding to the grid-element volume-averaged heads Y_i , $i = 1, 2, \dots, 3, 107$. As shown previously, these ω_k vary from 0.4 to 1.7. For model layers 2 through 11, the values of ω_s $s = 1, 2, \dots, 10$ are: 1.1, 0.5, 0.4, 0.5, 1.1, 0.8, 0.8, 0.5, 0.6, and 1.7. Thus, for layer 2 in the third model, for example, the probability is approximately 95 percent that $f_k(\hat{B}) - 141(1.1)^{-1/2} < Y_k < f_k(\hat{B}) + 141(1.1)^{-1/2}$. In other words, the probability is 95 percent that the observed values of grid-element volume-averaged head in layer 2 lie within $\pm 141(1.1)^{-1/2}$ ft of the model predicted values. This prediction interval applies to grid-element volume-averaged heads at or in the vicinity of the grid-element volume-averaged heads in layer 2 (fig. 33). Because all of the grid-element volume-averaged heads from water wells were at relatively shallow depths, this prediction interval does not apply to deep head values.

For the 33 observations of the logarithm of the hydraulic conductivities of sand, Y_i , the number shown for $\omega_k^{1/2} e_k$ needs to be divided by 149 to yield the desired prediction interval half width. The factor 149 is $(\omega_i/\omega'_i)^{1/2}$ of the previous section. For flow model 3, for example, the probability is approximately 95 percent that $\log_{10}(29.9) - 0.8dd_k - (141/149) < Y_k < \log_{10}(29.9) - 0.8dd_k + (141/149)$, or that $\log_{10}(29.9) - (141/149) < (Y_k + 0.8dd_k) < \log_{10}(29.9) + (141/149)$. Here, Y_k is the log of the volume-averaged logarithm of hydraulic conductivity (ft/d) of sand of zone k, one of the 33 zones based on the logarithm of the hydraulic conductivity of sand, or a zone in the vicinity of these zones. The average depth of hydraulic conductivity zone k, measured in kilometers, is dd_k . Each Y_k has the same predicted value $\log_{10}(29.9) - 0.8dd_k$. The single hydraulic conductivity of sand parameter for each hydraulic conductivity zone k is 29.9 ft/d. Note that the 33 observed values of $Y_i + 0.8dd_i$ shown in table 2 have the average value $1.481 = \log_{10}(30.3)$ and fall within the 95-percent prediction interval $\log_{10}(29.9) \pm (141/149)$. As with head, the 33 Y_i are at relatively shallow depths.

Appearing in the third through sixth rows in table 4 are $(S(B)/(n-p)\epsilon^2) = (1+u)$, the mean weighted residual $(1/n) \sum_{i=1}^n [Y_i - f_i(\hat{B})] \omega_i^{1/2}$, the root-mean square-weighted residual $[(1/n) \sum_{i=1}^n (Y_i - f_i(\hat{B}))^2 \omega_i]^{1/2} = [S(\hat{B})/n]^{1/2}$, and Chi^2 to be discussed in the next section. Also shown in table 4 are the values obtained for the regression parameter estimates (the elements of the $p \times 1$ vector \hat{B}), and also the confidence intervals of these values as obtained from equation (7). For example, model 3 in table 4 shows $\hat{b}_9 = \hat{B}_2$, the specific storage, equal to $0.45 \times 10^{-6} \text{ft}^{-1}$ (the specific storage for pure water is approximately $1.5 \times 10^{-6} \text{ft}^{-1}$). The 95-percent confidence interval for $b_9 = B_2$ is from $0.45 \times 10^{-6}(1.73)^{-1} \text{ft}^{-1}$ to $0.45 \times 10^{-6}(1.73) \text{ft}^{-1}$. As with the other regression parameters, the confidence interval is expressed in multiplicative factor form because the parameter variable used in the minimization routine was the base 10 logarithm of the parameter rather than the parameter itself. The units of b_1, \dots, b_9 are: 1, feet, 1, (day) $^{-1}$, 1, 1, 1, 1, and (feet) $^{-1}$. The units of the hydraulic conductivity of clay and sand parameters are ft/d.

Choosing the Best Regression Model

Draper and Smith (1981), chapter 6, suggest several methods for selecting the "best" regression equation or model. One procedure is to plot mean square residual as a function of the number of parameters p . Such a plot is shown in their figure 6.1, p. 298. Draper and Smith state that when mean square residual versus p ceases to decrease with increasing p , then an optimal choice for the number of parameters is the value of p where further decline in the mean-square residual is small. Values for root-mean square-weighted residual, $(S(\hat{B})/n)^{\frac{1}{2}}$, are shown in table 4. Note that the values shown for $(S(B)/n)^{\frac{1}{2}}$, and thus also the variances $[S(\hat{B})/(n-p)]\omega_k^{-1}$ of the Y_k (recall that the variance of Y_k is $[S(\hat{B})/(n-p)][\hat{X}_k(\hat{X}^T\omega\hat{X})^{-1}\hat{X}_k^T+\omega_k^{-1}]=[S(\hat{B})/(n-p)]\omega_k^{-1}$), do not decrease appreciably with increasing p . For example, model 4 with $p = 4$ has a root-mean square-weighted residual of 41.5, but model 12 with almost eight times as many regression parameters has a root-mean square residual of 35.9, only 13 percent less. This would suggest that an optimal choice for p would be quite small and that $p = 4$ would perhaps be a reasonable choice.

A second trend shown in table 4 is that although the root-mean square-weighted residual generally decreases as the number of regression parameters p used increases, the prediction interval half width e_k increases as p increases if p is greater than 4. In other words, even though the fit of the 3,107 heads and 33 logarithm values of hydraulic conductivity of sand becomes better as the number of regression parameters increases, the certainty that one has in the predicted values for head and hydraulic conductivity decreases with increasing p , if p exceeds 4.

A related trend in table 4 is that the confidence that one has in the values obtained for the regression parameters tends to decrease (the 95-percent confidence intervals increase) as the number of parameters increases above 4. For example, model 3 predicts that the value of regression parameter B_4 for the hydraulic conductivity of sand of model layers 2 through 11 is 29.9 ft/d, and that there is 95-percent confidence that the actual value of B_4 is between 29.9/1.20 ft/d and $(29.9)(1.20)$ ft/d. For model 10 with $p = 18$, which has the regression parameters B_9 through B_{18} for the hydraulic conductivity of sand for model layers 2 through 11, values for B_9 through B_{18} are not known with the same amount of confidence as in model 3. For example, model 10 has a value for B_{10} of 7.6 ft/d, but the 95-percent confidence interval is from $7.6(4.27)^{-1}$ ft/d to $(7.6)(4.27)$ ft/d. Note that model 12, with 31 regression parameters, shows larger confidence intervals for the 10 parameters for the hydraulic conductivity of sand of model layers 2 through 11 than does model 10 with 18 regression parameters.

The above discussions regarding prediction and confidence interval behavior as a function of the number of parameters p tend to lend support to the choice of a small value for p , if values for the prediction and confidence intervals are assumed to be accurate or accurate relative to each other. This assumption would be in question if the residuals were to exhibit a considerable lack of normality. As discussed below, such lack of

normality was in fact the case, so that the prediction interval half widths e_k calculated and shown in table 4 may not be accurate. The regression parameter confidence intervals shown may also be inaccurate for the same reason. Thus using the widths of these intervals as a criteria for selecting an optimal $f(B)$ or p may be in question.

Regression parameter variances, mentioned previously but not shown in table 4, increase as p increases. For example, model 4 has 30.3 ft/d for the hydraulic conductivity of sand parameter (P_s). The variation of $\log_{10}(P_s)$ within one standard deviation of $\log_{10}(30.3)$ allows P_s to vary in the range $30.3(1.06)^{-1}$ to $30.3(1.06)$ ft/d. However, for model 12 layer 8 for example, the range is $125(1.18)^{-1}$ to $1.25(1.18)$ ft/d. As with prediction and confidence interval half widths, regression parameter variances will be in error if there is a lack of normality.

The above results regarding: the very slow decrease of root-mean square-weighted residual with p greater than 4, the increase of prediction interval half-widths with p greater than 4, and the increase of regression parameter variances with p , lead to the conclusion that a model with a relatively small number of regression parameters would probably be the best choice.

Analysis of Residuals

The weighted residuals for all models used were tested to see if they differed significantly from those drawn from a normal distribution. Deviations from a normal distribution indicate the possible presence of factors that cause residuals to differ from those resulting solely from random fluctuations in the hydraulic conductivity or other properties of the porous medium, and (or) random measurement error. Significant deviations also preclude further model testing based on Chi^2 , F , or t distributions. The standard Chi^2 test for normality (Croxtton, 1953, p. 282-283) was used, for which the number of classes was approximated using the relation $5 \log(n) = 16$ (Panofsky and Brier, 1965, p. 4). The variance used for the test is given by

$$v^2 = \frac{1}{n} \sum_{i=1}^n (Y_i - f_i(\hat{B}))^2 \omega_i - \text{Mu}^2 = S(B) - \text{Mu}^2 ,$$

where the mean-weighted residual Mu (shown in table 4) is given by

$$\text{Mu} = \frac{1}{n} \sum_{i=1}^n (Y_i - f(B)) \omega_i^{\frac{1}{2}} .$$

Normality of the weighted residuals would result in $Z_i = \{[Y_i - f_i(B)] \omega_i^{\frac{1}{2}} - \text{Mu}\} / v$ being $N(0,1)$. Because of the use of v and also Mu , the number of degrees of freedom for the Chi^2 test is (number of classes) - 3 = 16 - 3 = 13. It may be preferable to test whether Z_i with Mu set equal to zero is $\sim N(0,1)$, because the model $f(B)$ should at least be able to produce $f_i(\hat{B})$ such that $\text{Mu}^2 \ll v^2$. This approach would give essentially the same results because as table 4 shows, values for Mu^2 were much smaller than v^2 .

For 13 degrees of freedom, the hypothesis of normality of the weighted residuals is rejected at the 1-percent significance level for $\text{Chi}^2 > 27.7$ (Hogg and Craig, 1965). That normality is rejected in every case by a considerable margin is shown in table 4. Typical results for the number of points falling into the 16 classes of equal probability on the $N(0,1)$ curve show a nonuniform distribution, generally with a sizable number of excess points falling into the far right interval corresponding to the largest positive values for the residual defined as $Y_i - f_i(B)$. For example, model 4 has the following numbers of points in the 16 classes: 131, 153, 185, 229, 248, 288, 276, 261, 184, 197, 179, 163, 134, 98, 109, and 305. A uniform spread indicating normality would have approximately 196 points in each interval.

At one point in the study, the observed grid-element volume-averaged heads Y_i were rejected when, for the original set of 3,140 predicted values $f_i(B)$, they fell in the far right class of the 16 classes. After eliminating these approximately 300 observations, a new B was found. The new Chi^2 value for the new B was dramatically reduced from its original value. When an application of this culling procedure was applied to model 4, the number of observations was reduced by 314 from 3,140 to 2,826, and the value for Chi^2 fell from 324 to 65. The new model $f(B)$ gave different results, because it was based on the new culled set of 2,826 observations. The root-mean square-weighted residual fell from 41.5 to 28.8. The value for $\omega_k^{1/2} e_k$ fell from 141 to 128. The hydraulic conductivity of clay and sand parameters, 0.362×10^{-3} and 30.3 ft/d, changed to 0.407×10^{-3} and 37.3 ft/d. When this culling procedure was applied to model 9 with 11 regression parameters, the value of Chi^2 fell from 260 to 56. Since the Chi^2 values 65 and 56 are greater than 27.7, the hypothesis of normality is rejected at the 1-percent significance level.

The possibility that the logarithms of the hydraulic conductivities of sand and the grid-element volume-averaged heads were incompatible, thus causing large Chi^2 values, was investigated by deleting the use of the logarithms of the hydraulic conductivities of sand as observables and determining the corresponding Chi^2 values. No decrease in Chi^2 values was found so that this possibility is rejected.

The most likely cause of the large Chi^2 values is that the 10-mi grid spacing is very large with respect to the variability of the head. Most of the head data is from shallow depths and is heavily influenced by land-surface altitude. This can be seen from the very close similarity between water-table altitude in figure 6 and land-surface altitude in figure 2. Note that within only a single 10 mi by 10 mi grid, land-surface altitude may have a complex nature and that there may be several hill tops and valleys along a given cross section. It is thus unlikely that the residuals for grid-element volume-averaged head would be approximately statistically normal, which is what is required for small Chi^2 values. More likely, the residual would express some land-surface altitude characteristic. This would be true even if the effective hydraulic conductivity was constant or had an exact log normal distribution.

A model with a 30-mi grid spacing was used early in the study and gave residuals that were considerably larger than those for a 10-mi grid spacing. Although Chi^2 values were not actually determined, the residuals had a pronounced pattern that suggest the model would have had very large Chi^2 values for this reason.

A complicating factor is that head measurements have some tendency to be located near areas of pumping which may be near the edge of a grid element, but the model approximates the somewhat centrally weighted average drawdown that would be produced in a grid element as if all the pumping in the grid element was located at the center of the grid element.

It would be appropriate to use a much smaller grid spacing in those parts of the aquifer system where the head shows considerable variability. This was not done because of the already large number of nodes in the computer model.

Several methods (Draper and Smith, 1981, p. 34-40) are available to investigate lack of fit and the presence of model bias. Bias causes the inflation of what is, herein, called apparent variance with respect to true variance. Plots of residuals $Y_i - f_i(B)$ for grid-element volume-average head were observed for each of the model layers 2 through 11. No discernible pattern or bias was seemingly present using this simple approach to investigate lack of fit. Values for mean residual grid-element volume-averaged head by layers were less than 10 ft in magnitude for each of the layers 2 through 11 for each of the models with four or more parameters. For these same models, values for the mean-weighted residual (table 4) for all of the observations were ususally less than 3 ft.

Other methods available to investigate the presence of lack of fit make use of prior estimates of variance or repeat measurements and are thus not applicable.

Comparison of Models

To show self consistency of the regression approach, it is appropriate that the 12 models in table 4 be compared with respect to their predictions $f_i(\hat{B})$ for the observed quantities Y_i , which are composed of the 3,107 grid-element volume-averaged heads, and the 33 or 6 observations of the logarithm of the hydraulic conductivities of sand. The models should also be compared with respect to their predictions for flow even though there are no prediction intervals for flow.

Models 1 and 2, with two and three regression parameters, respectively, gave flow rates from the upland surface recharge areas to the lower altitude discharge areas on land or the sea floor which were approximately 10 times larger than those of the other models, and also larger than would be expected from precipitation data and infiltration estimates. This might be

expected, because the observations did not include flow rates, and these two models allowed only a single hydraulic conductivity for both the clay and sand components in the entire domain of solution. These two models are thus rejected and will not be considered.

The 10 models 3 through 12 gave nearly the same value for the mean weighted residual head. The predicted heads $f_i(\hat{B})$, $i = 1, 2, \dots, 3, 107$, averaged by layer, differ between the 10 models by as much as 30 ft for one layer, but less than 5 ft for most of the layers. These values are well within the 95-percent prediction interval half widths e_k , which in table 4 show values of from $141 \text{ ft}/(1.7)^{\frac{1}{2}} = 108 \text{ ft}$ to $243 \text{ ft}/(.4)^{\frac{1}{2}} = 384 \text{ ft}$. Figures 10 through 19 show the values for head as produced by model 4, the model in table 4 with the smallest value for $\omega_k^{\frac{1}{2}}e_k$, for the year 1982. Predicted heads at deep parts of the aquifer system showed differences of up to 800 ft between the 10 models, 3 through 12.

Results for predictions of the 33 logarithm values of hydraulic conductivity of sand also show good overlap between the prediction intervals of the 10 models. Model 3, with four regression parameters, has the interval $\log_{10}(29.9) - 0.8dd_k \pm 141/149$ as the 95-percent prediction interval for each of the 33 logarithm values of hydraulic conductivity of sand, each of which has the predicted value of $\log_{10}(29.9) - 0.8dd_k$. The other prediction intervals for hydraulic conductivity of sand in the 10 models overlap to a high degree. The most extreme case is that of the predicted value of $\log_{10}(650) - 0.8dd_k$ for the 33 logarithm values of hydraulic conductivity of sand in layer 2 in model 12. The prediction interval in this case is $\log_{10}(650) - 0.8dd_k \pm 243/149$, which is a wide interval that overlaps $\log_{10}(29.9) - 0.8dd_k \pm 141/149$ of model 3.

The flow rates obtained from the models in table 4 were compared by looking at the total flow across various surfaces cutting across the domain of solution and also by looking at the flow rates across the many individual grid element faces. One of these sets of surfaces separate the layers. Values were obtained for the flow into and out of the top and bottom surfaces of each of the 10 model layers, a total of 40 flow rates. Comparison of these 40 flow rates for models 3 through 11 shows a considerable amount of consistency. Models 1 and 2 are rejected for the reasons given previously. Model 12 with 31 regression parameters gave flow rates considerably different from the other models, probably as a result of instability resulting from having too many parameters, so that flow rates for model 12 are not considered either. Rows 1 through 5 in table 5 show respectively (1) the flow out of the geopressured zone; (2) the recharge into the aquifer system from model layer 12 through the top of the aquifer system; (3) the flow out of the aquifer system into layer 12 through the top of the aquifer system; (4) the net total flow into the aquifer system from layer 12 through the top of the aquifer system; and (5) the total recharge to the aquifer system from both the geopressured zone and model layer 12. The second flow minus the third is equal to the fourth, and the first plus the fourth is equal to the fifth. Rows 6 through 15 in table 5

TABLE 5.-- 1982 Ground-water flow rates for models 3 through 11

[The number above/below the slash is the flow rate into/out of the tops of the 10 aquifer layers; units are 10⁵ cubic feet per day]

	Model									
	3	4	5	6	7	8	9	10	11	
Flow out of the geopressed zone	993	0	-18	973	844	9	0	775	539	
Recharge into the aquifer system from layer 12 through the top of the aquifer system	13500	13600	13600	13600	13900	13600	13600	13400	13700	
Flow out of the aquifer system into layer 12 through the top of the aquifer system	2270	1360	1350	2330	2560	1340	1500	2100	1950	
Net total flow into the aquifer system from layer 12 through the top of the aquifer system	11300	12200	12300	11200	11300	12200	12100	11300	11800	
Total recharge to the aquifer system from both the geopressed zone and layer 12	12250	12250	12240	12200	12170	12240	12130	12110	12300	
Flow rate into/out of top of: layer 2	177/1080	178/86	198/87	175/1060	235/988	181/98	205/114	402/1090	239/686	
layer 3	651/467	654/471	653/470	700/544	961/794	645/467	417/269	514/408	516/356	
layer 4	1020/404	1020/408	1020/408	864/406	963/492	1020/403	982/389	1140/593	1190/614	
layer 5	1490/517	1490/517	1480/515	1140/474	1300/623	1480/511	1110/273	1090/434	1320/497	
layer 6	765/286	766/284	765/282	444/283	493/319	760/273	482/219	530/296	801/456	
layer 7	203/485	216/138	218/133	174/445	159/390	216/142	160/84	163/380	291/377	
layer 8	657/566	676/319	679/309	630/509	515/449	673/318	656/310	726/590	839/559	
layer 9	663/669	687/312	691/305	649/614	605/530	684/318	564/240	579/559	773/509	
layer 10	949/663	984/321	988/315	949/613	917/534	981/325	851/171	776/445	994/391	
layer 11	10100/1190	10100/321	10100/318	9990/1190	10000/1120	10100/321	10600/849	10100/1050	10300/1080	

show the flow rates into and out of the tops of the 10 model layers for models 3 through 11. All numbers in table 5 have three significant figures except row 5 which has four. All flow rates shown are for the year 1982, at which time an approximately steady-state situation existed. The pumping rate for 1982 was 0.1265×10^{10} ft³/d. The difference between this pumping rate and the total recharge to the aquifer system on row 5 is the rate that water is coming from storage. Note that the values for the total recharge to the aquifer system are in each case greater than 95 percent of the 1982 pumping rate, indicating that less than 5 percent is coming from storage, and that a near steady-state condition exists.

Because the possible error of estimates for maximum allowable recharge (discharge) into the aquifer system from model layer 12 are large in comparison with the differences for this flow among models 3 through 11, none of the models seem any more likely to be valid than the others. The reason for this is that the flow rates into the aquifer system from model layer 12 in table 4 are very small compared to flow rates that occur at land surface, such as precipitation, runoff, evapotranspiration, etc. For example, the flow rate out of the aquifer system into layer 12 is 0.136×10^9 ft³/d for model 4. This water would either evaporate, be transpired, or flow into streams in lowland areas. However, this amount of water spread over 100,000 mi², an area approximately a third the size of the study area, is equivalent to a flow rate of only 0.21 in/yr, which is very small compared to evapotranspiration or runoff rates.

The direction and general location of ground-water flow that corresponds in a general way to the flow rates of table 5 are shown in figure 35. Figure 35 represents the actual aquifer system and actual flow locations and directions only in a very general and schematic manner. Actual flow patterns, both in the model and in the field, are far more complex. The recharge (discharge) into the aquifer system from model layer 12 through the top of the aquifer system for each grid element for the year 1982, model 4 is shown in figure 36. Equivalent freshwater drawdown since 1937 for the year 1982, model 4, is shown in figures 37 through 46.

Models 3, 4, 5, and 8 have a similar structure in that they all have a single regression parameter assigned to the hydraulic conductivity of sand for the entire aquifer system, and a single parameter assigned to hydraulic conductivity of clay. All four models also have a regression parameter for b_0 , specific storage, and regression parameter b_1 , even though model 3 has the same regression parameter B_1 assigned to both b_1 and b_3 . The values obtained for the parameter for hydraulic conductivity of sand are 29.9, 30.3, 30.3, and 29.0 ft/d for the four models, respectively. For hydraulic conductivity of clay, the four values are 0.365×10^{-3} , 0.362×10^{-3} , 0.361×10^{-3} , and 0.374×10^{-3} ft/d. The values obtained for the predicted heads $f_i(\hat{B})$ $i = 1, 2, \dots, 3, 107$ are very close. When averaged by layer, the four models give values for head that differ by less than 1.1 ft. Clearly the four models are very similar in structure and give nearly the same results for hydraulic conductivity of clay and sand and

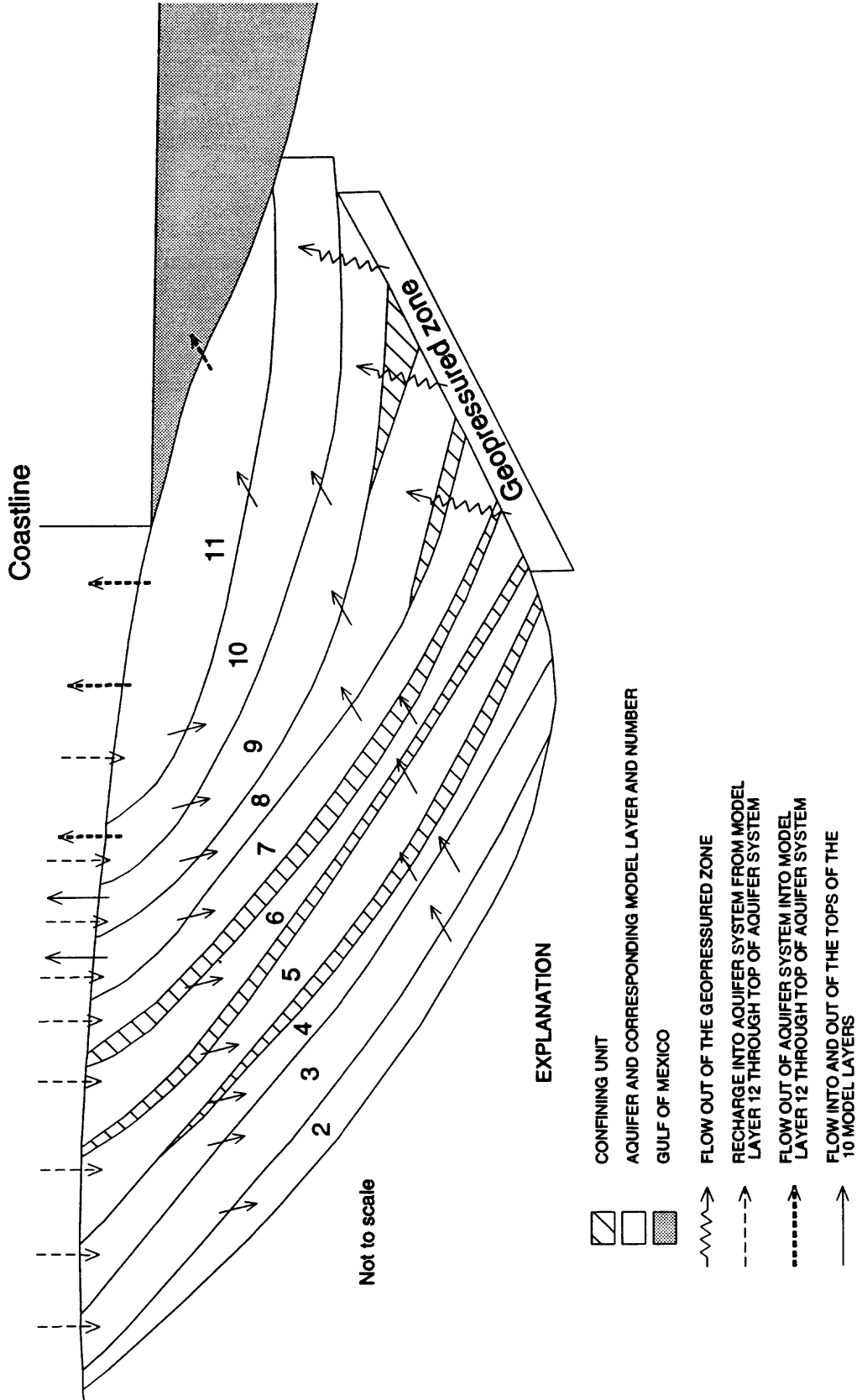


Figure 35. Generalized pattern of ground-water flow.

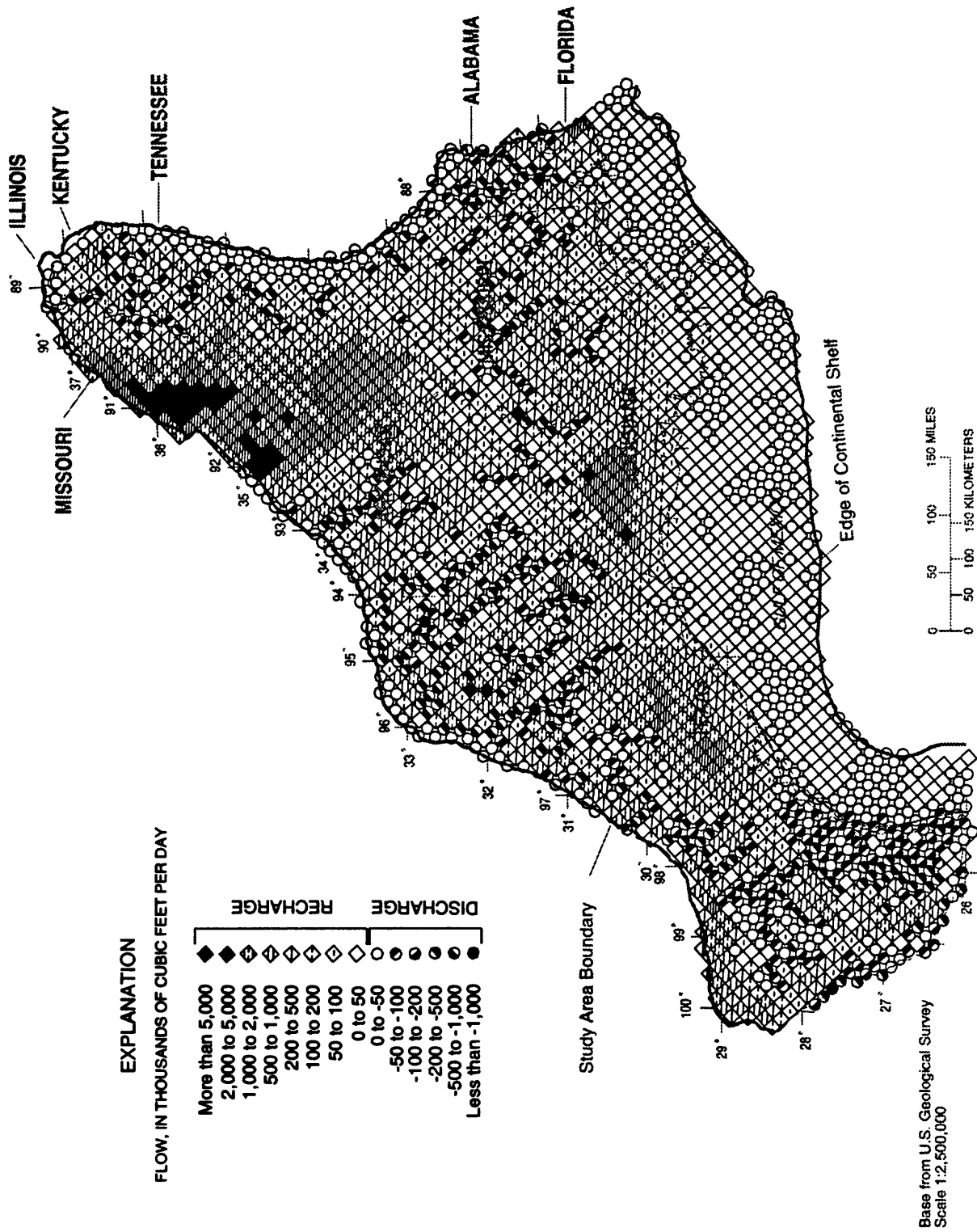


Figure 36. Simulated recharge (discharge) into the top of the aquifer system for 1982, model 4.

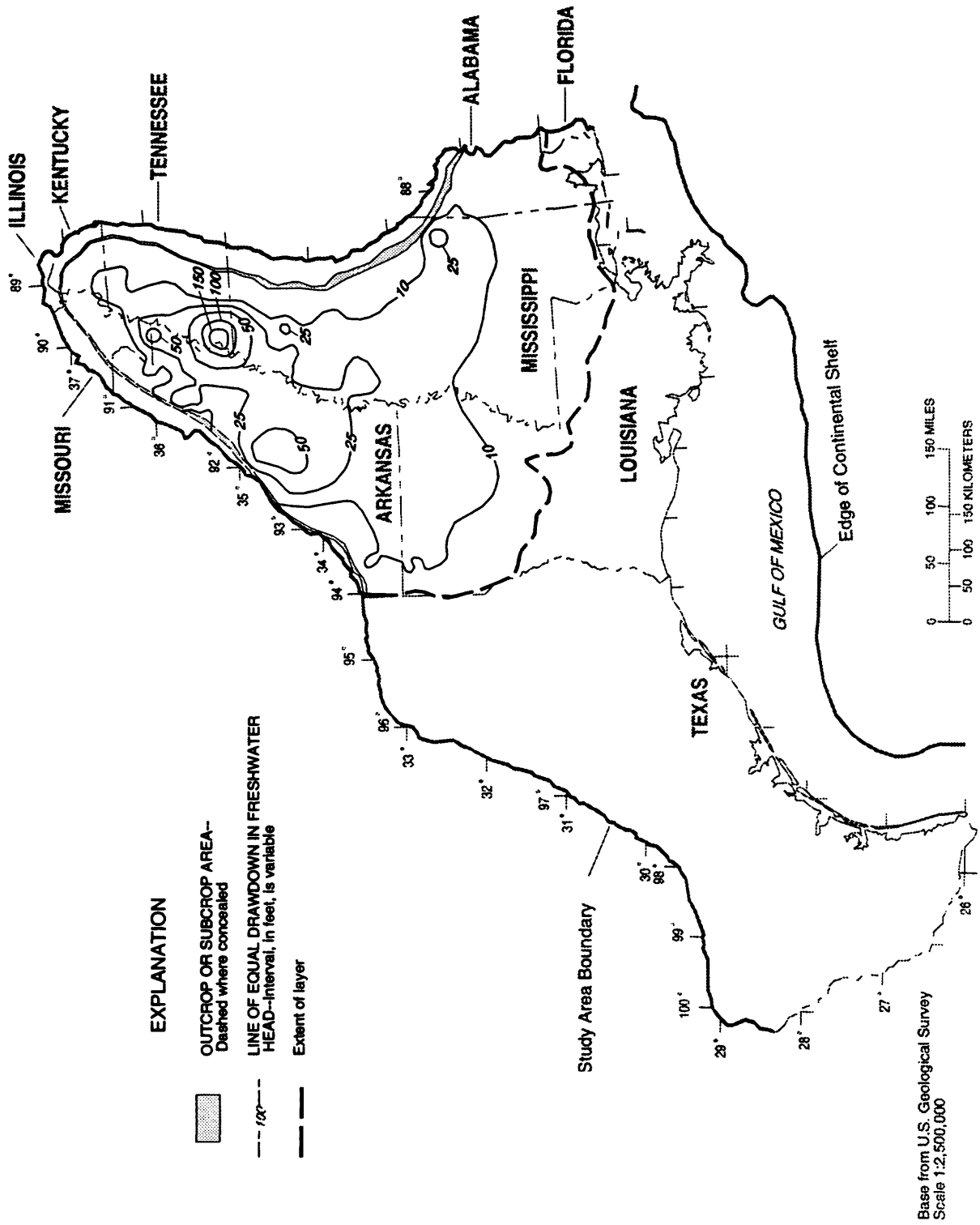


Figure 37. Simulated drawdown of equivalent freshwater head from 1937-82, model 4, model layer 2.

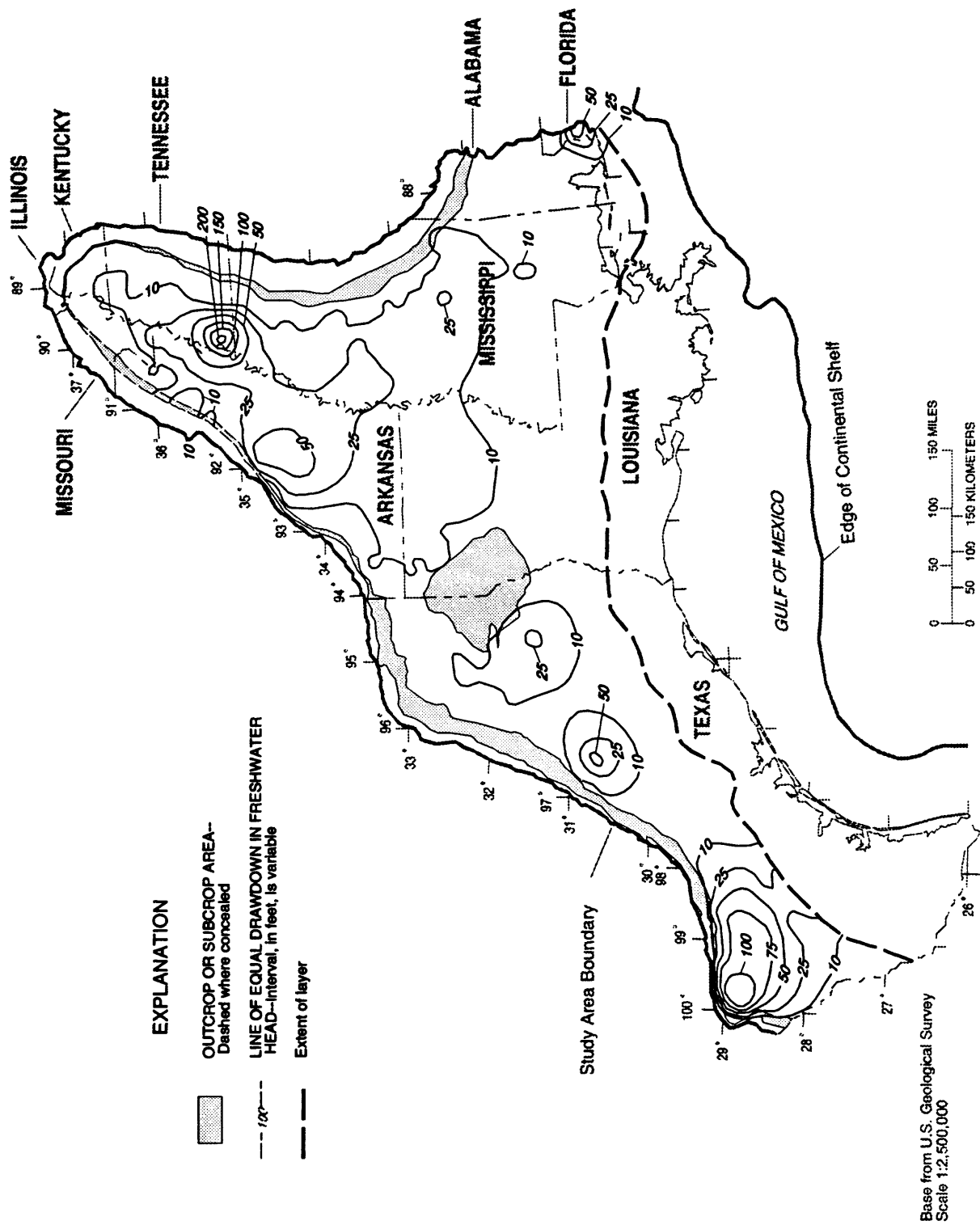


Figure 38. Simulated drawdown of equivalent freshwater head from 1937-82, model 4, model layer 3.

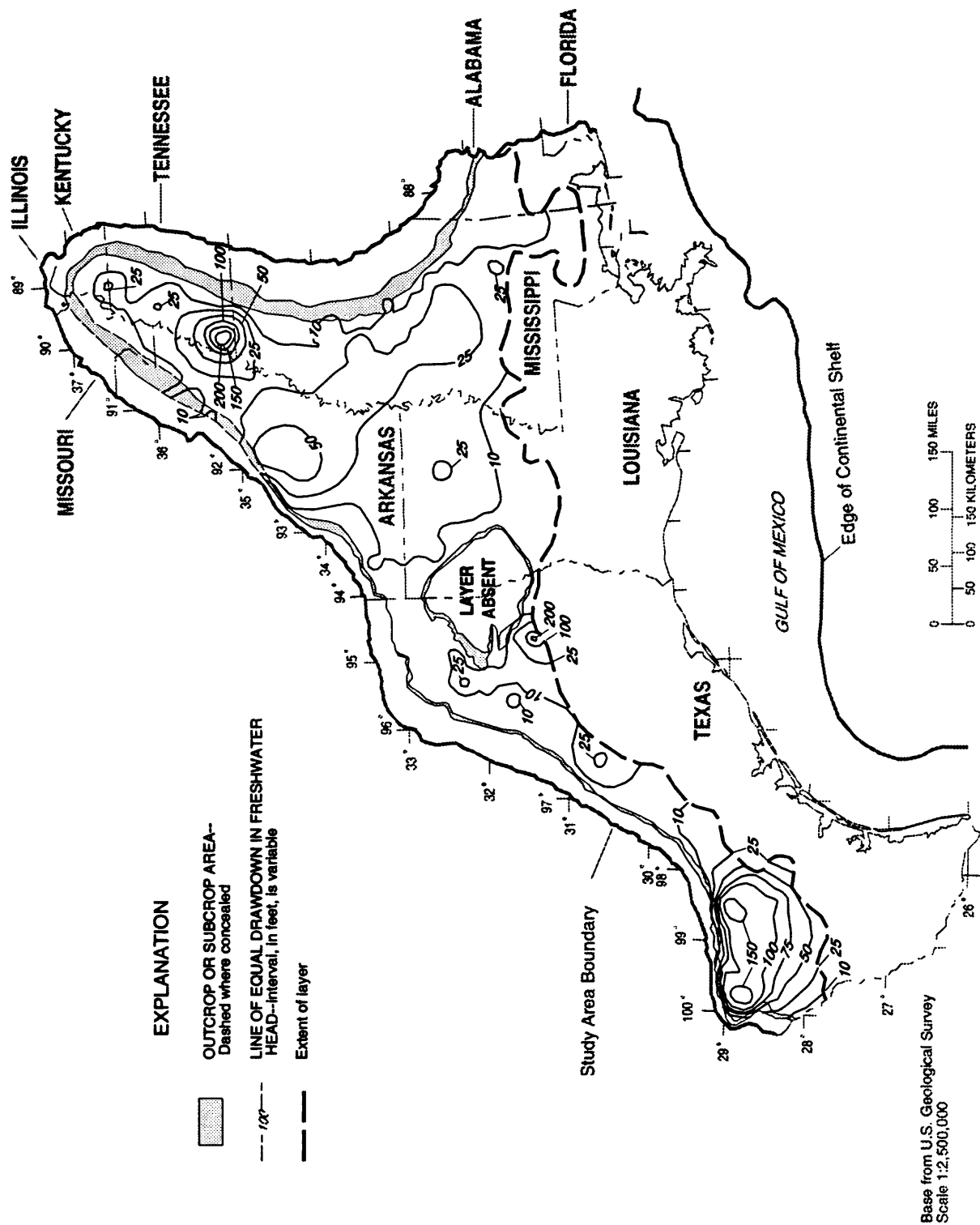


Figure 39. Simulated drawdown of equivalent freshwater head from 1937-82, model layer 4.

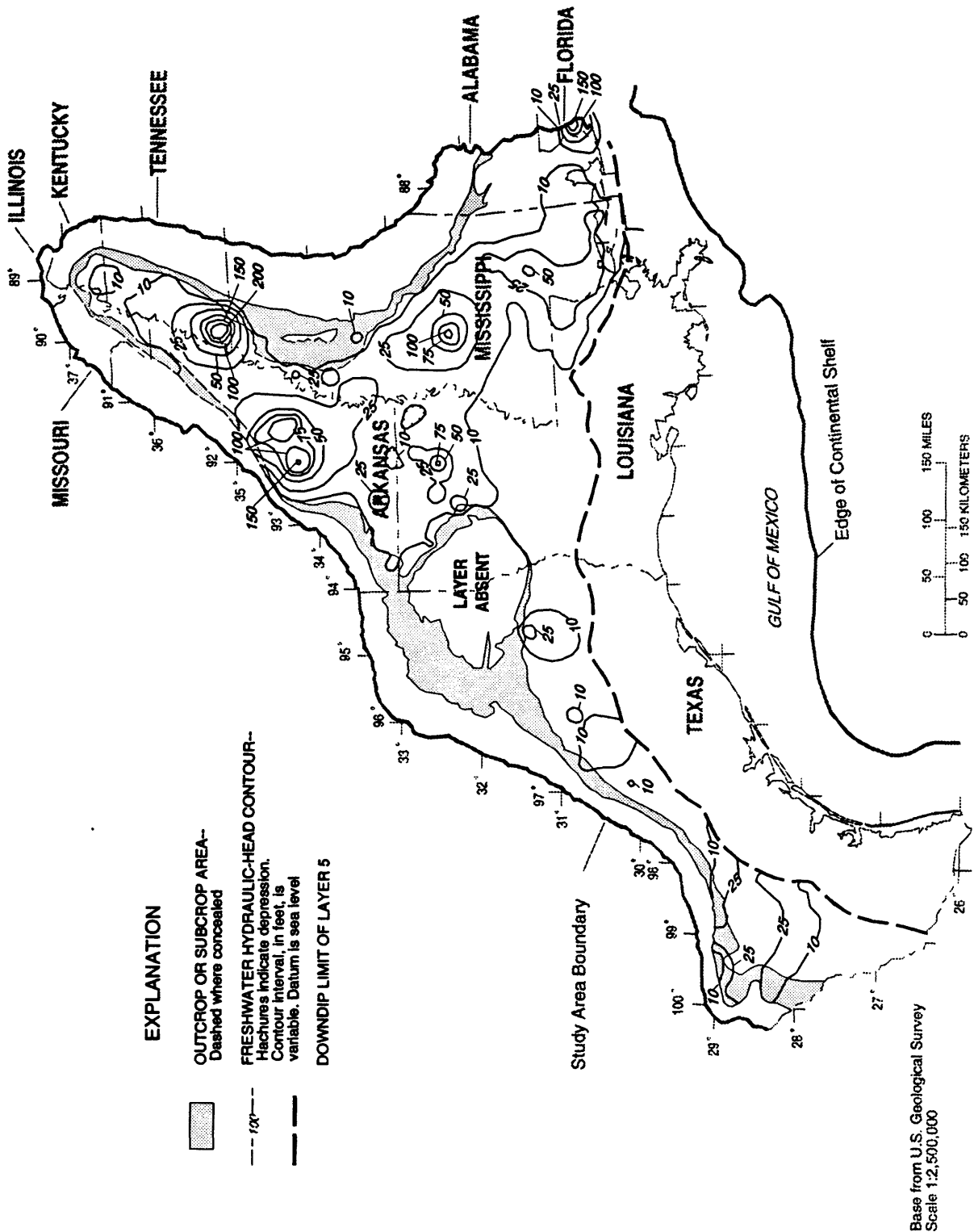


Figure 40. Simulated drawdown of equivalent freshwater head from 1937-82, model 4, model layer 5.

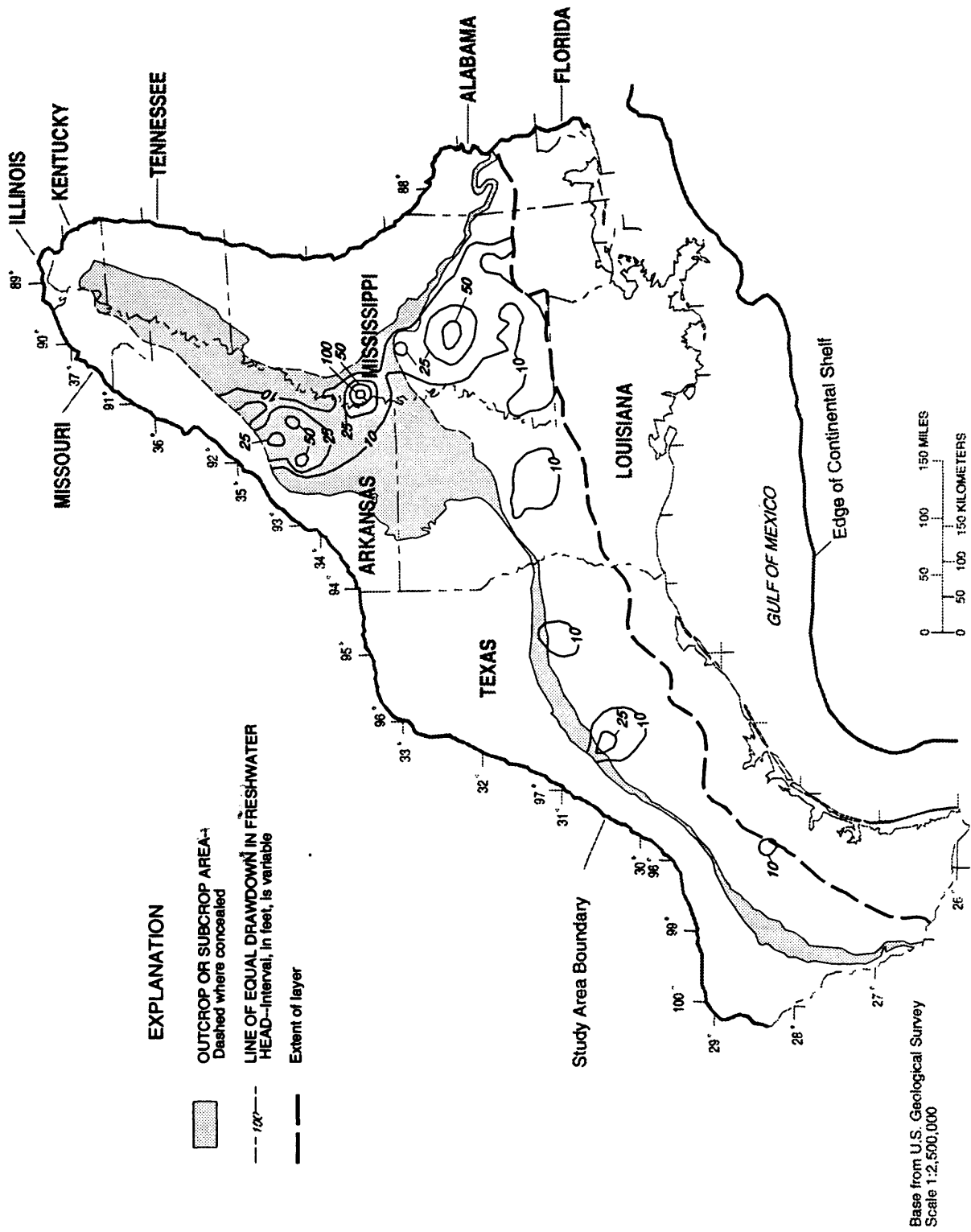


Figure 41. Simulated drawdown of equivalent freshwater head from 1937-82, model 4, model layer 6.

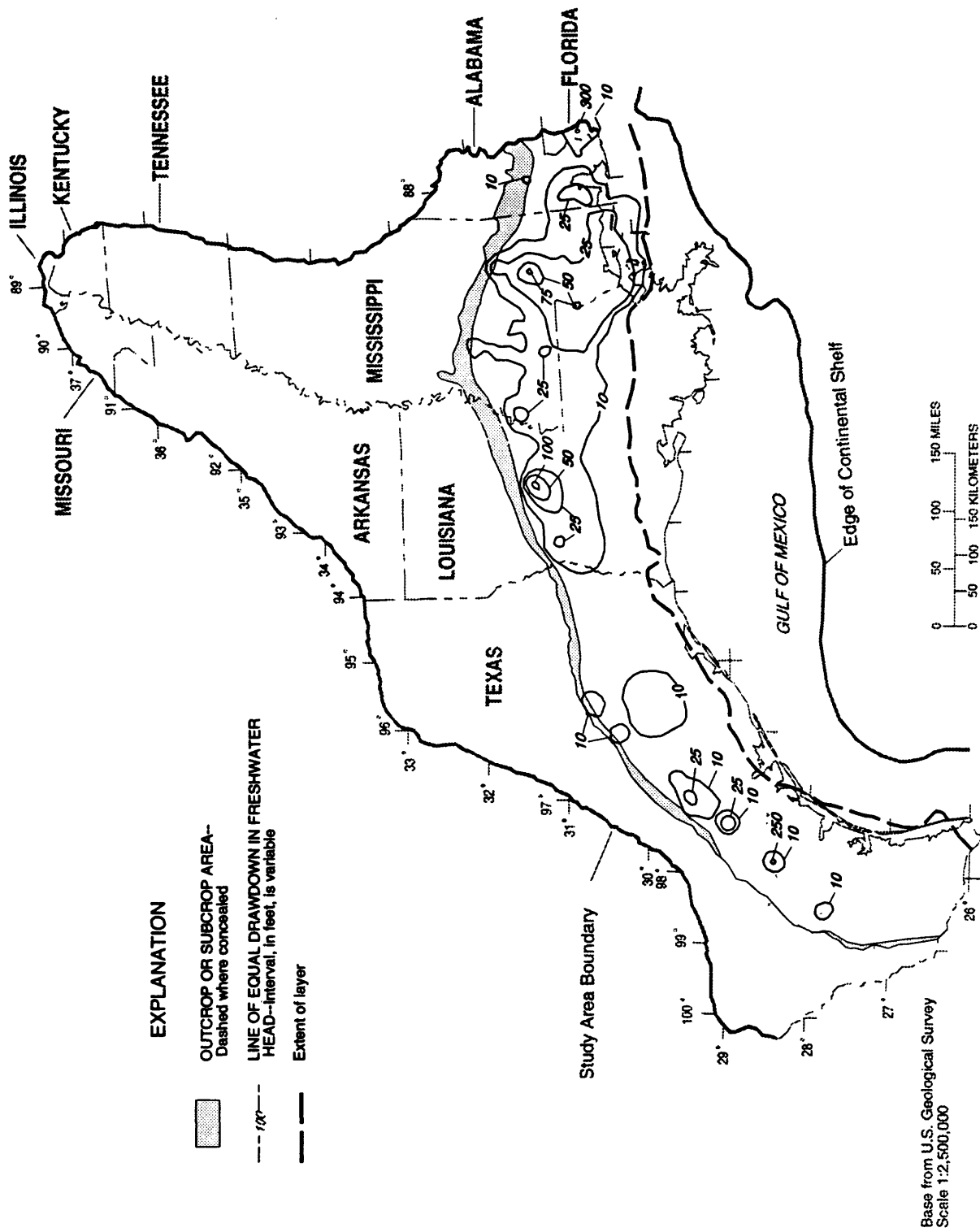


Figure 42. Simulated drawdown of equivalent freshwater head from 1937-82, model 4, model layer 7.

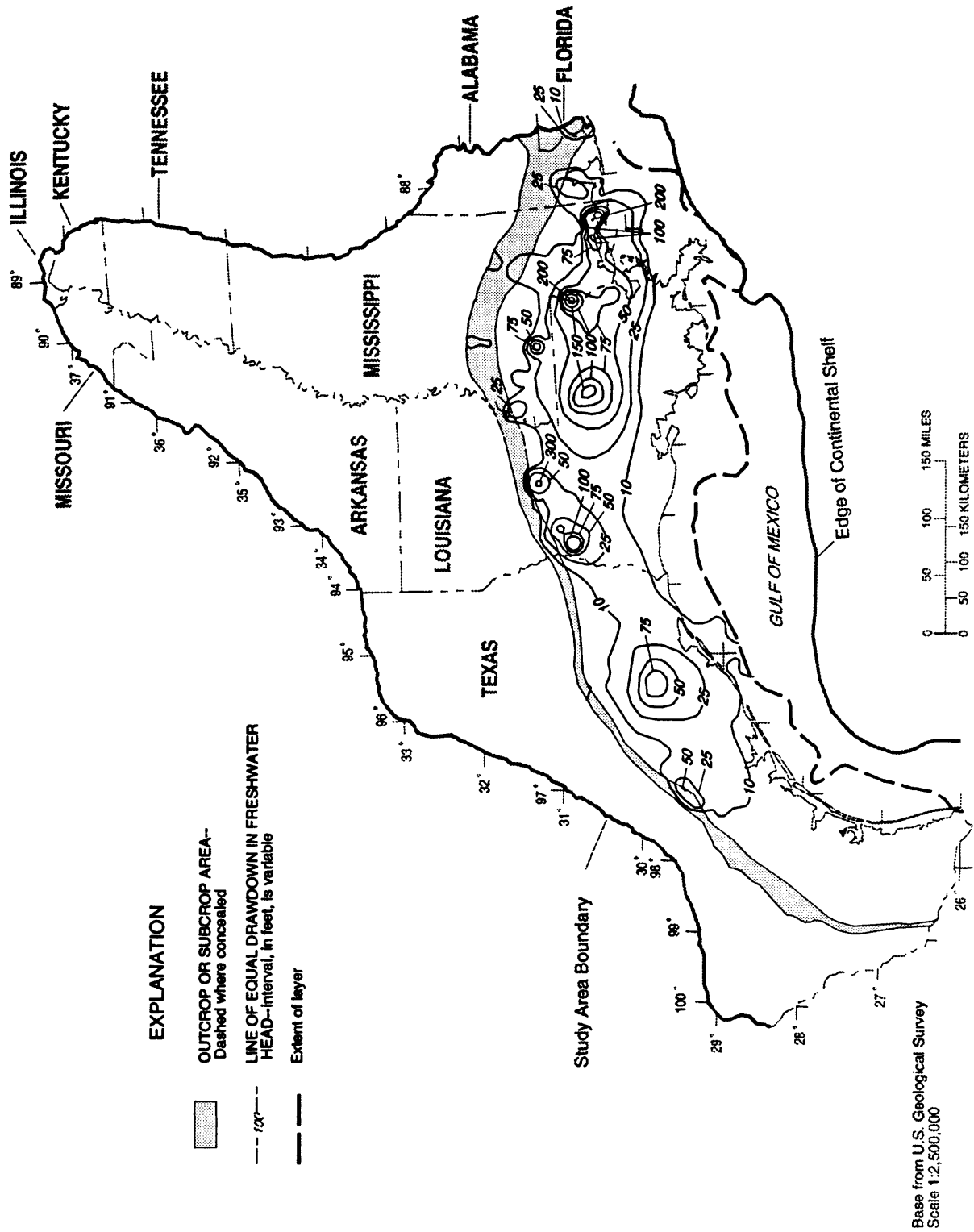


Figure 43. Simulated drawdown of equivalent freshwater head from 1937-82, model 4, model layer 8.

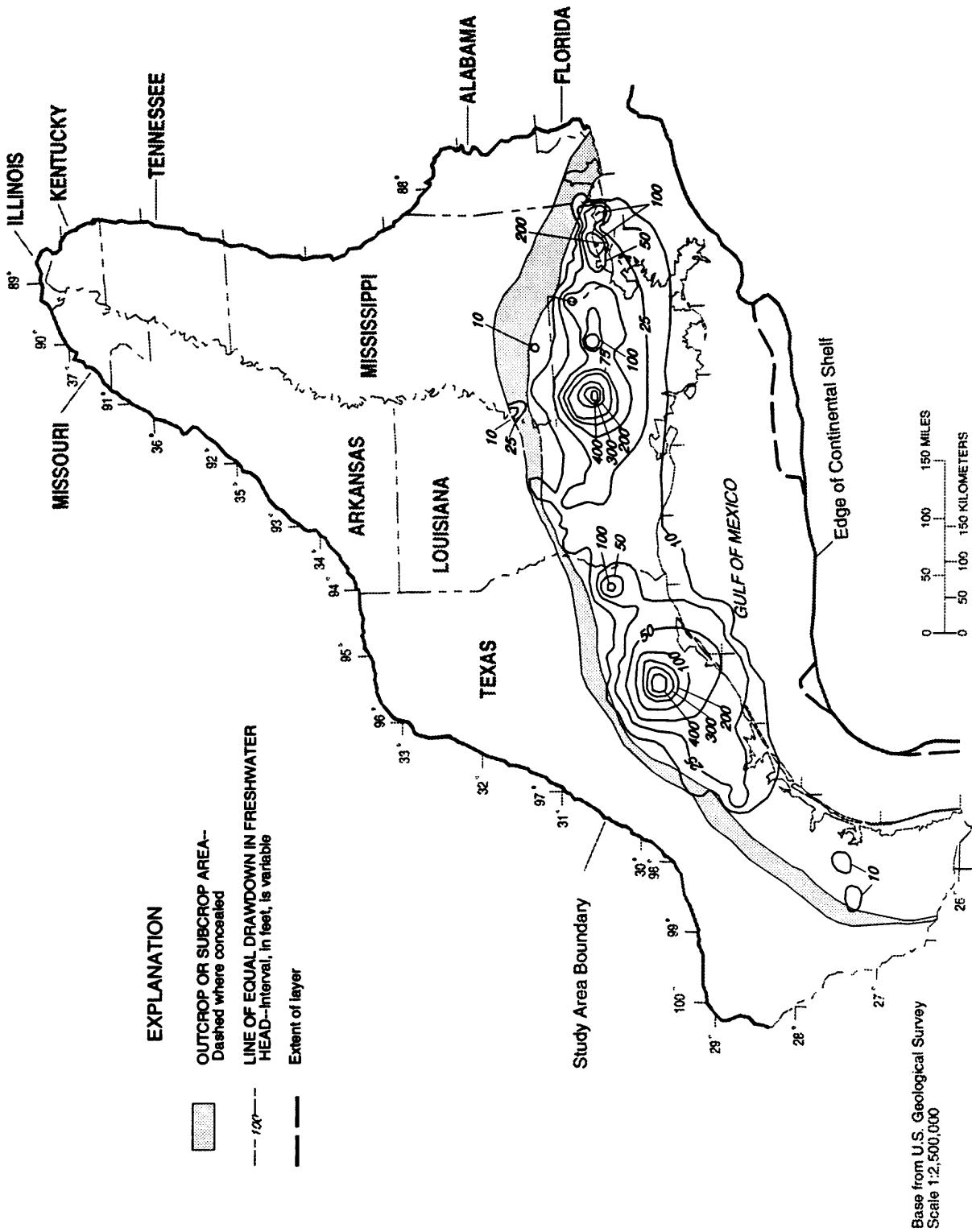


Figure 44. Simulated drawdown of equivalent freshwater head from 1937-82, model 4, model layer 9.

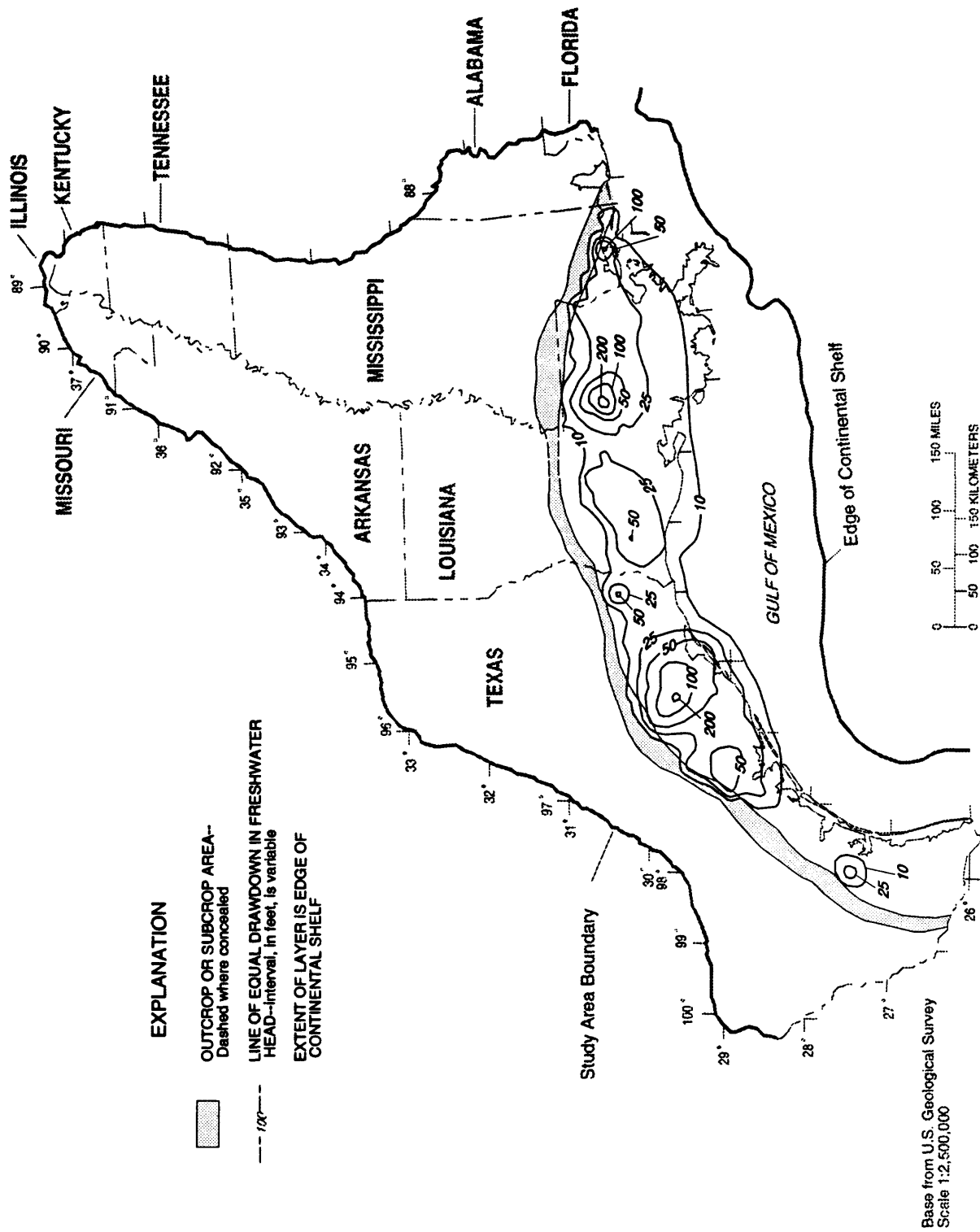


Figure 45. Simulated drawdown of equivalent freshwater head from 1937-82, model layer 10.

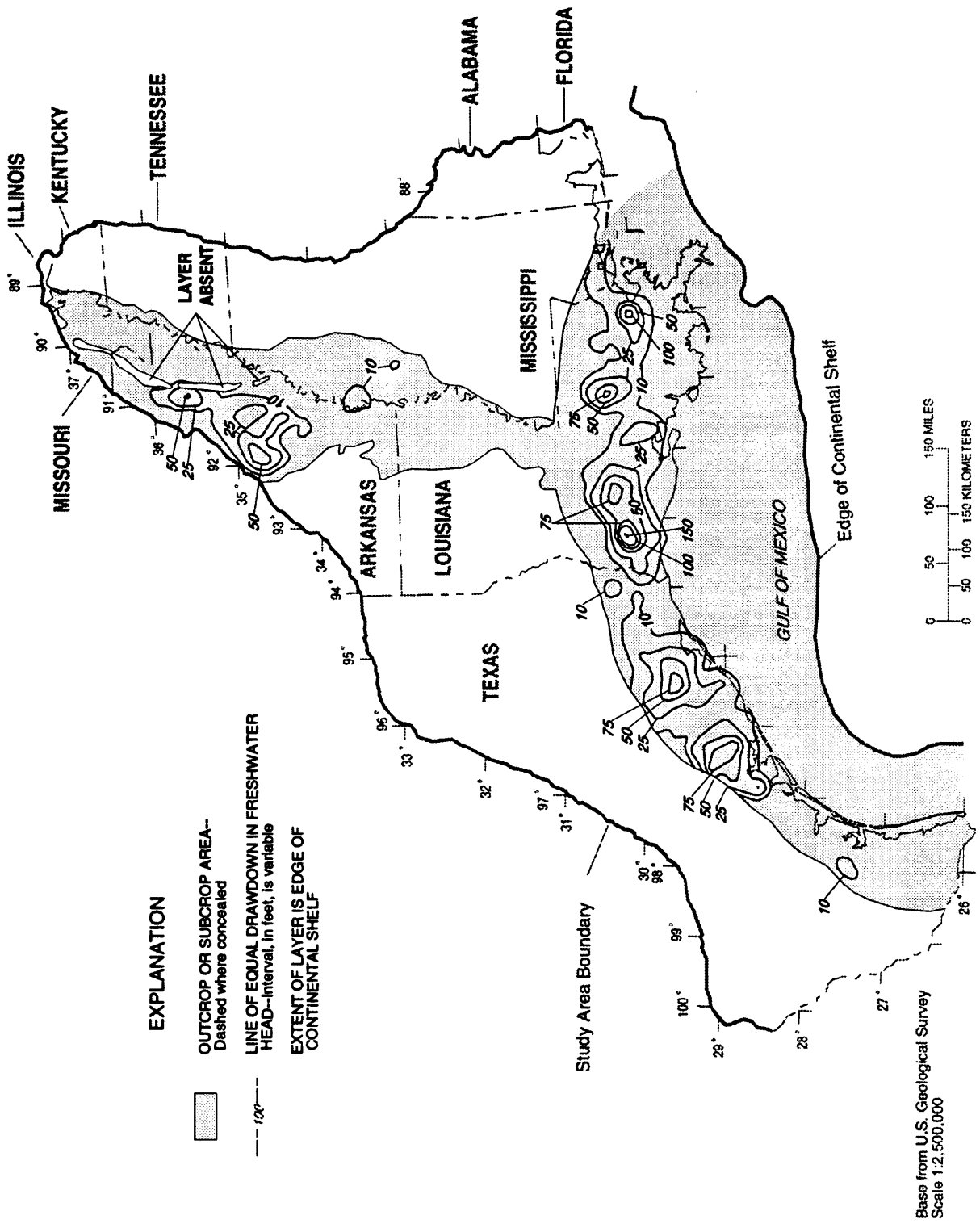


Figure 46. Simulated drawdown of equivalent freshwater head from 1937-82, model 4, model layer 11.

predicted shallow heads $f_i(B)$, $i = 1, 2, \dots, 3, 107$. However, table 5 shows that the flow rates are not the same, the main difference being differing amounts of flow from the geopressured zone passing up through the aquifer system through model layers 7 through 12. Also, heads at depth differ by as much as 800 ft. Note that in table 5, model 3 has a flow of 0.993×10^8 ft³/d from the geopressured zone. Model 4, however, has a zero flow condition because b_4 is set to zero. Models 5 and 8 have almost zero flow because of the values obtained for b_3 and b_4 , even though the confidence intervals for b_3 and b_4 are extremely large. A model not shown in tables 4 and 5 and having the same selection of regression parameters as model 5, but using grid-element volume-averaged heads from drill-stem test as well as the 3,107 grid-element volume-averaged heads from water wells, gave a flow from the geopressured zone of 0.544×10^8 ft³/d. Models 6, 7, 9, 10, and 11 have flow from the geopressured zone of from 0 to 0.973×10^8 ft³/d. The conclusion is that the modeling efforts of this study are very approximate with regard to deep flow and heads. This result is not unexpected because almost all of the data for hydraulic head and hydraulic conductivity were taken from shallow depths.

A flow from the geopressured zone as large as that shown by model 3 could exist because order of magnitude calculations show that with a large value of specific storage, the geopressured zone under the aquifer system could maintain an average upward flow of approximately 10^8 ft³/d if experiencing a rate of drop in head of several thousand feet per 100 million years ($S(\Delta h/\Delta t)$) (volume of geopressured zone) = flow rate:
 $(0.5/\text{ft})(5 \times 10^3 \text{ft}/365 \times 10^8 \text{d})(10^{15} \text{ft}^3) = 0.7 \times 10^8 \text{ft}^3/\text{d}$. However, as shown above, the models of this study give values of the flow from the geopressured zone of from 0 to 10^8 ft³/d with no indication of which is more correct. Values of head at depth also vary widely.

Model Error

It has been shown above that most of the various models show agreement regarding prediction of shallow heads and hydraulic conductivity values (the 3,107 grid-element volume-averaged heads and the 33 logarithm values of hydraulic conductivity of sand). The overlapping of the associated prediction intervals has also been demonstrated. It is appropriate to consider the extent to which the predictions of shallow heads and hydraulic conductivity could be in error because of conditions or constructions that are common to all of the models $f(B)$ used.

Before considering model error, it is appropriate to mention that many possible sources of error have already been removed by assigning regression parameters to unknown values such as: b_1 and b_2 for the top surface specified head, b_3 and b_4 for the geopressured zone, b_5 for the way in which effective hydraulic conductivity is determined from the hydraulic conductivity of the sand and clay components, b_6 for anisotropy, b_7 and b_8 for the subsidence mechanism, and b_9 for specific storage. Remaining sources of model error are (1) the evaluation of the density function $\rho(x, y, z)$ from data that may be in error or lacking; (2) the depth dependence of clay and

hydraulic conductivity of sand as described previously, specifically the functions used for the rate of decrease with depth; (3) the procedure for obtaining grid element effective hydraulic conductivity values by Desbarats (1987); and (4) the selection of the hydraulic conductivity zones. These four sources of error are considered in order in the following four paragraphs, and results of model alterations to explore these sources of error are summarized in table 6. An additional source of error which is very likely the major cause of the large root-mean square-weighted residuals and the large 95 percent prediction interval half widths e_k (table 4) is the relatively large 10 mi grid spacing, as discussed previously. Unfortunately, no tests with smaller grid spacing were performed because of the large number of grid elements that would be needed. Consequences of the use of 30-mi grid spacing have been discussed previously.

Several models were used in which grid-element volume-averaged density ρ was smoothed between grid elements in the same layer. This smoothing was done by assigning to ρ the average of ρ over nine locations, the neighboring eight grid elements and the center grid element for which the smoothed value of ρ is being sought. Changes in predicted $f_i(\hat{B})$ for observed quantities were very minimal. Using model 4, the maximum change in layer-averaged predicted head was 0.2 ft. The values for the hydraulic conductivity of clay and sand parameters, 0.362×10^{-3} and 30.3 ft/d, changed to 0.364×10^{-3} and 30.2 ft/d. The value of $\omega_k^{1/2}e_k$ was unchanged at 141, so that the confidence and prediction interval widths were unchanged. However, small local perturbations in head, flow velocity, and flow direction resulted in those parts of the aquifer system with high grid element densities if smoothing caused significant changes in these grid element densities. This would be expected from theoretical considerations regarding the variable-density flow equations (1) and (3). Larger changes in density, other than just smoothing, cause larger changes in predicted shallow head and hydraulic conductivity values. Using model 4, with the density ρ that of freshwater throughout the entire aquifer system, the maximum change in layer-averaged predicted head was 1.3 ft. The values for the hydraulic conductivity of clay and sand parameters, 0.362×10^{-3} and 30.3 ft/d in model 4, changed to 0.357×10^{-3} and 29.8 ft/d. The value for $\omega_k^{1/2}e_k$ was 141, unchanged. The 15 flow rates from model 4 appearing in table 5 changed by as much as 3 percent. Deep heads, in areas of high density originally, decreased as much as 600 ft due to the absence of the elevated pressure caused by the dense saline water.

As mentioned previously, the rates of decrease with depth of hydraulic conductivity of clay and sand were approximated by the functions $10^{-0.8dd}$ and $10^{-(1.167dd-0.0833dd^2)}$, respectively, where dd is measured in kilometers. Also as mentioned, these functions were assigned an exponent regression parameter in several models, but the confidence intervals for these regression parameters were very large. In accordance with these large confidence intervals, changes in the depth functions affected predicted heads $f_i(\hat{B})$ very little, provided only that the depth functions caused the hydraulic conductivity values of clay and sand to decrease in some substantial manner with depth.

TABLE 6.--The effect of model alterations on: (1) layer-averaged predicted head, h_{layer} ; (2) hydraulic conductivity of clay and sand, P_c and P_s ; (3) $w_k^{1/2}e_k$; (4) the 15 flows of table 5; and (5) deep head for models 3 through 11 and model 4

[Model 4 comparisons are on rows 2 and below; unaltered model 4 has $P_c = 0.362 \times 10^{-3}$ feet per day, (ft/d), $P_s = 30.3$ ft/d, and $w_k^{1/2}e_k = 141$. >, Greater than; <, less than; gm/cm³, grams per cubic centimeter]

Alteration	h_{layer} (ft)	P_c (ft/d)	P_s (ft/d)	$w_k^{1/2}e_k$	15 flows (percent)	Deep head (ft)
Nine models, 3 through 11	< 30 usually < 5	see table 4	see table 4	141-243	large differences see table 5	800
Smoothed density	< 0.2	0.364×10^{-3}	30.2	141	< 1	53
Density of freshwater	< 1.3	0.357×10^{-3}	29.8	141	< 3	600
Depth dependence of hydraulic conductivity	< 2.7	0.335×10^{-3} 0.371×10^{-3}	23.8 32.8	140 142	< 30 usually < 10	60
Effective hydraulic conductivity procedure	< 10 usually < 2	0.1980×10^{-2}	30.2	145	< 70 usually < 30	34
Truncation at density > 1.005 gm/cm ³	< 2.1	0.336×10^{-3}	32.0	142	< 35 usually < 7	no deep heads
Truncation at 3,000 ft below ground surface	< 2.3	0.336×10^{-3}	31.8	142	< 20 usually < 5	no deep heads

Multiplying both of the exponents of the functions $10^{-0.8dd}$ and $10^{-(1.167dd-0.0833dd^2)}$ by the factor 0.5 and also the factor 1.3 in model 4 gave predicted heads $f_1(\hat{B})$ that, when averaged by layer, differed from those of model 4 without alteration by at most 2.7 ft. The values for the hydraulic conductivity of clay and sand parameters, 0.362×10^{-3} and 30.3 ft/d in model 4, changed to 0.335×10^{-3} and 23.8 ft/d and 0.371×10^{-3} and 32.8 ft/d for the factors 0.5 and 1.3, respectively. This type of result is expected from the previously described mechanism relating the hydraulic conductivity of a grid element in the model, the hydraulic conductivity parameter for the grid element, and the depth d of the center of the grid element in kilometers. The value for $\omega_k^{1/2} e_k$ was 140 for factor 0.5 and 142 for the factor 1.3, both very close to the value of 141 in model 4. Thus, the prediction intervals for head and hydraulic conductivity of sand did not change significantly. Several of the 15 flow rates from model 4 appearing in table 5 changed by as much as 30 percent, but changes were usually less than 10 percent. As explained previously, the original hydraulic conductivity rate of decrease with depth functions were chosen to approximate data taken from the literature, and thus presumably should cause the model $f(B)$ to be the most accurate with the exponents unaltered. In the event that this is not correct, the analysis above shows that the results change insignificantly for very substantial changes in the exponents.

An alternative to using the procedure of Desbarats (1987) to obtain grid element effective horizontal and vertical hydraulic conductivity values, is to use the harmonic mean to obtain effective vertical hydraulic conductivity, and to use the arithmetic mean to obtain effective horizontal hydraulic conductivity. This procedure yields effective vertical and horizontal hydraulic conductivity values that correspond to the assumption that the clay in the grid element extends horizontally and continuously across the entire grid element as a single or several uniform layers. It would thus tend to give a larger than actual effective horizontal conductivity and a smaller than actual effective vertical conductivity. The formulas for effective vertical and horizontal hydraulic conductivity, K_z and K_h , for a grid element are:

$$K_z = [(V_c/K_c) + ((1-V_c)/K_s)]^{-1}, \quad (16)$$

and

$$K_h = (V_c K_c + (1-V_c) K_s), \quad (17)$$

where, as in formulas (10) and (11), K_c and K_s denote the hydraulic conductivity of the clay and sand components respectively, and V_c denotes the clay fraction of the grid element. Equations (16) and (17) were used in several of the models in table 4 as a replacement for equations (10) and (11). This was done by the direct use of equations (16) and (17), and also by using replacements for a and a^{-1} in equations (10) and (11), causing these equations to give nearly the same values for K_z and K_h as equations (16) and (17). Use of equations (16) and (17) as opposed to equations (10) and (11)

produced changes in the values for the hydraulic conductivity of clay and sand parameters for the various hydraulic conductivity zones. This would be expected from the functionally different manner that K_c and K_s appear in equations (10) and (11), as compared to the way they appear in equations (16) and (17). By use of equations (16) and (17) in model 4 gave predicted heads $f_i(B)$, which when averaged by layer differed by 10 ft at most and generally less than 2.0 ft from predicted heads obtained using equations (10) and (11). However, the values for the hydraulic conductivity of clay and sand parameters, 0.362×10^{-3} and 30.3 ft/d in model 4, changed to 0.198×10^{-2} and 30.2 ft/d, respectively. Due to the difference between equations (10) and (11) as compared to equations (16) and (17), effective hydraulic conductivity values K_z and K_h did not generally change by more than 50 percent, despite the substantial change of the hydraulic conductivity of clay parameter value from 0.362×10^{-3} ft/d to 0.198×10^{-2} ft/d. The value for $\omega_k^{1/2} e_k$ was 145, only slightly larger than the value of 141 in model 4, so that the prediction intervals for head and hydraulic conductivity of sand did not change significantly. Several of the 15 model 4 flow rates appearing in table 5 changed by as much as 70 percent, but changes were usually less than 30 percent. The value for Chi^2 did not change appreciably.

The manner of selecting the hydraulic conductivity zones was not changed, except for the use of various choices for the boundaries of the 10 regions in figure 31. However, because the various models had different choices for the assignment of the more than 100 hydraulic conductivity zones to a given set of hydraulic conductivity of clay and sand parameters, model error due to discretization of the aquifer system domain of solution with regard to the values used for hydraulic conductivity was partially eliminated. This is true only if a sufficiently large number of different chosen assignments of hydraulic conductivity zones was used. Since more than 40 different assignments were used (seven of which are shown in table 4), model error due to discretization is probably largely eliminated. This should be interpreted relative to the differences in results noted in the previous section.

Model Truncation

Some studies of aquifer systems with saline water at depth use a constant freshwater density model and truncate the domain of solution at or near that depth where the density begins to increase substantially, treating this truncation surface as a no-flow boundary. This approach may be seen as an approximation to the method of this study which, by the use of a variable-density model, models both the shallow freshwater system and the underlying saline water system as a total system. Obviously the truncation of the deep saline part of the aquifer system precludes the modeling of this deep part. The hope, however, is that in spite of truncation, the results for the remaining shallow part of the aquifer system are reasonably accurate.

With the truncation approaches described below, predicted shallow head and hydraulic conductivity were similar to values obtained by the variable density model. Flow from the geopressed zone in some of the models is shown in table 5. This flow, if it occurs, passes up through the no-flow truncation surface of the truncated system. Thus, flow at the depth of the

truncation surface differs substantially between the two approaches because, when modeling the full system, flow occurs across the truncation surface which is a no-flow boundary for the truncated system. Heads at depth cannot be compared between the two approaches, because the truncated aquifer system does not have any deep heads. Heads just above the truncation surface were found to be fairly close. Heads adjacent to the truncation surface and in areas of heavy pumping differed the most.

Model 4 was used with a truncation surface defined as that surface at which grid element density first exceeds 1.005 gm/cm^3 when proceeding downward from the top grid element at each horizontal location. This truncation reduced the number of observed grid-element volume-averaged heads Y_i from 3,107 to 3,067, because 50 heads Y_i were located below the truncation surface. Density in the grid elements above the truncation surface was set to that of freshwater. The maximum change in layer-averaged predicted head was 2.1 ft. The values for the hydraulic conductivity of clay and sand parameters, 0.362×10^{-3} and 30.3 ft/d in model 4, changed to 0.336×10^{-3} and 32 ft/d. The value for $\omega_k^{1/2} e_k$ was 142. The 15 flow rates from model 4 appearing in table 5 changed by as much as 35 percent, but changes were usually less than 7 percent. The maximum change in the 3,067 predicted heads was 49 ft. This occurred at a grid element located adjacent to the truncation surface that had a drawdown of almost 400 ft due to heavy pumping. Most of the changes in the 3,067 predicted heads were less than 5 ft. Flows in the area of the grid elements with heavy pumping were different in the truncated model due to the proximity of the no-flow truncation surface.

Model 4 was also used with a truncation surface at 3,000 ft below land surface. This truncation decreased the number of grid-element volume-averaged heads Y_i to 3,087. Density was set to that of freshwater. The maximum change in layer-averaged predicted head was 2.3 ft. The values for the hydraulic conductivity of clay and sand parameters, 0.362×10^{-3} and 30.3 ft/d in model 4, changed to 0.336×10^{-3} and 31.8 ft/d. The value for $\omega_k^{1/2} e_k$ was 142. The 15 flow rates from model 4 appearing in table 5 changed by as much as 20 percent, but changes were usually less than 5 percent.

Note that with both methods of truncation, layer-averaged predicted head does not change by more than 2.3 ft. This small change occurs in spite of the fact that some of the layers have a reduced number of heads Y_i , so that the average for the layer is over a reduced set of those Y_i that were in the layer before truncation. The 15 flow rates in table 5 show change, as mentioned, but some of this change occurs because the extent of the truncated layers has decreased, in some cases by a considerable amount. Because flow decreases substantially with depth due to decreasing hydraulic conductivity of clay and sand, the truncation of the deeper part of a layer may have a relatively small effect on the total flow going into or out of its top surface.

Changes that occur in layer-averaged predicted head and flow due to the truncation of model 4 are less than those that occur between the nine models in table 5, all without truncation (table 6). These results with the truncation of model 4 indicate that in general little predictive ability is lost by the use of a truncated model because neither the full nor truncated models are able to make any useful predictions for deep head and flow. The only exception to this would be that the full model is more accurate for the prediction of head and flow near the truncation surface, particularly if there is heavy pumping nearby.

SUMMARY AND CONCLUSIONS

SUMMARY

The major results of the study are:

1. Of the 12 models evaluated in this report, the model with the smallest prediction interval half widths, model 4, had only four regression parameters. With all models, the residuals failed the Chi^2 test for normality at the 1-percent significance level, possibly as a result of the large 10-mi grid spacing used.
2. The dominant factor controlling shallow hydraulic heads in the simulated aquifer system is the specified head along the top surface of the aquifer system, which consists of the water-table altitude and equivalent freshwater head at the sea floor. Because the water-table altitude surface is usually not far below land surface and has a very similar shape, a dominant factor controlling shallow heads is land-surface altitude. These shallow heads are also affected by pumping. Heads at depth may be affected by flow from the geopressured zone. However, the models used show almost no ability to predict deep heads and flow, including flow from the geopressured zone.

The various models used show considerable overlap among the prediction intervals for shallow head and hydraulic conductivity of sand. The 95-percent prediction interval half widths for grid-element volume-averaged head all exceed 108 ft, and those for volume-averaged \log_{10} hydraulic conductivity of sand all exceed $0.94(141/149) = 0.89$.

3. The essential feature of the flow system is the flow of water from upland surface recharge areas to discharge areas at lower altitude on land or the sea floor. No prediction intervals were obtained for flow. The variability from model to model in values obtained for shallow flow varies greatly. The flow across some surfaces is not known to within a factor of 10. For other surfaces, the flow rates are known to within a smaller factor. There is little certainty about the flow across many of the individual grid element surfaces, particularly those that have relatively small flow.

Because the possible error of estimate for maximum allowable recharge (discharge) into the aquifer system from model layer 12 is large in comparison with the differences for this flow among models 3 through 11, none of the models seem any more likely to be valid than another. The reason for this is that the flow rates into the aquifer system from model layer 12 are very small compared to flow rates in the hydrologic budget, such as precipitation, runoff, evapotranspiration, etc. Estimates for the flow rate from the geopressed zone are sufficiently approximate that they also provide no basis for selecting any one of the models 3 through 11 as being better than any of the others.

4. Truncating the domain of solution of one of the models below a certain ground-water density or depth below land surface and setting the density to that of freshwater in the remaining shallow part of the domain of solution did not appreciably change results for hydraulic head and flow produced by the model, except for locations close to the truncation surface.
5. The regression methodology allowed the testing of a very wide range of models for the simulation of the aquifer system. The time saved by being able to find the optimal selection of the regression parameters for a given model in only a single computer run was used to formulate and test many different types of models and procedures.

The regression methodology also provided estimates of the accuracy of results, in the form of prediction and confidence intervals. These accuracy estimates point out the limitations of the predictive ability of a model, and are thus very valuable. Testing, to determine the most likely sources of model error, led to the conclusion that the 10-mi grid element spacing was quite large relative to the variability of hydraulic head and is thus the probable cause of significant error.

CONCLUSIONS

The predictive ability of the models used was quite low in many aspects. The models showed almost no ability to predict deep heads and flow, including flow from the geopressed zone. Regression analysis shows that even the best of the models used had a rather poor ability to accurately predict head in any of the layers. Evidence of this is the 95-percent prediction interval half width of 108 ft mentioned previously. For predicting hydraulic conductivity of sand, the 95-percent prediction interval half widths for \log_{10} hydraulic conductivity of sand all exceeded 0.89, thus hydraulic conductivity of sand could not be predicted to within a factor of almost 8 ($10^{.89}$). These results show the considerable inaccuracy of the models chosen and perhaps the inaccuracy of any model based on the same data and relatively large 10-mi grid spacing. The very important contribution of regression analysis is showing the limitations of the predictive ability of the models used. A less thorough study probably would have left the impression that the model or models used were significantly more accurate than they actually were.

REFERENCES CITED

- Ackerman, D.J., 1989, Hydrology of the Mississippi River Valley alluvial aquifer, south-central United States--a preliminary assessment of the regional flow system: U.S. Geological Survey Water-Resources Investigations Report 88-4028, 74 p.
- _____ in press, Hydrology of the Mississippi River Valley alluvial aquifer, south-central United States: U.S. Geological Survey Professional Paper 1416-D.
- Arthur, J.K., and Taylor, R.E., 1990, Definition of geohydrologic framework and preliminary simulation of ground-water flow in the Mississippi embayment aquifer system, south-central United States: U.S. Geological Survey Water-Resources Investigations Report 86-4364, 97 p.
- _____ in press, Ground-water flow analysis of the Mississippi embayment aquifer system, south-central United States: U.S. Geological Survey Professional Paper 1416-I.
- Bear, Jacob, 1979, *Hydraulics of groundwater*: McGraw-Hill, New York, 569 p.
- Bennett, G.D., 1980, Research and model development related to the regional aquifer-system analysis program [abs]: American Geophysical Union Eos Transactions, v. 61, no. 46, p. 951.
- Brahana, J.V., and Mesko, T.O., 1988, Hydrogeology and preliminary assessment of regional flow in the Upper Cretaceous and adjacent aquifers, northern Mississippi embayment: U.S. Geological Survey Water-Resources Investigations Report 87-4000, 65 p.
- Cooley, R.L., 1977, A method of estimating parameters and assessing reliability for models of steady state ground-water flow; 1, Theory and numerical properties: *Water Resources Research*, v. 13, no. 2, p. 318-324.
- _____ 1979, A method of estimating parameters and assessing reliability for models of steady state ground-water flow; 2, Application of statistical analysis: *Water Resources Research*, v. 15, no. 3, p. 603-617.
- _____ 1982, Incorporation of prior information on parameters into nonlinear regression ground-water flow models; 1, Theory: *Water Resources Research*, v. 18, no. 4, p. 965-976.
- Cooley, R.L., Konikow, L.F., and Naff, R.L., 1986, Nonlinear-regression groundwater flow modeling of a deep regional aquifer system: *Water Resources Research*, v. 22, no. 13, p. 1759-1778.
- Croxtton, F.E., 1953, *Elementary statistics with applications in medicine and the biological sciences*: New York, Dover Publications, 376 p.
- Desbarats, A.J., 1987, Numerical estimation of effective permeability in sand-shale formations: *Water Resources Research*, v. 23, no. 2, p. 273-286.
- De Wiest, R.J.M., 1969, Fundamental principles of ground-water flow, in De Wiest, R.J.M., ed., *Flow through porous media*: New York, Academic Press, p. 1-52.
- Donaldson, J.R., and Schnabel, R.B., 1987, Computational experience with confidence regions and confidence intervals for nonlinear least squares: *Technometrics*, v. 29, p. 67-82.
- Draper, N.R., and Smith, H., 1981, *Applied regression analysis* (2d ed.): New York, John Wiley, 709 p.
- Durbin, T.J., 1983, Application of Gauss algorithm and Monte Carlo simulation to the identification of aquifer parameters: U.S. Geological Survey Open-File Report 81-688, 26 p.
- Fenneman, N.M., 1938, *Physiography of eastern United States*: New York, McGraw-Hill Book Company, 714 p.
- Fertl, W.H., 1976, Abnormal formation pressures; implications to exploration, drilling, and production of oil and gas resources: New York, Elsevier Scientific Publishing Company, 382 p.

- Gamut, J.H., 1986, Approximation; theory and practice: New York, Academic Press, 410 p.
- Gebert, W.A., Graczyk, D.J., and Krug, W.R., 1987, Average annual runoff in the United States, 1951-80: U.S. Geological Survey Hydrologic Investigations Atlas HA-710, 1 sheet.
- Gill, P.E., Murray, Walter, and Wright, M.H., 1981, Practical optimization: London, Academic Press, 401 p.
- Godson, R.H., 1981, Digital terrain map of the United States: U.S. Geological Survey Miscellaneous Investigations Map I-1318, 1 sheet, scale 1:7,500,000.
- Grubb, H.F., 1984, Planning report for the Gulf Coast Regional Aquifer-System Analysis, Gulf of Mexico Coastal Plain, United States: U.S. Geological Survey, Water-Resources Investigations Report 84-4219, 30 p.
- _____, 1987, Overview of the Gulf Coast Regional Aquifer-System Analysis, in Vecchiolli, John, and Johnson, A.I., eds., Aquifers of the Atlantic and Gulf Coastal Plain: American Water Resources Association Monograph, no. 9, p. 101-118.
- Hogg, R.V., and Craig, A.T., 1965, Introduction to mathematical statistics: New York, Macmillan Company, 383 p.
- Hosman, R.L., and Weiss, J.S., 1991, Geohydrologic units of the Mississippi embayment and Texas coastal uplands aquifer systems, south-central United States: U.S. Geological Survey Professional Paper 1416-B, 19 p.
- Konikow, L.F., 1978, Calibration of ground-water models: American Society of Civil Engineers Conference on verification of mathematical and physical models in hydraulic engineering, College Park, Maryland, August 9-11, 1978, Proceedings, p. 87-93.
- Kuiper, L.K., 1983, A numerical procedure for the solution of the steady-state variable-density ground-water flow equation: Water Resources Research, v. 19, no. 1, p. 234-240.
- _____, 1985, Documentation of a numerical code for the simulation of variable density ground-water flow in three dimensions: U.S. Geological Survey Water-Resources Investigations Report 84-4302, 90 p.
- Lake, L.W., and H.B. Carroll, Jr., 1986, Reservoir characterization: New York, Academic Press, 660 p.
- Leake, S.A., and Prudic, D.E., 1988, Documentation of a computer program to simulate aquifer-system compaction using the modular finite-difference ground-water flow model: U.S. Geological Survey Open-File Report 88-482, 80 p.
- Lobmeyer, D.H., 1985, Freshwater heads and ground-water temperatures in aquifers of the Northern Great Plains in parts of Montana, North Dakota, South Dakota, and Wyoming: U.S. Geological Survey Professional Paper 1402-D, 11 p.
- Loucks, R.G., Dodge, M.M., and Galloway, W.E., 1986, Controls on porosity and permeability of hydrocarbon reservoirs in lower Tertiary sandstones along the Texas Gulf Coast: The University of Texas at Austin Bureau of Economic Geology Report of Investigations 149, p. 78.
- Martin, Angel, Jr., and Whiteman, C.D., Jr., 1989, Geohydrology and regional ground-water flow of the coastal lowlands aquifer system in parts of Louisiana, Mississippi, Alabama, and Florida--A preliminary analysis: U.S. Geological Survey Water-Resources Investigations Report 88-4100, 88 p.
- _____, in press, Hydrology of the coastal lowlands aquifer system in parts of Alabama, Florida, Louisiana, and Mississippi: U.S. Geological Survey Professional Paper 1416-H.
- McDonald, M.G., and Harbaugh, A.W., 1988, A modular three-dimensional finite-difference ground-water flow model: U.S. Geological Survey Techniques of Water-Resources Investigations, book 6, chap. A1, 576 p.

- Mesko, T.O., Williams, T.A., Ackerman, D.J., and Williamson, A.K., 1990, Ground-water pumage from the gulf coast aquifer systems, 1960-85, south-central United States: U.S. Geological Survey Water-Resources Investigations Report 89-4180, 177 p.
- Neglia, Stefino, 1979, Migration of fluids in sedimentary basins: The American Association of Petroleum Geologists Bulletin, v. 63, no. 4, p. 573-597.
- Neuman, S.P., 1980, A statistical approach to the inverse problem of aquifer hydrology--3, Improved solution method and added perspective: Water Resources Research, v. 16, no. 2, p. 331-346.
- Panofsky, H.A., and Brier, G.W., 1965, Some applications of statistics to meteorology: University Park, Pennsylvania State University Press, 224 p.
- Prudic, D.E., 1991, Hydraulic conductivity in the Gulf Coast Regional Aquifer-System Analysis, south-central United States: U.S. Geological Survey Water-Resources Investigations Report 90-4121, 38 p.
- Ryder, P.D., 1988, Hydrogeology and predevelopment flow in the Texas Gulf Coast aquifer systems: U.S. Geological Survey Water-Resources Investigations Report 87-4248, 109 p.
- Ryder, P.D., and Ardia, A.F., in press, Hydrology of the Texas Gulf Coast aquifer systems: U.S. Geological Survey Professional Paper 1416-E.
- Sun, R.J., 1986, Regional Aquifer-System Analysis program of the U.S. Geological Survey--Summary of projects, 1978-84: U.S. Geological Survey Circular 1002, 263 p.
- Sundararaj, Narasimhaiyengar, 1978, A method for confidence regions for nonlinear models: Australian Journal of Statistics, v. 20, p. 270-74.
- Vecchia, A.V., and Cooley, R.L., 1987, Simultaneous confidence and prediction intervals for nonlinear regression models with application to a groundwater flow model: Water Resources Research, v. 23, no. 7, p. 1237-1250.
- Wallace, J.R., and Grant, J.L., 1977, A least squares method for computing statistical tolerance limits: Water Resources Research, v. 13, no. 5, p. 819-823.
- Weiss, E.J., 1982, A model for the simulation of flow of variable-density ground water in three dimensions under steady-state conditions: U.S. Geological Survey Open-File Report 82-353, 59 p.
- Weiss, J.S., 1987, Determining dissolved-solids concentrations in mineralized ground water of the gulf coast aquifer systems using electric logs, in Vecchioli, John, and Johnson, A.I., eds., Regional Aquifer Systems of the United States, Aquifers of the Atlantic and Gulf Coastal Plain: American Water Resources Association Monograph, no. 9, p. 139-150.
- _____, 1992, Geohydrologic units of the coastal lowlands aquifer system, south-central United States: U.S. Geological Survey Professional Paper 1416-C, 32 p.
- Weiss, J.S., and Williamson, A.K., 1985, Subdivision of thick sedimentary units into model layers for simulation of ground-water flow: Ground Water, v. 23, no. 6, p. 767-774.
- Williams, T.A., and Williamson, A.K., 1989, Estimating water-table altitudes regional ground-water flow modeling, U.S. Gulf Coast: Ground Water, v. 27, no. 3, p. 333-340.
- Williamson, A.K., Grubb, H.F., and Weiss, J.S., 1990, Ground-water flow in the gulf coast aquifer systems, south-central United States--A preliminary analysis: U.S. Geological Survey Water-Resources Investigations Report 89-4071, 124 p.
- Yeh, W.W-G., and Yoon, Y.S., 1981, Aquifer parameter identification with optimum dimension in parameterization: Water Resources Research, v. 17, no. 3, p. 664-672.

ATTACHMENTS

Introduction

The computer code used to find the p vector \hat{B} which minimizes the weighted mean square error $S(B) = \frac{1}{n} \sum_{i=1}^n (Y_i - f_i(B))^2 \omega_i$, consists of two parts. The first part is taken from Durbin (1983). The second part is Kuiper's variable-density ground-water flow model, VARDEN (Kuiper 1985), which is used to evaluate the $f_i(B)$. The first part consists mainly of a section called MAIN in the code which chooses a sequence of parameter vectors B_{st} , $s = 1, 2, \dots, t = 1, 2, \dots, p$, which are used to find a sequence B_s , $s = 1, 2, \dots$, which converges to \hat{B} . This process is an implementation of the Levenberg-Marquardt method for the minimization of a sum of squares. The remainder of the first part is a linear-system solver called SOLEQU, which is used as a subroutine to MAIN. MAIN uses Kuiper's (1985) variable density ground-water flow model VARDEN, by calling MODEL when an evaluation of $f(B)$ is required for B equal to one of the vectors B_{st} or B_s which MAIN has chosen. In turn, MODEL calls the linear-system solvers PCG, and SIP.

MODEL, PCG, and SIP make up VARDEN and have been explained in detail by Kuiper (1985). MAIN from Durbin (1983) and MODEL from Kuiper (1985) were substantially modified for this application and the modifications are explained below. Some of the modifications consist of inserted code used to calculate prediction and confidence intervals as given by equations (6) and (7) in the prediction and confidence interval section of this report. Several slight modifications were made to PCG and SIP and they also are explained below. SOLEQU was not modified. The FORTRAN code for MAIN, MODEL, SOLEQU, PCG, and SIP are listed below in their respective sections. The sections for MAIN and MODEL contain a listing of meaningful variables. Dummy variables used only to implement a calculation are not listed. The manner of selection of the sequences B_{st} and B_s as dictated by the Leven-Marquardt procedure is explained in the next section.

The Levenberg-Marquardt Method

The Levenberg-Marquardt method (Durbin, 1983; Gill, Murray, and Wright, 1981) for the minimization of a sum of squares $S(B) = \sum_{i=1}^n (Y_i - f_i(B))^2 \omega_i$, is:

$$(X^T \omega X + \lambda I) \Delta B = X^T \omega (Y - f(B)) \quad (18)$$

Here $X(B)$ is the sensitivity matrix defined as $X_{ij} = \partial f_i / \partial B_j$, $i = 1, 2, \dots, n$, $j = 1, 2, \dots, p$, where n is the number of observations Y_i and p is the number of parameters. B is the p vector of parameters, I is the identity matrix,

and vector ΔB is the change in B . $\lambda(B)$ is equal to $(\sum_{i=1}^n r_i^2)^{1/2} / RLEVM$,

where n vector $r = Y - f(B)$ and RLEVM is the "maximum Levenberg radius." Weights in $S(B)$ are denoted by ω_i .

Equation (18) is applied iteratively, starting with some initial B of choice and corresponding ΔB from (18). For the next iteration B is replaced with $B + \Delta B$, which value is then used in (18) in $X(B)$, $\lambda(B)$, and $f(B)$ to produce a new ΔB , etc. The successive values of the vector B are labeled B_s where s is the iteration count. In order to evaluate $X(B)$ it is necessary to find the $n \times p$ derivatives $\partial f_i / \partial B_j$. These are found n at a time from p evaluations of $f(B)$ at $B = B_{st}$, $t = 1, 2, \dots, p$ and also $f(B)$ at $B = B_s$. The derivative $\partial f_i / \partial B_j$ at $B = B_s$ is approximated by

$$\partial f_i / \partial B_j = (f_i(B_{st}) - f_i(B_s)) / ((B_{st})_j - (B_s)_j)$$

where

$$(B_{st})_j - (B_s)_j = (TST)(B_s)_j, (B_{st})_\ell = (B_s)_\ell \text{ for } \ell \neq j,$$

and TST is called the "perturbation factor." Having evaluated $X(B_s)$ by this means, equation (18) is used to find $B_{s+1} = B_s + \Delta B$.

It is readily shown from equation (18) that $\Sigma(\Delta B)_j^2$ cannot exceed $(RLEVM)^2$. Thus RLEVM can be chosen to limit the size of ΔB . In general RLEVM should be chosen large enough that ΔB is larger than $(TST)B$, but not so large that the number of iterations needed for B_j , $j = 1, 2, \dots$, to arrive at a suitable approximation to \hat{B} is caused to increase. TST should be chosen as small as possible before deterioration in the accuracy of the derivatives of $f(B)$ with respect to B occurs. The parameters B_j should be scaled in $f(B)$ so that approximately equal percentage changes occur in $S(B)$ corresponding to equal percentage change in the individual members B_j of vector B.

MAIN

The function of MAIN is to implement the Levenberg-Marquardt method. It calls subroutine MODEL when it needs $f(B)$ for some chosen value of B as dictated by the Levenberg-Marquardt method. MODEL is actually called by either a call to MODEL1 or MODEL2; MODEL1 being used only for an initial call which reads in data needed for the evaluation of $f(B)$ for any value of B.

Function $f(B)$ is the ground-water flow model VARDEN. The values for $f_i(B)$, $i = 1, 2, \dots, n$ are the flow model predictions for the observations Y_i , many of which are grid-element volume-averaged heads. Model $f(B)$ requires the specification of the sand and clay component of hydraulic conductivities for each of the grid elements. The mapping of the p values for grid-element sand and clay component hydraulic conductivity and other parameters of $f(B)$ is accomplished by the following procedure. $PARAMX(I) = PARMO(I) * PARAM(IPARAM(I))$ $I = 1, 2, \dots, IPARX$, where IPARX is the number of global parameters, the total number of parameters needed for model $f(B)$ including many thousand grid-element sand and clay hydraulic conductivity values. PARAM is a p ($p = IPAR$) vector equal to the parameter vector B. IPARAM(I), $I = 1, 2, \dots, IPARX$ has the values 1 through p and maps I to an associated parameter number IPARAM(I). PARMO(I) is a multiplicative factor. PARAMX(I) is used within the model $f(B)$. In the case of the sand and clay component hydraulic conductivities, the PARAMX(I) are used to arrive at multiplicative factors which are multiplied by read-in values for sand and clay component hydraulic conductivity.

Explanation of MAIN Listing

COMMENT	LINE NUMBERS WITH MAN PREFIX
Read in the number of columns, rows, layers and intervening confining beds in the modeled area: NI10, NJ10, NK10, NK4.	700
Read in: Number of global parameters Number of active parameters Maximum number of iterations Perturbation factor Maximum error change Maximum Levenberg radius IPARX, IPAR, JITU, TST, PCHL, RLEVM.	830
Read in IPARAM.	990-1170
Read in PARAMO.	1180-1480
Do initial model call (MODEL1).	1550-1710
If JITU=0 go to 255 CONTINUE for final model run, print out, and stop.	1730
This is the final run, print, and stop section addressed by 255 CONTINUE.	1750-2060
Set initial conditions (JIT = 1).	2090-2400
1017 CONTINUE.	2420
Set JIT = JIT+1.	2430
Calculate new PRARMX corresponding to new PARAM and call MODEL2.	2440-2520

COMMENT

LINE NUMBERS
WITH MAN PREFIX

Calculate $SB=S(B)$ and root mean square weighted residual $PZ \equiv (n^{-1} S(B))^{1/2}$. Print out PZ , new estimates of the parameters B_j , $j = 1, 2, \dots, p$ ($PARAM(I), I = 1, 2, \dots, IPAR$), the change in these parameters from the previous iteration ($MU(I)$, $I = 1, 2, \dots, IPAR$), and $\partial(PZ)/\partial B_j$, $j=1, 2, \dots, p$ ($GRAP(I)$, $I=1, 2, \dots, IPAR$).

2530-2700

If: 1) The iteration number JIT is greater than the "maximum number of iterations" $JITU$, or 2) the change in the root mean square weighted residual PZ was less than $PCHL$, the "maximum error change," go to 255 CONTINUE for eventual stop.

2800-2890

Do numerical gradient computations. The $p = IPAR$ values for the $PARAM$ vector used are the B_{st} mentioned previously. Here $s = JIT$ the iteration number and $t = 1, 2, \dots, p = IPAR$. $GRSS$ is the sensitivity matrix appearing in equations (6) and (7) in the text. $PARO$ is used to scale $PARAM$.

2980-3150

Get $B2 = X^T \omega(Y-f(B))$ on the right hand side of equation (18) above. GRP is $\nabla S(B)$ here.

3170-3240

Do regression pack.

3260-3840

5050 CONTINUE.

3900

Get $A2 = (X^T \omega X + \lambda I)$, the matrix on the left hand side of equation (18) above.

3910-4030

Solve $(A2)\Delta B = (B2)$ for $MU = \Delta B$.

4050-4090

If new B is out of imposed constraining region, go to 5050 CONTINUE for a recalculation of ΔB . This recalculation will have those members of new B which were placed out of their respective constraint values.

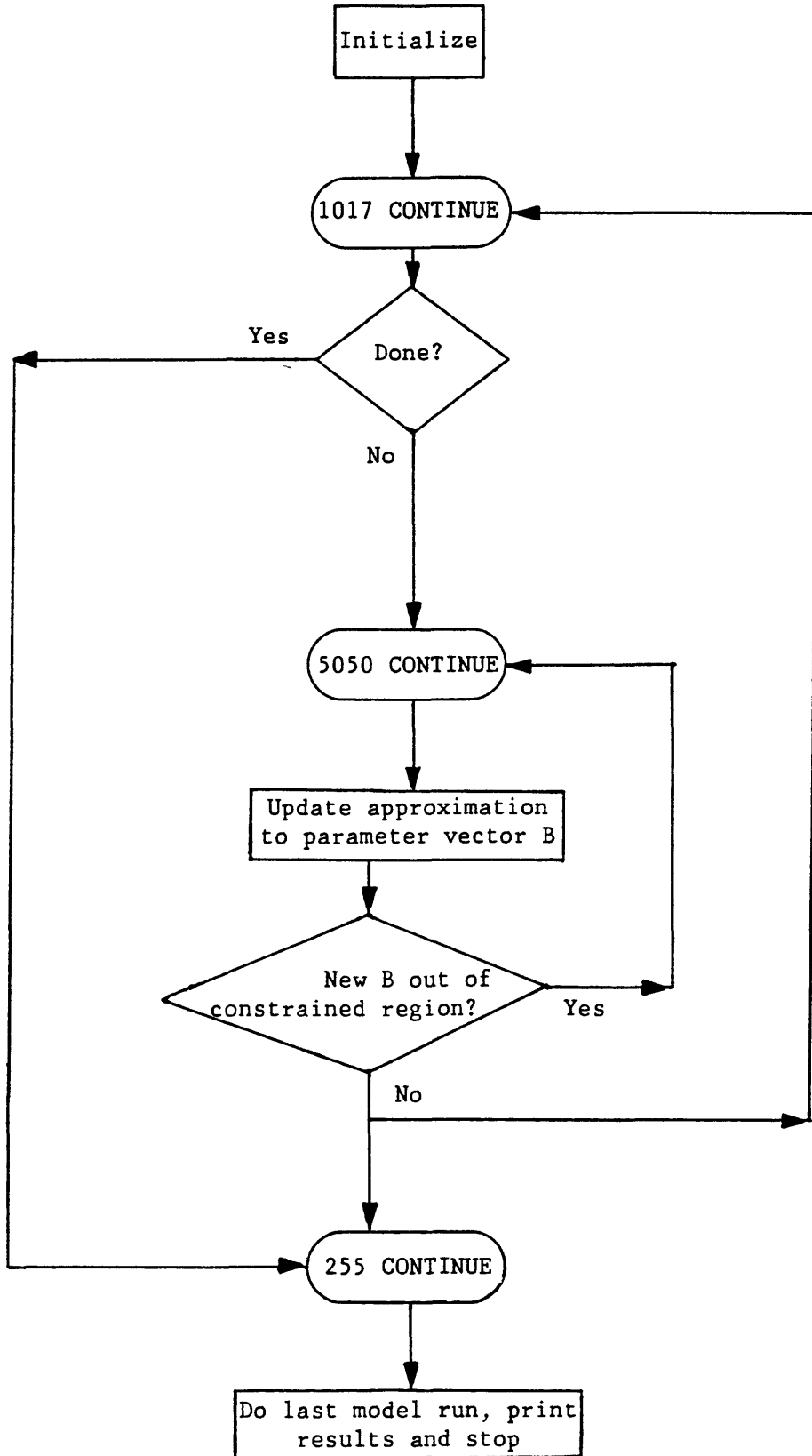
4120-4640

Calculate $\partial(PZ)/\partial B_t$, $t = 1, 2, \dots, p = IPAR$ ($GRP(I)$, $I = 1, 2, \dots, IPAR$).

4660-4690

Go to 1017.

Flow Chart of MAIN



Definition of Program Variables

EPS	$Y_i - f_i(B)$.
GRSS	Sensitivity matrix X in equations (6) and (7) above in body of report.
GRP	$\partial S(B)/\partial B_t$ or $\partial(PZ)/\partial B_t$.
IOUT	If IOUT = 1, MODEL1 or MODEL2 prints out certain results, if IOUT = 0, no printout occurs.
IPAR	Number of active parameters
IPARAM(I)	Maps global parameter numbers used by model f(B) to set of p active parameters of parameter vector B.
IPARX	Number of global parameters.
JIT	Iteration number (JIT = 5).
JITU	Maximum number of iterations.
MU	Change ΔB in the parameter vector B.
NI10	Number of columns in the modeled area.
NJ10	Number of rows in the modeled area.
NK10	Number of layers in the modeled area.
NK4	Number of intervening confining beds.
NWLMT	Number of observations Y_i
PARAMO(I)	Multiplicative factor in $PARAMX(I) = PARAMO(I)*PARAM(IPARAM(I))$ I = 1,2, . . . IPARX
PARAMX(I)	Global parameters used in model f(B)
PARO	Scale factor for parameters in parameter vector B
PCHL	Maximum error change
PDIV	Equal to NWLMT
PZ	$(\frac{1}{n} \sum S(B))^{1/2}$, root-mean-square-weighted residual

RLEVM Maximum Levenberg radius

SB $S(B) = \frac{1}{n} \sum_{i=1}^n (Y_i - f_i(B))^2$

TST Perturbation factor.

WLC Calculated values $f_i(B)$ for observations Y_i

WLM Measured values for observations Y_i

	IMPLICIT REAL*8(A-H,O-Z)	MAN0010
	COMMON WS,HMAX,RELX1,RELX2,COEF,ERR,XX10,DELT,ER5,SRZ,SUMRZ	MAN0020
	1,ERRSV,XX10SV,JIT,NIJ10,NI11,NJ11,NK11,NNN,NSKP1	MAN0030
	2,NSKP2,ITMAX,ICNT,IEVP,IWR1,NW1,NW2,NW3,N320,NUM4	MAN0040
	3,L9,LENGTH,NK1115,IT01,IT15,ICRO,DDK,BBK	MAN0050
	4,NI10,NJ10,NK10,NI12,NJ12,NK12,SVIJ,VV40,SV35	MAN0060
	COMMON /XX/ XX	MAN0070
	COMMON /DT/ DT	MAN0080
	COMMON /VV/ VV	MAN0090
	COMMON /E2/ E2	MAN0100
	COMMON /F2/ F2	MAN0110
	COMMON /G2/ G2	MAN0120
	COMMON /YQ/ YQ	MAN0130
	COMMON /NT/ NT	MAN0140
	COMMON /DD/ DD	MAN0150
	COMMON /BB/ BB	MAN0160
	COMMON /ZZ/ ZZ	MAN0170
	COMMON /XXS/ XXS	MAN0180
C	COMMON /ALN/ ALN	MAN0190
C	COMMON /XXE/ XXE	MAN0200
C	COMMON /SV/ SV	MAN0210
	COMMON /HL/ HL	MAN0220
	COMMON /LB/ LB	MAN0230
	COMMON /MHD/ MHD	MAN0240
	COMMON /C/ DXI,DYJ,N325,ISOR,IPDD	MAN0250
	1,NPINT,DT0,TOT,TFAC,NINT,IPRNT,IWRT,LFLOW,NK4,LLRO,IWRTXX,	MAN0260
	2,ILZ2,MAQ1,NU1,NU2,NU3,LFLO,IPH	MAN0270
	3,LBB,SUMF,SUNF,SQ2,SG2,SYQ,SVV,SUMFM,SUNFM	MAN0280
	COMMON /B/ COL,COU,PARAM,PARO,MU,W,EPS,WLM,LWLC,WLC,A2,B2,GRP	MAN0290
	1,CONA,CONB,SCALE	MAN0300
	2,NBND1,NBND2,ICON,NND,NWLM,NWLM1,NWLMT,IOUT	MAN0310
	COMMON /GRSS/ GRSS	MAN0320
	COMMON /XXSTR/ XXSTR	MAN0330
	COMMON /XKZZ/ XKZZ	MAN0340
	COMMON /LRO/ LRO	MAN0350
	COMMON /YQ1/ YQ1	MAN0360
	COMMON /LZ2/ LZ2	MAN0370
	COMMON /PARAMX/ PARAMX	MAN0380
	COMMON /PARAM0/ PARAM0	MAN0390
	COMMON /IPARAM/ IPARAM	MAN0400
	COMMON /YQ2/ YQ2	MAN0410
	REAL*4 YQ2(65078)	MAN0420
	DIMENSION A3(50,50)	MAN0430
	REAL*4COL(50),COU(50),PARAM(50),PARO(50),MU(50),W(3303),EPS(3303),	MAN0440
1	WLM(3303),LWLC(3303),WLC(3303),A2(50,50),B2(50),GRP(50),	MAN0450
2	CONA(50,50),CONB(50),SCALE(50),GRSS(3303,5),	MAN0460
3	PARAMX(159872),PARAM0(159872)	MAN0470
	INTEGER*4 NBND1(50),NBND2(50),ICON(50),	MAN0480
1	NND(3303)	MAN0490
	INTEGER*2 IPARAM(159872)	MAN0500
	REAL*4 DD(65078),BB(65078),ZZ(65078),YQ(65078),	MAN0510
	1XXS(65078),Q2(300),DDK(50),BBK(50),NT(94658),HL(65078)	MAN0520
2	,DXI(250),DYJ(250),XXSTR(65078),YQ1(65078,3)	MAN0530
3	,XKZZ(65078)	MAN0540

```

    INTEGER*2 LRO(94658),IPH(50),LFLO(4),J7(5),K7(5)
    1,NI(300),NJ(300),NK(300),MAQ1(50),NU1(3),NU2(3),NU3(3)
    DIMENSION DT(65078),E2(65078),F2(65078),G2(65078),VV(65078)
    DIMENSION XX(65078)
    1,WS(10),MHD(65078),LZ2(65078),LB(94658),LBB(5918)
    2,AOC(4),BOC(4),COC(4),DOC(4)
    3,SUMF(3,250),SUNF(3,250),SQ2(3,250),SG2(3,250),SYQ(3,250)
    4,SVV(3,250),SUMFM(3,250),SUNFM(3,250)
    *,IGR6(12,12)
    DATA PARAM/.9874,1.022,.8725,1.083,1.004,.7712,.9917,1.061,
    *1.017,.9249,1.041,.8042,.9301,1.180,.9482,.9572,
    *.9964,1.037,1.186,.9108,.9988,.9775,.9000,1.027,
    *1.002,.9558,
    *1.,1.,1.,1.,1.,1.,1.,1.,1.,1.,1.,1.,1.,1.,
    *1.,1.,1.,1.,1.,1.,1.,1.,1.,1.,1.,1./
    READ(5,99) NI10,NJ10,NK10,NK4
    NI11=NI10+1
    NJ11=NJ10+1
    NK11=NK10+1
    NIJ10=NI10*NJ10
    NIJK10=NIJ10*NK10
    N320=NIJK10+1
    N325=NIJ10*(NK10+NK4)+1
    NK15=NK11+NK4
C     NUMBER OF GLOBAL PARAMETERS, NUMBER OF ACTIVE PARAMETERS,
C     PERTURBATION FACTOR, MAXIMUM ERROR CHANGE, AND
C     MAXIMUM LEVENBERG RADIUS
C
    READ(5,940) IPARX,IPAR,JITU,TST,PCHL,RLEVM
    IPARX=N325+N320+2*NK10-1+10
    IPAR=4
    WRITE(6,941) IPARX,IPAR,JITU,TST,PCHL,RLEVM
C
    940  FORMAT(3I6,3F12.0)
    941  FORMAT(1H0,10X,'SERACH DEFINITION'/1H ,10X,17('- ')/
    1    1H0,10X,'NUMBER OF GLOBAL PARAMETERS',9X,I7/
    2    1H ,10X,'NUMBER OF ACTIVE PARAMETERS',9X,I3/
    3    1H ,10X,'MAXIMUM NUMBER OF ITERATIONS',8X,I3/
    4    1H ,10X,'PERTURBATION FACTOR',11X,1PE9.3/
    5    1H ,10X,'MAXIMUM ERROR CHANGE',10X,1PE9.3/
    6    1H ,10X,'MAXIMUM LEVENBERG RADIUS',6X,1PE9.3)
C
C     GLOBAL PARAMETER SET AND ASSIGNMENT TO ACTIVE PARAMETERS
C
C *****READ IPARAM
    NK1115=NK15
    IT15=1
    ICRO=0
    CALL RDWRT
    DO 209 IJ=2,N325
209    IPARAM(IJ)=1*NT(IJ)
    IPARAM(1)=0
    NK1115=NK11
    CALL RDWRT
    DO 211 IJ=2,N320

```

	I7=IJ+N325-1	MAN1100
211	IPARAM(I7)=1*NT(IJ)	MAN1110
	READ(5,99) (IPARAM(I7+I),I=1,NK10)	MAN1120
	WRITE(6,99) (IPARAM(I7+I),I=1,NK10)	MAN1130
	I8=I7+NK10	MAN1140
	READ(5,99) (IPARAM(I8+I),I=1,NK10)	MAN1150
	WRITE(6,99) (IPARAM(I8+I),I=1,NK10)	MAN1160
99	FORMAT(16I5)	MAN1170
C	READ PARAMO	MAN1180
	NK1115=NK15	MAN1190
	CALL RDWRT	MAN1200
	DO 309 IJ=2,N325	MAN1210
309	PARAMO(IJ)=NT(IJ)	MAN1220
	PARAMO(1)=0	MAN1230
	NK1115=NK11	MAN1240
	CALL RDWRT	MAN1250
	DO 311 IJ=2,N320	MAN1260
	I7=IJ+N325-1	MAN1270
311	PARAMO(I7)=NT(IJ)	MAN1280
	READ(5,98) (PARAMO(I7+I),I=1,NK10)	MAN1290
	WRITE(6,97) (PARAMO(I7+I),I=1,NK10)	MAN1300
	I8=I7+NK10	MAN1310
	READ(5,98) (PARAMO(I8+I),I=1,NK10)	MAN1320
	WRITE(6,97) (PARAMO(I8+I),I=1,NK10)	MAN1330
98	FORMAT(10G8.0)	MAN1340
97	FORMAT(10D12.3)	MAN1350
C	*****	MAN1360
	I1=IPARX-9	MAN1370
	DO 147 IL=I1,IPARX	MAN1380
	IPARAM(IL)=0	MAN1390
147	PARAMO(IL)=1	MAN1400
	PARAMO(I1+2)=.5900	MAN1410
	PARAMO(I1+7)=.8996	MAN1420
	IPARAM(I1+2)=1	MAN1430
	IPARAM(I1+7)=2	MAN1440
C	***	MAN1450
	WRITE(6,99) (IPARAM(IL),IL=I1,IPARX)	MAN1460
	WRITE(6,97) (PARAMO(IL),IL=I1,IPARX)	MAN1470
C	*****	MAN1480
C	ACTIVE PARAMETER VALUES, UPPER BOUNDS, AND LOWER BOUNDS	MAN1490
	DO 834 I=1,IPAR	MAN1500
	COL(I)= 01	MAN1510
	COU(I)=100	MAN1520
	PARAM(I)=1	MAN1530
834	CONTINUE	MAN1540
C	Determine PARAMX and do initial model call	MAN1550
	DO 210 I=1,IPARX	MAN1560
	X=PARAM(IPARAM(I))	MAN1570
	IF(IPARAM(I).EQ.0) X=1	MAN1580
	PARAMX(I)=PARAMO(I)*X	MAN1590
210	CONTINUE	MAN1600
	WRITE(6,946)	MAN1610
	WRITE(6,947) (I,PARAM(I),COL(I),COU(I),I=1,IPAR)	MAN1620
C		MAN1630
945	FORMAT(6X,3F12.0)	MAN1640

946	FORMAT(1H0,10X,'ACTIVE PARAMETER SET'/1H ,10X,20('-')/	MAN1650
1	1H0,10X,'ACTIVE',11X,'INITIAL',10X,'LOWER',10X,'UPPER' /	MAN1660
2	1H ,10X,'PARAMETER',8X,'VALUE',12X,'BOUND',10X,'BOUND' /)	MAN1670
947	FORMAT((1H ,10X,I9,3F15.4))	MAN1680
	JIT=-1	MAN1690
	IOUT=0	MAN1700
	CALL MODEL1	MAN1710
C	STOP	MAN1720
	IF(JITU.NE.0) GO TO 256	MAN1730
C	PRINT FINAL MODEL RUN	MAN1740
255	CONTINUE	MAN1750
	DO 251 I=1,IPARX	MAN1760
	X=PARAM(IPARAM(I))	MAN1770
	IF(IPARAM(I).EQ.0) X=1	MAN1780
	PARAMX(I)=PARAM(I)*X	MAN1790
251	CONTINUE	MAN1800
	IOUT=1	MAN1810
	CALL MODEL2	MAN1820
C		MAN1830
C	WATER-LEVEL RESIDUALS	MAN1840
C		MAN1850
	DO 656 I=1,NWLMT	MAN1860
	EPS(I)=WLM(I)-WLC(I)	MAN1870
656	CONTINUE	MAN1880
C		MAN1890
	WRITE(6,966)	MAN1900
C	WRITE(6,967) (NND(I),WLM(I),WLC(I),EPS(I),I=1,NWLMT)	MAN1910
	PDIV=NWLMT	MAN1920
	P=0.0	MAN1930
	DO 2566 IWL=1,NWLMT	MAN1940
	P=P+EPS(IWL)**2*W(IWL)	MAN1950
2566	CONTINUE	MAN1960
	PZ=DSQRT(P/PDIV)	MAN1970
	WRITE(6,9566) PZ	MAN1980
C		MAN1990
966	FORMAT(1H0,10X,'WATER-LEVEL RESIDUALS'/1H ,10X,21('-')/	MAN2000
1	1H0,10X,'STEP',3X,'NODE',3X,'MEASURED',3X,'COMPURED',	MAN2010
2	3X,'RESIDUAL' /)	MAN2020
967	FORMAT((1H ,10X,I4,3X,I4,3F11.1))	MAN2030
9566	FORMAT(1H0,10X,'STANDARD ERROR OF ESTIMATE',1X,1PE10.3)	MAN2040
C		MAN2050
	STOP	MAN2060
256	CONTINUE	MAN2070
C		MAN2080
C	SET INITIAL CONDITIONS	MAN2090
C		MAN2100
	FLAGA=0.	MAN2110
	IPARC=IPAR	MAN2120
	GDIV=IPAR	MAN2130
	PDIV=NWLMT	MAN2140
	PZP=0.	MAN2150
	PZPT=0.	MAN2160
	JIT=0.	MAN2170
	RLEV=0.0	MAN2180
	SCMIN=0.0	MAN2190

	IC=0	MAN2200
	DO 8000 I=1,IPAR	MAN2210
	MU(I)=0.0	MAN2220
	GRP(I)=0.0	MAN2230
	NBND1(I)=0	MAN2240
	NBND2(I)=0	MAN2250
8000	CONTINUE	MAN2260
C		MAN2270
	WRITE(6,960)	MAN2280
C		MAN2290
960	FORMAT(1H1,10X,'PARAMETER SEARCH RESULTS'/1H ,10X,24('-'))	MAN2300
C		MAN2310
C	INITIAL PARAMETERS	MAN2320
C		MAN2330
	DO 419 J=1,IPAR	MAN2340
	PARO(J)=PARAM(J)	MAN2350
	IF(COL(J).LE.1.0E-08.OR.COU(J).LE.1.0E-08) WRITE(6,130)	MAN2360
130	FORMAT(4(/),40X,'BOTH CONSTRAINTS MUST BE GREATER THAN 1.E-8')	MAN2370
	IF(PARO(J).GE.(COU(J)-1.E-5)) NBND1(J)=1	MAN2380
	IF(PARO(J).LE.(COL(J)+1.E-5)) NBND1(J)=-1	MAN2390
419	CONTINUE	MAN2400
C		MAN2410
1017	CONTINUE	MAN2420
	JIT=JIT+1	MAN2430
	DO 250 I=1,IPARX	MAN2440
	X=PARAM(IPARAM(I))	MAN2450
	IF(IPARAM(I).EQ.0) X=1	MAN2460
	PARAMX(I)=PARAMO(I)*X	MAN2470
250	CONTINUE	MAN2480
	IOUT=0	MAN2490
	WRITE(6,999) (PARAM(I),I=1,IPAR)	MAN2500
999	FORMAT(10E12.5)	MAN2510
	CALL MODEL2	MAN2520
	P=0.	MAN2530
	DO 7115 IWL=1,NWLMT	MAN2540
	LWLC(IWL)=WLC(IWL)	MAN2550
	EPS(IWL)=WLM(IWL)-WLC(IWL)	MAN2560
	P=P+EPS(IWL)**2*W(IWL)	MAN2570
7115	CONTINUE	MAN2580
	SB=P	MAN2590
	PZ=DSQRT(P/PDIV)	MAN2600
C		MAN2610
C	PRINT-OUT OF SEARCH RESULTS	MAN2620
C		MAN2630
	WRITE(6,7602) JIT,PZ,RLEV,SCMIN	MAN2640
7602	FORMAT(1H0),10X,'ITERATION',I4/1H,10X,13('-')/	MAN2650
1	1H0,10X,'STANDARD ERROR OF ESTIMATE',1X,1PE10.3/1H ,10X,	MAN2660
2	'LEVENBERG RADIUS',11X,1PE10.3/1H ,10X,'MINIMUM SCALING FACTOR',	MAN2670
3	5X,1PE10.3/1H0,10X,2('PARAMETER',3X,'ESTIMATE',7X,'CHANGE',5X,	MAN2680
4	'GRADIENT',5X)/)	MAN2690
	WRITE(6,7607)(I,PARAM(I),MU(I),GRP(I),I=1,IPAR)	MAN2700
	IF(IC.EQ.0) GO TO 8003	MAN2710
	WRITE(6,8002)	MAN2720
	WRITE(6,8001) (ICON(IC),IC=1,ICMAX)	MAN2730
8003	CONTINUE	MAN2740

C		MAN2750
	8002 FORMAT(1H0,10X,'CONSTRAINED PARAMETERS'/)	MAN2760
	8001 FORMAT(1H ,5X,10I8)	MAN2770
	7607 FORMAT((1H ,10X,2(I5,5X, 1PE10.3,3X,1PE10.3,3X,1PE10.3,4X)))	MAN2780
C		MAN2790
C	CONVERGENCE AND ITERATION TESTS	MAN2800
C		MAN2810
	IF(JIT.GE.JITU) GO TO 6260	MAN2820
	PCH=ABS(PZ-PZP)	MAN2830
	IF(PCH.LT.PCHL) GO TO 6274	MAN2840
	PZP=PZ	MAN2850
	GO TO 1305	MAN2860
	6260 WRITE(6,6261) JITU	MAN2870
	6261 FORMAT(1H0,10X,'NUMBER OF ITERATIONS GREATER THAN ',I5)	MAN2880
	GO TO 255	MAN2890
	6274 WRITE(6,6277) PCHL	MAN2900
	6277 FORMAT(1H0,10X,'OBJECTIVE FUNCTION CHANGES LESS THAN',F8.4)	MAN2910
	GO TO 255	MAN2920
C		MAN2930
C	BEGINNING OF NEW ITERATION	MAN2940
C		MAN2950
	1305 CONTINUE	MAN2960
C		MAN2970
C	NUMERICAL GRADIENT COMPUTATION	MAN2980
C		MAN2990
	DO 1732 J=1,IPAR	MAN3000
	DP=TST*PARAM(J)	MAN3010
	PARAM(J)=PARAM(J)+DP	MAN3020
C		MAN3030
	DO 252 I=1,IPARX	MAN3040
	X=PARAM(IPARAM(I))	MAN3050
	IF(IPARAM(I).EQ.0) X=1	MAN3060
	PARAMX(I)=PARAM0(I)*X	MAN3070
	252 CONTINUE	MAN3080
	IOUT=0	MAN3090
	CALL MODEL2	MAN3100
C		MAN3110
	PARAM(J)=PARAM(J)-DP	MAN3120
	DO 1730 IWL=1,NWLMT	MAN3130
	1730 GRSS(IWL,J)=(WLC(IWL)-LWLC(IWL))*PARO(J)/DP	MAN3140
	1732 CONTINUE	MAN3150
C		MAN3160
C	COMPUTATION OF A2 AND B2	MAN3170
C		MAN3180
	DO 1430 J=1,IPAR	MAN3190
	SUM=0	MAN3200
	DO 1427 IWL=1,NWLMT	MAN3210
	1427 SUM=SUM+GRSS(IWL,J)*EPS(IWL)*W(IWL)	MAN3220
	B2(J)=SUM	MAN3230
	1430 GRP(J)=-2.*SUM	MAN3240
	WRITE(6,999) (B2(J),J=1,IPAR)	MAN3250
C	#####Regression Insert Pack###	MAN3260
C	Get left hand side of inequality (9) in text	MAN3270
	DO 1675 JR=1,IPAR	MAN3280
	DO 1650 JS=1,IPAR	MAN3290

	SUM5=0.	MAN3300
	DO 1640 IWL=1,NWLMT	MAN3310
1640	SUM5=SUM5+GRSS(IWL, JR)*GRSS(IWL, JS)*W(IWL)	MAN3320
1650	A3(JR, JS)=SUM5	MAN3330
1675	CONTINUE	MAN3340
C	DO 619 JJ=1,IPAR	MAN3350
C619	WRITE(6,999) (A3(JJ,J),J=1,IPAR)	MAN3360
	DO 625 J1=1,IPAR	MAN3370
	DO 625 J2=1,IPAR	MAN3380
625	A2(J2,J1)=A3(J2,J1)	MAN3390
	CALL SOLEQU (A2,B2,IPAR)	MAN3400
	WRITE(6,999) (B2(J),J=1,IPAR)	MAN3410
	SUM=0.	MAN3420
	DO 620 J=1,IPAR	MAN3430
620	SUM=SUM+GRP(J)*B2(J)	MAN3440
	SUM=SUM*(-.5)	MAN3450
	X=SUM/(SB-SUM)	MAN3460
	WRITE(6,2999) 99,99,X,SB,SUM	MAN3470
C	Here, X is left hand side of inequality (9) in text	MAN3480
2999	FORMAT(2I8,6D16.9)	MAN3490
C	Take a look at several of the terms just preceding omega sub k	MAN3500
C	in equation (6) in the text to see how large they are relative	MAN3510
C	to omega sub k	MAN3511
	DO 693 I10=1,30	MAN3520
	IWL=100*I10	MAN3530
	IF(I10.EQ.27) IWL=3122	MAN3540
	IF(I10.EQ.28) IWL=3138	MAN3550
	IF(I10.EQ.29) IWL=3159	MAN3560
	IF(I10.EQ.30) IWL=3196	MAN3570
	DO 694 J=1,IPAR	MAN3580
694	B2(J)=GRSS(IWL,J)	MAN3590
	DO 626 J1=1,IPAR	MAN3600
	DO 626 J2=1,IPAR	MAN3610
626	A2(J2,J1)=A3(J2,J1)	MAN3620
	CALL SOLEQU(A2,B2,IPAR)	MAN3630
	SUM=0	MAN3640
	DO 695 J=1,IPAR	MAN3650
695	SUM=SUM+GRSS(IWL,J)*B2(J)	MAN3660
	WRITE(6,2999) I10,NND(IWL),SUM	MAN3670
C	SUM is one of the terms just preceding omega sub k	MAN3680
693	CONTINUE	MAN3690
C	Evaluate the term in the square root of equation (7) of the text	MAN3700
	DO 697 JS=1,IPAR	MAN3710
	DO 696 J=1,IPAR	MAN3720
696	B2(J)=0	MAN3730
	B2(JS)=1	MAN3740
	DO 627 J1=1,IPAR	MAN3750
	DO 627 J2=1,IPAR	MAN3760
627	A2(J2,J1)=A3(J2,J1)	MAN3770
	CALL SOLEQU(A2,B2,IPAR)	MAN3780
	ANS1=DSQRT(B2(JS)*SB)*PARO(JS)	MAN3790
	ANS=ANS1*DSQRT(X)	MAN3800
	WRITE(6,2999) JS,JS,ANS,ANS1,B2(JS),PARO(JS)	MAN3810
C	B2(JS) is the term	MAN3820
697	CONTINUE	MAN3830

C	#####End of Regression Insert Pack###	MAN3840
	DO 5070 J=1,IPAR	MAN3850
	CONB(J)=1.	MAN3860
	DO 5070 K=1,IPAR	MAN3870
	SCALE(J)=1.	MAN3880
5070	CONA(J,K)=1.	MAN3890
5050	CONTINUE	MAN3900
	SUM7=0.	MAN3910
	DO 1558 J=1,IPAR	MAN3920
	B2(J)=-.5*GRP(J)*CONB(J)	MAN3930
1558	SUM7=SUM7+B2(J)*B2(J)	MAN3940
	RLEV=RLEVM	MAN3950
	FLEV=DSQRT(SUM7)/RLEV	MAN3960
	DO 1575 JR=1,IPAR	MAN3970
	DO 1550 JS=1,IPAR	MAN3980
	SUM5=0.	MAN3990
	DO 1540 IWL=1,NWLMT	MAN4000
1540	SUM5=SUM5+GRSS(IWL, JR)*GRSS(IWL, JS)*W(IWL)	MAN4010
1550	A2(JR, JS)=SUM5*CONA(JR, JS)	MAN4020
1575	A2(JR, JR)=A2(JR, JR)+FLEV	MAN4030
C		MAN4040
C	SOLUTION OF THE SYSTEM OF LINEAR EQUATIONS	MAN4050
C		MAN4060
	CALL SOLEQU (A2,B2,IPARC)	MAN4070
	DO 1570 J=1,IPAR	MAN4080
1570	MU(J)=B2(J)*PARO(J)*CONB(J)	MAN4090
C	WRITE(6,97) (MU(I),I=1,IPAR)	MAN4100
C		MAN4110
C	COMPUTATION OF BOUNDARY SET	MAN4120
C		MAN4130
	DO 5100 J=1,IPAR	MAN4140
	THRR=PARAM(J)+MU(J)	MAN4150
	IF(THRR.GE.COU(J)) GO TO 5120	MAN4160
	IF(THRR.LE.COL(J)) GO TO 5140	MAN4170
	NBND2(J)=0	MAN4180
	GO TO 5100	MAN4190
5120	NBND2(J)=1	MAN4200
	GO TO 5100	MAN4210
5140	NBND2(J)=-1	MAN4220
5100	CONTINUE	MAN4230
C		MAN4240
C	SELECTION OF DECISION VARIABLES	MAN4250
C		MAN4260
	IC=0	MAN4270
	IF(FLAGA) 5160,5160,5170	MAN4280
5160	DO 5200 J=1,IPAR	MAN4290
	IF(NBND2(J).EQ.0) GO TO 5200	MAN4300
	IF(NBND2(J).NE.NBND1(J)) GO TO 5200	MAN4310
	CONB(J)=0.	MAN4320
	FLAGA=1.	MAN4330
	DO 5210 JJ=1,IPAR	MAN4340
	CONA(J, JJ)=0.	MAN4350
5210	CONA(JJ, J)=0.	MAN4360
	CONA(J, J)=1.	MAN4370
	IC=IC+1	MAN4380

ICON(IC)=J	MAN4390
WRITE(6,97) FLAGA,(CONB(I),I=1,IPAR)	MAN4400
5200 CONTINUE	MAN4410
ICMAX=IC	MAN4420
GO TO 5250	MAN4430
5170 FLAGA=0.	MAN4440
5250 IF(FLAGA) 5260,5260,5050	MAN4450
5260 CONTINUE	MAN4460
C	MAN4470
C UPDATE OF BOUNDARY SET	MAN4480
C	MAN4490
DO 5400 J=1,IPAR	MAN4500
THRR=PARAM(J)+MU(J)	MAN4510
C WRITE(6,97) MU(J),THRR	MAN4520
5430 IF(THRR.GE.(COU(J))) GO TO 5450	MAN4530
IF(THRR.LE.(COL(J))) GO TO 5460	MAN4540
NBND2(J)=0	MAN4550
GO TO 5420	MAN4560
5450 NBND2(J)=1	MAN4570
THRR=COU(J)	MAN4580
GO TO 5420	MAN4590
5460 NBND2(J)=-1	MAN4600
THRR=COL(J)	MAN4610
5420 CONTINUE	MAN4620
PARAM(J)=THRR	MAN4630
5400 CONTINUE	MAN4640
C Calculate gradient of PZ	MAN4650
DO 5500 J=1,IPAR	MAN4660
NBND1(J)=NBND2(J)	MAN4670
GRP(J)=GRP(J)/(2.*PZ*PDIV*PARO(J))	MAN4680
5500 CONTINUE	MAN4690
WRITE(6,99) (NBND1(I),I=1,IPAR)	MAN4700
GO TO 1017	MAN4710
END	MAN4720

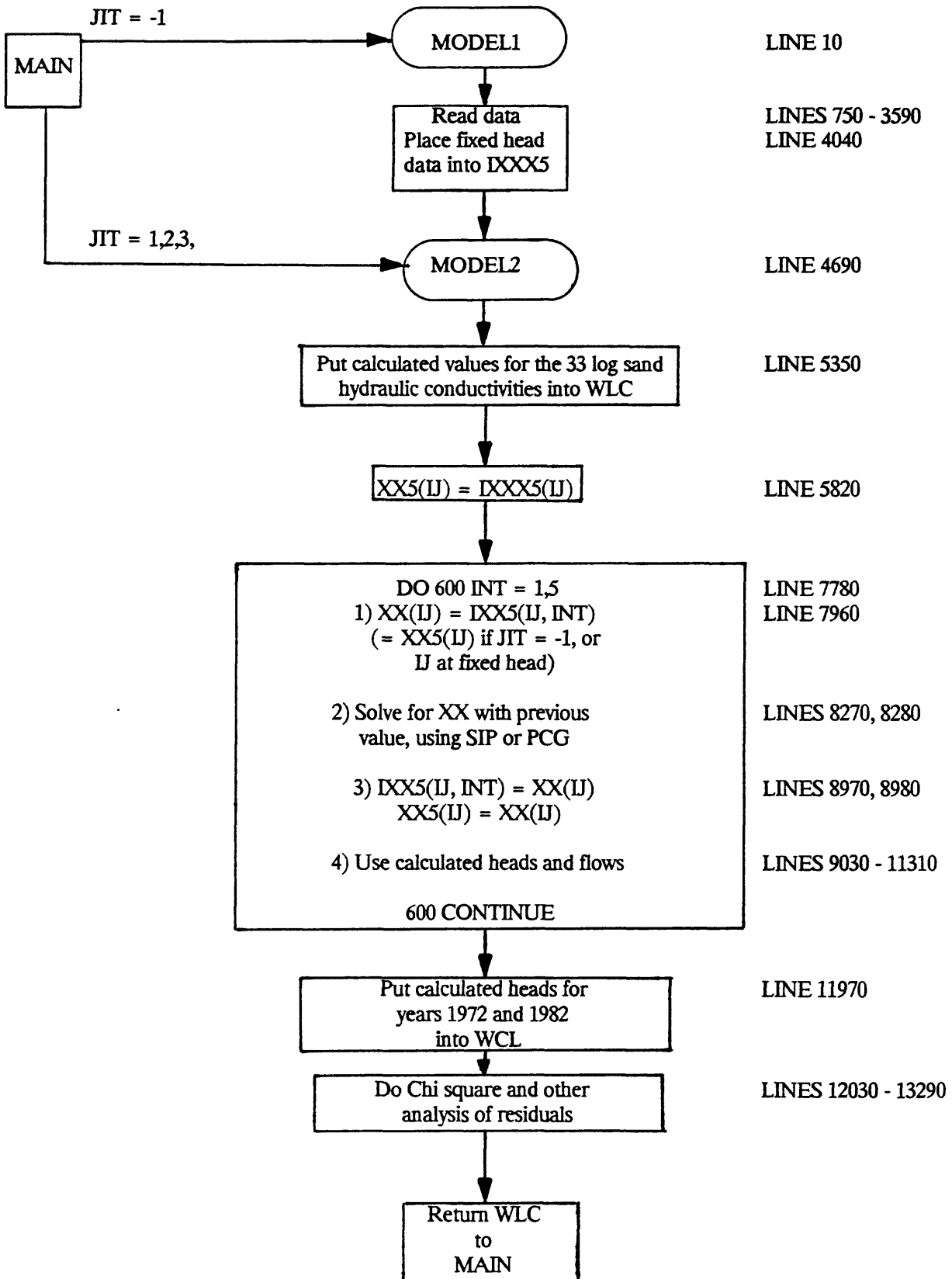
MODEL

The basic function of MODEL is to evaluate $f(B)$ given a value of B from MAIN. MAIN passes a value of $JIT = -1$ when going to MODEL1, and values of $JIT = 1, 2, 3, \dots$, when going to MODEL2. The approximations $f_i(B)$ to the observations Y_i include heads for the years 1972 and 1982 as well as 33 $f_i(B)$ corresponding to the 33 log sand hydraulic conductivity observations. Each time MODEL is called it finds heads for five different years corresponding to $INT = 1, 2, 3, 4, 5$. $INT = 3$ corresponds to 1972 and $INT = 5$ corresponds to 1982. Convergence of SIP or PCG is faster when good starting values for head ($= XX$) are used. Thus the values of $XX(IJ)$ found for a given INT and JIT are saved in $IXX5(IJ, INT)$ to be used as starting values for $XX(IJ)$ at $JIT = JIT + 1$. $XX5$ is used as the value of XX at $INT(t)$ when finding XX at $INT + 1(t + \Delta t)$, corresponding to the next time step.

$IOUT = 1$ is passed to MODEL by MAIN when various printouts are desired. When $IOUT = 0$ this printout does not occur

The most important changes of VARDEN necessary to produce MODEL are:
(1) The emplacement of the global parameters PARAMX into the calculation of the quantities DD , BB , and ZZ , the elements of the matrix the inversion of which gives $f(B)$; (2) implementation of the functions giving the rate of decrease with depth of sand and clay hydraulic conductivity combined with the use of equations (10) and (11) in the text and giving effective hydraulic conductivities. The first of these changes appears at lines MD06040 through MD06130 of the listing of MODEL. The second occurs at lines MD06140 through MD06440.

Essential Features of Model



Definition of Program Variables

ALFA	Parameter b_5 in text.
BBK	See FCNT.
DDK	See FCNT.
DD,BB,ZZ	Elements of the matrix, the inversion of which gives $f(B)$, the solution to the model with parameters B.
DEL	Array combining the five time intervals.
DELT	Time interval.
DXI,DYJ	DXI(I) is the I direction horizontal dimension of the grid elements in column I. DYJ(J) is the J direction horizontal dimension of the grid elements in row J.
ERR, XX10	<p>Iteration terminates when</p> $\max_{(\text{over } IJ)} XX^{ICNT} - XX^{(ICNT-1)} +$ $\max_{(\text{over } IJ)} XX^{(ICNT-1)} - XX^{(ICNT-2)} < ERR,$ <p>the maximum residual error</p> $\max_{(\text{over } IJ)} [M] XX^{ICNT} - YQ < XX10, \text{ or } ICNT \geq ITMAX.$
FC	Factors used to approximate pumping rates for first time interval.
FCNT,NT, DDK,BBK	$K_{xx}(IJ) = (NT(IJ) \times (DDK(K))),$ $K_{yy}(IJ) = (NT(IJ) \times (BBK(K))),$ <p>where $K_{xx}(IJ)$, $K_{yy}(IJ)$ denote the x, y components of K, the hydraulic conductivity for grid element IJ. NT is used as a dummy variable for various data sets.</p>
GP5	Multiplier for K_2/b for geopressure zone.

HL HL(IJ) is used for subsidence. It is the lowest value that XX(IJ) = head has achieved yet for any of the previous or the current time step.

HLS HLS is subsidence at ground surface.

HMAX SIP parameter β' (Trescott and Larson, 1977).

I Positional locator along a row, also column number.

ICT In SIP, a repeating counter for iteration parameter number.

IGP IGP(J) traces I along boundary of geopressured zone.

IJ Single subscript replacement for I,J,K corresponding to grid element I,J,K.

IJKM1 Replacement for I,J,K-1, or for I,J,K+1 when the K direction is reversed in SIP.

IJKP1 Replacement for I,J,K+1, or for I,J,K-1 when the K direction is reversed in SIP.

IJLB IJ for confining bed grid elements.

IJM1K Replacement for I,J-1,K, or for I,J+1,K when the J direction is reversed in SIP.

IJP1K Replacement for I,J+1,K, or for I,J-1,K when the J direction is reversed in SIP.

IM1JK Single subscript replacement for I-1,J,K.

IP1JK Single subscript replacement for I+1,J,K.

IOUT If IOUT = 1, MODEL prints various quantities. If IOUT = 0, it does not.

IP1JK Single subscript replacement for I+1,J,K.

IPH(K),
K=2 Set IPH(K) = 1 if you want: hydraulic head or freshwater head, flow rate data, or drawdown, for layer K. Set
NK11 IPH(K) = 0 if you do not want these quantities for layer K. The layers are numbered K = 2 through K = NK11 = NK10+1.

IPR,JPR At I = IPR(I10), J = JPR(I10) all of the layers present in region I10 (fig. 31) occur, I10 = 1,2,...,10.

ISOR ISOR = 0.

ITMAX Maximum number of iterations allowed.

IWRT Set IWRT to 1 if you want to watch the convergence of
 NU1(I), freshwater head $h' = XX$, at the three locations: I = NU1(1),
 I=1,3 J = NU1(2), K = NU1(3) I = NU2(1), J = NU2(2),
 NU2(I) K = NU2(3) and I = NU3(1), J = NU3(2), K = NU3(3).
 I=1,3),
 NU3(I),
 I=1,3

IXX5 Storage value for starting values for the solution finding
 XX, head.

IXXX5 Storage array for fixed (and other) head values.

J Positional locator along a column, also row number.

JIT Iteration number. Called s in previous text in this attachment.

K Layer number.

KOUT The total number of confining beds between layer 2 and layer K.
 Only one effective confining bed is allowed between any two
 layers. If there are more than two confining beds, they are
 combined into one effective confining bed.

L9 In SIP, L9 is: 1 for J direction reversal, 2 for J and K
 direction reversal, and 3 for K direction reversal.

LB LB(IJ) is the vertical dimension of grid element IJ.

LBB Elevation of the base of the lowermost layer, K = 2.

LENGTH Number of iteration parameters in SIP. Four types of flow-rate data are available (1) the flow rate out of each grid element in the negative I, J, and K directions, (2) the flow rate out of fixed head (MHD = 0) grid elements, (3) head dependent discharge flow rates from grid elements having such discharge, and (4) total flow rate budgets for sets of grid elements having the same I, the same J, and the same K. All flow rates are in units of mass divided by $\rho_0 = 1 \text{ gm/cm}^3$ per unit time (L^3/T) (see the section on "Units" in the text). Set LFLOW = 1 if you want any flow-rate data, set LFLOW = 0 if no flow rate data is desired. Set LFLO(i) = 0 if you do not want type i flow rate data. For i = 1, set LFLO(1) = 1, 2, 3, for type 1 flow rate data in the negative I, J, and K directions respectively. If LFLO(1) = 4 all directions are given.

Set LFLO(2) = 1 if you want type 2 flow rate data. Set LFLO(3) = 1 if you want type 3 flow rate data. Set LFLO(4) = 1, 2, 3, for the budgets of sets of grid elements having the same I, J, and K respectively. If LFLO(4) = 4 budgets are given for I, J, and K. Corresponding to the integers 1, 2, and 3 in the first column of output the second column gives I, J, and K respectively.

LRO $LRO(IJ) = (\rho'/\rho_0)$. $\rho = \rho' + \rho_0$ is the water density for grid element IJ. $LRO(IJLB) = (\rho'/\rho_0)$, where $\rho = \rho' + \rho_0$ is the water density for confining bed grid element IJLB. Values given are truncated after the fifth decimal place.

LZ2 $LZ2(IJ) = M$, where the integer M divided by 10 is the elevation of node point IJ located at the center of grid element IJ.

MAQ1 $MAQ1(K) = 0$ except when a confining bed lies between layers K-1 and K, in which case $MAQ1(K) = 1$.

MHD Holds read-in values for fixed heads initially. After these are read into IXXX5, MHD(IJ) is = 0,1,2, corresponding to: a regular active grid element, fixed element, and an element outside of the domain of solution, respectively.

NI10 Number of columns in the modeled area.

NINT Number of time intervals, NINT = 5.
 NJ10 Number of rows in the modeled area.

 NK10 Number of layers in the modeled area.

 NK4 Number of intervening confining beds.

 NND NND(I) is equal to the IJ location of observation I.

 NT See FCNT.

 NU1 See IWRT.

 NU2 See IWRT.

 NU3 See IWRT.

 NWLM Number of observations of grid-element volume-averaged head
 for years 1972 and 1982. Equal to 1,432 + 1,675 = 3,107.

 NWLM1 Number of observations of grid element volume averaged head
 for year 1972 only. Equal to 1,432.

 P1 Parameter b_4 in text.

 P2 Parameter b_9 in text.

 P3 Parameter b_7 in text.

 P7 Parameter b_8 in text.

 P8 Parameter b_3 in text.

 P9 Parameter b_7 in text.

 SV SV specifies specific storage S_s .

 SV35 P2*SV35 is specific storage for all grid elements (except as
 modified by subsidence which multiplies the value by VV40 for
 the clay component).

 VV40 VV40 = P7*40. VV40*SV35*P2 is specific storage for clay
 component in subsidence condition.

W W(I) is the weight of observation Y_i in the expression of S(B).

WLC WLC(IJ) is the calculated value $f_i(B)$ produced by the model.

WLM WLM(I) is the measured value Y_i of observation number i.

WMAX In SIP, $(XYFC)*(XY)$ is used for $(1-\alpha_{max})$ (Weinstein and others, 1969) when WMAX = 0. When WMAX = 0, $(1-\alpha_{max}) = WMAX$ is used.

XTV Chi square test data.

XX Freshwater head = (pressure head h) + z.

XX10 Error step for the residual $b - Ax$ in the solvers PCG and SIP.

XXS The value of XX for the previous time step.

XXSTR XXSTR(IJ) is percent sand in grid element IJ.

YQ Contains pumping rates and also psuedo sources prior to each solution by PCG or SIP.

YQ1 YQ1(IJ,I3) I3 = 1,2,3 has pumping rates for the years 1970, 1975, and 1980, respectively.

SUBROUTINE MODEL1	MD00010
IMPLICIT REAL*8 (A-H,O-Z)	MD00020
COMMON WS,HMAX,RELX1,RELX2,COEF,ERR,XX10,DELT,ER5,SRZ,SUMRZ	MD00030
1,ERRSV,XX10SV,JIT,NIJ10,NI11,NJ11,NK11,NNN,NSKP1	MD00040
2,NSKP2,ITMAX,ICNT,IEVP,IWR1,NW1,NW2,NW3,N320,NUM4	MD00050
3,L9,LENGTH,NK1115,IT01,IT15,ICRO,DDK,BBK	MD00060
4,NI10,NJ10,NK10,NI12,NJ12,NK12,SVIJ,VV40,SV35	MD00070
COMMON /XX/ XX	MD00080
COMMON /DT/ DT	MD00090
COMMON /VV/ VV	MD00100
COMMON /E2/ E2	MD00110
COMMON /F2/ F2	MD00120
COMMON /G2/ G2	MD00130
COMMON /YQ/ YQ	MD00140
COMMON /NT/ NT	MD00150
COMMON /DD/ DD	MD00160
COMMON /BB/ BB	MD00170
COMMON /ZZ/ ZZ	MD00180
COMMON /XXS/ XXS	MD00190
C COMMON /ALN/ ALN	MD00200
C COMMON /XXE/ XXE	MD00210
C COMMON /SV/ SV	MD00220
COMMON /HL/ HL	MD00230
COMMON /LB/ LB	MD00240
COMMON /MHD/ MHD	MD00250
COMMON /C/ DXI,DYJ,N325,ISOR,IPDD	MD00260
1,NPINT,DT0,TOT,TFAC,NINT,IPRNT,IWRT,LFLOW,NK4,LLRO,IWRTXX,	MD00270
2,ILZ2,MAQ1,NU1,NU2,NU3,LFLO,IPH	MD00280
3,LBB,SUMF,SUNF,SQ2,SG2,SYQ,SVV,SUMFM,SUNFM	MD00290
COMMON /B/ COL,COU,PARAM,PARO,MU,W,EPS,WLM,LWLC,WLC,A2,B2,GRP	MD00300
1,CONA,CONB,SCALE	MD00310
2,NBND1,NBND2,ICON,NND,NWLM,NWLM1,NWLMT,IOUT	MD00320
COMMON /GRSS/ GRSS	MD00330
COMMON /XXSTR/ XXSTR	MD00340
COMMON /XKZZ/ XKZZ	MD00350
COMMON /LRO/ LRO	MD00360
COMMON /YQ1/ YQ1	MD00370
COMMON /LZ2/ LZ2	MD00380
COMMON /PARAMX/ PARAMX	MD00390
COMMON /PARAMO/ PARAMO	MD00400
COMMON /IPARAM/ IPARAM	MD00410
COMMON /YQ2/ YQ2	MD00420
C *****EXTRAS*****	MD00430
COMMON /FC/ FC,DEL,ISO,OS4,GP5,LFLOA,IPHA	MD00440
COMMON /IXX5/ IXX5	MD00450
COMMON /IXXXS/ IXXXS	MD00460
COMMON /HLS/ HLS	MD00470
COMMON /IPR/ IPR,JPR,X3150,X493,IIII,XTV	MD00480
DIMENSION LA(40),IA(40),XL1(40),XTV(20),IX7(20)	MD00490
INTEGER*2 IXXXS(65078),IXX5(65078,5),LFLOA(4),IPHA(50)	MD00500
INTEGER*2 IGP(120),IPR(10),JPR(10)	MD00510
REAL*4 DPT(4),XSS(4),XSH(4),HLS(5918)	MD00520
C *****	MD00530
REAL*4 YQ2(65078)	MD00540
REAL*4COL(50),COU(50),PARAM(50),PARO(50),MU(50),W(3303),EPS(3303),	MD00550

1	WLM(3303), LWLC(3303), WLC(3303), A2(50, 50), B2(50), GRP(50),	MD00560
2	CONA(50, 50), CONB(50), SCALE(50), GRSS(3303, 5),	MD00570
3	PARAMX(159872), PARAM0(159872)	MD00580
	INTEGER*4 NBND1(50), NBND2(50), ICON(50),	MD00590
1	NND(3303)	MD00600
	INTEGER*2 IPARAM(159872)	MD00610
	REAL*4 DD(65078), BB(65078), ZZ(65078), YQ(65078),	MD00620
	1XXS(65078), Q2(300), DDK(50), BBK(50), NT(94658), HL(65078)	MD00630
2	, DXI(250), DYJ(250), XXSTR(65078), YQ1(65078, 3)	MD00640
3	, XKZZ(65078)	MD00650
	INTEGER*2 LRO(94658), IPH(50), LFLO(4), I7(5), J7(5), K7(5)	MD00660
1	, NI(300), NJ(300), NK(300), MAQ1(50), NU1(3), NU2(3), NU3(3)	MD00670
	DIMENSION DT(65078), E2(65078), F2(65078), G2(65078), VV(65078)	MD00680
	DIMENSION XX(65078)	MD00690
1	, WS(10), MHD(65078), LZ2(65078), LB(94658), LBB(5918)	MD00700
2	, AOC(4), BOC(4), COC(4), DOC(4)	MD00710
3	, SUMF(3, 250), SUNF(3, 250), SQ2(3, 250), SG2(3, 250), SYQ(3, 250)	MD00720
4	, SVV(3, 250), SUMFM(3, 250), SUNFM(3, 250), FC(5, 15), DEL(5)	MD00730
*	, IC7(65)	MD00740
	PI=3.1415926	MD00750
	DATA DEL/1.D40, 10950.D0, 1825.D0, 1825.D0, 1825.D0/	MD00760
	DATA IPR/12, 16, 18, 23, 28, 27, 20, 28, 35, 30/	MD00770
	DATA JPR/90, 56, 41, 36, 29, 94, 66, 44, 38, 60/	MD00780
	DATA XTV/-1.D20, -1.53413, -1.15035, -.88715, -.67449, -.48877,	MD00790
*	-.31864, -.15731, .0, .0, .0, .0, .0, .0, .0, .0, .0, .0/	MD00800
	DO 719 I=10, 17	MD00810
719	XTV(I)=-XTV(18-I)	MD00820
	WRITE(6, 3555) (XTV(I), I=1, 17)	MD00830
	WRITE(6, 3555) (DEL(I), I=1, 5)	MD00840
	DO 10 I=1, 50	MD00850
10	MAQ1(I)=0	MD00860
	READ(5, 8877) ((FC(I, J), J=1, 10), I=1, 2)	MD00870
	FC(1, 11)=1	MD00880
	FC(2, 11)=1	MD00890
8877	FORMAT(10F8.0)	MD00900
	WRITE(6, 8877) ((FC(I, J), J=1, 10), I=1, 2)	MD00910
	READ(5, 2003) (IGP(I), I=2, 103)	MD00920
	WRITE(6, 2003) (IGP(I), I=2, 103)	MD00930
	OS4=1.E-25	MD00940
	GP5=5.E-30	MD00950
	VV40=40	MD00960
	WRITE(6, 9022)	MD00970
	WRITE(6, 3555) VV40, OS4, GP5	MD00980
	L9=2	MD00990
	LENGTH=5	MD01000
	XYFC=1	MD01010
	WMAX=0	MD01020
	READ(5, 2000) ISOR	MD01030
	IF (ISOR.GE.0) READ(5, 2000) ITMAX, ERR, XX10, HMAX	MD01040
	ISOR=0	MD01050
	ITMAX=70	MD01060
	ERR=.001	MD01070
	XX10=8	MD01080
C	ERR=.0002	MD01090
C	XX10=1	MD01100

	HMAX=1.0	MD01110
	READ(5,2020) NI10,NJ10,NK10,NK4	MD01120
	READ(5,2003) IWRT,(NU1(I),I=1,3),(NU2(I),I=1,3),(NU3(I),I=1,3)	MD01130
	IWRT=0	MD01140
	READ(5,2003) LFLOW,(LFLO(I),I=1,4),(LFLOA(I),I=1,4)	MD01150
	NK11=NK10+1	MD01160
	READ(5,2003) (IPH(K),K=2,NK11)	MD01170
	READ(5,2003) (IPHA(K),K=2,NK11)	MD01180
	NUM4=ISOR-1	MD01190
	NUM4=3	MD01200
	NI11=NI10+1	MD01210
	NJ11=NJ10+1	MD01220
	NK15=NK11+NK4	MD01230
	NI12=NI10+2	MD01240
	NJ12=NJ10+2	MD01250
	NK12=NK10+2	MD01260
	NIJ10=NI10*NJ10	MD01270
	NIJK10=NIJ10*NK10	MD01280
	NNN=NIJK10+2	MD01290
	N315=NIJ10+1	MD01300
	N320=NIJK10+1	MD01310
	N325=NIJ10*(NK10+NK4)+1	MD01320
	NW1=NU1(1)+NI10*(NU1(2)-2)+NIJ10*(NU1(3)-2)	MD01330
	NW2=NU2(1)+NI10*(NU2(2)-2)+NIJ10*(NU2(3)-2)	MD01340
	NW3=NU3(1)+NI10*(NU3(2)-2)+NIJ10*(NU3(3)-2)	MD01350
C	READ IN AND PRINT ARRAYS MHD,LRO,LBB,LB,XX,SV,XXSTR, XKZZ, FCNT,	MD01360
C	DDK,BBK,NT,MAQ1,DXI,DYJ,YQ1	MD01370
C	GROUP II	MD01380
	WRITE(6,5000)	MD01390
	NK1115=NK11	MD01400
	IT15=1	MD01410
	ICRO=0	MD01420
	CALL RDWRT	MD01430
	DO 20 IJ=2,N320	MD01440
20	MHD(IJ)=NT(IJ)*(10)+.1	MD01450
	WRITE(6,5002)	MD01460
	NK1115=NK15	MD01470
	CALL RDWRT	MD01480
	DO 90 IJ=2,N325	MD01490
90	LRO(IJ)=NT(IJ)*1.D+5+.1	MD01500
	WRITE(6,5003)	MD01510
	NK1115=2	MD01520
	CALL RDWRT	MD01530
	DO 100 IJ=2,N315	MD01540
100	LBB(IJ)=NT(IJ)	MD01550
	WRITE(6,5004)	MD01560
	NK1115=NK15	MD01570
	IT15=10	MD01580
	CALL RDWRT	MD01590
	DO 110 IJ=2,N325	MD01600
110	LB(IJ)=NT(IJ)	MD01610
	LB(1)=1	MD01620
	IT15=1	MD01630
C	***** Insert LB=1 for geopressed zone *****	MD01640
	DO 219 J=2,NJ11	MD01650

```

IGPJ=IGP(J) MD01660
DO 217 I=2,NI11 MD01670
IF=I+NI10*(J-2) MD01680
C %%%%%%%%% If LB<10 at any location, set to zero and adjust LBB MD01690
C accordingly MD01691
LL=0 MD01700
DO 216 K=2,NK10 MD01710
IJ=IF+(K-2)*NIJ10 MD01720
LBIJ=LB(IJ) MD01730
IF(LBIJ.GE.10) GO TO 215 MD01740
LL=LL+LBIJ MD01750
LB(IJ)=0 MD01760
215 CONTINUE MD01770
216 CONTINUE MD01780
LBB(IF)=LBB(IF)+LL MD01790
C %%%%%%%%% LB<10 to zero done MD01800
LB1=LB(IF) MD01810
I2236=22*I+36*J-2349 MD01820
IF(I2236.LE.0) GO TO 218 MD01830
IF(LB(IF+NIJ10*9).EQ.0) GO TO 218 MD01840
IF(I.LT.IGPJ) GO TO 218 MD01850
C LB1=1 MD01860
218 LB(IF)=LB1 MD01870
C218 CONTINUE MD01880
217 CONTINUE MD01890
C WRITE(6,3004) J,(LB(I+NI10*(J-2)),I=2,NI11) MD01900
219 CONTINUE MD01910
C ***** LB=1 for geopressed zone done ***** MD01920
C Read in observations Yi(=WLM) of grid element volume averaged MD01930
C head for the years 1970 and 1980. Number them consecutively MD01931
C using I9 as shown. NWLM is the total number of these. NND is MD01940
C the IT location of each observation MD01950
C ***** MD01960
NK11 15=NK11 MD01970
IT15=10 MD01980
CALL RDWRT MD01990
DO 246 I=1,3303 MD02000
WLM(I)=0 MD02010
W(I)=0 MD02020
WLC(I)=0 MD02030
246 NND(I)=0 MD02040
I9=0 MD02050
DO 247 IJ=2,N320 MD02060
XNTIJ=NT(IJ) MD02070
IF((XNTIJ*LB(IJ)).EQ.0.) GO TO 247 MD02080
I9=I9+1 MD02090
NND(I9)=IJ MD02100
WLM(I9)=XNTIJ MD02110
247 CONTINUE MD02120
NWLM1=I9 MD02130
CALL RDWRT MD02140
IT15=1 MD02150
DO 274 IJ=2,N320 MD02160
XNTIJ=NT(IJ) MD02170
IF((XNTIJ*LB(IJ)).EQ.0.) GO TO 274 MD02180

```

	I9=I9+1	MD02190
	NND(I9)=IJ	MD02200
	WLM(I9)=XNTIJ	MD02210
274	CONTINUE	MD02220
	NWLM=I9	MD02230
	NWLMT=NWLM+100	MD02240
C	***** Done getting grid element value averaged head	MD02250
C	observations *****	MD02251
C	Set weights for gerah observations	MD02260
	CALL RDWRT	MD02270
	DO 248 I=1,NWLM	MD02280
	IJ=NND(I)	MD02290
248	W(I)=(39.093*39.093)/NT(IJ)**2	MD02300
	WRITE(6,952)	MD02310
	DO 249 I=1,NWLM	MD02320
	IF (W(I).LE.0.0) W(I)=1.0	MD02330
249	CONTINUE	MD02340
C	WRITE(6,953) (NND(I),WLM(I),W(I),I=1,20)	MD02350
	WRITE(6,2020) NWLM	MD02360
C		MD02370
953	FORMAT((1H ,10X,I4,3X,I4,F12.1,F10.4))	MD02380
C	***** Set weights done *****	MD02390
C	Determine observations and corresponding weights for the 33	MD02400
C	zone averaged hydraulic conductivities	MD02410
C	GO TO 876	MD02420
	N33=33	MD02430
	SUM=0	MD02440
	LAA=2	MD02450
	Y1=0	MD02460
	Y2=0	MD02470
	NL=0	MD02480
	DO 125 I=1,N33	MD02490
	READ(5,2777) LA(I),IA(I),M1,V1,V2,M2,V3,V4,M3,XL1(I)	MD02500
	WRITE(6,2777) LA(I),IA(I),66,XL1(I)	MD02510
	IF((LA(I).EQ.LAA).AND.(I.NE.33)) GO TO 1266	MD02520
	SUM=SUM+(Y2-Y1*Y1/NL)/NL	MD02530
	NL=0	MD02540
	Y1=0	MD02550
	Y2=0	MD02560
	LAA=LAA+1	MD02570
1266	CONTINUE	MD02580
	X=XL1(I)	MD02590
	Y2=Y2+X*X	MD02600
	Y1=Y1+X	MD02610
	NL=NL+1	MD02620
125	CONTINUE	MD02630
	AV65=SUM/10	MD02640
	X493=39.093/DSQRT(AV65)	MD02650
	DO 126 I=1,N33	MD02660
	II=NWLM+(LA(I)-2)*10+IA(I)	MD02670
	W(II)=1	MD02680
	WLM(II)=X493*(XL1(I))	MD02690
	WRITE(6,3 001) I,II,XL1(I),W(II),WLM(II),AV65,X493	MD02700
3001	FORMAT(2I7,7D12.3)	MD02710
126	CONTINUE	MD02720

2777	FORMAT(2I4,3(I4,2F8.3))	MD02730
C876	CONTINUE	MD02740
C	***** Done with 33 observations and weights *****	MD02750
	WRITE(6,5052)	MD02760
	NK1115=NK11	MD02770
	CALL RDWRT	MD02780
	DO 150 IJ=2,N320	MD02790
150	XX(IJ)=NT(IJ)*10	MD02800
	XX(1)=0	MD02810
	XX(NNN)=0	MD02820
	WRITE(6,5054)	MD02830
	CALL RDWRT	MD02840
C	DO 160 IJ=2,N320	MD02850
C160	SV(IJ)=NT(IJ)*1	MD02860
	SV35=.3D-5	MD02870
	WRITE(6,3555) SV35	MD02880
	WRITE(6,9954)	MD02890
	CALL RDWRT	MD02900
	DO 1601 IJ=2,N320	MD02910
1601	XXSTR(IJ)=NT(IJ)	MD02920
	WRITE(6,5060)	MD02930
	CALL RDWRT	MD02940
	DO 166 IJ=2,N320	MD02950
166	XKZZ(IJ)=NT(IJ)	MD02960
C	Read pumping rate for 3 time periods 1970, 1975, and 1980	MD02970
C	into YQ1	MD02971
	READ(5,2000) NINT	MD02980
	WRITE(6,5053)	MD02990
	NK1115=NK11	MD03000
	DO 1642 I3=1,3	MD03010
	CALL RDWRT	MD03020
	DO 1681 IJ=2,N320	MD03030
1681	YQ1(IJ,I3)=1*NT(IJ)	MD03040
1642	CONTINUE	MD03050
	WRITE(6,5005)	MD03060
	NK1115=NK15	MD03070
	IT15=2	MD03080
	CALL RDWRT	MD03090
C	***** REMOVE PINCHED OUT NODES WHEN APPROPRIATE *****	MD03100
	DO 163 I=2,NI11	MD03110
	DO 163 J=2,NJ11	MD03120
	IJIJ=I+NI10*(J-2)	MD03130
	DO 163 K=2,NK11	MD03140
	IJ=IJIJ+NIJ10*(K-2)	MD03150
	IF(LB(IJ).NE.0) GO TO 165	MD03160
	IF((K.EQ.2).OR.(K.EQ.NK11)) GO TO 164	MD03170
	IT5=0	MD03180
	KM1=K-1	MD03190
	DO 161 K1=2,KM1	MD03200
	IJ1=IJIJ+NIJ10*(K1-2)	MD03210
161	IF(LB(IJ1).NE.0) IT5=IT5+1	MD03220
	IT6=0	MD03230
	KP1=K+1	MD03240
	DO 162 K2=KP1,NK11	MD03250
	IJ2=IJIJ+NIJ10*(K2-2)	MD03260

162	IF(LB(IJ2).NE.0) IT6=IT6+1	MD03270
	IF((IT5*IT6).GT.0) GO TO 165	MD03280
164	NT(IJ)=0	MD03290
165	CONTINUE	MD03300
	IF(NT(IJ).EQ.0) XKZZ(IJ)=0	MD03310
	IF((IKZZ.NE.0).AND.(XKZZ(IJ).EQ.0)) NT(IJ)=0	MD03320
163	CONTINUE	MD03330
C	***** DONE Pinched out nodes DONE *****	MD03340
C	GROUP III	MD03350
	IF(NK4.EQ.0) GO TO 170	MD03360
	READ(5,2003) (MAQ1(K),K=2,NK11)	MD03370
	WRITE(6,5010)	MD03380
	WRITE(6,4002) (K,MAQ1(K),K=2,NK11)	MD03390
170	CONTINUE	MD03400
	READ(5,2000) FDXI,FDYJ,MDXI1,MDYJ1,MD2	MD03410
	IF(MDXI1.EQ.1) READ(5,2000) (DXI(I),I=2,NI11)	MD03420
	IF(MDYJ1.EQ.1) READ(5,2000) (DYJ(J),J=2,NJ11)	MD03430
	IF(MDXI1.EQ.1) GO TO 190	MD03440
	DO 180 I=2,NI11	MD03450
180	DXI(I)=FDXI	MD03460
190	IF(MDYJ1.EQ.1) GO TO 210	MD03470
	DO 200 J=2,NJ11	MD03480
200	DYJ(J)=FDYJ	MD03490
210	IF(MD2.NE.0) GO TO 220	MD03500
	WRITE(6,5001)	MD03510
	WRITE(6,3010) (DXI(I),I=2,NI11)	MD03520
	WRITE(6,3010) (DYJ(I),I=2,NJ11)	MD03530
220	CONTINUE	MD03540
	DXI(1)=1	MD03550
	DYJ(1)=1	MD03560
	DXI(NI12)=1	MD03570
	DYJ(NJ12)=1	MD03580
C	READ IN AND PRINTING OF ARRAYS NOW COMPLETE	MD03590
C	INITIALIZE VARIOUS ARRAYS TO ZERO	MD03600
	DO 230 IJ=1,NNN	MD03610
	HL(IJ)=0	MD03620
	DD(IJ)=0	MD03630
	BB(IJ)=0	MD03640
	ZZ(IJ)=0	MD03650
	DT(IJ)=0	MD03660
	E2(IJ)=0	MD03670
	F2(IJ)=0	MD03680
	G2(IJ)=0	MD03690
	YQ2(IJ)=0	MD03700
230	VV(IJ)=0	MD03710
C	DETERMINE LZ2	MD03720
	KOUT=0	MD03730
	DO 280 K=2,NK11	MD03740
	KOUT=KOUT+MAQ1(K)	MD03750
	DO 280 J=2,NJ11	MD03760
	DO 280 I=2,NI11	MD03770
	I2236=22*I+36*J-2349	MD03780
	DXY=DXI(I)*DYJ(J)	MD03790
	IJF=I+NI10*(J-2)	MD03800
	IJ=IJF+NIJ10*(K-2)	MD03810

	LBIJ=LB(IJ)	MD03820
	KLB=NK11+KOUT	MD03830
	IJLB=IJF+NIJ10*(KLB-2)	MD03840
	DTIJ=LRO(IJ)*1.0D-5	MD03850
C	SV(IJ)=SV(IJ)*DXY*LBIJ	MD03860
C	DETERMINE LZ2	MD03870
	IJKM1=IJ-NIJ10	MD03880
	IF(K.EQ.2) GO TO 240	MD03890
	LZ2(IJ)=LZ2(IJKM1)+5*(LBIJ+LB(IJKM1))+10*MAQ1(K)*LB(IJLB)	MD03900
	GO TO 250	MD03910
240	LZ2(IJ)=LBIJ*5+10*(LBB(IJ)+MAQ1(K)*LB(IJLB))	MD03920
250	CONTINUE	MD03930
C	Place layer 12 head from MHD and also head of zero for	MD03940
C	geopressed zone into IXXX5 for storage.	MD03950
C	Set MHD=0,1,2 for active, fixed, and out of domain	MD03960
C	elements respectively	MD03961
	XXMHD=XX(IJ)	MD03970
	MHDIJ=MHD(IJ)	MD03980
	IF(K.EQ.NK11) XXMHD=MHDIJ	MD03990
	LZ2IJ=LZ2(IJ)	MD04000
	X=((XXMHD-LZ2IJ)*(DTIJ+1)+LZ2IJ)*.1D0	MD04010
	IF((K.EQ.2).AND.(I2236.GT.0)) X=3000	MD04020
	IF(NT(IJ).EQ.0.0) X=0.0	MD04030
	IXXXS(IJ)=X+.5	MD04040
	IX=0	MD04050
	IF((K.EQ.2).AND.(I2236.GT.0)) IX=1	MD04060
	IF(K.EQ.NK11) IX=1	MD04070
	IF(NT(IJ).EQ.0.0) IX=2	MD04080
	MHD(IJ)=IX	MD04090
C	PUT PUMPING RATES to zero if out of domain of solution	MD04100
	DO 1643 I3=1,3	MD04110
	X=YQ1(IJ,I3)	MD04120
	IF(IX.EQ.2) X=0	MD04130
	YQ1(IJ,I3)=X	MD04140
1643	CONTINUE	MD04150
280	CONTINUE	MD04160
C	***** DO removal (W(I)=0) OF WLM'S that lie outside of domain of	MD04170
C	solution *****	MD04180
	ISM9=0	MD04190
	DO 643 I=1,NWLM	MD04200
	IJ=NND(I)	MD04210
	IF(.NOT.(MHD(IJ).GE.1)) GO TO 644	MD04220
	ISM9=ISM9+1	MD04230
	W(I)=0	MD04240
	WRITE(6,1003) ISM9,IJ,MHD(IJ),777.,WLM(I)	MD04250
644	CONTINUE	MD04260
643	CONTINUE	MD04270
	DO 895 I10=1,10	MD04280
	I2464=IPR(I10)+(JPR(I10)-2)*NI10	MD04290
	DO 993 I=1,10	MD04300
	IJ=I2464+(I-1)*NIJ10	MD04310
	II3=I+1	MD04320
	I8=NWLM+(II3-2)*10+I10	MD04330
	IF(MHD(IJ).GE.1) W(I8)=0	MD04340
	IF(MHD(IJ).GE.1) WRITE(6,2020) I8,I10,I,IJ,MHD(IJ)	MD04350

993	CONTINUE	MD04360
895	CONTINUE	MD04370
C	STOP	MD04380
C	***** DONE *****	MD04390
	LZ2(1)=0	MD04400
	SVIJ=SV35*DXY	MD04410
C	Put elevation of top layer 12 into LBB for later use, print	MD04420
	WRITE(6,8002)	MD04430
	WRITE(6,6000)	MD04440
	WRITE(6,4002) NK11	MD04450
	DO 300 J=2,NJ11	MD04460
	DO 290 I=2,NI11	MD04470
	IJF=I+NI10*(J-2)	MD04480
	IJ=IJF+NIJ10*(NK11-2)	MD04490
	X=(LZ2(IJ)*.1D0+LB(IJ)*.5D0+.1)	MD04500
	LBB(IJF)=X	MD04510
290	CONTINUE	MD04520
300	CONTINUE	MD04530
	DO 301 J=2,NJ11	MD04540
	I5=NI10*(J-2)	MD04550
C	WRITE(6,3004) J,(LBB(I5+I),I=2,NI11)	MD04560
301	CONTINUE	MD04570
C	STOP	MD04580
C	Set up several variables which are to be used in subsequent	MD04590
C	calls to model2	MD04600
	N98=N320+N325-2	MD04610
	N99=N98+NK10	MD04620
	ERRSV=ERR	MD04630
	XX10SV=XX10	MD04640
	X3150=NWLM+N33	MD04650
	IIII=-1	MD04660
C		MD04670
C		MD04680
	ENTRY MODEL2	MD04690
C		MD04700
C		MD04710
	I92=60	MD04720
	J92=74	MD04730
	R42=37*37	MD04740
	N324=N325-1	MD04750
C	Set error criteria for solution dependent upon iteration	MD04760
C	count JIT	MD04761
	XL5=1.0*JIT	MD04770
	IF(XL5.GT.9.) XL5=9.	MD04780
	ERR=(19.-2.*XL5)*ERRSV	MD04790
	XX10=(19.-2.*XL5)*XX10SV	MD04800
C	Error criteria ERR and XX10 now set	MD04810
	N111=N99+NK11	MD04820
	N121=N111+7	MD04830
C	^^	MD04840
	IF(IOUT.EQ.0) GO TO 780	MD04850
	WRITE(6,9030)	MD04860
	DO 792 I=1,27	MD04870
	IJ=I*NIJ10-100	MD04880
792	WRITE(6,4502) PARAMX(IJ)	MD04890

```

WRITE(6,3555) (PARAMX(N111+I),I=1,8) MD04900
780 CONTINUE MD04910
C ^^ For IJ=2,N121(N121=IPARX-3,N111=IPARX-10) MD04920
C Change PARAMX(IJ) to EXP[(PARAMX(IJ)-1)*LS] MD04930
C LS=5 for sand and clay hydraulic conductivities MD04940
C DO 312 IJ=2,N121 MD04950
L5=5 MD04960
IF(IJ.GE.(N111+2)) L5=2 MD04970
312 PARAMX(IJ)=10**((PARAMX(IJ)-1)*L5) MD04980
C Change done MD04990
C Assign those PARAMX(IJ) for IJ>N111 to specific parameters MD05000
P1=PARAMX(N111+1) MD05010
P2=PARAMX(N111+3) MD05020
P3=PARAMX(N111+4) MD05030
ALFA=PARAMX(N111+5) MD05040
P7=PARAMX(N111+6) MD05050
P8=PARAMX(N111+7) MD05060
P9=PARAMX(N111+8) MD05070
VV40=P7*40 MD05080
C Write out PARAMX,XKZZ,NT, and resulting effective MD05090
C conductivities and their logarithms for depths of 600 and MD05100
C 6000 ft for each of the 10 regions of figure 31 in the text. MD05110
C Determine calculated values WLC for observations corresponding MD05120
C to the 33 log sand hydraulic conductivities at line MD05350 MD05130
C ^^ MD05140
DO 795 I10=1,10 MD05150
I2464=IPR(I10)+(JPR(I10)-2)*NI10 MD05160
IF(IOUT.EQ.1) WRITE(6,9031) I10 MD05170
DO 793 I=1,27 MD05180
IJ=I2464+(I-1)*NIJ10 MD05190
PP=PARAMX(IJ) MD05200
IJ32=IJ-N324 MD05210
IF(I.GE.17) W8=XKZZ(IJ32)*(LB(IJ32)/(LB(IJ32)+1.D-6)) MD05220
IF(I.LT.17) W8=NT(IJ) *(LB(IJ) /(LB(IJ) +1.D-6)) MD05230
X=PP*W8 MD05240
II=I+1 MD05250
II3=II MD05260
IF(I.GE.17) II=II-16 MD05270
X1=DLOG10(X+1.D-20) MD05280
C ^^ MD05290
C DPTI4=(LBB(I2464)-LZ2(IJ))/6000. MD05300
C IF(DPTI4.LT.0.) DPTI4=0 MD05310
C XFAC=10**(-DPTI4/6.72) MD05320
C X2=DLOG10(X*XFAC+1.D-20) MD05330
C ^^ MD05340
IF(II3.LE.11) WLC(NWLM+(II3-2)*10+I10)=X1*X493 MD05350
IF(IOUT.EQ.1) WRITE(6,4501) II,PP,X,X1 MD05360
793 CONTINUE MD05370
IF(IOUT.EQ.0) GO TO 795 MD05380
WRITE(6,3555) P1,P6,P2,P3,ALFA,P7,P8,P9 MD05390
DO 794 I44=1,2 MD05400
DO 794 I=1,11 MD05410
IJ=I2464+(I-1)*NIJ10 MD05420
XSS(1)=NT(IJ)*PARAMX(IJ) MD05430
XSH(1)=XKZZ(IJ)*PARAMX(IJ+N324) MD05440

```

	DPTI4=.67	MD05450	
	IF(I44.EQ.2) DPTI4=10	MD05460	
	X=.1829*DPTI4	MD05470	
	FACSH=1*10**((.08333*X*X-1.1677*X)*1.0)	MD05480	
	FACSS=1*10**(-DPTI4/6.72)	MD05490	
	XSH(1)=XSH(1)*FACSH	MD05500	
	XSS(1)=XSS(1)*FACSS	MD05510	
	X=1-.5	MD05520	
	AL25=ALFA*4	MD05530	
	ALP5=1./AL25	MD05540	
	C0 =XSS(1)*(XSH(1)/(XSS(1)+1.D-20))**((X)**AL25)	MD05550
	C01=XSS(1)*(XSH(1)/(XSS(1)+1.D-20))**((X)**ALP5)	MD05560
	X0=DLOG10(C0+1.D-20)	MD05570	
	X01=DLOG10(C01+1.D-20)	MD05580	
	WRITE(6,4501) I+1,C0,C01,X0,X01	MD05590	
794	CONTINUE	MD05600	
795	CONTINUE	MD05610	
C	Write out DONE	MD05620	
	I3684=NWLM+1	MD05630	
	I3783=NWLM+100	MD05640	
	IF(JIT.EQ.-1) WRITE(6,4502) (WLC(I),I=I3684,I3783)	MD05650	
C	^^^	MD05660	
	KOUT=0	MD05670	
	DO 322 K=2,NK11	MD05680	
	MAQ1K=MAQ1(K)	MD05690	
	KOUT=KOUT+MAQ1K	MD05700	
	KLB=NK11+KOUT	MD05710	
	DO 321 J=2,NJ11	MD05720	
	DO 320 I=2,NI11	MD05730	
	I2236=22*I+36*J-2349	MD05740	
	IJF=I+NI10*(J-2)	MD05750	
	IJ=IJF+NIJ10*(K-2)	MD05760	
C	+++++++ FIXED HEAD TO XXS ++++++++	MD05770	
	I5=IXXS(IJ)	MD05780	
C	X=I5*P9+20-P8	MD05790	
	X=I5*P9	MD05800	
	IF(I5.GT.(3000-5)) X=P8*3000	MD05810	
	XXS(IJ)=X	MD05820	
C	+++++++	MD05830	
	IJLB=IJF+NIJ10*(KLB-2)	MD05840	
	IM1JK=IJ-1	MD05850	
	IJM1K=IJ-NI10	MD05860	
	IJKM1=IJ-NIJ10	MD05870	
	IF(IJM1K.LT.1) IJM1K=1	MD05880	
	IF(IJKM1.LT.1) IJKM1=1	MD05890	
	DXII=DXI(I)	MD05900	
	DYJJ=DYJ(J)	MD05910	
	DXIM1=DXI(I-1)	MD05920	
	DYJM1=DYJ(J-1)	MD05930	
	B0=LB(IJ)	MD05940	
	LBIM1=LB(IM1JK)	MD05950	
	LBIJM=LB(IJM1K)	MD05960	
	BDD=(LBIM1*DXII+B0*DXIM1)/(DXII+DXIM1)	MD05970	
	BBB=(LBIJM*DYJJ+B0*DYJM1)/(DYJJ+DYJM1)	MD05980	
	WDD=LBIM1*B0	MD05990	

	WBB=LBIJM*B0	MD06000
	IF(WDD.EQ.0.0) BDD=0	MD06010
	IF(WBB.EQ.0.0) BBB=0	MD06020
	B4=LB(IJKM1)	MD06030
C	***** Use PARAMX as multicative factor for sand (XSS) and	MD06040
C	clay (XSH) hydraulic conductivities *****	MD06050
	XSS(1)=NT(IJ)*PARAMX(IJ)	MD06060
	XSS(2)=NT(IM1JK)*PARAMX(IM1JK)	MD06070
	XSS(3)=NT(IJM1K)*PARAMX(IJM1K)	MD06080
	XSS(4)=NT(IJKM1)*PARAMX(IJKM1)	MD06090
	XSH(1)=XKZZ(IJ)*PARAMX(IJ+N324)	MD06100
	XSH(2)=XKZZ(IM1JK)*PARAMX(IM1JK+N324)	MD06110
	XSH(3)=XKZZ(IJM1K)*PARAMX(IJM1K+N324)	MD06120
	XSH(4)=XKZZ(IJKM1)*PARAMX(IJKM1+N324)	MD06130
C	***** Multiply these factors (XSJ and XSH) by decrease of	MD06140
C	sand and clay hydraulic conductivity with depth functions	MD06150
C	from text *****	MD06151
	LBB0=LBB(IJF)	MD06160
	DPT(1)=(LBB0-LZ2(IJ)*.1)/600.	MD06170
	DPT(2)=(LBB(IJF-1)-LZ2(IM1JK)*.1)/600.	MD06180
	IJF8=IJF-NI10	MD06190
	IF(IJF8.LT.1) IJF8=1	MD06200
	DPT(3)=(LBB(IJF8)-LZ2(IJM1K)*.1)/600.	MD06210
	DPT(4)=(LBB0-LZ2(IJKM1)*.1)/600.	MD06220
	FACA=0	MD06230
	DO 897 I4=1,4	MD06240
	DPTI4=DPT(I4)	MD06250
	IF(DPTI4.LT.0.) DPTI4=0	MD06260
	IF(DPTI4.GT.100.) DPTI4=100	MD06270
	X=.1829*DPTI4	MD06280
	FACSH=1*10**((.08333*X*X-1.1677*X)*1.0)	MD06290
	FACSS=1*10**(-DPTI4/6.72)	MD06300
	XSH(I4)=XSH(I4)*FACSH	MD06310
	XSS(I4)=XSS(I4)*FACSS	MD06320
	IF((I4.EQ.1).OR.(I4.EQ.4)) FACA=FACA+FACSH*.5	MD06330
897	CONTINUE	MD06340
C	**** Use equations (10) and (11) of text to arrive at effective	MD06350
C	conductivities. XXSTR is percentage sand=1-clay function ***	MD06360
	X=1-XXSTR(IJ)	MD06370
	AL25=ALFA*4	MD06380
	ALP5=1./AL25	MD06390
	CO =XSS(1)*(XSH(1)/(XSS(1)+1.D-20))**((X	MD06400
	CD =XSS(2)*(XSH(2)/(XSS(2)+1.D-20))**((1-XXSTR(IM1JK))**AL25)	MD06410
	CB =XSS(3)*(XSH(3)/(XSS(3)+1.D-20))**((1-XXSTR(IJM1K))**AL25)	MD06420
	C01=XSS(1)*(XSH(1)/(XSS(1)+1.D-20))**((X	MD06430
	CZ1=XSS(4)*(XSH(4)/(XSS(4)+1.D-20))**((1-XXSTR(IJKM1))**ALP5)	MD06440
C	UUUUUUUUUUUUUUUUUUUU	MD06450
C	Introduce parparameter P1 (b4 in text)	MD06460
	IF((K.EQ.3).AND.(I2236.GT.0)) CZ1=LB(IJKM1)*P1*GP5	MD06470
	IF(K.NE.NK11) GO TO 1123	MD06480
1123	CONTINUE	MD06490
319	CONTINUE	MD06500
	IF(I.EQ.2) CD=0	MD06510
	IF(J.EQ.2) CB=0	MD06520
	IF(K.EQ.2) CZ1=0	MD06530

	DD(IJ)=-DYJJ*2*DDK(K)*PARAMX(N98+K)*BDD*CD*CO/(DXII*CD+1DXIM1*CO+1.D-30)	MD06540
	BB(IJ)=-DXII*2*BBK(K)*PARAMX(N99+K)*BBB*CB*CO/(DYJJ*CB+1DYJM1*CO+1.D-30)	MD06550
	CC=FACA*NT(IJLB)*PARAMX(IJLB)	MD06560
	IF(MAQ1K.EQ.0) CC=1	MD06570
	ALP=.5D0*(B0*CC*CZ1+B4*CC*CO1)+MAQ1K*LB(IJLB)*CO1*CZ1	MD06580
	CCC=CO1*CC*CZ1	MD06590
	ZZIJ=1.D0	MD06600
	IF(ALP.NE.0.0) ZZIJ=CCC/ALP	MD06610
	IF(CCC.EQ.0.0) ZZIJ=0	MD06620
	ZZ(IJ)=-DXI(I)*DYJ(J)*ZZIJ	MD06630
320	CONTINUE	MD06640
321	CONTINUE	MD06650
322	CONTINUE	MD06660
C	THE QUANTITIES DD, BB, AND ZZ, ARE NOW DETERMINED.	MD06670
C	Calculate pseudo sources and put into YQ2	MD06680
	SUX=0	MD06690
	NCNT=0	MD06700
	NI2=NI10*NI10	MD06710
	NJ2=NJ10*NJ10	MD06720
	NK2=NK10*NK10	MD06730
	KOUT=0	MD06740
	DO 350 K=2,NK11	MD06750
	KOUT=KOUT+MAQ1(K)	MD06760
	KLB=NK11+KOUT	MD06770
	DO 350 J=2,NJ11	MD06780
	DO 340 I=2,NI11	MD06790
	IJF=I+NI10*(J-2)	MD06800
	IJ=IJF+NIJ10*(K-2)	MD06810
	IF(MHD(IJ).GE.1) GO TO 340	MD06820
	NCNT=NCNT+1	MD06830
	IJLB=IJF+NIJ10*(KLB-2)	MD06840
	IJLB1=IJLB+NIJ10	MD06850
	IP1JK=IJ+1	MD06860
	IM1JK=IJ-1	MD06870
	IJP1K=IJ+NI10	MD06880
	IJM1K=IJ-NI10	MD06890
	IJKP1=IJ+NIJ10	MD06900
	IJKM1=IJ-NIJ10	MD06910
	IF(IJM1K.LT.1) IJM1K=1	MD06920
	IF(IJKM1.LT.1) IJKM1=1	MD06930
	IF(IJP1K.GT.NNN) IJP1K=NNN	MD06940
	IF(IJKP1.GT.NNN) IJKP1=NNN	MD06950
	IF(IJLB1.GT.N325) IJLB1=N325	MD06960
	DD1=DD(IJ)	MD06970
	DD2=DD(IP1JK)	MD06980
	BB1=BB(IJ)	MD06990
	BB2=BB(IJP1K)	MD07000
	ZZ1=ZZ(IJ)	MD07010
	ZZ2=ZZ(IJKP1)	MD07020
C	IF((WMAX.NE.0.0).OR.(ISOR.NE.0.0)) GO TO 806	MD07030
	D1=(BB1+BB2+ZZ1+ZZ2)/(DD1+DD2-1.D-30)	MD07040
	B1=(DD1+DD2+ZZ1+ZZ2)/(BB1+BB2-1.D-30)	MD07050
		MD07060
		MD07070
		MD07080

	Z1=(DD1+DD2+BB1+BB2)/(ZZ1+ZZ2-1.D-30)	MD07090
	IF(D1.GT.1.D+9) D1=0	MD07100
	IF(B1.GT.1.D+9) B1=0	MD07110
	IF(Z1.GT.1.D+9) Z1=0	MD07120
	D1=1/(NI2*(1+D1))	MD07130
	B1=1/(NJ2*(1+B1))	MD07140
	Z1=1/(NK2*(1+Z1))	MD07150
	X=D1	MD07160
	IF(B1.LT.X) X=B1	MD07170
	IF(Z1.LT.X) X=Z1	MD07180
	SUX=SUX+X	MD07190
806	CONTINUE	MD07200
C	****	MD07210
	B0=LB(IJ)	MD07220
	B4=LB(IJKM1)	MD07230
	B5=LB(IJKP1)	MD07240
	BT0=LRO(IJ)*1.D-5	MD07250
	BT4=LRO(IJKM1)*1.D-5	MD07260
	BT5=LRO(IJKP1)*1.D-5	MD07270
	BTDD=LRO(IM1JK)*1.D-5	MD07280
	BTFF=LRO(IP1JK)*1.D-5	MD07290
	BTBB=LRO(IJM1K)*1.D-5	MD07300
	BTHH=LRO(IJP1K)*1.D-5	MD07310
	NB1=LB(IJLB)	MD07320
	NB2=LB(IJLB1)	MD07330
C	FB1=NB1/(NB1+.01)	MD07340
C	FB2=NB2/(NB2+.01)	MD07350
	X=(.5D0*(BT0*B0+BT4*B4)+MAQ1(K)*(LRO(IJLB)*1.0D-5)*NB1)*ZZ1	MD07360
	1-(.5D0*(BT0*B0+BT5*B5)+MAQ1(K+1)*(LRO(IJLB1)*1.0D-5)*NB2)*ZZ2	MD07370
C	3+(ZZ2*FB2*MAQ1(K+1)*(BT5-BT0)+ZZ1*FB1*MAQ1(K)*(BT4-BT0))*OS4	MD07380
	LZ0=LZ2(IJ)	MD07390
	DXII=DXI(I)	MD07400
	DXIM1=DXI(I-1)	MD07410
	DXIP1=DXI(I+1)	MD07420
	DYJJ=DYJ(J)	MD07430
	DYJM1=DYJ(J-1)	MD07440
	DYJP1=DYJ(J+1)	MD07450
	BTOX=BT0*DXII	MD07460
	BTOY=BT0*DYJJ	MD07470
	YQ2(IJ)=X-(((BTDD*DXIM1+BTOX)/(DXIM1+DXII))*DD1*(LZ2(IM1JK)-LZ0)	MD07480
1	+((BTFF*DXIP1+BTOX)/(DXIP1+DXII))*DD2*(LZ2(IP1JK)-LZ0)	MD07490
2	+((BTBB*DYJM1+BTOY)/(DYJM1+DYJJ))*BB1*(LZ2(IJM1K)-LZ0)	MD07500
3	+((BTHH*DYJP1+BTOY)/(DYJP1+DYJJ))*BB2*(LZ2(IJP1K)-LZ0)	MD07510
	4)*.1D0	MD07520
340	CONTINUE	MD07530
350	CONTINUE	MD07540
C	YQ2 NOW DETERMINED	MD07550
C	Get iteration parameters for SIP subroutine	MD07560
	IF(ISOR.NE.0) GO TO 390	MD07570
	XY=.5D0*PI*PI*SUX/NCNT	MD07580
C	XY IS NOW DETERMINED	MD07590
	XY=XYFC*XY	MD07600
	IF(WMAX.NE.0.0) XY=WMAX	MD07610
C	DETERMINE ITERATION PARAMETERS WS(I)	MD07620
	DO 360 I=1,LENGTH	MD07630

360	WS(I)=1-XY**((I-1.)/(LENGTH-1))	MD07640
C	WRITE(6,5056)	MD07650
C	WRITE(6,5006)	MD07660
C	WRITE(6,3555) (WS(I),I=1,LENGTH)	MD07670
390	CONTINUE	MD07680
C	Have coefficients	MD07690
	IF(JIT.EQ.-1) WRITE(6,1003) 99,ISOR,ITMAX,ERR,XX10	MD07700
	1,HMAX,XYFC,WMAX	MD07710
	DO 599 IJ=2,N315	MD07720
599	HLS(IJ)=0	MD07730
	NINT=5	MD07740
C	Begin main loop of pgn.	MD07750
C	There are 5 time intervals INT=1,2,...5.	MD07760
C	DELT is time interval	MD07770
	DO 600 INT=1,5	MD07780
	INT2=INT-2	MD07790
	IF(INT2.LT.1) INT2=1	MD07800
	DELT=DEL(INT)	MD07810
	DELT=DELT/P2	MD07820
	SUMYQ=0	MD07830
	DO 231 IDBZ=1,3	MD07840
	DO 231 N=1,250	MD07850
231	SYQ(IDBZ,N)=0	MD07860
C	Put pumping for this time interval into YQ	MD07870
	DO 331 K=2,NK11	MD07880
	K1=K-1	MD07890
	DO 330 J=2,NJ11	MD07900
	DO 329 I=2,NI11	MD07910
	IJ=I+NI10*(J-2)+NIJ10*(K-2)	MD07920
C	*** GOOD FIRST GUESS AND FIXED HEAD TO XX ***	MD07930
	X=IXX5(IJ,INT)*.1	MD07940
	IF((JIT.EQ.-1).OR.(MHD(IJ).EQ.1)) X=XXS(IJ)	MD07950
	XX(IJ)=X	MD07960
C	*****	MD07970
	XDEN=FC(2,K1)	MD07980
	X=XDEN	MD07990
	IF(INT.EQ.1) X=0	MD08000
	IF(INT.EQ.2) X=FC(1,K1)*.79	MD08010
	FCX=X/XDEN	MD08020
	XQ=YQ1(IJ,INT2)*FCX	MD08030
	IF(IOUT.EQ.0) GO TO 701	MD08040
	SYQ(1,I)=SYQ(1,I)+XQ	MD08050
	SYQ(2,J)=SYQ(2,J)+XQ	MD08060
	SYQ(3,K)=SYQ(3,K)+XQ	MD08070
	SUMYQ=SUMYQ+XQ	MD08080
701	CONTINUE	MD08090
329	YQ(IJ)=XQ+YQ2(IJ)	MD08100
330	CONTINUE	MD08110
331	CONTINUE	MD08120
C	YQ now has pumping including pseudo sources	MD08130
	I01=1	MD08140
	IWR1=IWR1*I01	MD08150
	LFLO1=LFLOW*I01	MD08160
	IF(IWR1.NE.1) GO TO 420	MD08170
	WRITE(6,5007)	MD08180

	WRITE(6,5072) NU1(1),NU2(1),NU3(1)	MD08190
	WRITE(6,5073) NU1(2),NU2(2),NU3(2)	MD08200
	WRITE(6,5074) NU1(3),NU2(3),NU3(3)	MD08210
420	CONTINUE	MD08220
C	BEGIN SIP,OR PCG ITERATIONS.	MD08230
C	Call PCG for firsit time interval,	MD08240
C	SIP for second through fifth intervals	MD08250
	ISO=ISO+1	MD08260
	IF(INT.GT.1) CALL SIP	MD08270
	IF(INT.EQ.1) CALL PCG	MD08280
	WRITE(6,1003) JIT,INT,ICNT,ER5,SRZ,SUMRZ,HMAX,XX(9583),XX(30904)	MD08290
C	@@@@@ GET SUBSIDENCE STORAGE (RATE) @@@@@	MD08300
	IF(IOUT.EQ.0) GO TO 673	MD08310
	WRITE(6,9020)	MD08320
	DO 670 K=2,NK11	MD08330
	SUMT=0	MD08340
	SUMS=0	MD08350
	DO 671 I=2,NI11	MD08360
	DO 671 J=2,NJ11	MD08370
	IJ=I+NI10*(J-2)+NIJ10*(K-2)	MD08380
	IF(MHD(IJ).GE.1) GO TO 672	MD08390
	XXIJ=XX(IJ)	MD08400
	X=HL(IJ)-XXIJ	MD08410
	SM=XXS(IJ)-HL(IJ)	MD08420
	S1=X	MD08430
	SS=0	MD08440
	IF(X.LE.0) GO TO 675	MD08450
	S1=X*VV40*(1-XXSTR(IJ))	MD08460
	SS=S1	MD08470
675	CONTINUE	MD08480
	SUMT=SUMT+(SM+S1)*LB(IJ)	MD08490
	SUMS=SUMS+SS*LB(IJ)	MD08500
672	CONTINUE	MD08510
671	CONTINUE	MD08520
	SUMT=SUMT*SVIJ/DELT	MD08530
	SUMS=SUMS*SVIJ/DELT	MD08540
	WRITE(6,4501) K,SUMS,SUMT	MD08550
670	CONTINUE	MD08560
C	@@@@@@@@@@@@@@@@@@@@	MD08570
	DO 771 I=2,NI11	MD08580
	DO 771 J=2,NJ11	MD08590
C	RXY=1/(DXI(I)*DYJ(J))	MD08600
	IJJ=I+NI10*(J-2)	MD08610
	SUM=0	MD08620
	DO 770 K=2,NK11	MD08630
	IJ=IJJ+NIJ10*(K-2)	MD08640
	IF(MHD(IJ).GE.1) GO TO 772	MD08650
	XXIJ=XX(IJ)	MD08660
	X=HL(IJ)-XXIJ	MD08670
	SM=XXS(IJ)-HL(IJ)	MD08680
	S1=X	MD08690
	SS=0	MD08700
	IF(X.LE.0) GO TO 775	MD08710
	S1=X*VV40*(1-XXSTR(IJ))	MD08720
	SS=S1	MD08730

775	CONTINUE	MD08740
	SUM=SUM+(SM+S1)*LB(IJ)	MD08750
772	CONTINUE	MD08760
770	CONTINUE	MD08770
	IF(INT.NE.1) HLS(IJJ)=HLS(IJJ)+SUM*SV35*P2	MD08780
771	CONTINUE	MD08790
673	CONTINUE	MD08800
C	@@@@@@@@@@@@ End subsidence @@@@@@@@@@@@@	MD08810
C	Save XX in IXX5(IJ,INT) for use as the starting solution	MD08820
C	for XX at the next iteration (JIT+1), same time interval INT.	MD08830
C	Also save XX in XXS for use in PCG & SIP as the starting value	MD08840
C	for XX at the beginning of the next time interval (INT+1)	MD08850
C	Calculate HL(IJ), the lowest value for head yet achieved	MD08860
C	at location IJ	MD08861
	DO 430 K=2,NK11	MD08870
	DO 430 J=2,NJ11	MD08880
	DO 430 I=2,NI11	MD08890
	IJ=I+NI10*(J-2)+NIJ10*(K-2)	MD08900
	XXIJ=XX(IJ)	MD08910
	HLIJ=HL(IJ)	MD08920
	IF(XXIJ.LT.HLIJ) HL(IJ)=XXIJ	MD08930
	P380=P3*80	MD08940
	IF(K.LE.6) P380=1000	MD08950
	IF(INT.EQ.1) HL(IJ)=XXIJ-P380	MD08960
	IXX5(IJ,INT)=XXIJ*10.+5	MD08970
430	XXS(IJ)=XXIJ	MD08980
C	Done with IXX5,XX5,HLIJ	MD08990
	IF((JIT.EQ.-1).AND.(INT.EQ.5)) GO TO 7197	MD09000
	IF((LFLO1*IOUT).EQ.0) GO TO 560	MD09010
7197	CONTINUE	MD09020
C	DETERMINE WATER FLOW RATES	MD09030
C	Much of this is in VARDEN and deals with calculation of various	MD09040
C	flow rates. See WRIR 84-4302, p. B-6, Kuiper	MD09050
	DO 440 IJ=1,NNN	MD09060
440	G2(IJ)=0	MD09070
	DO 511 IDBZ=1,3	MD09080
	DO 450 N=1,250	MD09090
	SUMFM(IDBZ,N)=0	MD09100
	SUNFM(IDBZ,N)=0	MD09110
	SUNF(IDBZ,N)=0	MD09120
450	SUMF(IDBZ,N)=0	MD09130
	IRITE=0	MD09140
	L1=LFLO(1)	MD09150
	IF((L1.EQ.IDBZ).OR.(L1.EQ.4)) IRITE=1	MD09160
	IF(((INT-3).NE.2).OR.(IOUT.NE.1)) IRITE=0	MD09170
	IF(IRITE.NE.1) GO TO 460	MD09180
	IF(IDBZ.EQ.1) WRITE(6,5101)	MD09190
	IF(IDBZ.EQ.2) WRITE(6,5102)	MD09200
	IF(IDBZ.EQ.3) WRITE(6,5103)	MD09210
	WRITE(6,6000)	MD09220
460	CONTINUE	MD09230
	IRITEA=0	MD09240
	L1=LFLOA(1)	MD09250
	IF((L1.EQ.IDBZ).OR.(L1.EQ.4)) IRITEA=1	MD09260
	IF(((IABS(INT-3).NE.2).OR.(IOUT.NE.1))) IRITEA=0	MD09270

	IF(IRITEA.NE.1) GO TO 461	MD09280
C	IF(IDBZ.EQ.1) WRITE(7,5101)	MD09290
C	IF(IDBZ.EQ.2) WRITE(7,5102)	MD09300
C	IF(IDBZ.EQ.3) WRITE(7,5103)	MD09310
C	WRITE(7,6000)	MD09320
461	CONTINUE	MD09330
	KOUT=0	MD09340
	DO 511 K=2,NK11	MD09350
	KOUT=KOUT+MAQ1(K)	MD09360
	KLB=NK11+KOUT	MD09370
	IF((IRITE.EQ.1).AND.(IPH(K).GE.0)) WRITE(6,4002) K	MD09380
C	IF((IRITEA.EQ.1).AND.(IPHA(K).EQ.1)) WRITE(7,4002) K	MD09390
	I88=0	MD09400
	SM9=0	MD09410
	DO 510 J=2,NJ11	MD09420
	I88=I88+1	MD09430
	IF(I88.EQ.11) I88=1	MD09440
	IJMI=NI10*(J-2)+NIJ10*(K-2)	MD09450
	IJLBMI=NI10*(J-2)+NIJ10*(KLB-2)	MD09460
	DO 500 I=2,NI11	MD09470
	IJ=IJMI+I	MD09480
	IJLB=IJLBMI+I	MD09490
	XX0=XX(IJ)	MD09500
	BT0=LRO(IJ)*1.0D-5	MD09510
	LZ0=LZ2(IJ)	MD09520
	IF(IDBZ.NE.1) GO TO 470	MD09530
	DBZ=DD(IJ)	MD09540
	IF(I.EQ.2) GO TO 490	MD09550
	IM1JK=IJ-1	MD09560
	XXI=XX(IM1JK)	MD09570
	BTDD=LRO(IM1JK)*1.0D-5	MD09580
	DXII=DXI(I)	MD09590
	DXIM1=DXI(I-1)	MD09600
	BTOX=BT0*DXII	MD09610
	FLOW=((BTDD*DXIM1+BTOX)/(DXIM1+DXII))*(LZ2(IM1JK)-LZ0)*.1D0	MD09620
	GO TO 490	MD09630
470	IF(IDBZ.NE.2) GO TO 480	MD09640
	DBZ=BB(IJ)	MD09650
	IF(J.EQ.2) GO TO 490	MD09660
	IJM1K=IJ-NI10	MD09670
	XXI=XX(IJM1K)	MD09680
	BTBB=LRO(IJM1K)*1.0D-5	MD09690
	DYJJ=DYJ(J)	MD09700
	DYJM1=DYJ(J-1)	MD09710
	BTOY=BT0*DYJJ	MD09720
	FLOW=((BTBB*DYJM1+BTOY)/DYJM1+DYJJ)*(LZ2(IJM1K)-LZ0)*.1D0	MD09730
	GO TO 490	MD09740
480	DBZ=ZZ(IJ)	MD09750
	IF(K.EQ.2) GO TO 490	MD09760
	IJKM1=IJ-NIJ10	MD09770
	XXI=XX(IJKM1)	MD09780
	B0=LB(IJ)	MD09790
	B4=LB(IJKM1)	MD09800
	BT4=LRO(IJKM1)*1.0D-5	MD09810
	NB1=LB(IJLB)	MD09820

	IF(IDBZ.EQ.2) IJK=J	MD10370
	IF(IDBZ.EQ.3) IJK=K	MD10380
	IF(LB(IJ).EQ.0) GO TO 491	MD10390
	IF(X.GT.0) SUMF(IDBZ,IJK)=SUMF(IDBZ,IJK)+X	MD10400
	IF(X.LT.0) SUNF(IDBZ,IJK)=SUNF(IDBZ,IJK)-X	MD10410
491	IF(LB(IJM).EQ.0) GO TO 492	MD10420
	IF(X.GT.0) SUMFM(IDBZ,IJK)=SUMFM(IDBZ,IJK)+X	MD10430
	IF(X.LT.0) SUNFM(IDBZ,IJK)=SUNFM(IDBZ,IJK)-X	MD10440
492	CONTINUE	MD10450
	G2(IJ)=G2(IJ)+X	MD10460
500	CONTINUE	MD10470
C	IF(I88.NE.-1) GO TO 934	MD10480
	IF(.NOT.(((J.LE.69).AND.(J.GE.62)).OR.((J.LE.19).AND.(J.GE.15))))	MD10490
	*GO TO 934	MD10500
	IF((IRITE.EQ.1).AND.(IPH(K).EQ.1)) WRITE(6,4500) J,(DT(I),I=2	MD10510
	1,NI11)	MD10520
934	CONTINUE	MD10530
C	IF((IRITEA.EQ.1).AND.(IPHA(K).EQ.1)) WRITE(7,5500) J-1,	MD10540
C	1(DT(I),I=2,NI11)	MD10550
510	CONTINUE	MD10560
	IF(IOUT.EQ.1) WRITE(6,1003) IDBZ,K,5555,SM9	MD10570
511	CONTINUE	MD10580
	IF((LFLO1*IOUT).EQ.0) GO TO 560	MD10590
	IF(LFLO(2).EQ.1) WRITE(6,8010)	MD10600
	I5=0	MD10610
	SUMG2=0	MD10620
	DO 549 IDBZ=1,3	MD10630
	DO 549 N=1,250	MD10640
549	SG2(IDBZ,N)=0	MD10650
	DO 550 K=2,NK11	MD10660
	DO 550 J=2,NJ11	MD10670
	DO 550 I=2,NI11	MD10680
	IJ=I+NI10*(J-2)+NIJ10*(K-2)	MD10690
	IF(MHD(IJ).NE.1) GO TO 540	MD10700
	G2IJ=G2(IJ)	MD10710
	I5=I5+1	MD10720
	DT(I5)=G2IJ	MD10730
	I7(I5)=I	MD10740
	J7(I5)=J	MD10750
	K7(I5)=K	MD10760
	SG2(1,I)=SG2(1,I)+G2IJ	MD10770
	SG2(2,J)=SG2(2,J)+G2IJ	MD10780
	SG2(3,K)=SG2(3,K)+G2IJ	MD10790
	SUMG2=SUMG2+G2IJ	MD10800
540	IF(I5.NE.5) GO TO 550	MD10810
	I5=0	MD10820
	IF(LFLO(2).EQ.1) WRITE(6,3560) (I7(L),J7(L),K7(L),DT(L),L=1,5)	MD10830
550	CONTINUE	MD10840
	IF((LFLO(2).EQ.1).AND.(I5.GE.1))	MD10850
	1WRITE(6,3560) (I7(L),J7(L),K7(L),DT(L),L=1,I5)	MD10860
	IF(LFLO(3).EQ.1) WRITE(6,9010)	MD10870
	I5=0	MD10880
	SUMVV=0	MD10890
	DO 649 IDBZ=1,3	MD10900
	DO 649 N=1,250	MD10910

649	SVV(IDBZ,N)=0	MD10920
	DO 650 K=2,NK11	MD10930
	DO 650 J=2,NJ11	MD10940
	DO 650 I=2,NI11	MD10950
	IJ=I+NI10*(J-2)+NIJ10*(K-2)	MD10960
C	X=XX(IJ)-XXE(IJ)	MD10970
C	VVIJ=X*ALN(IJ)	MD10980
	IF(.NOT.((IEVP.EQ.1).AND.(VVIJ.GT.0))) GO TO 641	MD10990
	I5=I5+1	MD11000
	DT(I5)=VVIJ	MD11010
	I7(I5)=I	MD11020
	J7(I5)=J	MD11030
	K7(I5)=K	MD11040
	SVV(1,I)=SVV(1,I)+VVIJ	MD11050
	SVV(2,J)=SVV(2,J)+VVIJ	MD11060
	SVV(3,K)=SVV(3,K)+VVIJ	MD11070
	SUMVV=SUMVV+VVIJ	MD11080
641	IF(I5.NE.5) GO TO 650	MD11090
	I5=0	MD11100
	IF(LFLO(3).EQ.1) WRITE(6,3560) (I7(L),J7(L),K7(L),DT(L),L=1,5)	MD11110
650	CONTINUE	MD11120
	IF((LFLO(3).EQ.1).AND.(I5.GE.1))	MD11130
	1WRITE(6,3560) (I7(L),J7(L),K7(L),DT(L),L=1,I5)	MD11140
	WRITE(6,8011) SUMYQ,SUMG2,SUMVV	MD11150
	IF(LFLO(4).EQ.0) GO TO 530	MD11160
	WRITE(6,7001)	MD11170
	IDBZ1=LFLO(4)	MD11180
	IDBZ3=IDBZ1	MD11190
	IF(IDBZ1.GE.4) IDBZ1=1	MD11200
	IF(IDBZ3.GE.4) IDBZ3=3	MD11210
	DO 520 IDBZ=IDBZ1,IDBZ3	MD11220
	N20=NI11	MD11230
	IF(IDBZ.EQ.2) N20=NJ11	MD11240
	IF(IDBZ.EQ.3) N20=NK11	MD11250
	DO 519 N=2,N20	MD11260
	NP1=N+1	MD11270
519	WRITE(6,8012) IDBZ,N,SYQ(IDBZ,N),SG2(IDBZ,N),SVV(IDBZ,N)	MD11280
	1,SUNF(IDBZ,N),SUMFM(IDBZ,NP1),SUMF(IDBZ,N),SUNFM(IDBZ,NP1)	MD11290
520	CONTINUE	MD11300
530	CONTINUE	MD11310
560	IF((1*IOUT).EQ.0) GO TO 590	MD11320
C	End of flow rate section	MD11330
C	Printout heads in various formats and media. Change things	MD11340
C	in this section to choose media, which heads, etc.	MD11350
	WRITE(6,5008)	MD11360
	WRITE(6,6000)	MD11370
C	IF(IABS(INT-3).GE.0) WRITE(8,5008)	MD11380
C	IF(IABS(INT-3).GE.0) WRITE(8,6000)	MD11390
C	WRITE(10,5009)	MD11400
C	WRITE(10,6000)	MD11410
C	DETERMINE HYDRAULIC HEAD FROM XX = H PRIME = (PRESSURE HEAD H) + Z	MD11420
	XSM=0	MD11430
	DO 580 K=2,NK11	MD11440
C	IF(IABS(INT-3).GE.0) WRITE(8,4002) K	MD11450
C	WRITE(10,4002) K	MD11460

	XXSM=0	MD11470
	WRITE(6,2020) 1,1,0,K	MD11480
	DO 579 J=2,NJ11	MD11490
	IJMI=NI10*(J-2)+NIJ10*(K-2)	MD11500
	DO 570 I=2,NI11	MD11510
	IJ=IJMI+I	MD11520
	XZ210=LZ2(IJ)*.1D0	MD11530
	DTI=(1/(LRO(IJ)*1.0D-5+1))*(XX(IJ)-XZ210)+XZ210	MD11540
	IF(MHD(IJ).EQ.2) DTI=0	MD11550
	X9=1	MD11560
	IF(LB(IJ).EQ.0) X9=0	MD11570
	XXF=XX(IJ)*X9	MD11580
	XXH=DTI*X9	MD11590
	IF(K.NE.NK11) XSM=XSM+XXF	MD11600
	IF(K.NE.NK11) XXSM=XXSM+XXF	MD11610
	E2(I)=XXF	MD11620
	E2(2)=J	MD11630
	IF(XXF.EQ.0) XXF=-1.E+38	MD11640
	IF(XXH.EQ.0) XXH=-1.E+38	MD11650
	G2(I)=XXF	MD11660
570	DT(I)=XXH	MD11670
	IF((INT.EQ.5).AND.(IPH(K).GE.1)) WRITE(6,1008) (E2(I),	MD11680
	*I=2,NI11)	MD11690
C	IF(IWRTXX.LE.1) WRITE(10,1001) J-1,(DT(I),I=2,NI11)	MD11700
C	IF(IABS(INT-3).GE.0) WRITE(8,5500) J-1,(G2(I),I=2,NI11)	MD11710
1008	FORMAT(20F6.0)	MD11720
579	CONTINUE	MD11730
	WRITE(6,3555) XXSM	MD11740
580	CONTINUE	MD11750
	WRITE(6,3555) XSM	MD11760
C	End of head printout	MD11770
590	CONTINUE	MD11780
600	CONTINUE	MD11790
C	End of MAIN loop	MD11800
C	***** PRINT OUT TOTAL SUBSIDENCE *****	MD11810
	IF(IOUT.EQ.0) GO TO 664	MD11820
	WRITE(6,9021)	MD11830
	DO 779 J=2,NJ11	MD11840
	IJMI=NI10*(J-2)	MD11850
C	WRITE(6,1001) J,(HLS(IJMI+I),I=2,NI11)	MD11860
779	CONTINUE	MD11870
664	CONTINUE	MD11880
C	***** DONE WITH SUBSIDENCE PRINT OUT *****	MD11890
C	Put calculated heads into WLC=f(B) for use by MAIN	MD11900
	DO 642 I=1,NWLM	MD11910
	IJ=NND(I)	MD11920
	XZ210=LZ2(IJ)*.1D0	MD11930
C642	WLC(I)=(1/(LRO(IJ)*1.0D-5+1))*(XX(IJ)-XZ210)+XZ210	MD11940
	IF(I.LE.NWLM1) XXX=IXX5(IJ,3)*.1	MD11950
	IF(I.GT.NWLM1) XXX=XX(IJ)	MD11960
642	WLC(I)=XXX	MD11970
C	Read into WLC done	MD11980
	IF(IOUT.EQ.0) GO TO 736	MD11990
C	Insert pack for observation of residual errors	MD12000
C	Y-f(B)=WLM(IJ)-WLC(IJ)	MD12001

C	Various formats occur: Average residual error by layer and	MD12010
C	by total model. Root mean square residual error by layer and	MD12011
C	total model	MD12020
	K40=1	MD12030
	K40M1=0	MD12040
	CUM=0	MD12050
	CCUM=0	MD12060
	DO 737 I2=1,2	MD12070
	K41=0	MD12080
	SSUM=0	MD12090
	TSUM=0	MD12100
	SWLMT=0	MD12110
	WRITE(6,9998)	MD12120
	DO 735 K=2,NK11	MD12130
	K39=0	MD12140
	PSUM=0	MD12150
	PSUM1=0	MD12160
	SWLM=0	MD12170
	WRITE(6,4003) K	MD12180
	DO 734 J=2,NJ11	MD12190
	DO 733 I=2,NI11	MD12200
	IJ=I+NI10*(J-2)+NIJ10*(K-2)	MD12210
	DT(I)=0	MD12220
	IF(IJ.NE.NND(K40)) GO TO 732	MD12230
	XXX=WLC(K40)	MD12240
	WLM40=WLM(K40)	MD12250
	W40=W(K40)	MD12260
	K40=K40+1	MD12270
	IF(W40.LT.1.D-20) GO TO 732	MD12280
	SWLMT=SWLMT+WLM40	MD12290
	SWLM =SWLM +WLM40	MD12300
	X=XXX-WLM40	MD12310
	DT(I)=X	MD12320
	K39=K39+1	MD12330
	K40M1=K40M1+1	MD12340
	K41=K41+1	MD12350
	SSUM=SSUM+X*X	MD12360
	TSUM=TSUM+X*1	MD12370
	PSUM=PSUM+X*1	MD12380
	CUM=CUM+X*1	MD12390
	PSUM1=PSUM1+X*X	MD12400
	CCUM=CCUM+X*X	MD12410
732	CONTINUE	MD12420
733	CONTINUE	MD12430
C	IF(I2.EQ.2) WRITE(6,1007) J,(DT(I),I=2,NI11)	MD12440
734	CONTINUE	MD12450
	PSUM=PSUM/(K39+1.D-20)	MD12460
	PSUM1=DSQRT(PSUM1/(K39+1.D-20))	MD12470
	SWLM=SWLM/(K39+1.D-20)	MD12480
	WRITE(6,4501) K39,PSUM,PSUM1,SWLM	MD12490
735	CONTINUE	MD12500
	SSUM=DSQRT(SSUM/(K41))	MD12510
	TSUM=TSUM/(K41)	MD12520
	SWLMT=SWLMT/(K41)	MD12530
	WRITE(6,1003) K40M1,66,K41,TSUM,SSUM,SWLMT	MD12540

737	CONTINUE	MD12550
	CUM=CUM/K40M1	MD12560
	CCUM=DSQRT(CCUM/K40M1)	MD12570
	WRITE(6,1003) 66,66,66,CUM,CCUM	MD12580
C	End of residual error pack	MD12590
C	***** DO CHI square test for normalcy of residuals	MD12600
C	Discarding of outlying data lying outside of certain	MD12610
C	normalcy bounds is optimal, at JIT=K4	MD12620
C	Subsequent values of JIT will use reduced data set with	MD12630
C	others discarded	MD12631
736	CONTINUE	MD12640
	K4=1	MD12650
	IF(JIT.EQ.K4) IIII=IIII+1	MD12660
	J8=JIT+IIII	MD12670
	WRITE(6,2020) 5555,5555,K4,JIT,IIII,J8	MD12680
	IF(.NOT.((J8.EQ.K4).OR.(IOUT.NE.0))) GO TO 1849	MD12690
	DO 1839 IW=0,1	MD12700
	CUM=0	MD12710
	CCUM=0	MD12720
	DO 1836 K40=1,NWLMT	MD12730
	X=WLC(K40)-WLM(K40)	MD12740
	W40=W(K40)	MD12750
	IJ=NND(K40)	MD12760
	IF(W40.LE.1.D-20) GO TO 1836	MD12770
	X=X*DSQRT(W40)	MD12780
	CUM=CUM+X	MD12790
	CCUM=CCUM+X*X	MD12800
1836	CONTINUE	MD12810
	CUM=CUM/X3150	MD12820
	CCUM=DSQRT(CCUM/X3150)	MD12830
	DO 1837 I=1,16	MD12840
1837	IX7(I)=0	MD12850
	RHO1=DSQRT(CCUM*CCUM-CUM*CUM)	MD12860
	F2242=(RHO1/(RHO1S+1.D-40))	MD12870
	RHO1S=RHO1	MD12880
	LR=0	MD12890
	DO 1838 K40=1,NWLMT	MD12900
	W40=W(K40)	MD12910
	IF(W40.LE.1.D-20) GO TO 1939	MD12920
	X=WLC(K40)-WLM(K40)	MD12930
	X=(X-CUM)/RHO1	MD12940
	IF((X.LT.1.54).AND.(X.GT.-3.4)) GO TO 1950	MD12950
	IF(K40.GT.NWLM) GO TO 1950	MD12960
	LR=LR+1	MD12970
	WRITE(6,3011) LR,K40,NND(K40),888,X,WLC(K40),WLM(K40)	MD12980
3011	FORMAT(4I8,6D11.3)	MD12990
	IF((J8.EQ.K4).AND.(IW.EQ.0)) W(K40)=0	MD13000
1950	CONTINUE	MD13010
	DO 1792 II=1,16	MD13020
	XR=XTV(II+1)	MD13030
	XL=XTV(II)	MD13040
	IF((XL.LT.X).AND.(X.LE.XR)) IX7(II)=IX7(II)+1	MD13050
1792	CONTINUE	MD13060
1939	CONTINUE	MD13070
1838	CONTINUE	MD13080

	XNP=X3150/16.	MD13090
	SUM=0	MD13100
	DO 893 I=1,16	MD13110
	IXI=IX7(I)	MD13120
	X=IXI-XNP	MD13130
893	SUM=SUM+X*X	MD13140
	SUM=SUM/XNP	MD13150
	WRITE(6,2020) (IX7(I),I=1,16)	MD13160
	WRITE(6,3555) SUM,CUM,CCUM,RHO1,XNP,X3150	MD13170
	IF((J8.EQ.K4).AND.(IW.EQ.0)) X3150=X3150-LR	MD13180
	WRITE(6,1003) 3333,3333,LR,X3150	MD13190
1839	CONTINUE	MD13200
	IF(J8.NE.K4) GO TO 1952	MD13210
	X493=X493*F2242	MD13220
	NWLM3=NWLM+1	MD13230
	DO 1951 NN=NWLM3,NWLMT	MD13240
	WLC(NN)=WLC(NN)*F2242	MD13250
1951	WLM(NN)=WLM(NN)*F2242	MD13260
1952	CONTINUE	MD13270
	WRITE(6,1003) 3333,3333,LR,X3150,F2242,X493	MD13280
1849	CONTINUE	MD13290
1001	FORMAT(I12,20F6.1/(12X,20F6.1))	MD13300
1003	FORMAT(3I10,7D12.4)	MD13310
1004	FORMAT(12X,15F8.1)	MD13320
1007	FORMAT(I12,20F6.0/(12X,20F6.0))	MD13330
2000	FORMAT(8G10.0)	MD13340
2003	FORMAT(20I4)	MD13350
2007	FORMAT(4(3I3,D11.3))	MD13360
2020	FORMAT(8I10)	MD13370
3004	FORMAT(I12,20I6/(12X,20I6))	MD13380
3005	FORMAT(22I6)	MD13390
3007	FORMAT(4(I12,2I4,D11.3))	MD13400
3010	FORMAT(' ',12F10.1)	MD13410
3555	FORMAT(8D15.7)	MD13420
3560	FORMAT(' ',5(3I4,D12.3))	MD13430
4002	FORMAT(I6,I12)	MD13440
4003	FORMAT('1',5I6)	MD13450
4500	FORMAT(I12,10D12.3/(12X,10D12.3))	MD13460
5500	FORMAT(I12,13D9.3/(12X,13D9.3))	MD13470
4501	FORMAT(I12,9D12.3)	MD13480
4502	FORMAT(10D10.3)	MD13490
4997	FORMAT('1',44X,'LENGTH IN FEET OF WATER COLUMN IN WELL BORE')	MD13500
4998	FORMAT('1',64X,'MOLALITY')	MD13510
4999	FORMAT('1',53X,'TEMPERATURE DEGREES CENTIGRADE')	MD13520
5000	FORMAT('1',52X,'FIXED HYDRAULIC HEAD')	MD13530
5001	FORMAT('1',49X,'X AND Y DIMENSIONS OF GRID ELEMENTS')	MD13540
5002	FORMAT('1',41X,'(DENSITY OF WATER RHO, IN GRAMS PER CUBIC CENTIMETMD13550 1ER)-1.0')	MD13560
5003	FORMAT('1',59X,'BASE ELEVATION')	MD13570
5004	FORMAT('1',52X,'Z DIMENSION OF GRID ELEMENTS')	MD13580
5005	FORMAT('1',54X,'HYDRAULIC CONDUCTIVITY')	MD13590
5052	FORMAT('1',56X,'INITIAL HYDRAULIC HEAD')	MD13600
5053	FORMAT('0',53X,'RECHARGE RATE YQ (L*L*L/T)')	MD13610
5054	FORMAT('1',57X,'SPECIFIC STORAGE')	MD13620
5055	FORMAT('1',53X,'RECHARGE RATES Q2 (L*L*L/T)')	MD13630

5056 FORMAT('1',51X,'SIP CONVERGENCE PARAMETERS CHOSEN'// MD13640
18X,'L9',5X,'ITMAX',4X,'LENGTH',14X,'HMAX',14X,'XYFC', MD13650
215X,'ERR',14X,'WMAX',14X,'XX10') MD13660

5057 FORMAT('1',51X,'SOR CONVERGENCE PARAMETERS CHOSEN'// MD13670
15X,'NSKP1',5X,'NSKP2',5X,'ITMAX',13X,'RELX1',13X,'RELX2', MD13680
214X,'COEF',15X,'ERR',14X,'XX10') MD13690

5058 FORMAT('1',51X,'PCG(',I1,') CONVERGENCE PARAMETERS CHOSEN'// MD13700
17X,'ITMAX',9X,'ERR',8X,'XX10') MD13710

5060 FORMAT('1',50X,'Z COMPONENT OF HYDRAULIC CONDUCTIVITY') MD13720

5006 FORMAT('0',58X,'SIP COEFFICIENTS') MD13730

5007 FORMAT('0',56X,'WATCHING CONVERGENCE'//25X,'I,J,K, IS THE LOCATION MD13740
1 AT WHICH THE MAXIMUM CHANGE IN XX OCCURED.'/25X,'MAXIMUM RESIDUAL MD13750
2 ERROR = THE MAXIMUM OVER ALL THE GRID ELEMENTS OF THE'/25X,'DIFF MD13760
3ERENCE BETWEEN THE WATER FLOW RATE INTO AND OUT OF EACH GRID ELEM MD13770
4NT.') MD13780

5074 FORMAT(7X,' I J K',9X,'XX(I,J,K)',9X,'XX(I,J,K)',13X,'ERROR' MD13790
1,3(12X,'K=',I4)) MD13800

5072 FORMAT('0',72X,3(6X,'XX AT I=',I4)) MD13810

5073 FORMAT(46X,'CHANGE IN',6X,'MAX RESIDUAL',3(12X,'J=',I4)) MD13820

5075 FORMAT('0', 'ITERATIONS USED =', I3, MD13830
1' MAXIMUM CHANGE IN XX BETWEEN LAST 2 ITERATIONS =', D11.3/ MD13840
2' MAXIMUM RESIDUAL ERROR FOR GRID ELEMENTS NOT HAVING FIXED HYDRAU MD13850
3LIC HEAD =', D11.3, ' TOTAL =', D11.3) MD13860

5008 FORMAT('1',59X,'FRESH WATER HEAD') MD13870

5009 FORMAT('1',59X,'WATER WELL HEAD') MD13880

5010 FORMAT('1',37X, MD13890
1'LAYERS UNDERLAIN BY A CONFINING BED HAVE 1, OTHER LAYERS 0') MD13900

5101 FORMAT('1',46X,'WATER FLOW RATE IN NEGATIVE I DIRECTION') MD13910

5102 FORMAT('1',46X,'WATER FLOW RATE IN NEGATIVE J DIRECTION') MD13920

5103 FORMAT('1',46X,'WATER FLOW RATE OUT GRID ELEMENT BOTTOM') MD13930

6000 FORMAT('0', 'LAYER ROW') MD13940

7000 FORMAT('1', 'TIME INTERVAL NUMBER', I3, ' DURATION =', D11.4, ' MD13950
1 TOTAL ELAPSED TIME =', D11.4) MD13960

7001 FORMAT('0',31X,'FLOW FROM',1X,'HEAD DEPENDENT',8X,'FLOW IN' MD13970
1,8X,'FLOW IN',7X,'FLOW OUT',7X,'FLOW OUT' MD13980
2/18X,'RECHARGE',4X,'FIXED HEADS',6X,'DISCHARGE',9X,'BOTTOM' MD13990
3,12X,'TOP',9X,'BOTTOM',12X,'TOP'//) MD14000

8000 FORMAT('1',25X,'THE ELEVATION OF THE HYDRAULIC HEAD (MEASURED RELA MD14010
1TIVE TO THE CENTER OF'/26X,'THE GRID ELEMENT) AT WHICH HEAD DEPEND MD14020
2ANT DISCHARGE BEGINS') MD14030

8001 FORMAT('1',20X,'(RATE OF LOSS (L/T))/(((HYDRAULIC HEAD)-(ELEVATION MD14040
1 AT WHICH DISCHARGE BEGINS)) (L))') MD14050

8002 FORMAT ('1',36X,'THE ELEVATION OF THE TOP OF THE UPPERMOST GRID EL MD14060
1EMENT LAYER') MD14070

8003 FORMAT('1', 'PUMPING INTERVAL=', I5) MD14080

8004 FORMAT('1',45X,'DRAWDOWN DURING THIS PUMPING INTERVAL') MD14090

8010 FORMAT('1',30X,'WATER FLOW RATES OUT OF FIXED HEAD GRID ELEMENTS') MD14100

8011 FORMAT('1',50X,'MASS FLOW BUDGETS'//5X MD14110
1,'TOTAL RECHARGE TO MODELED REGION=', D13.4/5X MD14120
2,'TOTAL FLOW FROM FIXED HEAD GRID ELEMENTS INTO MODELED REGION=' MD14130
3, D13.4/5X, 'TOTAL HEAD DEPENDANT DISCHARGE FROM MODELED REGION' MD14140
4, D13.4) MD14150

8012 FORMAT(' ',2I5,7D15.3) MD14160

9010 FORMAT('1',50X,'HEAD DEPENDANT DISCHARGE RATES') MD14170

9011 FORMAT('0',4X,'TOTAL YQ RECHARGE RATE TO MODELED REGION=', D13.4/ MD14180

```

15X,'TOTAL Q2 RECHARGE RATE TO MODELED REGION=',D13.4/ MD14190
25X,'TOTAL RECHARGE RATE TO MODELED REGION=',D13.4) MD14200
9954 FORMAT('0',45X,'PERCENT SAND') MD14210
9998 FORMAT('0',45X,'ERROR, CALCULATED MINUS MEASURED FRESH WATER HD') MD14220
9020 FORMAT('1','RATE OF RELEASE OF WATER FROM STORAGE BY LAYER','1X,' MD14230
1SUBSIDENCE ONLY, TOTAL') MD14240
9021 FORMAT('1','TOTAL SUBSIDENCE FROM ALL LAYERS FOR THIS PUMPING INTEND MD14250
1RVAL') MD14260
9022 FORMAT('1',9X,'SUBSIDENCE SPECIFIC STORAGE MULTIPLICATION FACTOR') MD14270
9023 FORMAT('0','DEPTH BELOW INITIAL FRESH WATER HEAD AT WHICH SUBSIDEN MD14280
1CE BEGINS IS',D10.1) MD14290
9030 FORMAT('1','PARAMETERS IN LOG FORM-FOR NEW PARAMO') MD14300
9031 FORMAT('0','PARAMETERS ACTUAL VALUE',I10) MD14310
RETURN MD14320
END MD14330
SUBROUTINE RDWRT MD14340
IMPLICIT REAL*8 (A-H,O-Z) MD14350
COMMON WS,HMAX,RELX1,RELX2,COEF,ERR,XX10,DELT,ER5,SRZ,SUMRZ MD14360
1,ERRSV,XX10SV,JIT,NIJ10,NI11,NJ11,NK11,NNN,NSKP1 MD14370
2,NSKP2,ITMAX,ICNT,IEVP,IWR1,NW1,NW2,NW3,N320,NUM4 MD14380
3,L9,LENGTH,NK1115,IT01,IT15,ICRO,DDK,BBK MD14390
4,NI10,NJ10,NK10,NI12,NJ12,NK12,SVIJ,VV40,SV35 MD14400
COMMON /XX/ XX MD14410
COMMON /DT/ DT MD14420
COMMON /VV/ VV MD14430
COMMON /E2/ E2 MD14440
COMMON /F2/ F2 MD14450
COMMON /G2/ G2 MD14460
COMMON /YQ/ YQ MD14470
COMMON /NT/ NT MD14480
COMMON /DD/ DD MD14490
COMMON /BB/ BB MD14500
COMMON /ZZ/ ZZ MD14510
COMMON /XXS/ XXS MD14520
C COMMON /ALN/ ALN MD14530
C COMMON /XXE/ XXE MD14540
C COMMON /SV/ SV MD14550
COMMON /HL/ HL MD14560
COMMON /LB/ LB MD14570
COMMON /MHD/ MHD MD14580
REAL*4 DD(65078),BB(65078),ZZ(65078),XXS(65078), MD14590
1YQ(65078),DDK(50),BBK(50),NT(94658),HL(65078) MD14600
DIMENSION DT(65078),E2(65078),F2(65078),G2(65078),VV(65078) MD14610
DIMENSION XX(65078) MD14620
1,WS(10),MHD(65078),LB(94658) MD14630
2,IF1(10),IF2(10),NNT(250) MD14640
READ(5,1000) II,(IF1(I1),I1=1,9),(IF2(I2),I2=1,10) MD14650
WRITE(6,6000) MD14660
DO 161 K=2,NK1115 MD14670
READ(5,2000) FCNTK,IVAR,IPRN,DDK(K),BBK(K) MD14680
IF(IPRN.EQ.1) GO TO 158 MD14690
IF(IT15.EQ.10) WRITE(6,7000) K,FCNTK MD14700
IF(IT15.EQ.1) WRITE(6,1002) K,FCNTK MD14710
IF(IT15.EQ.2) WRITE(6,1002) K,FCNTK,DDK(K),BBK(K) MD14720
158 DO 161 J=2,NJ11 MD14730

```

	IJMI=NI10*(J-2)+NIJ10*(K-2)	MD14740
	IF(IVAR.EQ.1) READ(5,IF1) (NT(IJMI+I),I=2,NI11)	MD14750
	DO 159 I=2,NI11	MD14760
	IJ=IJMI+I	MD14770
	X=1	MD14780
	IF(IVAR.EQ.1) X=NT(IJ)	MD14790
159	NT(IJ)=X	MD14800
	IF(ICRO.EQ.0) GO TO 1605	MD14810
	DO 13 I=2,NI11	MD14820
	IJ=IJMI+I	MD14830
	LBIJ=LB(IJ)	MD14840
	IF(LBIJ.NE.-30000) NT(IJ)=LBIJ*1.D-5/FCNTK	MD14850
13	CONTINUE	MD14860
1605	IF(.NOT.((IPRN.EQ.0).AND.(IVAR.EQ.1))) GO TO 41	MD14870
	DO 40 I=2,NI11	MD14880
40	NNT(I)=NT(IJMI+I)	MD14890
	IF(II.EQ.0) WRITE(6,IF2) J,(NNT(I),I=2,NI11)	MD14900
	IF(II.EQ.1) WRITE(6,IF2) J,(NT(IJMI+I),I=2,NI11)	MD14910
41	CONTINUE	MD14920
	DO 42 I=2,NI11	MD14930
	IJ=IJMI+I	MD14940
42	NT(IJ)=NT(IJ)*FCNTK	MD14950
161	CONTINUE	MD14960
1000	FORMAT(I4,19A4)	MD14970
1002	FORMAT(I6,6D18.4)	MD14980
2000	FORMAT(8G10.0)	MD14990
4000	FORMAT(I6,I10)	MD15000
6000	FORMAT('0','LAYER ROW')	MD15010
7000	FORMAT('1',I6,6D18.4)	MD15020
	RETURN	MD15030
	END	MD15040

	SUBROUTINE SOLEQU (A,X,N)	SLQ0010
C		SLQ0020
C	THIS SUBROUTINE SOLVES A SET OF SYMMETRIC LINEAR EQUATIONS	SLQ0030
C		SLQ0040
	REAL*4A(50,50),X(50)	SLQ0050
	NM=N-1	SLQ0060
	DO 85 I=1,NM	SLQ0070
	IP=I+1	SLQ0080
	DO 25 J=IP,N	SLQ0090
	IF(ABS(A(I,I)).LT.1.E-8) GO TO 200	SLQ0100
	A(I,J)=A(I,J)/A(I,I)	SLQ0110
25	CONTINUE	SLQ0120
	DO 50 J=IP,N	SLQ0130
	DO 45 K=J,N	SLQ0140
	IF(A(I,J)) 35,50,35	SLQ0150
35	A(K,J)=A(K,J)-A(K,I)*A(I,J)	SLQ0160
	A(J,K)=A(K,J)	SLQ0170
45	CONTINUE	SLQ0180
50	CONTINUE	SLQ0190
	X(I)=X(I)/A(I,I)	SLQ0200
	DO 75 K=IP,N	SLQ0210
	X(K)=X(K)-A(K,I)*X(I)	SLQ0220
75	CONTINUE	SLQ0230
85	CONTINUE	SLQ0240
	IF(ABS(A(N,N)).LT.1.E-8) GO TO 202	SLQ0250
	X(N)=X(N)/A(N,N)	SLQ0260
100	DO 125 II=1,NM	SLQ0270
	I=N-II+1	SLQ0280
	DO 125 K=I,N	SLQ0290
	X(I-1)=X(I-1)-A(I-1,K)*X(K)	SLQ0300
125	CONTINUE	SLQ0310
	AD=0.	SLQ0320
	GO TO 130	SLQ0330
200	WRITE(6,1)	SLQ0340
	WRITE(6,300) I, A(I,I)	SLQ0350
300	FORMAT(//,40X,I5,E20.6)	SLQ0360
	GO TO 130	SLQ0370
202	WRITE(6,1)	SLQ0380
	WRITE(6,300) N, A(N,N)	SLQ0390
	AD=2.	SLQ0400
130	RETURN	SLQ0410
1	FORMAT(//,8X,'BAD INVERSE, ZERO ON DIAGONAL')	SLQ0420
	END	SLQ0430

	SUBROUTINE PCG	PCG0010
	IMPLICIT REAL*8 (A-H,O-Z)	PCG0020
	COMMON WS,HMAX,RELX1,RELX2,COEF,ERR,XX10,DELT,ER5,SRZ,SUMRZ	PCG0030
	1,ERRSV,XX10SV,JIT,NIJ10,NI11,NJ11,NK11,NNN,NSKP1	PCG0040
	2,NSKP2,ITMAX,ICNT,IEVP,IWR1,NW1,NW2,NW3,N320,NUM4	PCG0050
	3,L9,LENGTH,NK1115,IT01,IT15,ICRO,DDK,BBK	PCG0060
	4,NI10,NJ10,NK10,NI12,NJ12,NK12,SVIJ,VV40,SV35	PCG0070
	COMMON /XX/ XX	PCG0080
	COMMON /DT/ DT	PCG0090
	COMMON /VV/ VV	PCG0100
	COMMON /E2/ E2	PCG0110
	COMMON /F2/ F2	PCG0120
	COMMON /G2/ G2	PCG0130
	COMMON /YQ/ YQ	PCG0140
	COMMON /NT/ NT	PCG0150
	COMMON /DD/ DD	PCG0160
	COMMON /BB/ BB	PCG0170
	COMMON /ZZ/ ZZ	PCG0180
	COMMON /XXS/ XXS	PCG0190
C	COMMON /ALN/ ALN	PCG0200
C	COMMON /XXE/ XXE	PCG0210
C	COMMON /SV/ SV	PCG0220
	COMMON /HL/ HL	PCG0230
	COMMON /LB/ LB	PCG0240
	COMMON /MHD/ MHD	PCG0250
	COMMON /E22/ E22	PCG0260
	COMMON /D2S/ D2S	PCG0270
	COMMON /XXSTR/ XXSTR	PCG0280
C	***	PCG0290
	COMMON /XXSS/ XXSS	PCG0300
	REAL*4 XXSS(65078)	PCG0310
C	****	PCG0320
	DIMENSION E22(65078),D2S(65078)	PCG0330
	REAL*4 DD(65078),BB(65078),ZZ(65078),XXS(65078),	PCG0340
	1YQ(65078),DDK(50),BBK(50),NT(94658),HL(65078)	PCG0350
	2,XXSTR(65078)	PCG0360
	DIMENSION DT(65078),E2(65078),F2(65078),G2(65078),VV(65078)	PCG0370
	DIMENSION XX(65078)	PCG0380
	1,WS(10),MHD(65078),LB(94658)	PCG0390
C	IF YOU WANT TO SAVE STORAGE, REMOVE D2S AND E22 FROM THE DIMENSION	PCG0400
C	STATEMENT AND CARDS "76 CONTINUE" THROUGH "56 CONTINUE", AND "86	PCG0410
C	CONTINUE" THROUGH "662 CONTINUE". THIS REMOVES PCG METHODS SIPCG	PCG0420
C	AND SFPCG.	PCG0430
	ICNT=0	PCG0440
	DO 999 IC=1,ITMAX	PCG0450
	DO 1 IJ=1,NNN	PCG0460
	DT(IJ)=0	PCG0470
	E2(IJ)=0	PCG0480
	F2(IJ)=0	PCG0490
	G2(IJ)=0	PCG0500
1	VV(IJ)=0	PCG0510
C	Modification to PCG from VARDEN due to subsidence. Replaces	PCG0520
C	DO 16 and DO 2 loops immediately following this modification	PCG0530
	DO 998 IJ=2,N320	PCG0540
	XXIJ=XX(IJ)	PCG0550

	HLIJ=HL(IJ)	PCC0560
	XXSIJ=XXS(IJ)	PCC0570
	E2(IJ)=XXIJ	PCC0580
	SVIJX=SVIJ*LB(IJ)	PCC0590
	SVDT=SVIJX/DELT	PCC0600
	SVDT40=SVDT*VV40*(1-XXSTR(IJ))	PCC0610
	SVDT1=SVDT	PCC0620
	IF(XXSIJ.LT.HLIJ) SVDT1=SVDT40	PCC0630
	SVDT2=SVDT40	PCC0640
	IF(XXIJ.GT.HLIJ) SVDT2=SVDT	PCC0650
	SHODT=SVDT1*(XXSIJ-HLIJ)+SVDT2*HLIJ	PCC0660
	DELE=0	PCC0670
	IF(MHD(IJ).GE.1) GO TO 997	PCC0680
	DELE=SVDT2	PCC0690
	VV(IJ)=YQ(IJ)+SHODT	PCC0700
997	CONTINUE	PCC0710
	XXSS(IJ)=DELE	PCC0720
998	CONTINUE	PCC0730
C	End of modification	PCC0740
C	DO 16 IJ=2,N320	PCC0750
C	E2(IJ)=XX(IJ)	PCC0760
C	IF(MHD(IJ).GE.1) GO TO 16	PCC0770
C	SVIJX=SVIJ*LB(IJ)	PCC0780
C	DELY=(SVIJX/DELT)*XXS(IJ)	PCC0790
C	IF((IEVP.EQ.1).AND.(XX(IJ).GT.XXE(IJ))) DELY=DELY+ALN(IJ)*XXE(IJ)	PCC0800
C	VV(IJ)=YQ(IJ)+DELY	PCC0810
C16	CONTINUE	PCC0820
C	DO 2 IJ=2,N320	PCC0830
C	DELE=0	PCC0840
C	IF(MHD(IJ).GE.1) GO TO 19	PCC0850
C	SVIJX=SVIJ*LB(IJ)	PCC0860
C	DELE=SVIJX/DELT	PCC0870
C	IF((IEVP.EQ.1).AND.(XX(IJ).GT.XXE(IJ))) DELE=DELE+ALN(IJ)	PCC0880
C19	XXS(IJ)=DELE	PCC0890
C2	CONTINUE	PCC0900
	GO TO (71,71,71,74,74,74),NUM4	PCC0910
71	CONTINUE	PCC0920
	Y1=0	PCC0930
	Z1=0	PCC0940
	DO 51 IJ=2,N320	PCC0950
	IF(.NOT.(MHD(IJ).GE.1)) GO TO 777	PCC0960
	Y1=0	PCC0970
	Z1=0	PCC0980
	GO TO 51	PCC0990
777	CONTINUE	PCC1000
	IJP1K=IJ+NI10	PCC1010
	IJM1K=IJ-NI10	PCC1020
	IJKP1=IJ+NIJ10	PCC1030
	IJKM1=IJ-NIJ10	PCC1040
	IF(IJP1K.GT.NNN) IJP1K=NNN	PCC1050
	IF(IJKP1.GT.NNN) IJKP1=NNN	PCC1060
	IF(IJM1K.LT.1) IJM1K=1	PCC1070
	IF(IJKM1.LT.1) IJKM1=1	PCC1080
	X=DD(IJ)	PCC1090
	Y=BB(IJ)	PCC1100

	Z=ZZ(IJ)	PCG1110
	EEIJ=-(X+Y+Z+DD(IJ+1)+BB(IJP1K)+ZZ(IJKP1))+XXSS(IJ)	PCG1120
	IF(MHD(IJ-1).GE.1) X=0	PCG1130
	IF(MHD(IJM1K).GE.1) Y=0	PCG1140
	IF(MHD(IJKM1).GE.1) Z=0	PCG1150
	Y1Z1=0	PCG1160
	XP=X	PCG1170
	YP=Y	PCG1180
	F2X=F2(IJ-1)	PCG1190
	F2Y=F2(IJM1K)	PCG1200
	F2Z=F2(IJKM1)	PCG1210
	IF(NUM4.EQ.1) GO TO 20	PCG1220
	JP1=IJM1K+1	PCG1230
	KP1=IJKM1+1	PCG1240
	IJMMN=IJ-(NIJ10-NI10)	PCG1250
	IF(IJMMN.LT.1) IJMMN=1	PCG1260
	WY1=0	PCG1270
	WZ1=0	PCG1280
	IF(F2Y.NE.0.0) WY1=Y/F2Y	PCG1290
	IF(F2Z.NE.0.0) WZ1=Z/F2Z	PCG1300
	XP=X-(WY1*Y1+WZ1*Z1)	PCG1310
	G2(IJ)=XP	PCG1320
	YP=Y-WZ1*D2S(IJM1K)	PCG1330
	E22(IJ)=YP	PCG1340
	Y1=-WY1*G2(JP1)	PCG1350
	Z1=-WZ1*G2(KP1)	PCG1360
	ZB=-WZ1*E22(IJMMN)	PCG1370
	D2S(IJ)=ZB	PCG1380
	F21=F2(JP1)	PCG1390
	F22=F2(KP1)	PCG1400
	F23=F2(IJMMN)	PCG1410
	P1=0	PCG1420
	P2=0	PCG1430
	P3=0	PCG1440
	IF(F21.NE.0.0) P1=Y1*Y1/F21	PCG1450
	IF(F22.NE.0.0) P2=Z1*Z1/F22	PCG1460
	IF(F23.NE.0.0) P3=ZB*ZB/F23	PCG1470
	Y1Z1=P1+P2+P3	PCG1480
20	CONTINUE	PCG1490
	XF=0	PCG1500
	YF=0	PCG1510
	ZF=0	PCG1520
	IF(F2X.NE.0.0) XF=XP*XP/F2X	PCG1530
	IF(F2Y.NE.0.0) YF=YP*YP/F2Y	PCG1540
	IF(F2Z.NE.0.0) ZF=Z*Z/F2Z	PCG1550
	F2(IJ)=EEIJ-(XF+YF+ZF+Y1Z1)	PCG1560
51	CONTINUE	PCG1570
	GO TO 80	PCG1580
74	CONTINUE	PCG1590
	DO 54 IJ=2,N320	PCG1600
	IF(MHD(IJ).GE.1) GO TO 54	PCG1610
	IJP1K=IJ+NI10	PCG1620
	IJKP1=IJ+NIJ10	PCG1630
	IF(IJP1K.GT.NNN) IJP1K=NNN	PCG1640
	IF(IJKP1.GT.NNN) IJKP1=NNN	PCG1650

	EEIJ= -(DD(IJ)+BB(IJ)+ZZ(IJ)+DD(IJ+1)	PCG1660
	1+BB(IJP1K)+ZZ(IJKP1))+XXSS(IJ))	PCG1670
	IF(NUM4.LE.5) GO TO 539	PCG1680
	X=DD(IJ)	PCG1690
	F2X=F2(IJ-1)	PCG1700
	XF=0	PCG1710
	IF(F2X.NE.0.0) XF=X*X/F2X	PCG1720
	F2(IJ)=EEIJ-XF	PCG1730
	GO TO 54	PCG1740
539	F2(IJ)=EEIJ	PCG1750
54	CONTINUE	PCG1760
80	CONTINUE	PCG1770
	SPR=1.D-50	PCG1780
	ER5S=100	PCG1790
	L78=2.5*ER5S	PCG1800
C	L78=8	PCG1810
	DO 100 ITER=1,L78	PCG1820
	ICNT=ICNT+1	PCG1830
	IF(ICNT.EQ.ITMAX) GO TO 202	PCG1840
	SPP=0	PCG1850
	DO 3 IJ=2,N320	PCG1860
	IF(MHD(IJ).GE.1) GO TO 3	PCG1870
	IP1JK=IJ+1	PCG1880
	IJP1K=IJ+NI10	PCG1890
	IJM1K=IJ-NI10	PCG1900
	IJKP1=IJ+NIJ10	PCG1910
	IJKM1=IJ-NIJ10	PCG1920
	IF(IJP1K.GT.NNN) IJP1K=NNN	PCG1930
	IF(IJKP1.GT.NNN) IJKP1=NNN	PCG1940
	IF(IJM1K.LT.1) IJM1K=1	PCG1950
	IF(IJKM1.LT.1) IJKM1=1	PCG1960
	DDIJ=DD(IJ)	PCG1970
	DDIP1=DD(IP1JK)	PCG1980
	BBIJ=BB(IJ)	PCG1990
	BBIJP=BB(IJP1K)	PCG2000
	ZZIJ=ZZ(IJ)	PCG2010
	ZZIJK=ZZ(IJKP1)	PCG2020
	E2IJ=E2(IJ)	PCG2030
	DTIJ=(-(DDIJ+DDIP1+BBIJ+BBIJP+ZZIJ+ZZIJK)+XXSS(IJ))*E2IJ	PCG2040
	1+DDIJ*E2(IJ-1)+DDIP1*E2(IP1JK)	PCG2050
	2+BBIJ*E2(IJM1K)+BBIJP*E2(IJP1K)	PCG2060
	3+ZZIJ*E2(IJKM1)+ZZIJK*E2(IJKP1)	PCG2070
	DT(IJ)=DTIJ	PCG2080
	SPP=SPP+E2IJ*DTIJ	PCG2090
3	CONTINUE	PCG2100
	A1=SPR/(SPP+1.D-70)	PCG2110
	A2=A1	PCG2120
	IF(ITER.GT.1) GO TO 35	PCG2130
	A1=0	PCG2140
	A2=1.	PCG2150
35	SRZ=0	PCG2160
	SUMRZ=0	PCG2170
	ER5=0	PCG2180
	DO 4 K=2,NK11	PCG2190
	DO 4 J=2,NJ11	PCG2200

	DO 4 I=2,NI11	PCG2210
	IJ=I+NI10*(J-2)+NIJ10*(K-2)	PCG2220
	IF(MHD(IJ).GE.1) GO TO 4	PCG2230
	DX=A1*E2(IJ)	PCG2240
	X=XX(IJ)+DX	PCG2250
	XX(IJ)=X	PCG2260
	ADX=DABS(DX)	PCG2270
	IF(ADX.LT.ER5) GO TO 111	PCG2280
	IMX=I	PCG2290
	JMX=J	PCG2300
	KMX=K	PCG2310
	XXPMX=X	PCG2320
	ER5=ADX	PCG2330
111	CONTINUE	PCG2340
	X=VV(IJ)-A2*DT(IJ)	PCG2350
	SUMRZ=SUMRZ+X	PCG2360
	DSR=DABS(X)	PCG2370
	IF(DSR.GT.SRZ) SRZ=DSR	PCG2380
	VV(IJ)=X	PCG2390
4	CONTINUE	PCG2400
C	GO TO 202	PCG2410
	IF(IWR1.EQ.1) WRITE(6,1000) IC,ICNT,IMX,JMX,KMX,XXPMX,ER5,SRZ,	PCG2420
	1XX(NW1),XX(NW2),XX(NW3)	PCG2430
C	IF((ER5+ER5S).LT.ERR) GO TO 202	PCG2440
C	C OUT NEXT FOR NONLINEAR	PCG2450
	IF(SRZ.LT.XX10) GO TO 202	PCG2460
	IF((SRZ.LT.XX10).AND.(ITER.EQ.1)) GO TO 202	PCG2470
	ER5S=ER5	PCG2480
	SPRS=SPR	PCG2490
	SPR=0	PCG2500
	GO TO (81,81,81,87,83,85),NUM4	PCG2510
81	CONTINUE	PCG2520
	DO 10 IJ=2,N320	PCG2530
	IF(MHD(IJ).GE.1) GO TO 10	PCG2540
	IJM1K=IJ-NI10	PCG2550
	IJKM1=IJ-NIJ10	PCG2560
	IF(IJM1K.LT.1) IJM1K=1	PCG2570
	IF(IJKM1.LT.1) IJKM1=1	PCG2580
	B6=0	PCG2590
	Z6=0	PCG2600
	DDIJ=DD(IJ)	PCG2610
	BBIJ=BB(IJ)	PCG2620
	IF(NUM4.EQ.1) GO TO 21	PCG2630
	DDIJ=G2(IJ)	PCG2640
	BBIJ=E22(IJ)	PCG2650
	JP1=IJ-NI10+1	PCG2660
	KP1=IJ-NIJ10+1	PCG2670
	IF(JP1.LT.1) JP1=1	PCG2680
	IF(KP1.LT.1) KP1=1	PCG2690
	IJMMN=IJ-(NIJ10-NI10)	PCG2700
	IF(IJMMN.LT.1) IJMMN=1	PCG2710
	B6=0	PCG2720
	Z6=0	PCG2730
	F2J=F2(IJM1K)	PCG2740
	F2K=F2(IJKM1)	PCG2750

	IF(F2J.NE.0.DO) B6=DT(JP1)*G2(JP1)/F2J	PCG2760
	IF(F2K.NE.0.DO) Z6=(DT(KP1)*G2(KP1)+DT(IJMMN)*E22(IJMMN))/F2K	PCG2770
21	CONTINUE	PCG2780
	DT(IJ)=(VV(IJ)-DDIJ*DT(IJ-1)-BBIJ*(DT(IJM1K)-B6)	PCG2790
	1-ZZ(IJ)*(DT(IJKM1)-Z6))/F2(IJ)	PCG2800
10	CONTINUE	PCG2810
	DO 11 IJB=2,N320	PCG2820
	IJ=N320+2-IJB	PCG2830
	IF(MHD(IJ).GE.1) GO TO 11	PCG2840
	IP1JK=IJ+1	PCG2850
	IJP1K=IJ+NI10	PCG2860
	IJKP1=IJ+NIJ10	PCG2870
	IF(IJP1K.GT.NNN) IJP1K=NNN	PCG2880
	IF(IJKP1.GT.NNN) IJKP1=NNN	PCG2890
	XAD=0	PCG2900
	DDD=DD(IP1JK)	PCG2910
	BBB=BB(IJP1K)	PCG2920
	IF(NUM4.EQ.1) GO TO 22	PCG2930
	JM1=IJ+NI10-1	PCG2940
	KM1=IJ+NIJ10-1	PCG2950
	IF(JM1.GT.NNN) JM1=NNN	PCG2960
	IF(KM1.GT.NNN) KM1=NNN	PCG2970
	IJM1K=IJ-NI10	PCG2980
	IJPMN=IJ+(NIJ10-NI10)	PCG2990
	IF(IJM1K.LT.1) IJM1K=1	PCG3000
	IF(IJPMN.GT.NNN) IJPMN=NNN	PCG3010
	DDD=G2(IP1JK)	PCG3020
	BBB=E22(IJP1K)	PCG3030
	XAD1=0	PCG3040
	XAD2=0	PCG3050
	F2I=F2(IJ-1)	PCG3060
	F2J=F2(IJM1K)	PCG3070
	IF(F2I.NE.0.DO) XAD1=- (E22(JM1)*DT(JM1)+ZZ(KM1)*DT(KM1))*	PCG3080
	1G2(IJ)/F2I	PCG3090
	IF(F2J.NE.0.DO) XAD2=- ZZ(IJPMN)*E22(IJ)*DT(IJPMN)/F2J	PCG3100
	XAD=XAD1+XAD2	PCG3110
22	CONTINUE	PCG3120
	DTIJ=DT(IJ)-(DDD*DT(IP1JK)+BBB*DT(IJP1K)+ZZ(IJKP1)	PCG3130
	1*DT(IJKP1)+XAD)/F2(IJ)	PCG3140
	DT(IJ)=DTIJ	PCG3150
	SPR=SPR+DTIJ*VV(IJ)	PCG3160
11	CONTINUE	PCG3170
	GO TO 90	PCG3180
83	CONTINUE	PCG3190
	DO 63 IJ=2,N320	PCG3200
	IF(MHD(IJ).GE.1) GO TO 63	PCG3210
	F2IJ=F2(IJ)	PCG3220
	VVIJ=VV(IJ)	PCG3230
	DTIJ=VVIJ/F2IJ	PCG3240
	DT(IJ)=DTIJ	PCG3250
	SPR=SPR+DTIJ*VVIJ	PCG3260
63	CONTINUE	PCG3270
	GO TO 90	PCG3280
85	CONTINUE	PCG3290
	DO 651 IJ=2,N320	PCG3300

	IF(MHD(IJ).GE.1) GO TO 651	PCG3310
	DT(IJ)=(VV(IJ)-DD(IJ)*DT(IJ-1))/F2(IJ)	PCG3320
651	CONTINUE	PCG3330
	DO 652 IJB=2,N320	PCG3340
	IJ=N320+2-IJB	PCG3350
	IF(MHD(IJ).GE.1) GO TO 652	PCG3360
	IP1JK=IJ+1	PCG3370
	DTIJ=DT(IJ)-DD(IP1JK)*DT(IP1JK)/F2(IJ)	PCG3380
	DT(IJ)=DTIJ	PCG3390
	SPR=SPR+DTIJ*VV(IJ)	PCG3400
652	CONTINUE	PCG3410
	GO TO 90	PCG3420
C	***** NEW SSOR METHOD*****	PCG3430
87	CONTINUE	PCG3440
	IF(HMAX.EQ.0.DO) HMAX=1	PCG3450
	DO 771 IJ=2,N320	PCG3460
	IF(MHD(IJ).GE.1) GO TO 771	PCG3470
	IM1JK=IJ-1	PCG3480
	IJM1K=IJ-NI10	PCG3490
	IJKM1=IJ-NIJ10	PCG3500
	IF(IJM1K.LT.1) IJM1K=1	PCG3510
	IF(IJKM1.LT.1) IJKM1=1	PCG3520
	C2S=DD(IJ)	PCG3530
	B2S=BB(IJ)	PCG3540
	A2S=ZZ(IJ)	PCG3550
	DT(IJ)=(VV(IJ)-C2S*DT(IJ-1)-B2S*DT(IJM1K)	PCG3560
	1-A2S*DT(IJKM1))/(F2(IJ)/HMAX)	PCG3570
771	CONTINUE	PCG3580
	DO 772 IJB=2,N320	PCG3590
	IJ=N320+2-IJB	PCG3600
	IF(MHD(IJ).GE.1) GO TO 772	PCG3610
	IP1JK=IJ+1	PCG3620
	IJP1K=IJ+NI10	PCG3630
	IJKP1=IJ+NIJ10	PCG3640
	IF(IJP1K.GT.NNN) IJP1K=NNN	PCG3650
	IF(IJKP1.GT.NNN) IJKP1=NNN	PCG3660
	DTIJ=DT(IJ)	PCG3670
	1-(DD(IP1JK)*DT(IP1JK)+BB(IJP1K)*DT(IJP1K)	PCG3680
	2+ZZ(IJKP1)*DT(IJKP1))/F2(IJ)	PCG3690
	DT(IJ)=DTIJ*HMAX	PCG3700
772	CONTINUE	PCG3710
	DO 773 IJ=2,N320	PCG3720
	DTIJ=DT(IJ)*(2-HMAX)/HMAX	PCG3730
	SPR=SPR+DTIJ*VV(IJ)	PCG3740
773	DT(IJ)=DTIJ	PCG3750
C	*****END SSOR METHOD*****	PCG3760
90	CONTINUE	PCG3770
	B6=SPR/SPRS	PCG3780
	IF(ITER.EQ.1) B6=0	PCG3790
	DO 5 IJ=2,N320	PCG3800
	E2IJ=DT(IJ)+B6*E2(IJ)	PCG3810
	IF(MHD(IJ).GE.1) E2IJ=0	PCG3820
	E2(IJ)=E2IJ	PCG3830
5	CONTINUE	PCG3840
100	CONTINUE	PCG3850

```
999 CONTINUE
202 CONTINUE
1000 FORMAT(' ', 2I3, 3I5, 6D18.7)
      RETURN
      END
```

```
PCG3860
PCG3870
PCG3880
PCG3890
PCG3900
```

	SUBROUTINE SIP	SIP0010
	IMPLICIT REAL*8 (A-H,O-Z)	SIP0020
	COMMON WS,HMAX,RELX1,RELX2,COEF,ERR,XX10,DELT,ER5,SRZ,SUMRZ	SIP0030
	1,ERRSV,XX10SV,JIT,NIJ10,NI11,NJ11,NK11,NNN,NSKP1	SIP0040
	2,NSKP2,ITMAX,ICNT,IEVP,IWR1,NW1,NW2,NW3,N320,NUM4	SIP0050
	3,L9,LENGTH,NK1115,IT01,IT15,ICRO,DDK,BBK	SIP0060
	4,NI10,NJ10,NK10,NI12,NJ12,NK12,SVIJ,VV40,SV35	SIP0070
	COMMON /XX/ XX	SIP0080
	COMMON /DT/ DT	SIP0090
	COMMON /VV/ VV	SIP0100
	COMMON /E2/ E2	SIP0110
	COMMON /F2/ F2	SIP0120
	COMMON /G2/ G2	SIP0130
	COMMON /YQ/ YQ	SIP0140
	COMMON /NT/ NT	SIP0150
	COMMON /DD/ DD	SIP0160
	COMMON /BB/ BB	SIP0170
	COMMON /ZZ/ ZZ	SIP0180
	COMMON /XXS/ XXS	SIP0190
C	COMMON /ALN/ ALN	SIP0200
C	COMMON /XXE/ XXE	SIP0210
C	COMMON /SV/ SV	SIP0220
	COMMON /HL/ HL	SIP0230
	COMMON /LB/ LB	SIP0240
	COMMON /MHD/ MHD	SIP0250
	COMMON /E22/ E22	SIP0260
	COMMON /D2S/ D2S	SIP0270
	COMMON /XXSTR/ XXSTR	SIP0280
	DIMENSION E22(65078),D2S(65078)	SIP0290
	REAL*4 DD(65078),BB(65078),ZZ(65078),XXS(65078),	SIP0300
	1YQ(65078),DDK(50),BBK(50),NT(94658),HL(65078)	SIP0310
	2,XXSTR(65078)	SIP0320
	DIMENSION DT(65078),E2(65078),F2(65078),G2(65078),VV(65078)	SIP0330
	DIMENSION XX(65078)	SIP0340
	1,WS(10),MHD(65078),LB(94658)	SIP0350
	DO 889 IJ=1,NNN	SIP0360
	E2(IJ)=0	SIP0370
	F2(IJ)=0	SIP0380
	G2(IJ)=0	SIP0390
	VV(IJ)=0	SIP0400
889	DT(IJ)=0	SIP0410
	ICNT=0	SIP0420
	ICT=0	SIP0430
	ER5S=100	SIP0440
	DO 501 ITER0=1,60	SIP0450
	DO 499 I33=1,2	SIP0460
	I3=I33	SIP0470
	I4=1	SIP0480
	IF(L9.EQ.2) I4=I3	SIP0490
	IF(L9.LT.3) GO TO 195	SIP0500
	I3=1	SIP0510
	I4=I33	SIP0520
195	CONTINUE	SIP0530
	ICT=ICT+1	SIP0540
	IF(ICT.EQ.(LENGTH+1)) ICT=1	SIP0550

ICNT=ICNT+1	SIP0560
IF(ICNT.EQ.ITMAX) GO TO 202	SIP0570
W=WS(ICT)	SIP0580
JJM1=2*I3-3	SIP0590
JJP1=-JJM1	SIP0600
KKM1=2*I4-3	SIP0610
KKP1=-KKM1	SIP0620
C ACCOMPLISH EQUATIONS (10) AND (14) BY WEINSTEIN [1969]	SIP0630
SRZ=0	SIP0640
SUMRZ=0	SIP0650
DO 100 KB=2,NK11	SIP0660
ISF1=0	SIP0670
IF((KB.GE.3).AND.(KB.LE.NK10)) ISF1=1	SIP0680
DO 100 JB=2,NJ11	SIP0690
ISF2=0	SIP0700
IF((JB.GE.3).AND.(JB.LE.NJ10)) ISF2=1	SIP0710
J=JB	SIP0720
K=KB	SIP0730
IF(I3.EQ.2) J=NJ12+1-JB	SIP0740
IF(I4.EQ.2) K=NK12+1-KB	SIP0750
DO 50 I=2,NI11	SIP0760
IJF=I+NI10*(J-2)	SIP0770
IJ=IJF+NIJ10*(K-2)	SIP0780
IF(MHD(IJ).GE.1) GO TO 49	SIP0790
IM1JK=IJ-1	SIP0800
IP1JK=IJ+1	SIP0810
IJM1K=IJ+JJM1*NI10	SIP0820
IJP1K=IJ+JJP1*NI10	SIP0830
IJP2K=IJ+NI10	SIP0840
IJKM1=IJ+KKM1*NIJ10	SIP0850
IJKP1=IJ+KKP1*NIJ10	SIP0860
IJKP2=IJ+NIJ10	SIP0870
IF(ISF1.EQ.1) GO TO 91	SIP0880
IF(IJKM1.LT.1) IJKM1=1	SIP0890
IF(IJKM1.GT.NNN) IJKM1=NNN	SIP0900
IF(IJKP1.LT.1) IJKP1=1	SIP0910
IF(IJKP1.GT.NNN) IJKP1=NNN	SIP0920
IF(IJKP2.GT.NNN) IJKP2=NNN	SIP0930
IF(ISF2.EQ.1) GO TO 91	SIP0940
IF(IJM1K.LT.1) IJM1K=1	SIP0950
IF(IJM1K.GT.NNN) IJM1K=NNN	SIP0960
IF(IJP1K.LT.1) IJP1K=1	SIP0970
IF(IJP1K.GT.NNN) IJP1K=NNN	SIP0980
IF(IJP2K.GT.NNN) IJP2K=NNN	SIP0990
91 CONTINUE	SIP1000
XXIJ=XX(IJ)	SIP1010
HLIJ=HL(IJ)	SIP1020
XXSIJ=XXS(IJ)	SIP1030
Z=ZZ(IJ)	SIP1040
B=BB(IJ)	SIP1050
D=DD(IJ)	SIP1060
F=DD(IP1JK)	SIP1070
H=BB(IJP2K)	SIP1080
S=ZZ(IJKP2)	SIP1090
IF(I3.EQ.1) GO TO 42	SIP1100

	BS=B	SIP1110
	B=H	SIP1120
	H=BS	SIP1130
42	CONTINUE	SIP1140
	IF(I4.EQ.1) GO TO 43	SIP1150
	ZS=Z	SIP1160
	Z=S	SIP1170
	S=ZS	SIP1180
43	CONTINUE	SIP1190
C	Due to subsidence	SIP1200
C	Next 8 lines modified from SIP from VARDEN	SIP1210
C	SVDT2 replaces SVDT used before in equation for E	SIP1220
	SVIJX=SVIJ*LB(IJ)	SIP1230
	SVDT=SVIJX/DELTA	SIP1240
	SVDT40=SVDT*VV40*(1-XXSTR(IJ))	SIP1250
	SVDT1=SVDT	SIP1260
	IF(XXSIJ.LT.HLIJ) SVDT1=SVDT40	SIP1270
	SVDT2=SVDT40	SIP1280
	IF(XXIJ.GT.HLIJ) SVDT2=SVDT	SIP1290
	E=-(Z+B+D+F+H+S)+SVDT2	SIP1300
C	DH1=XXSIJ-HLIJ	SIP1310
C	DH2=HLIJ-XXIJ	SIP1320
C	IF(SVDT1.NE.SVDT2) SVDTA=(DH1*SVDT1+DH2*SVDT2)/(DH1+DH2)	SIP1330
C	IF(SVDT1.EQ.SVDT2) SVDTA=SVDT1	SIP1340
C	E=-(Z+B+D+F+H+S)+SVDTA	SIP1350
	LEV=0	SIP1360
C	IF((IEVP.EQ.1).AND.(XXIJ.GT.XXE(IJ))) LEV=1	SIP1370
	IF(LEV.NE.1) GO TO 44	SIP1380
C	ALNI=ALN(IJ)	SIP1390
	E=E+ALNI	SIP1400
44	CONTINUE	SIP1410
	E2I=E2(IM1JK)	SIP1420
	E2J=E2(IJM1K)	SIP1430
	E2K=E2(IJKM1)	SIP1440
	F2I=F2(IM1JK)	SIP1450
	F2J=F2(IJM1K)	SIP1460
	F2K=F2(IJKM1)	SIP1470
	G2I=G2(IM1JK)	SIP1480
	G2J=G2(IJM1K)	SIP1490
	G2K=G2(IJKM1)	SIP1500
	A2=Z/(1+W*(E2K+F2K))	SIP1510
	B2=B/(1+W*(G2J+E2J))	SIP1520
	C2=D/(1+W*(G2I+F2I))	SIP1530
	AC=W*(A2*E2K+B2*E2J)	SIP1540
	TG=W*(A2*F2K+C2*F2I)	SIP1550
	WU=W*(C2*G2I+B2*G2J)	SIP1560
	D2=E+(AC+TG+WU)-C2*E2I-B2*F2J-A2*G2K	SIP1570
	D2=1/D2	SIP1580
	E2(IJ)=D2*(F-AC)	SIP1590
	F2(IJ)=D2*(H-TG)	SIP1600
	G2(IJ)=D2*(S-WU)	SIP1610
	RZ=YQ(IJ)-(XX(IM1JK)*D+XX(IP1JK)*F+XX(IJM1K)*B+XX(IJP1K)*H	SIP1620
	1+XX(IJKM1)*Z+XX(IJKP1)*S+XXIJ*E)	SIP1630
C	Next line added to SIP from VARDEN	SIP1640
	2+SVDT1*(XXSIJ-HLIJ)+SVDT2*HLIJ	SIP1650

C	Next line was used by SIP from VARDEN	SIP1651
C	2+SVDTA*XXSIJ	SIP1660
C	Next line was used by SIP from VARDEN	SIP1670
C	IF(LEV.EQ.1) RZ=RZ+ALNI*XXE(IJ)	SIP1680
	SUMRZ=SUMRZ+RZ	SIP1690
	DSR=DABS(RZ)	SIP1700
	IF(DSR.GT.SRZ) SRZ=DSR	SIP1710
	VV(IJ)=D2*(RZ-A2*VV(IJKM1)-B2*VV(IJM1K)-C2*VV(IM1JK))	SIP1720
49	CONTINUE	SIP1730
50	CONTINUE	SIP1740
100	CONTINUE	SIP1750
C	EQUATIONS (10) AND (14) ARE NOW ACCOMPLISHED	SIP1760
C	ACCOMPLISH EQUATION (15) BY WEINSTEIN [1969]	SIP1770
	ER5=0	SIP1780
	DO 102 KB=2,NK11	SIP1790
	ISF1=0	SIP1800
	IF((KB.GE.3).AND.(KB.LE.NK10)) ISF1=1	SIP1810
	DO 102 JB=2,NJ11	SIP1820
	ISF2=0	SIP1830
	IF((JB.GE.3).AND.(JB.LE.NJ10)) ISF2=1	SIP1840
	J=NJ12+1-JB	SIP1850
	K=NK12+1-KB	SIP1860
	IF(I3.EQ.2) J=JB	SIP1870
	IF(I4.EQ.2) K=KB	SIP1880
	DO 62 IB=2,NI11	SIP1890
	I=NI12+1-IB	SIP1900
	IJ=I+NI10*(J-2)+NIJ10*(K-2)	SIP1910
	IF(MHD(IJ).GE.1) GO TO 61	SIP1920
	IP1JK=IJ+1	SIP1930
	IJP1K=IJ+JJP1*NI10	SIP1940
	IJKP1=IJ+KKP1*NIJ10	SIP1950
	IF(ISF1.EQ.1) GO TO 92	SIP1960
	IF(IJKP1.LT.1) IJKP1=1	SIP1970
	IF(IJKP1.GT.NNN) IJKP1=NNN	SIP1980
	IF(ISF2.EQ.1) GO TO 92	SIP1990
	IF(IJP1K.LT.1) IJP1K=1	SIP2000
	IF(IJP1K.GT.NNN) IJP1K=NNN	SIP2010
92	CONTINUE	SIP2020
	X=VV(IJ)-E2(IJ)*DT(IP1JK)-F2(IJ)*DT(IJP1K)-G2(IJ)*DT(IJKP1)	SIP2030
	DT(IJ)=X	SIP2040
	X=X*HMAX	SIP2050
	XXP=XX(IJ)+X	SIP2060
	XX(IJ)=XXP	SIP2070
	X=DABS(X)	SIP2080
	IF(X.LE.ER5) GO TO 111	SIP2090
	IMX=I	SIP2100
	JMX=J	SIP2110
	KMX=K	SIP2120
	XXPMX=XXP	SIP2130
	ER5=X	SIP2140
111	CONTINUE	SIP2150
61	CONTINUE	SIP2160
62	CONTINUE	SIP2170
102	CONTINUE	SIP2180
C	EQUATION (15) IS NOW ACCOMPLISHED	SIP2190

	IF(IWR1.EQ.1) WRITE(6,1000)	SIP2200
	1 ICNT,IMX,JMX,KMX,XXPMX,ER5,SRZ,XX(NW1),XX(NW2),XX(NW3)	SIP2210
	IF((ER5+ER5S).LT.ERR) GO TO 202	SIP2220
	IF(SRZ.LT.XX10) GO TO 202	SIP2230
	ER5S=ER5	SIP2240
499	CONTINUE	SIP2250
501	CONTINUE	SIP2260
202	CONTINUE	SIP2270
1000	FORMAT(' ',I3,3I5,6D18.7)	SIP2280
	RETURN	SIP2290
	END	SIP2300